GLOBAL INVESTIGATIONS OF RADIATED SEISMIC ENERGY AND REAL-TIME IMPLEMENTATION

A Dissertation
Presented to
The Academic Faculty

by

Jaime Andres Convers Arjona

In Partial Fulfillment
of the Requirements for the Degree
Doctor of Philosophy in the
School of Earth and Atmospheric Sciences

Georgia Institute of Technology
December 2013

GLOBAL INVESTIGATIONS OF RADIATED SEISMIC ENERGY AND REAL-TIME IMPLEMENTATION

Approved by:

Dr. Andrew Newman, Advisor
School of Earth and Atmospheric Sciences
Georgia Institute of Technology

Dr. Zhigang Peng
School of Earth and Atmospheric Sciences
Georgia Institute of Technology

Dr. Hermann M. Fritz
School of Civil and Environmental Engineering
Georgia Institute of Technology

Dr. Josef Dufek
School of Earth and Atmospheric Sciences
Georgia Institute of Technology

Dr. Stewart Weinstein
Pacific Tsunami Warning Center

Date Approved: August 21,2013

To Jaime and Lucy

ACKNOWLEDGEMENTS

I would like first to express my gratitude to my advisor, Dr. Andrew Newman, for letting me work on a motivating project, which I grew more passionate about as I made progress, and for giving me all the scientific and technical knowledge to achieve my goals and hopefully continue to grow as a scientist.

I would like to thank also my dissertation committee, Dr. Zhigang Peng, Dr. Josef Dufek, Dr. Hermann Fritz and Dr. Stuart Weisntein, for their time, their feedback, and of course their knowledge, I have learned from each one of them one way or another, they are a great example of what excellence represents in science.

Especial thanks to Dr. Kurt Frankel, rest in peace, great scientist, amazing person, and contagious laughter, for his valuable insights and suggestions and his support. Also, for giving me the opportunity to work in the field when I had no funding, thanks to him I had the motivation and encouragement to continue in the program.

To my fellow Georgia Tech and Geophysics members, they practically became my family for the last few years making my life enjoyable. They are, Ozge Karakas, Lujia Feng, Peng Zhao, Kevin Chao, Jenn Telling, Brendan Sullivan, Chastity Aiken, Xiaofeng Meng, Chunquan Wu, Josh Mendez, Cindy Young, and the rest of the geophysics group.

Special heartfelt thanks to Jeremy Riousset, Andres Felipe Hernandez and Ozge Karakas at Georgia Tech for their unlimited support and their help through difficult times.

To Ekaterina Krylova and Anna Grabar, distance is no obstacle for their support and kindness, from wake up calls to inspirational motivation; they helped me stay on task and their ongoing moral support still influence me during my personal and professional life.

My parents, Jaime and Lucy, to whom I dedicate this dissertation, without their unconditional love and support I would not be where I am.

This manuscript contains parts from two published manuscripts, one in review and one in prepare:

Convers, J. A., and A. V. Newman (2011), "Global evaluation of large earthquake energy from 1997 through mid-2010", Journal of Geophysical Research, 116, B08304

Convers, J. A. and A. V. Newman. "Rapid Earthquake Rupture Duration Estimates from Teleseismic Energy Rates, with Application to Real-Time Warning", *Geophysical Research Letters*. (2013). In review.

Convers, J. A. and A. V. Newman. "RTerg: Radiated Seismic Energy and Rupture Duration Calculation for Large Earthquakes". *Computers & Geosciences*, In prep.

Newman, A. V., G. Hayes, Y, Wei, J. A. Convers, "The 25 October 2010 Mentawai Tsunami Earthquake, from real-time discriminant, finite-fault rupture, and tsunami excitation", *Geophysical Research Lett*ers, 38, L05302.

TABLE OF CONTENTS

LIST OF TABLES

LIST OF FIGURES

Page

LIST OF SYMBOLS AND ABBREVIATIONS

M_0	Seismic Moment
M_W	Moment Magnitude
M_e	Energy Magnitude
m_b	Body Wave Magnitude
M_S	Surface Wave Magnitude
E	Radiated Seismic Energy
θ	Energy-to-Moment Ratio
E_{bb}	Broadband Radiated Energy (0.5 – 70 s)
E_{hf}	High Frequency Radiated Energy (0.5 – 2 s)
E_{rate}	Rate of Increase in Cumulative Radiated Seismic Energy
T_r	Rupture Duration
V_r	Rupture velocity
TsE	Tsunami Earthquake
MAT	Middle America Trench
IRIS	Incorporated Research Institutions for Seismology
NEIC	National Earthquake Information Center
ISC	International Seismological Centre
EHB	Engdahl et al. algorithm used for ISC catalog

SUMMARY

This dissertation contains investigations of radiated seismic energy measurements from large earthquakes and duration determinations as significant properties of the dynamic earthquake rupture and its applications in the identification of very large and slow source rupturing earthquakes. This includes a description of earthquake released seismic energy from 1997 to 2010 and identification of slow source tsunami earthquakes in that time period. The implementation of these measurements in real-time since the beginning of 2009, with a case study of the Mentawai 2010 tsunami earthquake are also discussed. Further studies of rupture duration assessments and its technical improvements for more rapid and robust solutions are investigated as well, with application to the Tohoku-Oki 2011 earthquake an a case of directivity in the 2007 M_w 8.1 Solomon islands earthquake. Finally, the set of routines and programs developed for implementation at Georgia Tech and IRIS to produce the real-time results since 2009 presented in this study are described.

CHAPTER 1

INTRODUCTION

Recent studies of tectonics, earthquake physics and modern instrumentation have allowed us identify important earthquake parameters that not only improve our understanding about earthquakes in general, but they have also played a role in our damage mitigation efforts. From classifying magnitude scale of earthquakes [*Richter*, 1935], and estimations of their physical size [*Aki*, 1966], to non-saturating modern magnitude scales [*Hanks and Kanamori*, 1979], we can now promptly assess location and timing of such events, and soon after its occurrence, we also estimate important descriptive parameters, such as size and even focal mechanisms for most earthquakes. All of these measurements aid categorization of the nature of an earthquake and its hazard implications.

However, the occurrence in recent years of some of the largest earthquakes in seismically recorded history has put our methods of rapidly characterizing their hazard to the test, in many cases with limited success (such as the case for the Sumatra 2004 earthquake, with a recorded moment magnitude of 9.1). Fortunately, advances in instrumentation and data transmission have minimized many limitations regarding station coverage, timing, quantity and quality of seismic data, consequently not only allowing us to perform calculations of seismic parameters more rapidly, but integrating them with other quantities to help elucidate faulting nature and characterize earthquake hazard. One of such quantities is radiated seismic energy, around which this dissertation is centered.

This is a seismic observable that plays an important role in describing the earthquake dynamic rupture process.

While the seismic moment M_0, and hence moment magnitude M_W [*Hanks and Kanamori*, 1979], are highly valuable as estimates of the total static work done in an earthquake, in isolation they do not describe the dynamic component of earthquake rupture. Full determinations of seismic moment frequently require the inclusion of the full body-wave and/or substantial surface wave data for analysis [e.g., *Ekstrom et al.*, 2005], though real-time estimates may be made using integrated *P*-wave seismograms at teleseismic distances. This real-time adaptation, however, requires an assumption of constant stress drop for accurate moment estimations [*Tsuboi et al.*, 1999; *Tsuboi et al.*, 1995]. These issues make the use of seismic moment alone less useful for real-time hazard assessment [e.g., *Beresnev*, 2009; *Choy and Boatwright*, 2009]. Because events with the same seismic moment, M_0, can have considerable differences in their radiated energy, damage evaluations based solely on M_0 may inaccurately characterize the true damage caused by an earthquake. This is particularly the case for both high stress drop earthquakes that have disproportionally energetic shaking given their M_0 [*Choy and Kirby*, 2004], and tsunami earthquakes (TsE), which can be energetically deficient by more than a factor of ten relative to global averages of E/M_0, due to their slow rupture [*Newman and Okal*, 1998].

While any earthquake that creates a tsunami can be classified as "tsunamigenic", the specific name "tsunami earthquake" is reserved for a special class of events that generate tsunamis much larger than expected for their magnitude [*Kanamori*, 1972]. These earthquakes are relatively rare, and there have been less a dozen events in the past century or so. They are normally identified to have anomalously slow rupture velocities, and are thus inefficient at radiating seismic energy, often making such events only weakly felt by local populations, and posing challenges in hazard assessment and tsunami warning systems. Growing evidence suggests that TsE rupture slowly because they occur in the shallowest segment of the subduction megathrust [*Lay et al.*, 2012; *Polet and Kanamori*, 2000], which may have □1/10th the rigidity of the deeper thrust, causing a reduction in shear velocity V_S and hence the rupture velocity V_R, which is usually □0.8 V_S [*Bilek and Lay*, 1999].

This highlights the hazard implications from these earthquakes, and not only brings to attention the importance of studying the radiated seismic energy from slow source tsunami earthquakes, but of large earthquakes in general. Their radiated seismic energy reveals dynamic rupture characteristics that are not revealed by measurements of size, and now more than ever we find the convenience of using modern technological capabilities to address these in a timely matter.

Using known energy characteristics of tsunami earthquakes identified from their seismic observables, I catalog radiated seismic energy released by large earthquakes from 1997 to 2009 at a global scale to expand upon previous investigations of this character for the benchmarking of future procedures and studies, and I include a comparison of two regional studies for possible spatial and depth variations in the local released seismic energy. This serves as the precedent for the subsequent step: the real-time implementation of this methodology from early 2009, after which, the M_W 7.8 Mentawai earthquake on October 25 of 2010 was identified as a slow source tsunami earthquake. I also describe the real-time implementation and improvements on rupture duration estimates with application to the 2011 Tohoku-Oki earthquake. This is carried out in an effort to improve calculation capabilities by single stations. Finally, I describe the real-time set of software and routines for these calculations implemented at Georgia Tech and IRIS.

CHAPTER 2

RADIATED SEISMIC ENERGY AND DURATION

2.1 Introduction

The methodology to obtain the released seismic energy for this dissertation is obtained from *P*-waves at teleseismic distances (25° - 80°) and was used initially to compile a global catalog of post-processed events between 1997 and 2010, as well as a real-time adaptation beginning in early 2009. This approach is built upon the methods described in *Newman and Okal* [1998], and used to catalog prior global earthquake activity between 1982 and 1997, however, its application for this catalog utilizes advancements in computational code for more rapid and automated processing, and it is benefited by the vast improvement in the readily-available broad-band seismic data from globally distributed stations. Additionally, we introduce an improvement to account for the full rupture duration by computing increasing time windows of cumulative radiated seismic energy, as opposed to keeping a fixed 70 s duration used by *Newman and Okal* [1998]. We also investigate the independence of results with distance that were performed for the post-processed catalog, and although results are robust and can be considered as general, the evaluations of independence of results with distance from the source and comparison of duration are taken from the investigation performed for the 1997 to 2010 catalog.

2.2 Energy Calculations

Boatwright and Choy [1986] developed a method to calculate the energy radiated from seismic waves using the shaking recorded in the *P*-wave group (*P*+*pP*+*sP*). The group energy is selected because the energy fluxes from individual phases overlap for shallow rupturing and long-duration earthquakes (**Figure 2.1**). For shallow earthquakes, the phases travel along similar paths and hence a group attenuation correction can be made. However, the *pP* and *sP* phases of deeper earthquakes become distinctly separated from the direct arrival, and are preferentially attenuated because the direct *P*-phase no-longer travels through the weak source-side crust.

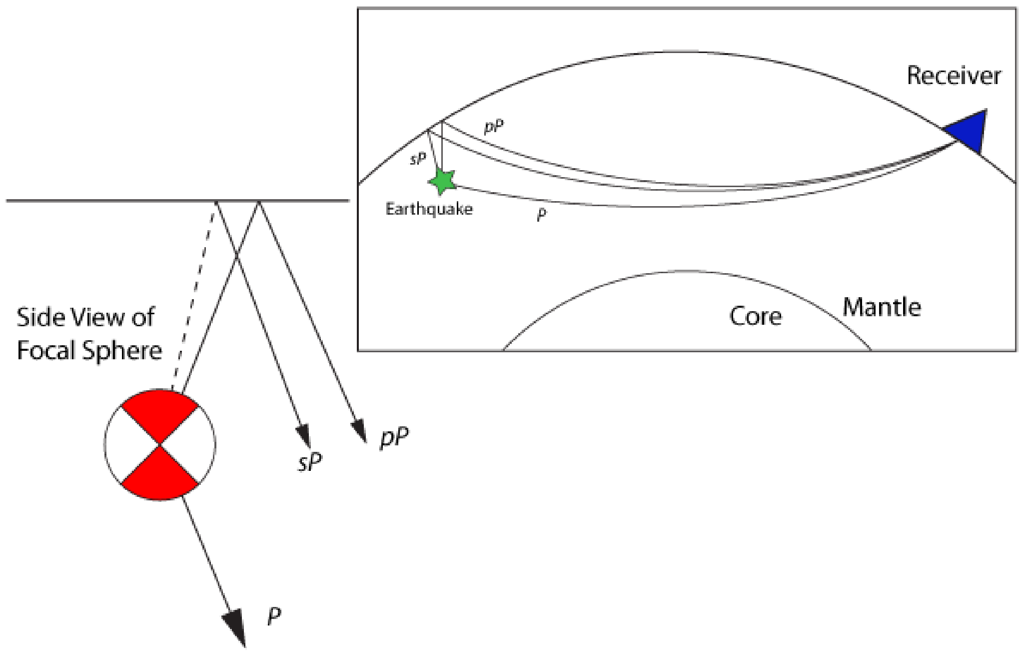

Figure 2.1: Schematic illustration showing the relative takeoff angles and the near-source free surface reflections of *pP* and *sP* depth phases for a thrust focal mechanism. The P-wave arrival for a shallow earthquake at teleseismic distances is modeled as the sum of arrivals due to the direct *P*-wave and the depth phases *pP* and *sP*. Modified from Figures 4.3-6 and 4.3-7 of *Stein and Wysession* [2003].

From the velocity records, the energy flux can be computed in the time-domain at each station, and integrated over the duration of the generalized *P*-wave group. However, by calculating the per-station energy flux in the frequency domain, it is possible to directly correct for frequency-dependent anelastic attenuation, obtaining a new theoretical station energy flux corrected for attenuation $\bar{\varepsilon}^*$ [*Boatwright and Choy*, 1986; *Newman and Okal*, 1998]:

$$\bar{\varepsilon}^* = \frac{\rho\ \alpha}{\pi} \int_0^\infty |u\omega|^2 \exp\left(t^*(\omega)\ \ \omega\right) d\omega \tag{2.1}$$

Where ρ=3000 kg/m^3 and α=7 km/s are the approximate near-source density and compressional wave velocity respectively. The square of the velocity seismogram u and frequency-dependent attenuation correction t^* are integrated over the angular frequency ω. Represented in seconds, t^* is the reciprocal of the characteristic ω representing the frequency by which an exponential decay of energy is *1/e* of its original value [*Der et al.*, 1982]. The values of t^* used in this study were introduced by *Choy and Boatwright* [1995], and quantified in *Newman and Okal* [1998].

We convert $\bar{\varepsilon}^*$ measured at each station back to radiated source energy E by correcting for geometric spreading, the depth and mechanism-dependent coefficients for radiated energy in the *P*-wave group, and the partitioning between *P* and *S* waves, similar to *Boatwright and Choy* [1995]. Our determination of the radiated earthquake energy at the source is then

$$E = (1+q)4\pi(R)^2 \frac{\left\langle (F_P)^2 \right\rangle}{(F_{gP})^2} \varepsilon^* \tag{2.2}$$

Where q=15.6 is the relative partitioning between *S* and *P* waves [*Boatwright and Fletcher*, 1984], R is the distance-dependent geometric spreading coefficient, $\left\langle (F_P)^2 \right\rangle$ =4/15 is the average squared radiation pattern of the direct *P*-wave [*Aki and Richards*, 1980], and F_{gP} is the mechanism-dependent radiation coefficient of the *P*-wave group including *pP* and *sP* given by *Boatwright and Choy* [1986] (**Figure 2.2**). Though F_{gP} is near 1 for dip-slip mechanisms, we require $F_{\mathrm{gP}} \geq 0.2$ to avoid a near-singularity that exists at distal stations ($\Delta > 60^{\mathrm{o}}$) for strike-slip mechanisms where the take-off orientation is near-nodal for the direct-*P* and depth phase arrivals.

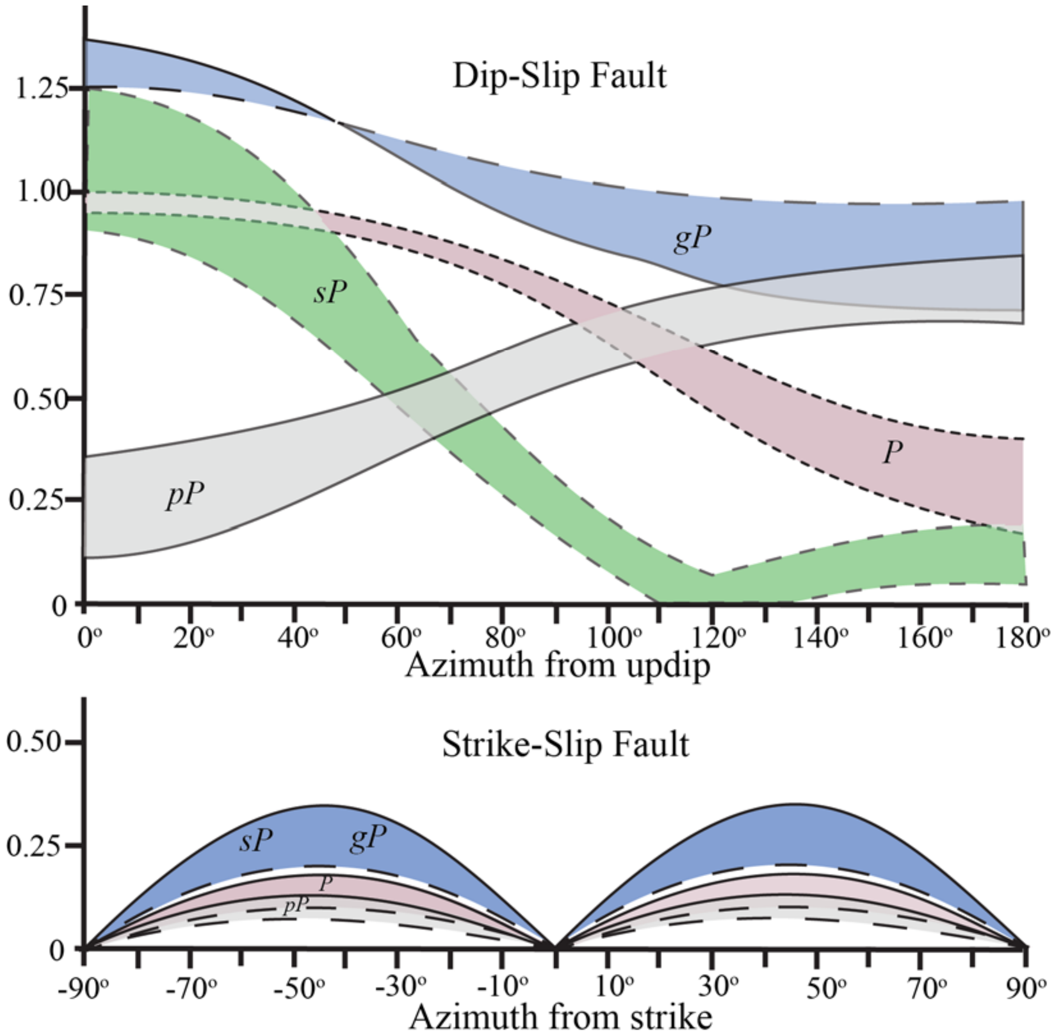

Figure 2.2: (a) Radiation patterns appropriate for a dip-slip fault: either a thrust fault dipping at 30° or a normal fault dipping at 60°. The colored regions show the range of the radiation pattern coefficients for each phase, for takeoff angles between 18° and 25° (the teleseismic window). (b) The radiation patterns for a vertical strike-slip fault. Re-created from Figure 1 in Boatwright and Choy [1986].

While the energy should ideally be calculated across an infinite frequency range (according to equation 2.1), digital recordings, anelastic attenuation, and the finiteness of the processing window limit the feasible range of calculation. To maintain consistency with the catalog of Newman and Okal [1998], we limit the frequency range between 14 mHz and 2 Hz (period range between 0.5 and 70 s). At frequencies above 2 Hz much of the signal falls below background noise levels, particularly for smaller events [e.g., *Choy and Boatwright*, 1995; *Newman and Okal*, 1998; *Vassiliou and Kanamori*, 1982]. The lower frequency limit of 14 mHz is chosen because it corresponds to the time-window of evaluation (70 s) in *Newman and Okal* [1998], and maintained for catalog comparisons

For many of the larger (M_W>7.8), and deep (depth >70 km) earthquakes, directivity is observable with increased strong shaking and shorter duration in the direction of rupture. Fortunately, directivity does not seem to significantly impact the teleseismic estimates of radiated energy [*Venkataraman and Kanamori*, 2004]. By taking advantage of available waveforms from stations within numerous permanent networks we improve estimates of *E* and minimize azimuthal dependency that may arise from directivity, inaccuracies in focal mechanisms, regional variations in attenuation, and individual station response issues.

In practice, teleseismic (epicentral distance between 30^{O} and 80^{O}) vertical recordings are used from broadband seismic stations. For a few events, stations as close as 25^{O} were used without visibly increased errors (**Figure 2.3**), however it should be noted that recordings from stations nearer than 30^{O} are potentially complicated by triplication of arrivals due to the shallow take-off angle, and contamination from reflected *PP* energy. Additionally, recordings from stations at distances greater than 80^{O} have reduced signal for smaller events and can reflect rapidly lost energy because of diffraction around the outer-core and are thus avoided.

The largely consistent E deviations observed across all distances used in this study suggest that contamination from later arrivals (including *PP*, *PcP*, etc.) is not substantial (**Figure 2.3**).

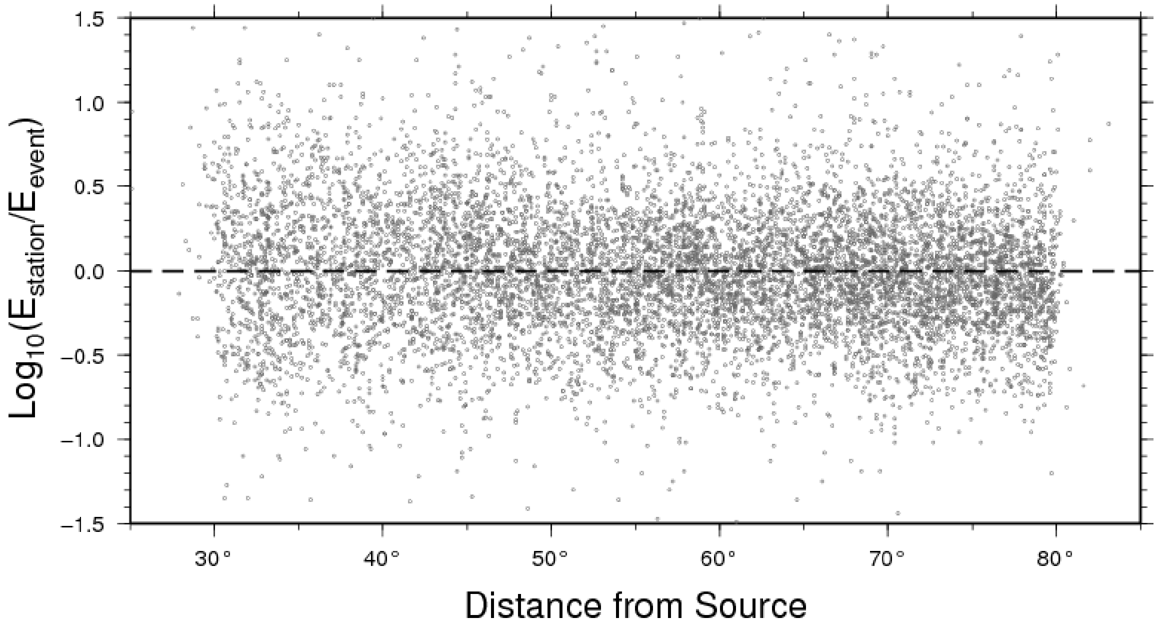

Figure 2.3: To evaluate the potential for distance-dependence in solutions, we show the per-station E deviation as a function of distance for all events M_w>6.7 in the time spam 1997 – 2010, shallower than 30 km (deeper earthquakes are excluded because of the relatively shallow take-off in the near-field. No significant trend is observed, suggesting that determinations are largely robust and not particularly sensitive to energy contamination from other arrivals including *PP* (<30°), and *PcP* (>50°), when calculating energy to 70 s.

The stations used to produce these measurements are those available from 51 networks: AD, AK, AT, AU, AV, AZ, BK, CC, CI, CN, CU, CZ, G, GB, GE, GR, GT, HL, HW, IC, II, IU, IW, JP, KN, KZ, LB, LD, LI, LX, MN, MS, MY, NE, NL, NM, NN, NO, PE, PM, PN, PR, PS, SS, TA, TS, TW, UO, US, UW, and XG. These networks were readily available from the Incorporated Research Institutions for Seismology (IRIS) Data Management Center (DMC).

2.3 Duration Determination

Because some large earthquakes have rupture durations that far exceed the 70 s window of evaluation in the *Newman and Okal* [1998] study, most notably the approximately 540 s rupture of the 2004 Sumatran earthquake [*Ammon et al.*, 2005; *Ni et al.*, 2005; *Weinstein and Okal*, 2005], it was necessary to adapt the method to all events for variable source durations. This is achieved by making averaged incremental measurements of energy starting with the initial *P*-arrival while also increasing the time window of the waveforms analyzed by 1 s increments (**Figure 2.4**). The incremental measurements are continued for at least 100 s beyond the expected event duration (normally ran to 300 s), and the per-second cumulative energy growth of each station is averaged to examine the composite energy growth of an event (**Figure 2.5**). The rupture duration is approximated by identifying the point of maximal fall-off in the growth of high-frequency rupture energy (between 0.5 and 2 Hz). The 0.5 to 2 Hz band is chosen because it avoids much of the energy from later arrivals that are largely attenuated at higher frequencies [*Ni et al.*, 2005].

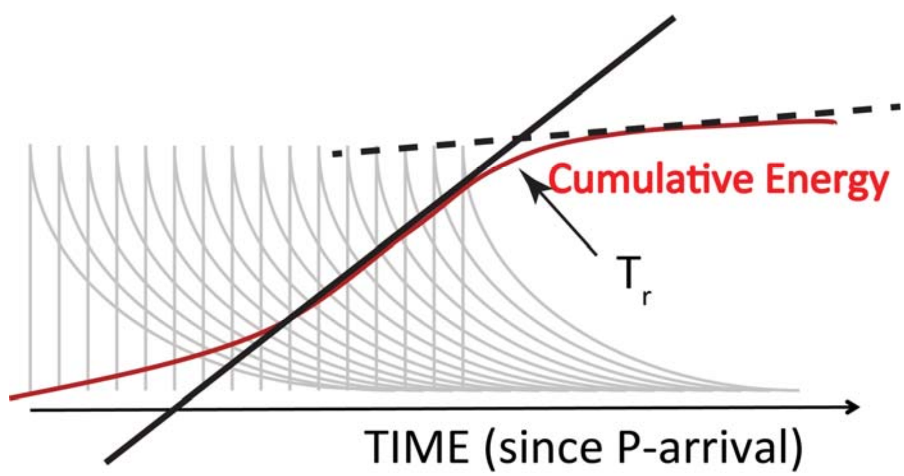

Figure 2.4: Schematic diagram of the cumulative high frequency energy calculated in increasing time windows for a synthetic series of pulsed energy (simulating a box-car source-time function with scattering). The cumulative energy is characterized as the result of overlapping energy pulses radiated throughout the earthquake rupture process, the energy pulses mimic scattering using a simple exponential decay.

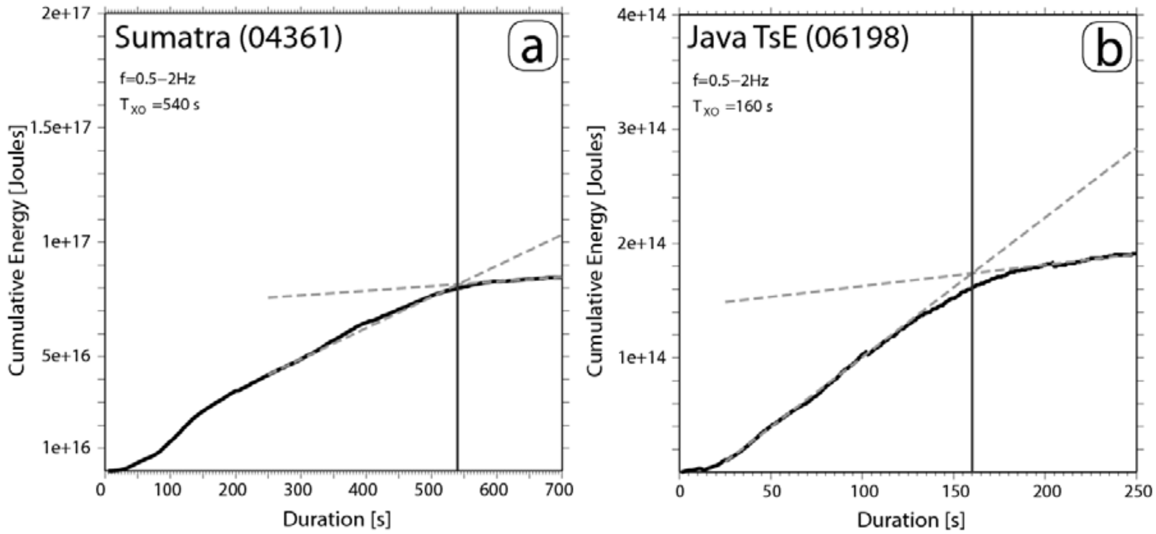

Figure 2.5: Cumulative high frequency energy growth as a function of time for (a) the MW 9.1 Sumatra 2004 earthquake, and (b) the MW 7.8 Java 2006 tsunami earthquake (TsE). The per-second averaged energy growth across all stations shows an initial ramp-up in the first 100s and 20s for the Sumatra and Java events, respectively, before increasing at a near-constant and independent energy rate before falling off to a much reduced background growth. The cross-over time T_{XO}, approximating the rupture duration, is the cross-over between linear growth and die-off slopes. Note that utilizing only the initial 70 s energy would underestimate the energy determination of the Sumatran earthquake by more than a factor of 6, and the Java TsE by more than a factor of 2.

The cross-over duration T_{XO} is estimated as the cross-over from the near-constant increasing energy-rate to the relative flat and slow continued growth due to scattered energy including later arrivals. Examples of the duration determination for the M_W 9.1 Sumatra 2004 earthquake and the M_W 7.8 Java TsE are shown in **Figure 2.5**. T_{XO} is shown here as the intersection of two linear fits to the rapid increase and the near-horizontal die-off of energy growth. While the method is particularly helpful for long-duration events, it modestly overestimates the duration of smaller events, and deeper earthquakes. In the case of deep events (depth ≥ 70 km), care must be taken to not miss the later arrivals of *pP* and *sP* energy, which would appear as a second corner in the energy growth, becoming more separated the deeper the event occurs. Estimated T_{XO} values are reported for all events in Appendix Table A-1, and are shown relative to the global Centroid Moment Tensor (gCMT) estimated durations (2x the reported half-duration) in **Figure 2.6** [*Ekstrom et al.*, 2005]

The resultant determination of T_{XO} from the high-frequency cumulative energy growth is then used as the cut-off time for our estimation of total radiated energy for all earthquakes. While for small earthquakes, this value has little effect on the final energy estimation (note the near flat continued growth after T_{XO} in **Figure 2.5**, it can greatly affect the results for very large earthquakes. In the case of the Sumatra 2004 event, the high-frequency energy was less than one-sixth the ultimate size when measured at the 70 s cut-off used by Newman and Okal [1998], rather than at T_{XO}=540 s (**Figure 2.5**a).

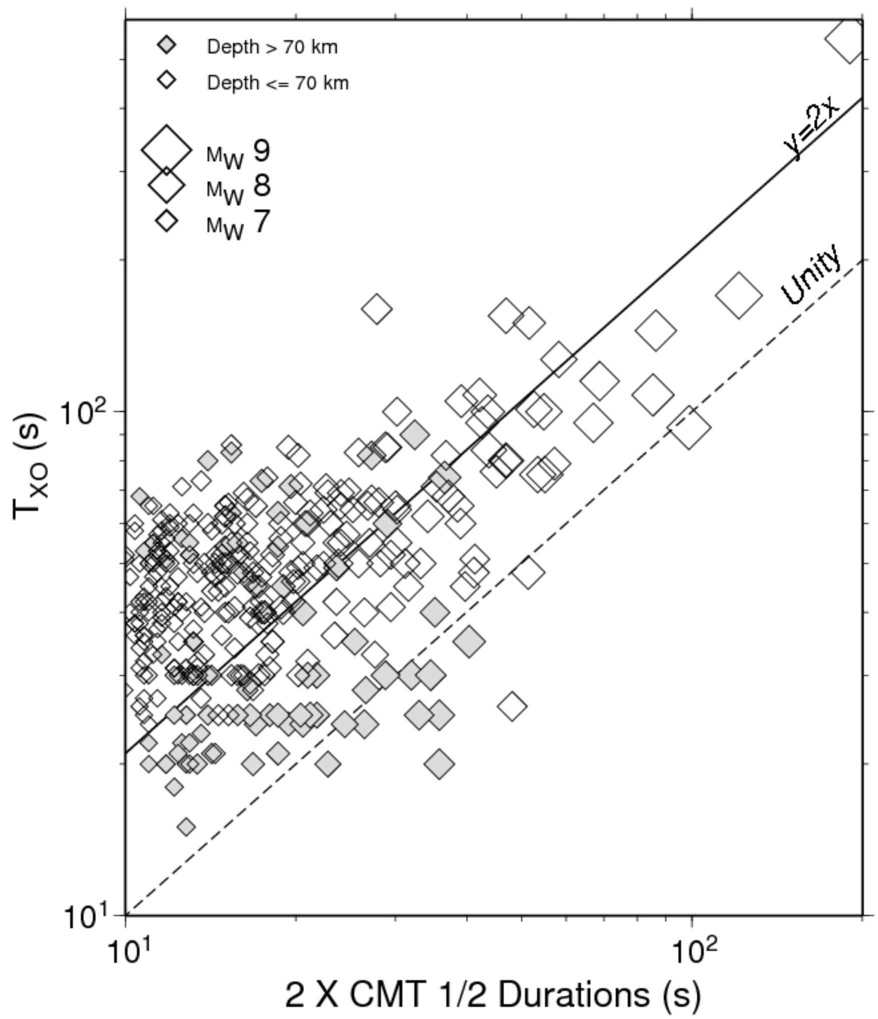

Figure 2.6: Duration estimates found for shallow (open symbols) and deep (filled symbols) earthquakes in the global catalog (1997 - 2010) are shown relative to twice the 1/2-duration estimates from the gCMT catalog. The latter are a fixed parameter in their inversion obtained using an empirical formula, and used to define the period for which moment tensors are determined, hence they are not necessarily representative of the full duration [*Ekstrom et al.*, 2005]. On average, durations determined here are twice of those within the gCMT, but have considerable scatter.

In the case of events with rupture durations longer than 70 s, the corner frequency will be below the minimum frequency of observation in this study (14 mHz). However, we find that the additional energy in these lower frequencies is mostly negligible. In the example of the 2006 Java TsE, which ruptured for approximately 160 s (**Figure 2.5**), the additional energy found in frequencies down to the earthquake's corner frequency (1/160 s = 6.25 mHz) was approximately 1% over that which was measured down to the minimum reported in this study. While in the most extreme case of the Giant 2004 Sumatran earthquake, which ruptured for approximately 540 s (**Figure 2.5**), energy calculations to the earthquakes approximate corner frequency (1/540 s = 1.85 mHz) yields 10% more energy. In each case, the additional energy is much less than the error in energy determination in most results.

CHAPTER 3
GLOBAL EVALUATION OF LARGE EARTHQUAKE ENERGY FROM 1997 TO MID-2010

3.1 Introduction

To better characterize the global distribution of earthquake energy release, we develop a catalog of recent earthquake energies and their energy-to-moment ratio using available broadband seismic recordings at teleseismic distances for events of $M_0 \geq 10^{19}$ Nm ($M_W \geq 6.7$), and include earthquakes up to 20 times larger in moment release than in previous systematic studies. Thus, by comparing E/M_0 ratio results of this study with those by *Ide and Beroza* [2001], we can evaluate whether earthquakes remain largely scale invariant for the largest observed natural events, and the smallest generated events in laboratory environments.

A detailed earthquake energy catalog provides a reliable base to explore ruptures in other large events, with the possibility of real-time applications in tsunami warning and disaster mitigation. For real-time calculations, existing records of global and regional activity are useful for determining zones with anomalous behavior. The methodology applied here is useful for real-time detection of earthquakes through: 1) a global improvement in the determination of average source and path characteristics; 2) identification and correction of station-specific deviations due to either local seismologic structure or potentially incorrect instrument responses; 3) identification of regional and tectonic controlled variations in source parameters; and 4) use of the real-time determined rupture duration.

Because of vast improvements in global station coverage, final energy determinations are made with 52 stations on average. This represents a significant improvement over *Newman and Okal* [1998] and *Weinstein and Okal* [2005], which use 10 and 27, respectively, and a modest improvement over the ongoing U.S. Geological Survey determinations [*Choy and Boatwright*, 1995], which used ~45 stations on average in energy determinations over the same time period.

3.2 Station Performance and Corrections

As global seismology becomes more data-rich, it is easy to be overwhelmed by the ever-increasing number of stations that become available. Unfortunately, in some cases the instrument response information may not be properly documented or updated, causing biased determinations of energy. To reduce the effect of this bias and to improve our ability to utilize fewer stations for some real-time applications, we investigate recordings from each station independently, to identify stations that consistently under- or overestimate the mean *E* of recorded events.

Of the 1342 stations used for energy determinations in this study, we examine the 514 stations that were used for 10 or more events. We define a simple per-station geometric deviation $\sigma^{\pm}$ that retains the sign of the offset as:

$$\sigma_g^{\pm} = \log_{10}\left(\frac{E_s}{\overline{E}^*}\right) \tag{3.1}$$

Where E_S and $\overline{E}^*$ are the single-station energy, and the initial mean event energy utilizing all stations. For those 514 stations, we evaluated the azimuthal and temporal behavior.

Examples of four stations are shown in **Figure 3.1**; two of each accurate and biased stations. Azimuthal and temporal deviations in energy calculations for stations with 50 or more recorded events are included in the Appendix Figures A-3 to A-6.

Of the stations observed, 31 exhibited clear and consistent over- or underestimations of radiated energy (Appendix A). Interestingly, none of the stations showed an obvious azimuthal dependence, suggesting that regional variability in crustal attenuation structure was not a major factor in the observed station errors. Additionally, no station was found to have a substantial change in results over time, suggesting no incorrectly or undocumented changes in station instrumentation or log files were observed in our study. Likewise, we found no consistent regional biases across the global network (e.g., **Figure 3.2**a), and hence regional variations in attenuation do not appear to significantly hamper global calculations. A case example are two stations in south eastern Australia, STKA(AU) and CAN(G), where each have consistent near-order-of-magnitude differences in their average energy determinations from the globally determined results, however, because these are opposite in direction, we conclude that over the period of our observation, deviations such as these appear to be largely due to persistent issues with instrument response files.

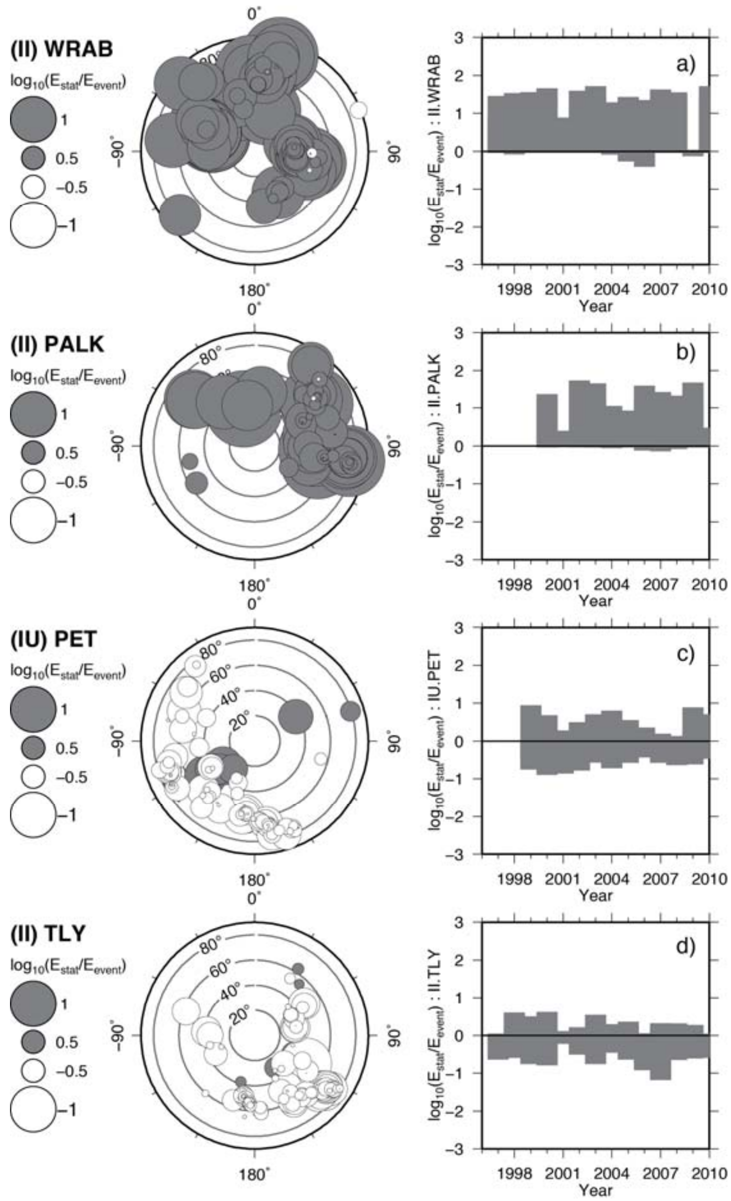

Figure 3.1: Four representative stations (rows), of the 1342 used for energy determinations, are shown with their azimuthal and distance distribution of per-event energy deviations (left column), as well as their temporal deviation (right column). Two stations with unbiased and relatively low error are shown (PET and TLY) for comparison with two stations that consistently reported biased results (WRAB and PALK). The space-time evaluations show that none of the stations were consistently reporting preferential errors at any locales, nor at time periods that could be attributed to source and path effects, or instrument and configuration changes.

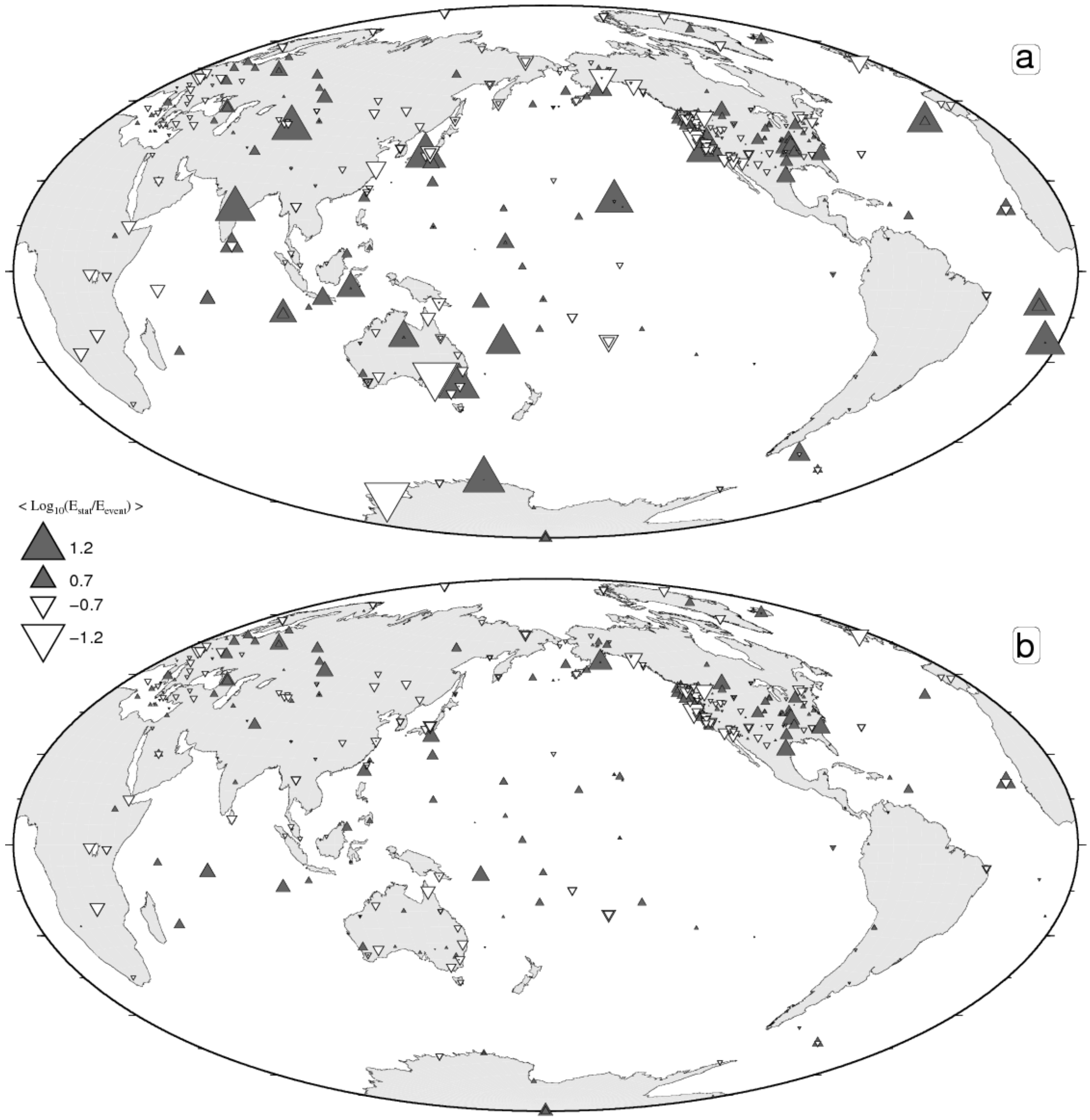

Figure 3.2: Seismic stations with at least 10 recorded events in the global catalog. The triangle size represents the mean logarithmic deviation the station reports from the determined event mean. The logarithmic deviations are displayed (a) before, and (b) after station corrections are applied to the 31 stations that revealed a clear and consistent deviation.

For each of the 31 identified stations with permanent deviations, we implemented a station correction based on the value of their mean deviation

$$\overline{\sigma}_g^{\pm} = \left(\frac{\sum \sigma_g^{\pm}}{N} \right) \qquad (3.2)$$

,

where $10^{-\overline{\sigma}_g^{\pm}}$ is the multiplicative factor by which a station's energy would be corrected for a new single-station energy estimation. The resultant new per-station deviations from the new mean energies are shown in **Figure 3.2**b. The final per-station energy estimates reported in this study are then used to calculate a new mean event energy $\overline{E}$ using the geometric average of all stations (hereafter simply *E*). We compare our individual event *E* to those analyzed by the U.S. Geological Survey's National Earthquake Information Center (NEIC, *http://earthquake.usgs.gov/earthquakes/).* Though both results follow *Boatwright and Choy* [1986], the NEIC method uses a modestly different adaptation for windowing and frequency, and generally relies on fewer, and potentially different stations. While results largely agree, there is nearly one-order of magnitude of scatter, and a modest tendency for relatively larger reported *E* for smaller and dip-slip events in this study (**Figure 3.3**).

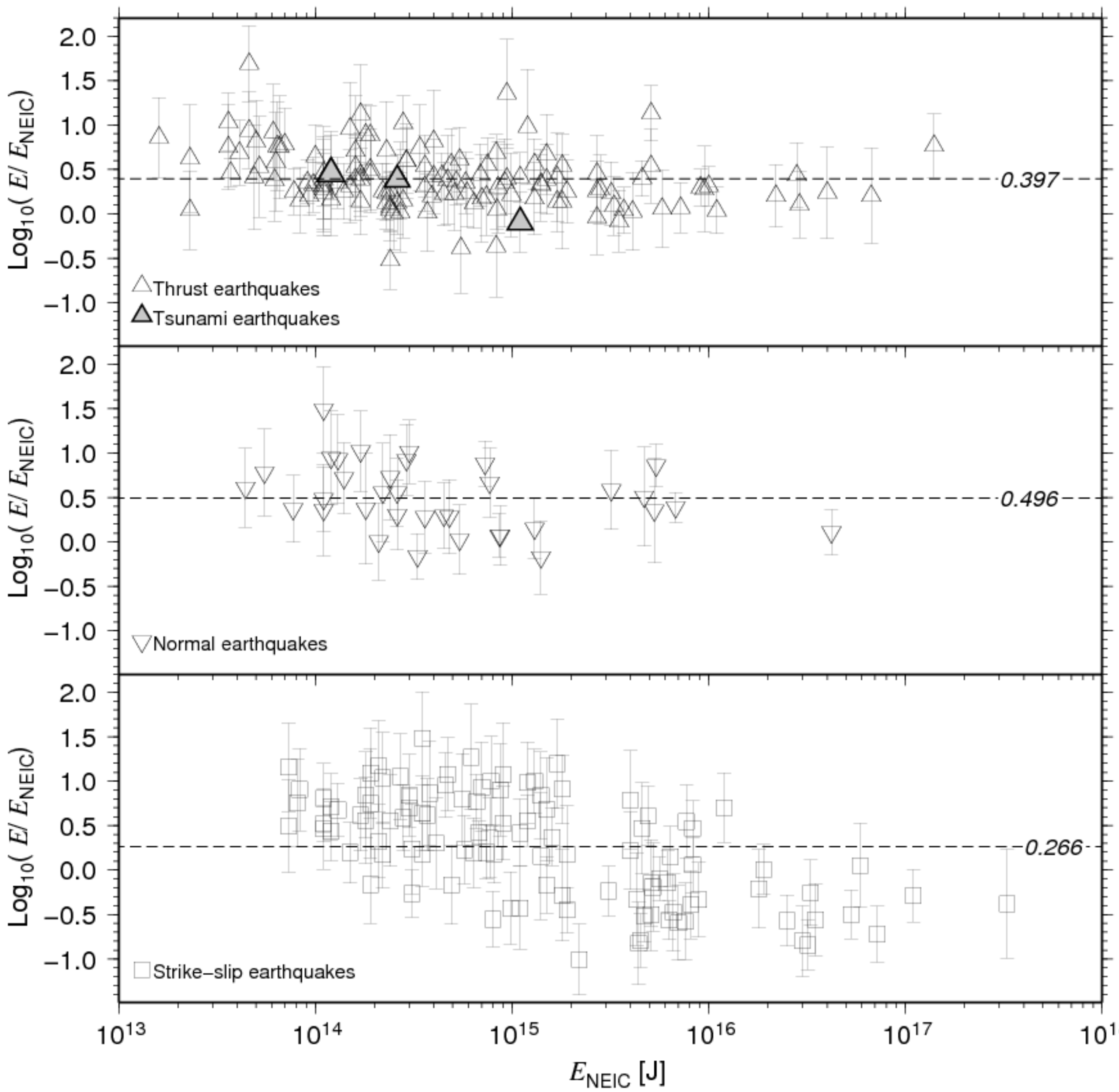

Figure 3.3: Comparison of energy determinations reported within the National Earthquake Information Center (NEIC) following *Boatwright and Choy* [1986] and this study, and distinguished by faulting mechanism. The error bar lengths correspond to 1σ from this study. Relative to the NEIC results, dip-slip earthquakes in this study are regularly reported to be higher in E, while strike-slip events are more variable.

3.3 Results

For each of the earthquakes in this study, we compare our determination of E with M_0 obtained from the gCMT catalog to reevaluate the energy-to-moment ratio discriminant θ of Newman and Okal [1998], defined as:

$$\theta = \log_{10}\left(E/M_0\right) \tag{3.3}$$

Because of its scale-invariance, and the fact that *E* does not saturate for large earthquakes, a simple conversion from *E* to an earthquake energy magnitude M_e is possible [*Choy and Boatwright*, 1995]:

$$M_e = \frac{2}{3}\log_{10} E \; - \; 2.9 \tag{3.4}$$

While θ is largely scale-invariant, there is substantial variability within this parameter that emerges when events have relatively stronger or weaker ruptures than their corresponding M_0 would suggest. An important case of these is slow-source TsE that are energetically deficient with more than 50% reduction in their rupture velocity [*Newman and Okal*, 1998; *Newman et al.*, 2011a; *Weinstein and Okal*, 2005].

3.3.1 Global Catalog

The global catalog (Supplementary Table A1) consists of all large earthquakes with $M_0 \geq 10^{19}$ Nm, which occurred between 1997 and mid-2010 as reported within the gCMT catalog (**Figure 3.4**). The catalog is composed of 342events recorded by 17849 seismograms from 1342 stations. As shown in **Figure 3.5**, energy determinations scale well with seismic moment, hence no obvious changes in seismic efficiency are observed over the nearly 4 orders-of-magnitude of this study. For all events in this study we find the average $\overline{\theta}$= -4.59 ± 0.36, somewhat higher than previous studies by Newman and Okal [1998], and *Weinstein and Okal* [2005] which found -4.98 and -5.12, respectively.

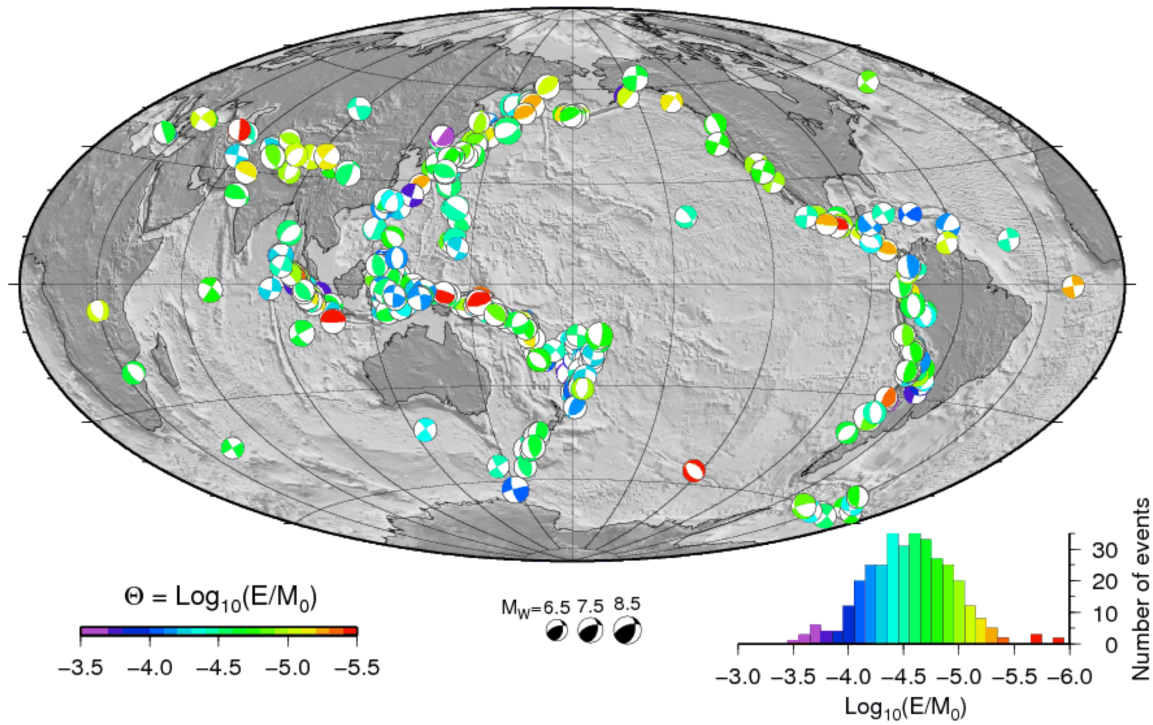

Figure 3.4: Distribution of focal mechanisms in the global catalog of earthquakes in this study (all recorded events between 1997 and mid-2010 with $M_0 \geq 10^{19}$). Focal mechanisms from the gCMT catalog [*Dziewonski and Woodhouse*, 1983; *Dziewonski et al.*, 1981; *Ekstrom et al.*, 2005] are plotted with shallower events overlapping deeper ones, and colored by their corresponding energy-to-moment ratio. Histogram shows the distribution of θ values plotted in map.

While the energy method works well for most events, there are rare instances when analysis of significantly smaller early aftershocks unrealistically overestimates energies. Two events, an M_W 6.7 event following 26 minutes after the 2006 M_W 8.3 Kuril Islands earthquake, and an M_W 6.9 event that occurred 32 minutes after the 2007 M_W 8.1 Solomon Islands earthquake both reported energies equivalent to an M_e 8.3, due to the overwhelming contribution of main-shock surface wave energy at lower frequencies. These events are documented in Appendix Table 1 and were excluded from all statistical analysis, and are noted here to illustrate the difficulty in determining robust energy calculations for smaller aftershocks immediately following very large earthquakes.

3.3.1.1 Focal Mechanism

We further evaluate how our calculated value of θ changes with mechanism by sub-setting the catalog into thrust (**Figure 3.5**b), normal (**Figure 3.5**c), and strike-slip (**Figure 3.5**d) earthquakes. We find that thrust earthquakes tend to be energetically deficient, having a mean $\overline{\theta}_T$= -4.74, while both normal and strike-slip earthquakes tend to be modestly stronger (or more energetic) than the global average with $\overline{\theta}_N$= -4.51 and $\overline{\theta}_{SS}$= -4.44, respectively. This apparent variation of θ is in agreement with observations of the focal mechanism dependence by *Perez-Campos and Beroza*, [2001] and *Choy and Boatwright* [1995]. Applying a student's T-test to each of the subsets [*Press et al.*, 1992], we find that while both thrust and strike-slip earthquakes are distinctly different from each other, and the group average at 99.9% confidence, the remaining normal faulting earthquakes can only be considered different from the group average at 80% confidence. Thus, we consider the groups to be distinct, with normal faulting earthquakes being intermediate between thrust and strike-slip events, in energy.

We observe no significant moment-dependence for any of the focal-mechanism subsets: a result that is somewhat surprising given the more than order-of-magnitude downward deviation found when comparing our results with those reported by the NEIC (**Figure 3.3**).

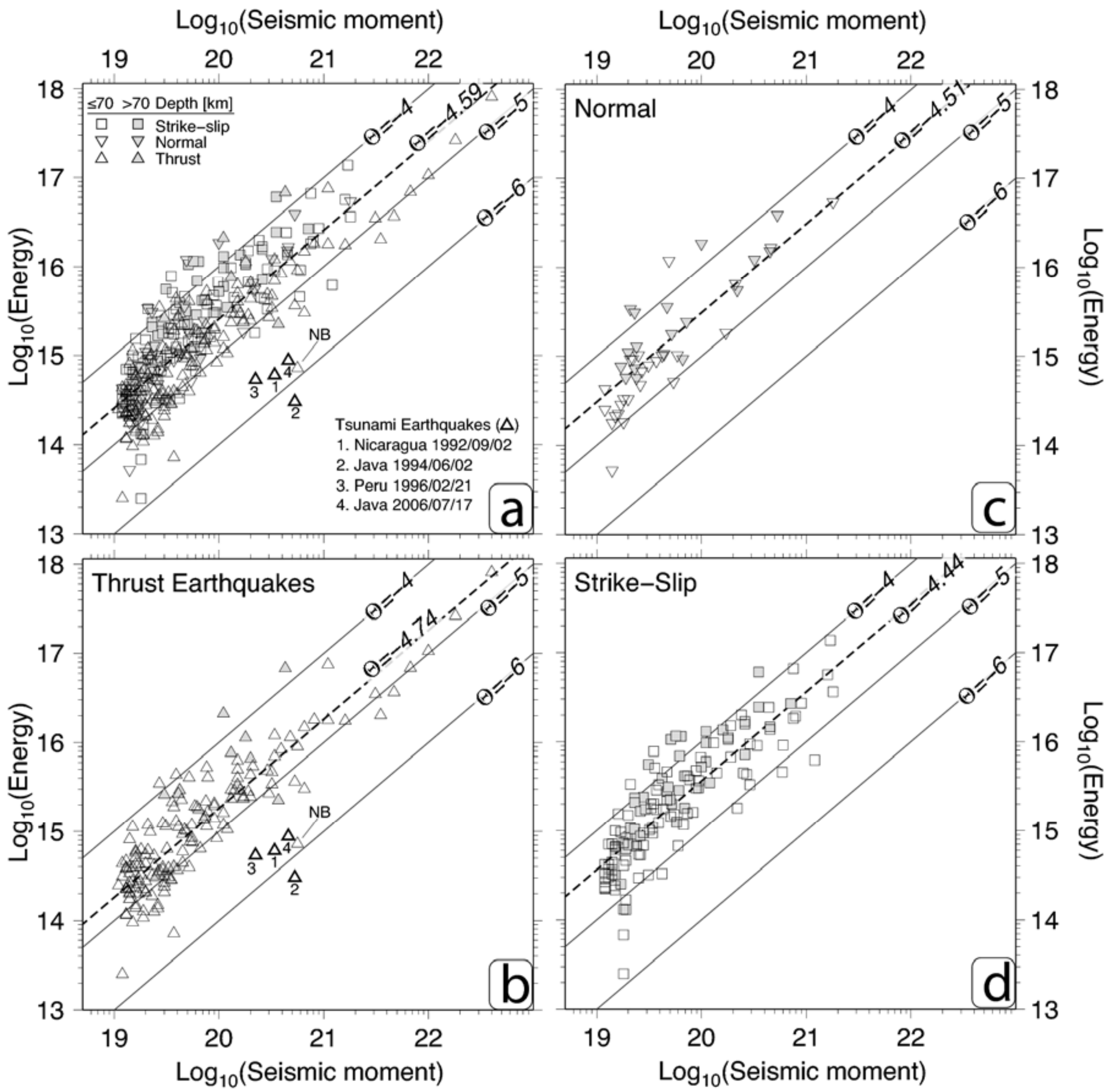

Figure 3.5: (a) E to M_0 comparison for the global catalog in this study (all events $M_0 \geq 10^{19}$ Nm between 1997 and mid-2010). Events are identified by their dominant mechanism and illustrated separately as (b) thrust (triangles), (c) normal (inverted triangles), and (d) strike-slip (squares). The dashed line represents the average value of the E/M_0 discriminant θ for each group. Events deeper than 70 km depth (shaded symbols), and TsE (bold triangles) are also differentiated. E energy deficient earthquakes tend to the lower right, while strong rupturing events tend to the upper-left. TsE before 1997 are included for comparison. Note the energy deficient New Britain earthquake (NB), which is not a known TsE.

3.3.1.2 Java 2006 Tsunami Earthquake

Within the subset of thrust events, one known TsE was newly determined, the 17 July 2006 M_W 7.8 Java earthquake. The event was found to have θ = -5.7, identifying it as a TsE following the discriminant threshold established in *Newman and Okal* [1998] ($\theta_{TsE} \leq$ -5.7), and updated utilizing the full rupture duration it changes to $\theta_{TsE} \leq$ -5.6. This event is shown with the 3 TsE events that occurred in the 1990s for comparison in **Figure 3.5**a,b.

3.3.1.3 Slow Source New Britain Earthquake

Interestingly, one event, the 17 November 2000 M_W 7.8 New Britain earthquake, is not known to have caused any tsunami [e.g., *Geist and Parsons*, 2005; *Sahal et al.*, 2010], yet shares several features identified in TsE, including comparable magnitude, long rupture duration (T_{XO} = 95 s), shallow depth (z = 17 km as reported in the gCMT catalog), and low θ = -5.9. While this earthquake cannot be considered a TsE by its definition of disproportionately large tsunami given by *Kanamori* [1972], it shares the essential characteristics of other slow-source TsE events [*Newman and Okal*, 1998; *Polet and Kanamori*, 2000], and hence we classify the earthquake as simply "slow-source". Interestingly, this event was the second major aftershock that followed another M_W 7.8 aftershock (occurring 14 hours earlier) and the November 16 M_W 8.0 main shock, both modestly deficient in energy, with θ = -5.3. A regional tsunami did occur from these events across the region (being recorded as far away as Honiara, Solomon Islands, and Port Vila, Vanuatu), but current evidence supports waves coming from either the main event, or its first aftershock, which preceded the slow-source New Britain event by more than 24 hours [*Geist and Parsons*, 2005].

3.3.2 Regional Catalogs

We construct two regional catalogs utilizing the same procedure and time range as the global catalog, but including smaller events ($M_0 \geq 2 \times 10^{17}$ Nm, $M_W \geq 5.5$). The regions selected include the subduction zones along the Middle America and Java trenches, both of which recorded recent TsEs; the 2 September 1992 M_W 7.7 earthquake offshore Nicaragua [*Ide et al.*, 1993; *Imamura et al.*, 1993], and the 2 June 1994 M_W 7.8 and the 17 July 2006 M_W 7.7 earthquakes offshore Java [*Abercrombie et al.*, 2001; *Ammon et al.*, 2006]. To determine if the subduction megathrusts in these environments are particularly susceptible to slow-rupturing events, we evaluate only the thrust earthquakes that occur in each region with gCMT depths less than 70 km. For each region, the datasets are complemented by thrust events above $M_0 \geq 5 \times 10^{17}$ Nm ($M_W \geq 5.7$), recorded between 1981 and 1997 in *Okal and Newman* [2001].

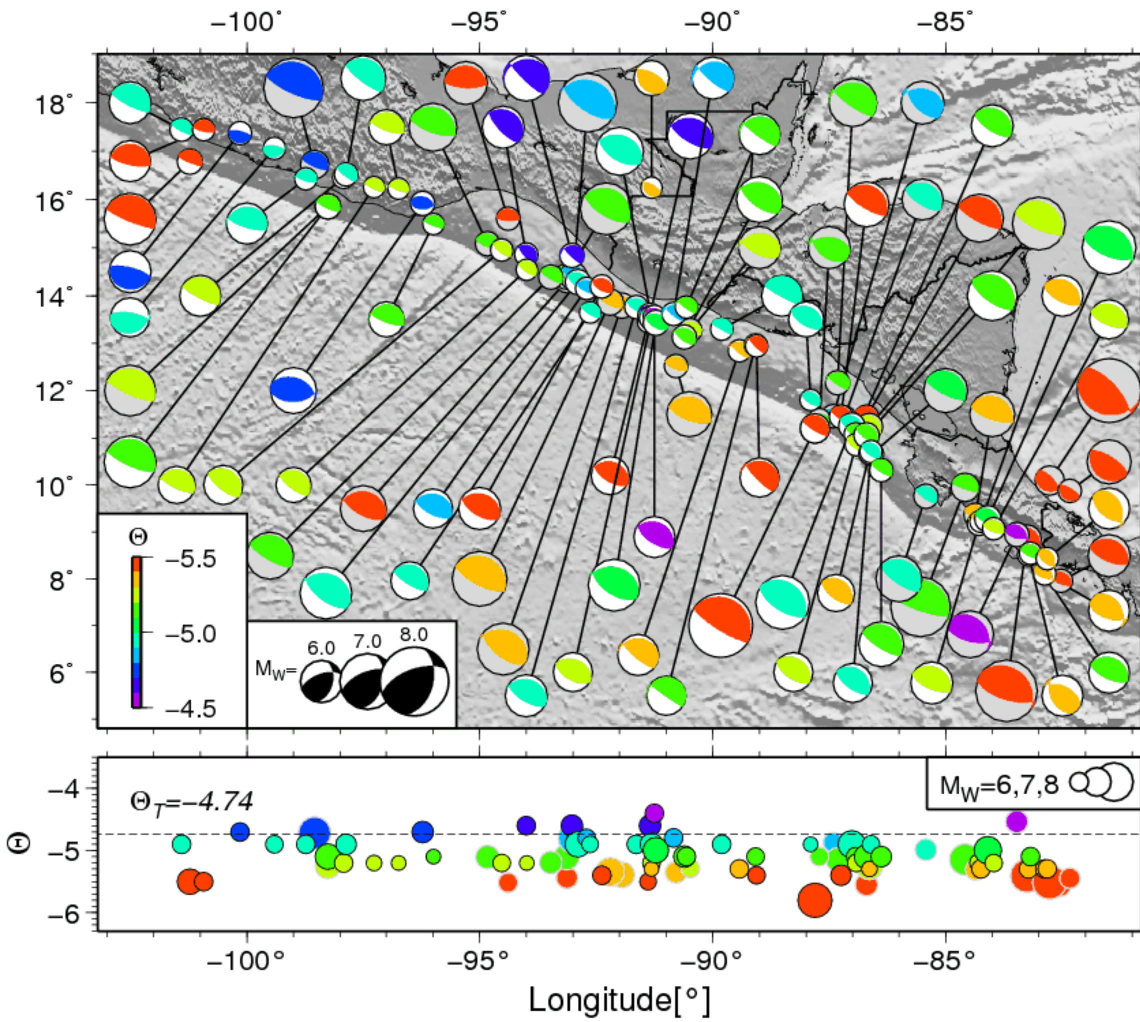

Figure 3.6: Top: Central American thrust events (gCMT epicenters and solutions), occurring primarily along the Middle America Trench (MAT) are shown for this study (49 events between 1997 to mid-2010, white P-quadrants) and from *Okal and Newman* [2001] (28 events between 1981 and 1997, gray P-quadrants). The focal mechanisms are colored corresponding to the energy-to-moment parameter θ. Bottom: The longitudinal variations in θ highlight the overall low energy ruptures in the region with almost all earthquakes being more energy deficient than the global thrust average of θ_T = -4.74 (dashed line).

3.3.2.1 Middle America Trench

Along the Middle America Trench (MAT), we determined the radiated seismic energy for 53 thrust events, and compared with those reported in *Okal and Newman*, [2001] (**Figure 3.6**); Appendix Table 3). From the two studies, the combined energy-to-moment discriminant results for thrust events along the MAT is $\bar{\theta}_{T-MAT}$=-5.15, one-third of global thrust average value (**Figure 3.7**). Using data from this study alone, we find $\bar{\theta}_{T-MAT}$= -5.1, modestly higher than observed in thrust events reported only in the study by *Newman and Okal* [1998], $\bar{\theta}_{T-MAT}$=-5.2. Changes in θ between the data sets occur, in part, due to the improved event-dependent time-window used for energy determinations in this study. On average, energy determinations should be modestly reduced because calculations in this study are run to T_{XO}. For most events, this value is less than the default window of 70 s used in the previous analysis by *Okal and Newman* [2001]. However, the 1992 TsE had T_{XO} = 165 s and yielded E=6.1×10^{14} J, almost 2.4 times larger than E=2.5×10^{14} J) reported in *Newman and Okal* [1998] using only a 70 s window. The significant increase in energy caused by using the event-dependent duration yields θ =-5.7, which is less energetically deficient than previously reported (old θ = - 6.1) [*Newman and Okal*, 1998]. The energy increase is roughly equivalent to the extended duration of determination, because radiated energy growth is observed to be near-constant for slow and other long-duration earthquakes [*Newman et al.*, 2011a; *Weinstein and Okal*, 2005].

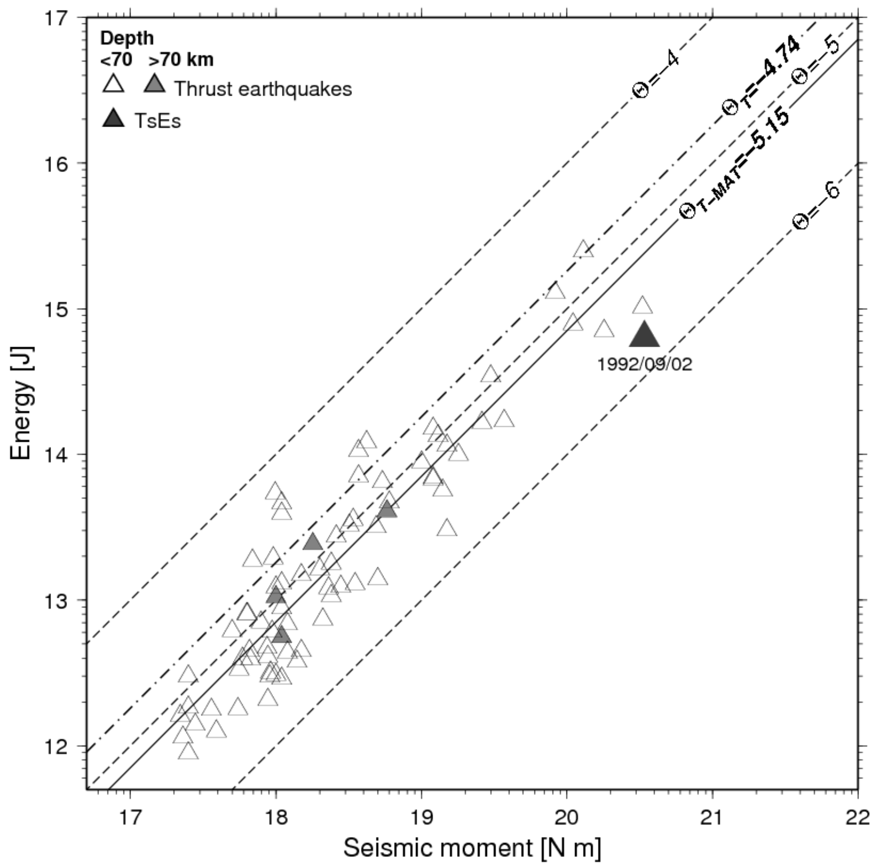

Figure 3.7: E to M_0 comparison for the Central American thrust events of this and the *Okal and Newman* [2001] studies (similar to **Figure 3.5**). The average regional $\overline{\theta}_{T-MAT}$ = -5.15 is visibly below the global $\overline{\theta}_T$ = -4.74, and does not have a clearly observable moment dependence.

Almost all thrust events along the MAT are deficient in radiated E compared to the global thrust average of θ= -4.74 (**Figure 3.6** and **Figure 3.7**). With the exception of one event from the *Okal and Newman* [2001] catalog, all earthquakes examined in the Nicaragua and Costa Rica region (East of 90° W, **Figure 3.6**), are below the average. Events occurring further to the northwest are mostly reduced in θ, but include more energetic events. Clearly, Central American thrust earthquakes are energetically deficient relative to the global dataset.

To evaluate whether the observed increase in source rupture speed with depth identified by *Bilek and Lay* [1999] yields a comparable increase in θ, we compare E to both hypocentral and gCMT depth determinations. While the former gives more precise information of the event initiation, the latter is a better descriptor of the mean depth by which most of the moment release occurs. The hypocentral solutions come from the EHB catalog when available [*ISC*, 2009], otherwise defaulting to depths reported by the NEIC Bulletin.

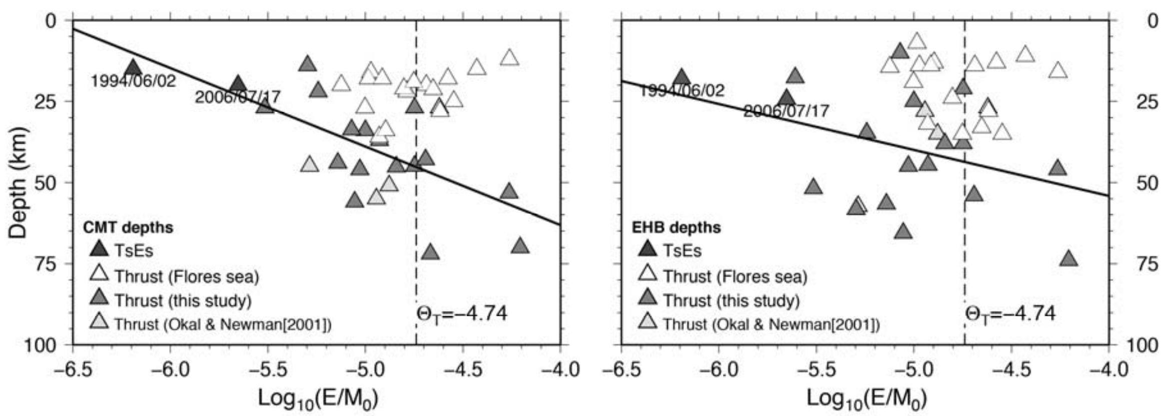

Figure 3.8: The same Central American events from **Figure 3.6** and **Figure 3.7** shown as a function of (a) gCMT and (b) hypocentral depth and θ ($\log_{10}\left(E/M_0\right)$). EHB depths were used when available [*ISC*, 2009], otherwise depths are from the NEIC. Events are observed to be depth dependent, and split into two groups. The linear trend (solid line) described events determined in this study (dark triangles) with linear fits using the gCMT depths (intercept 59 ± 44 km, and slope 3.37 ± 8.5 km/θ), and the EHB depths (intercept of 53.6 ± 36 km and slope 4.86 ± 7 km/θ).

For events along the MAT, we find an increase in θ with increasing gCMT depth but with large scatter (**Figure 3.8**a). The trend becomes less clear when examining merely hypocentral depths (**Figure 3.8**b). For events that dominantly slip in the shallow megathrust environment (gCMT depth ≤ 20 km), θ is consistently low and below the global thrust average. In contrast, as depth increases, earthquakes tend to have relatively larger values of θ, with events at gCMT depths greater than 40 km having θ close to the global average. Whereas the best linear trend of the variability of θ with depth z(θ) yields a slope of 3.4 ± 8.6 km/θ and intercept of a=59±44 km, and illustrated in **Figure 3.8**, the possible depth dependence of θ shows too much scatter to make a significant linear fit.

3.3.2.2 Java Trench

We similarly analyze the Java trench, the only source known to have two TsE since the development of the global seismic network. We performed energy determinations for 34 thrust events, and compared them to the 7 available from the *Okal and Newman* [2001] study (**Figure 3.9**; Appendix Table A.4). Unlike the results from the Central American study region, the thrust events here have average energy ratios $\overline{\theta}_{T-JV}$= -4.91, statistically equivalent to the global thrust average $\overline{\theta}_T$ = -4.74 (**Figure 3.10**). Little difference is observed between the thrust events in this study and the one obtained by *Okal and Newman* [2001], with the two having similar mean values $\overline{\theta}_T$ = -4.9 and -5.0, respectively. However, the inclusion of nearly 5-fold the data allows for a more robust evaluation of the depth dependence of θ.

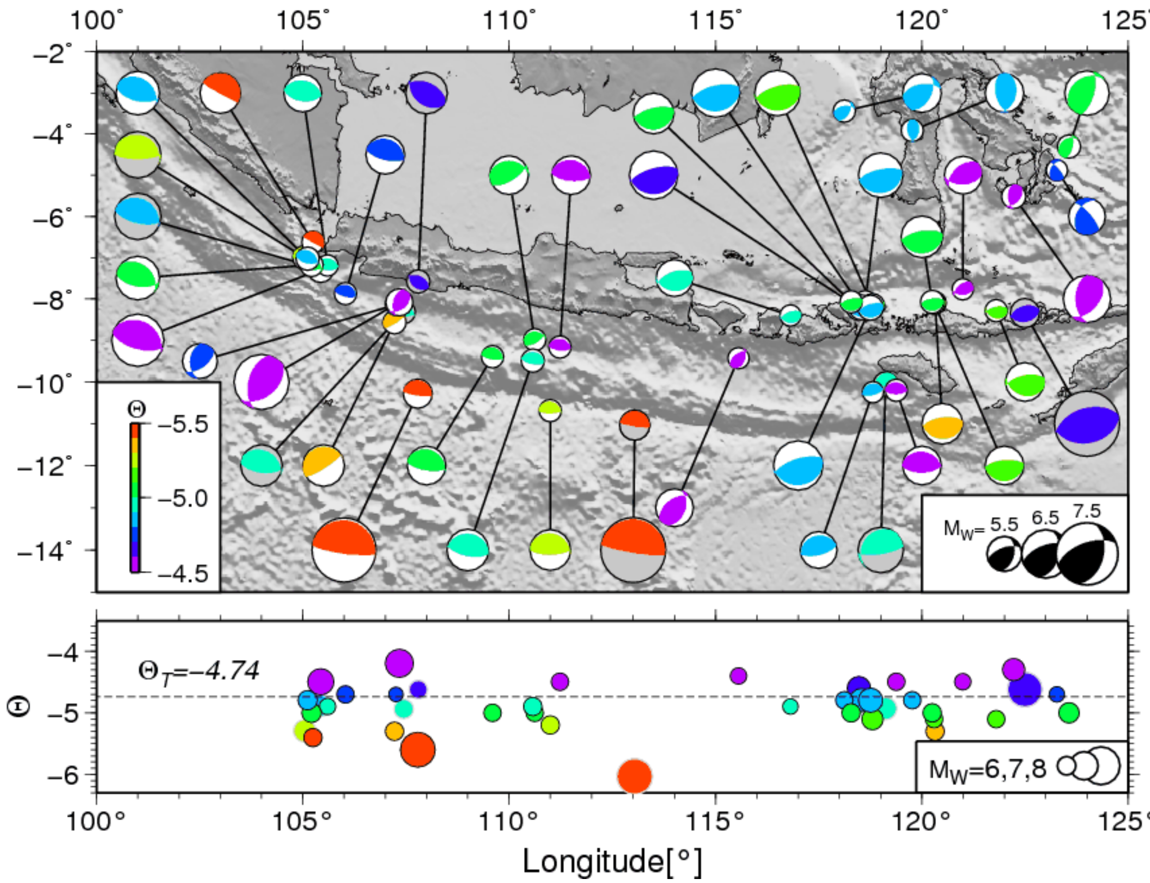

Figure 3.9: Top: Focal mechanisms for Java thrust earthquakes are shown for this study using the gCMT focal solutions and epicenters (34 events between 1997 to mid-2010, white *P*-quadrants) and from *Okal and Newman* [2001] (7 events between 1981 to 1997, gray *P*-quadrants); similar to **Figure 3.6**. Bottom: No longitudinal variation is apparent, with most seismicity having θ near the global thrust average of θ_T=-4.74 (dashed line).

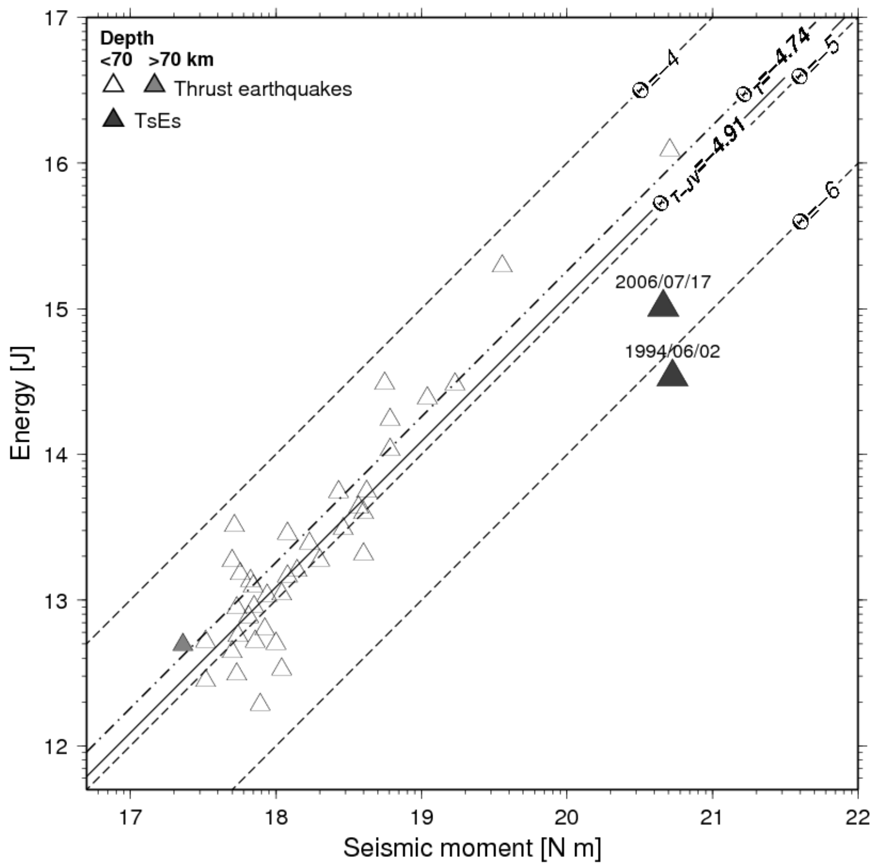

Figure 3.10: E to M_0 comparison for Java thrust events of this and the O*kal and Newman,* [2001] studies (similar to **Figure 3.5** and **Figure 3.7**). The average regional $\overline{\theta}_{T-JV}$=-4.91 is comparable to the global θ_T= -4.74, reduced mostly by the occurrence of the two known TsEs.

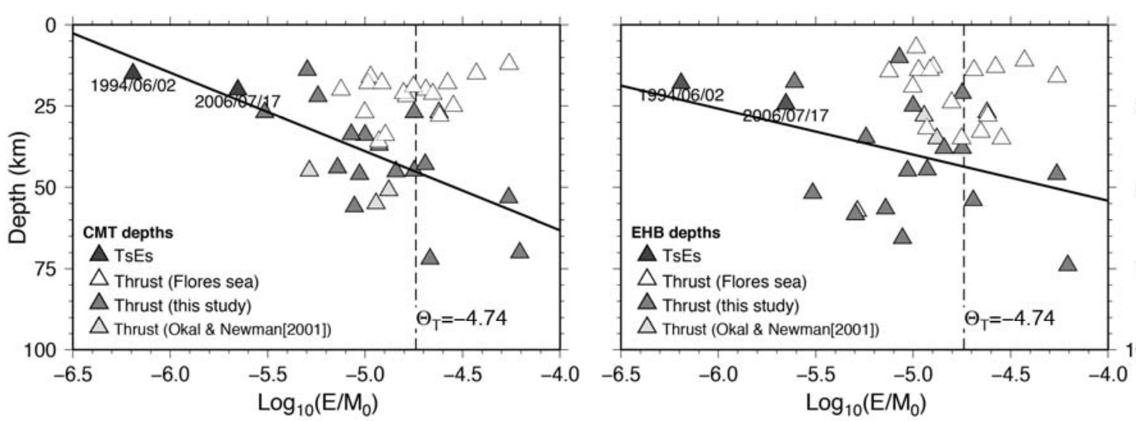

Figure 3.11: Events in the Java region from **Figure 3.9** and **Figure 3.10**, shown as a function of (a) gCMT and (b) hypocentral depth and θ ($\log_{10}\left(E/M_0\right)$). EHB depths were used when available [*ISC*, 2009], otherwise depths are from the NEIC. When excluding events within the Flores Sea (latitude ≥ -9°, longitude ≥115°; open triangles), a depth-dependent trend z(θ) is apparent from the gCMT depths with intercept 171 ± 31 km, and

a slope of 25.8 ± 6 km/θ following a linear fit. Note some events are deeper than the depth cut-off (70 km) based on gCMT reports.

Though the average of thrust events near Java are close to the global average, unlike Central America, the events show more robust depth dependence when using the gCMT reported values (**Figure 3.11**). Shallow earthquakes are highly scattered between the energetically deficient TsE events with $\theta < -5.7$ and energetic events with $\theta > -4.5$, but there is a trend where as depth increases, the values of θ become comparable to the global average. The distribution here is bifurcated with two trends; one of an apparent constant steeper gradient, and another showing a range of shallow earthquakes with higher values of θ that occur primarily in the Flores Sea region. Removing events from this region (Latitude ≥-9º, Longitude ≥ 115º), we find an apparent linear trend for $z(\theta)$ of increased θ with gCMT depths, where the slope is 25.8 ± 6.2 km/θ and intercept 171 ± 31 km.

3.4 Discussion

In evaluating the fractional energy of the global earthquake catalog in this study we find a mean energy-to-moment ratio $\bar{\theta}$=-4.59, similar to the scale-invariant solution θ=-4.5 that was identified between 3×10^{3} to 2×10^{21} Nm [*Ide and Beroza*, 2001]. Because of the recent occurrence of giant earthquakes in Sumatra and Chile, we can extend that range to 4×10^{22} Nm, yielding now 19 orders-of-magnitude of scale invariance.

This study finds moderately higher results than that of *Newman and Okal* [1998], with $\bar{\theta}$=-5.0. The difference between the two studies occurs from the inclusion of: 1) the full rupture duration; 2) deep earthquakes (depth ≥ 70 km); and 3) events from different time periods. The first two differences have the effect of increasing the determinations of energy. Utilizing the full rupture duration captures the additional energy in very large earthquakes (50 events with T_{XO}> 70 s in this study) that would not be measured at the 70 s cut-off of *Newman and Okal* [1998]. Most notably, the Sumatra 2004 earthquake has less than 15% of the total radiated energy in the first 70 s of its 540 s T_{XO}-determined rupture. Additionally, because TsE events all have T_{XO}> 70 s, their full energy would otherwise be lost. Reevaluation of θ as a discriminant for TsE events finds that when utilizing the full duration of rupture, a modestly lower value of $\theta_{TsE} \leq$ -5.6 is necessary, rather than $\theta_{TsE} \leq$ -5.7 found in *Newman and Okal* [1998]. The addition of 70 deep earthquakes (depth >70 km) in this study increases the global average values because these events rupture with higher relative radiated energies ($\bar{\theta}_{deep}$= -4.32). The last major difference between the two analysis is the inclusion of more events (342 events here vs. 52 events in *Newman and Okal* [1998]), most of these with significantly more available data. On average, more than 50 stations are used per determination in this study, as compared to only 10 in the earlier analysis by *Newman and Okal* [1998]. This, and the additional careful correction of 31 stations that yielded biased solutions, allows for improved *E* determinations for individual events, as well as the global average.

A direct physical interpretation of E/M_0 or θ is somewhat difficult since the ratio can be combined to approximate several parameters, when others are held constant. Most fundamentally, the ratio is a relationship between the dynamically radiated energy *E* and the amount of work done to cause the fault to slip, represented by M_0 [e.g., *Kanamori and Rivera*, 2006].

Assuming an earthquake is perfectly efficient at radiating energy (no work goes into tearing or heating the fault) the energy-to-moment ratio can be directly related to dynamic stress drop $\Delta\sigma$:

$$\Delta\sigma = 2G\left(E / M_0\right) \tag{3.5}$$

Where *G* is the near-source crustal rigidity [*Hanks and Kanamori*, 1979; *S Stein and Wysession*, 2003].

Alternatively, the radiated seismic efficiency η is useful for evaluating the 'snappiness' of earthquake rupture, given that the static stress drop $\Delta\sigma_S$ is assumed constant. *Husseini and Randall* [1976] first characterized the parameter as

$$\eta_R = \left(\frac{2G}{\Delta\sigma_S}\right)\left(\frac{E}{M_0}\right) \tag{3.6}$$

The radiated efficiency varies almost uniformly between 0 and 1 with the ratio of the rupture velocity V_R and the rupture limiting speed (usually the shear wave speed) [*Kanamori and Rivera*, 2006], and hence an earthquake that ruptures more/less rapidly would have increased/decreased radiation efficiency and θ parameter. Because an inherent trade-off exists between η_R and $\Delta\sigma_S$, which is not independently evaluated here, we prefer to characterize θ in terms of a third parameter, apparent stress τ_a. *Wyss and Brune* [1968] originally described τ_a as the product of the energy-to-moment ratio and the rigidity. By assuming dynamic and static stress drop are roughly equivalent, this relation can be directly related to η_R through:

$$\tau_a = G\left(\frac{E}{M_0}\right) = \frac{\eta_R}{2} \tag{3.7}$$

While describing the energy-to-moment ratio in terms of radiation efficiency is useful for events like slow-rupturing TsE that are limited by V_R, it may not be optimal as a generic characterization for global earthquake activity. Thus, we more generically describe E/M_0 in terms of τ_a, which requires only an assumption of G.

3.4.1 Mechanism Dependence

On average, strike-slip earthquakes are more energetic, having $\overline{\theta}_{SS}$=-4.44, higher than the global average (**Figure 3.5**b). While small, this difference is robust, and is suggested to stem from the rupture of strong lithosphere along the edges of oceanic transforms, or intraplate environments, both are observed to have increased $\Delta\sigma$ or τ_a [*Allmann and Shearer*, 2009; *Choy and McGarr*, 2002; *Choy et al.*, 2006; *Schorlemmer et al.*, 2005].

This is in contrast to thrust mechanisms that are generally less energetic, having $\overline{\theta}_T$= -4.74, corresponding to an approximate 30% reduction in τ_a. Though also occurring in intraplate regions, they occur dominantly along subduction megathrusts, the environments responsible for excessively energy deficient TsE events [*Newman and Okal*, 1998; *Polet and Kanamori*, 2000].

According to the dataset analyzed, we find normal faulting earthquakes to be intermediate between the other mechanisms, and not distinguishable from the global average. However, this is analog to results obtained for apparent stress, which also locate normal earthquakes between thrust and strike-slip earthquakes [*Choy and Boatwright*, 1995]. The relative higher value of θ_N=-4.51, compared to thrust earthquakes, has been related mostly to immature faults, such as those in cold and intact lithosphere, or intraslab earthquake ruptures [*Choy and Kirby*, 2004].

3.4.2 Depth Dependence

Examination of $\Delta\sigma$ or τ_a with various focal mechanisms and at different depths has been done for different magnitude ranges and settings, identifying the largest values for strike-slip earthquakes [e.g., *Allmann and Shearer*, 2009; *Choy and Boatwright*, 1995; *Choy et al.*, 2006; *Perez-Campos and Beroza*, 2001; *Venkataraman and Kanamori*, 2004]. While higher values are found in strike-slip environments and lowest for reverse faulting earthquakes, a clear characterization of the depth dependence of τ_a remains problematic. *Allmann and Shearer* [2009] find a median τ_a =2 MPa (converted from $\Delta\sigma$ = 4 MPa), with slight but non-conclusive depth dependence. As well, *Venkataraman and Kanamori* [2004] were unable to find definitive depth dependence in a global evaluation of earthquakes shallower than 100 km depth. The lack of a clear trend in these studies are in contrast to our results for regional and global thrust earthquakes (**Figure 3.8**, **Figure 3.11** and **Figure 3.12**), as well as those expected from the study of *Bilek and Lay* [1999], which attributed a depth dependent change in source durations due to a reduction of rigidity in shallow subduction environments possibly caused by increased sediment compaction. Decreasing rigidity potentially affects the rupture velocity, and consequently the overall rupture duration [*Bilek*, 2007; *Houston*, 2001; *Vidale and Houston*, 1993].

Alternatively, assuming no change in regional rigidity, the depth-dependent change in energy-to-moment ratio can be attributed to a change in τ_a due to increased lithostatic pressure. There is large scatter in our observed depth dependence of θ, with activity along the Java trench being highly dependent, compared to the moderate behavior of the Middle America Trench (**Figure 3.12**). While some shallow events that have relatively higher θ values (and τ_a), may represent intraplate crustal activity on immature faults, others can likely be attributed to complexities along the fault interface.

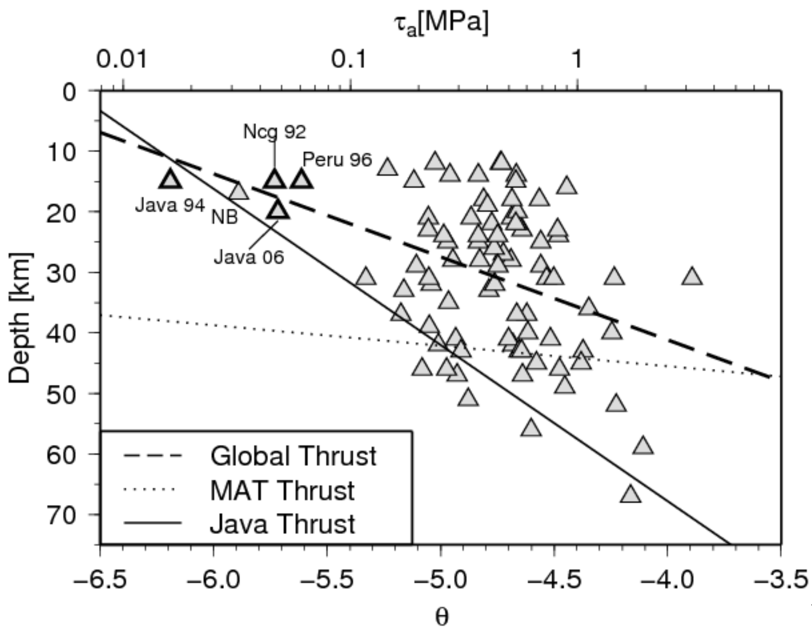

Figure 3.12: The gCMT depth dependence of global thrust earthquakes is shown relative to θ and its conversion to apparent stress τa using Equation (2.9). While steeper than the global distribution (dashed line; linear fit with intercept 95.9 ± 21 km and slope 13.7 ± 4 km/θ), the trend determined from the Java thrust earthquakes (solid line; **Figure 3.11**a) is considered more representative of subduction zone behavior, as the global thrust catalog contains results from intraplate environments. The trend for the Middle America Trench (MAT; dotted line) is also shown for completeness. The five slow-source earthquakes, comprising the 4 observed TsE events and the 2000 New Britain (NB) earthquake, all roughly follow this trend.

Conversion of θ to τ_a for subduction thrust earthquakes shows a linearly trending envelope, where τ_a increases from about 6 kPa at 0 km to 3 MPa at 70 km depth (**Figure 3.12**). Assuming $\tau_a=\Delta\sigma/2$, this result is comparable to the depth-$\Delta\sigma$ relationship of *Bilek and Lay* [1999] and *Lay et al*. [2012], which was found assuming constant rupture velocity. Events deeper than 70 km likely occur within the slab, and hence may represent immature fault behavior. Thus, our high θ values for these events are expected ($\bar{\theta}_{deep}$= -4.32).

A limitation in this generalized study is that we utilize a single frequency-dependent attenuation correction [*Choy and Boatwright*, 1995], that is not depth dependent. Such a correction, will overestimate the attenuation from the direct *P*-wave, while underestimating the contribution from *sP* and *pP*. We use this because a more complex depth-dependent attenuation would need to adequately account for the focal-mechanism-dependent contribution of the depth phases which travel a different path (through the source region crust twice, while the direct *P*-wave only travels through the crust at the receiver).

3.4.3 Regional Results

While analysis of the Java trench yielded no consistent energy deficiency (**Figure 3.9**), with most events occurring very near the global average thrusting $\bar{\theta}_T$, thrust events along the MAT were consistently deficient (**Figure 3.6**). The regional average across the MAT is $\bar{\theta}_{T-MAT}$=-5.15, about one-third the global thrust average and is consistent with other studies that have found low stress drop in the region [*Allmann and Shearer*, 2009; *Eissler et al.*, 1986; *Iglesias et al.*, 2003]. Interestingly, the negative deviation from the global thrust average appears to change linearly along-strike of the trench, becoming increasingly negative toward the southeast section. At the southeastern terminus of the regional study, near the Costa Rica-Panama border, (located towards the lower right region of map in **Figure 3.6**), θ values are most reduced, including events both along the MAT and along shallow thrusts along the back arc. At this locale the failed Cocos ridge subducts [e.g., *Protti et al.*, 1994], potentially increasing local high-frequency attenuation. Alternatively, because the rate of convergence gradually increases to the southeast from 70 to approximately 100 mm/yr [*DeMets*, 2001], there may be a modest increase in fault maturity due to increased cumulative slip, thus allowing for reduced τ_a [*Choy and Kirby,* 2004*; Choy and Boatwright,* 2009*; Schorlemmer et al.,* 2005].

When excluding events that occur northeast of the islands of Java (those mostly associated with subduction in the Flores Sea), we find that thrusts have a strong gCMT depth-dependence, with increasingly deep events being more energetic (**Figure 3.11**). This trend of increased θ with depth closely follows the trend observed for global thrust mechanisms (**Figure 3.12**).

3.5 Conclusions

The updated global catalog of radiated seismic energy from recent large earthquakes ($M_0 \geq 10^{19}$ Nm) is developed for 342 events using 17849 seismograms. Comparison of the *E* determinations of this study finds that the radiated seismic energy parameter θ is significantly higher ($\overline{\theta}$=-4.59 ± 0.36) than previously reported by *Newman and Okal* [1998] and *Weinstein and Okal* [2005] (-4.98, and -5.12, respectively). Utilizing the full duration of the event rupture significantly improves the estimation of very large and slow rupturing events such as giant and tsunami earthquakes. Because of the inclusion of recent giant earthquakes, we now extend the scale-invariant range of θ=-4.5 over 19 orders of magnitude, from 3×10^3 to 4×10^{22} Nm by augmenting the study of *Ide and Beroza* [2001] with events beyond 2×10^{21} Nm.

Similar to previous studies, we observe a robust variation of θ with focal mechanism, as thrust, strike-slip, and normal earthquakes exhibit $\overline{\theta}_T$= -4.74, $\overline{\theta}_{SS}$= -4.44, and $\overline{\theta}_N$ = -4.51, respectively. The deficiency in radiated seismic energy in thrust events is potentially due to the preferential occurrence of these events on mature subduction megathrusts [*Choy and Kirby*, 2004], while increased relative radiated energy in strike-slip events likely occur because of their preferential occurrence on immature continental and oceanic transforms.

Regional analyses of thrust events along the MAT and Java trench environments yield mixed results. While Java does not exhibit a preferentially deficient nature, the MAT thrust events are almost exclusively deficient in energy, representing an approximate 30% reduction in τ_a. However, only the Java trench environment exhibits a significant increase in θ with depth down to 70 km, that can be described as a gradual increase in earthquake τ_a from near 15 kPa near the trench to 2 MPa near 70 km depth. The five slow-source earthquakes, comprising the 4 observed TsE events and the 2000 New Britain earthquake, are the most energetically deficient end-members of this trend.

CASE: MENTAWAI TSUNAMI EARTHQUAKE

4.1 Introduction

On 25 October a moment magnitude M_W 7.8 earthquake struck just west of the Mentawai Islands off the west coast of Sumatra (**Figure 4.1**), generating a surprisingly large local tsunami that caused more than 400 causalities. The event ruptured immediately up-dip from the seismogenic zone and was possibly triggered by stress changes following the September 2007 M_W 8.5 Sumatran earthquake [*Stein*, 1999]. This area may have last ruptured as part of the 1797 and 1833 M_W 8.6 and 8.9 events, with as much as 18 m of megathrust slip to explain the coseismic uplift of local microatolls by 3 m [*Natawidjaja et al.*, 2006]. Further north, a segment that ruptured in 1861 was likely comparable in magnitude (M_W □8.5) to the 2005 M_W 8.6 Nias earthquake that ruptured the same approximate area [*Briggs et al.*, 2006; *Newcomb and McCann*, 1987]. Available high-resolution bathymetry along the trench adjacent to the giant 2004 M_W 9.1 Sumatran earthquake suggests that significant faulting in the region may be due to rupture through the prism toe during the 2004 and previous earthquakes [*Henstock et al.*, 2006; *Lay et al.*, 2012]. The large slip estimated in the shallow trench during the 1833 earthquake, and the considerable faulting near the trench toe further north support the hypothesis that the subduction zone off western Indonesia is capable of supporting shallow megathrust slip, the type seen in tsunami earthquake ruptures. This is supported by a recent study that suggests slow rupture of a magnitude 7.6 earthquake offshore Sumatra in 1907 (□2°N) caused a large local tsunami [*Kanamori et al.*, 2010].

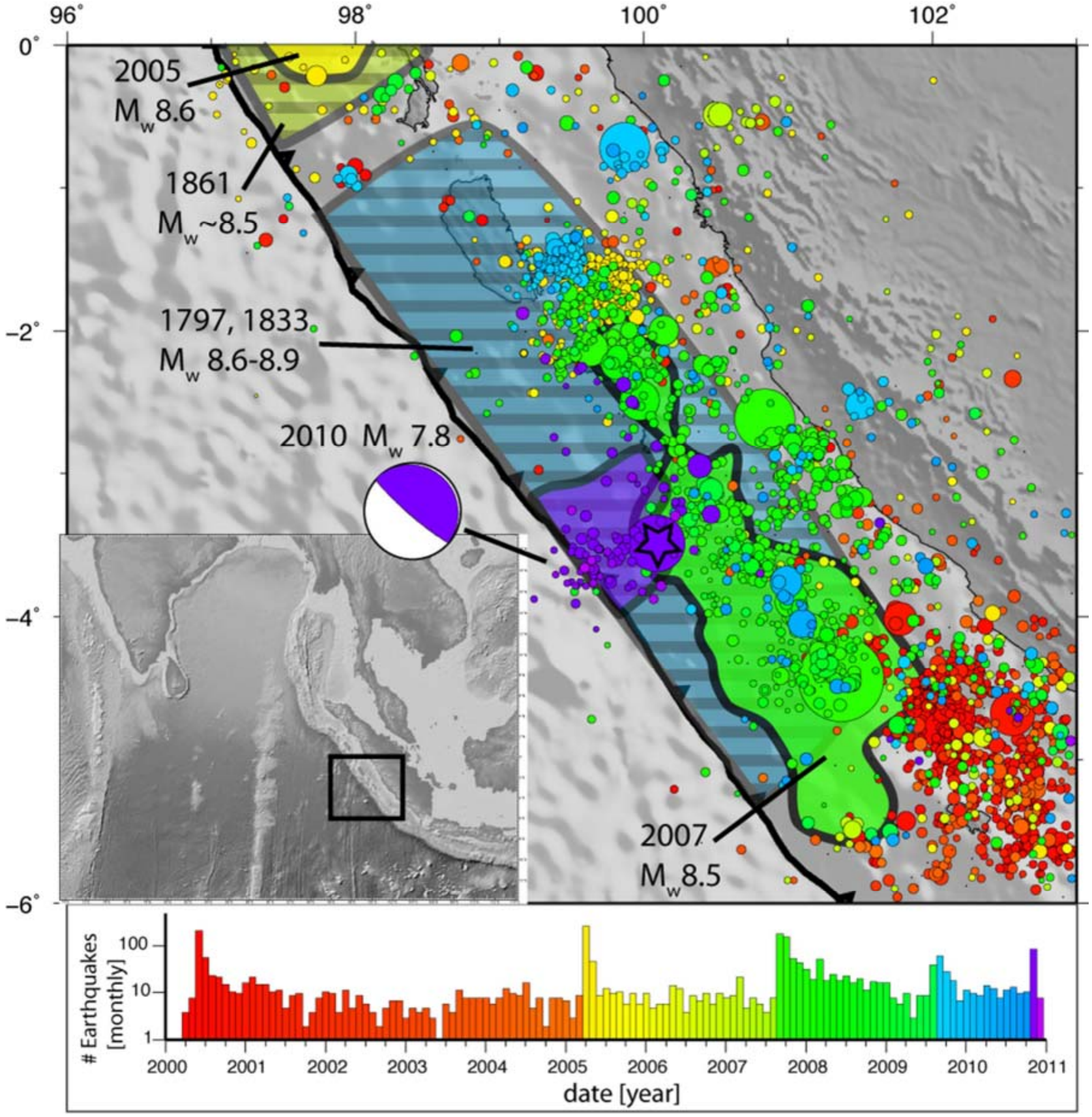

Figure 4.1: Approximate rupture area of the 2010 Mentawai, and previous historic and recent large earthquakes (inset is study region highlighted by box). Events include the combined rupture of the 1797 and 1833 MW 8.6 to 8.9 earthquakes [*Natawidjaja et al.*, 2006], the southern extent of the 1861 and 2005 M_W □8.6 events [*Briggs et al.*, 2006; *Newcomb and McCann*, 1987], and 2007 M_W 8.5 earthquake following *Ji et al.*, [2002]. Also shown is the gCMT mechanism and location, and other earthquakes with magnitude >4 since 2000 colored by date and corresponding to histogram.

4.2 Real-Time Detection and Performance

Using the set of programs called 'RTerg' implemented at Georgia Tech, utilizing the methodology previously described in CHAPTER 2, earthquake energies and estimated rupture durations were automatically determined in near real-time at Georgia Tech for global earthquakes greater than magnitude 6.5 since the beginning of 2009. This information is useful for rapidly characterizing strong shaking in large earthquakes and their tsunami potential. This automated system was active and running by the time of the Mentawai earthquake. Because the first iterations used data from stations that did not yet record the rupture termination, the event duration was underreported (**Table 4.**1). The first iteration found T_R = 53 s and M_e = 6.95, considerably smaller than the final reported M_W = 7.8. By the second iteration, 8.5 minutes after rupture initiation, T_R increased to 96 s and M_e to 7.17, a result that in retrospect could have identified the event as slow. By the fourth iteration, 16.5 minutes after the rupture began, RTerg stabilized to its near final solution with T_R = 126 s and M_e = 7.09. A final determination was made after an analyst reviewed the event, and corrected for the reported global Centroid Moment Tensor (gCMT) focal mechanism [*Ekstrom et al.*, 2005], finding T_R = 127 s and M_e = 7.03 using 51 stations, comparable but smaller than the final result determined independently by the USGS (M_e = 7.2) [*Choy and Boatwright*, 2007].

Table 4.1 Energy results in different iterations and final broadband energy (0.5 – 70 s), high frequency energy (0.5 – 2 s), duration and E/T_R^3 discriminant.

Iteration	Latency (s)	$N_{Stations}$	T_R (s)	$E(M_e)$ ($\times 10^{14}$J)	$E_{hf}(M_{e\text{-}hf})$ ($\times 10^{14}$J)	E_{hf}/T_R^3 ($\times 10^7$ J/s^3)
1	393	11	53	5.9 (6.95)	1.3 (6.97)	85
2	513	18	96	13.0 (7.17)	2.2 (7.12)	24
3	693	44	94	8.6 (7.06)	1.0 (6.90)	12
4	993	54	126	9.6 (7.09)	1.0 (6.91)	5.2
5	1615	51	124	7.6 (7.02)	0.90 (6.87)	4.7
Final	N/A	51	127	7.8 (7.03)	0.91 (6.87)	4.5

While real-time assessments***:*** of T_R, and E, are independently useful for assessing the size of a large earthquake, their combination yields a robust discriminant for TsE [e.g., *Lomax et al.*, 2007]. Because T_R^3 scales with M_0 for most earthquakes [*Houston*, 2001], the long duration of slow-source TsE stand out particularly well when compared to their deficient rupture energy. We identified that real-time high-frequency solutions are optimal and implemented in RTerg a discriminant threshold for TsE to be $E_{hf}/T_R^3 < 5 \times 10^7$ J/s^3. Thus, after iteration 5, the event was automatically classified as a possible TsE, and notifications were sent to a distribution list including individuals from the USGS National Earthquake Information Center (NEIC) and Pacific Tsunami Warning Center (PTWC). The progression of the discriminant in real time is shown along with other post-processed and real time solutions in Figure 4.2.

Like other TsE, the 2010 Mentawai earthquake can be uniquely identified as a slow-rupturing TsE through a comparison of its radiated seismic energy E to seismic moment M_0 ratio, θ. As previously discussed, while most events have $\theta = \log_{10}(E/M_0)$

between −4.0 and −5.0, slow TsE have $\theta \leq -5.7$ [*Newman and Okal*, 1998]. Using the final energy given the corrected gCMT mechanism, we find the Mentawai earthquake to have $\theta = -5.9$, clearly discriminating it as a slow-TsE (Figure 4.2a). Because RTerg does not determine focal mechanisms, the θ solution was not determined in real-time. However, θ determinations are routine at the PTWC [*Weinstein and Okal*, 2005].

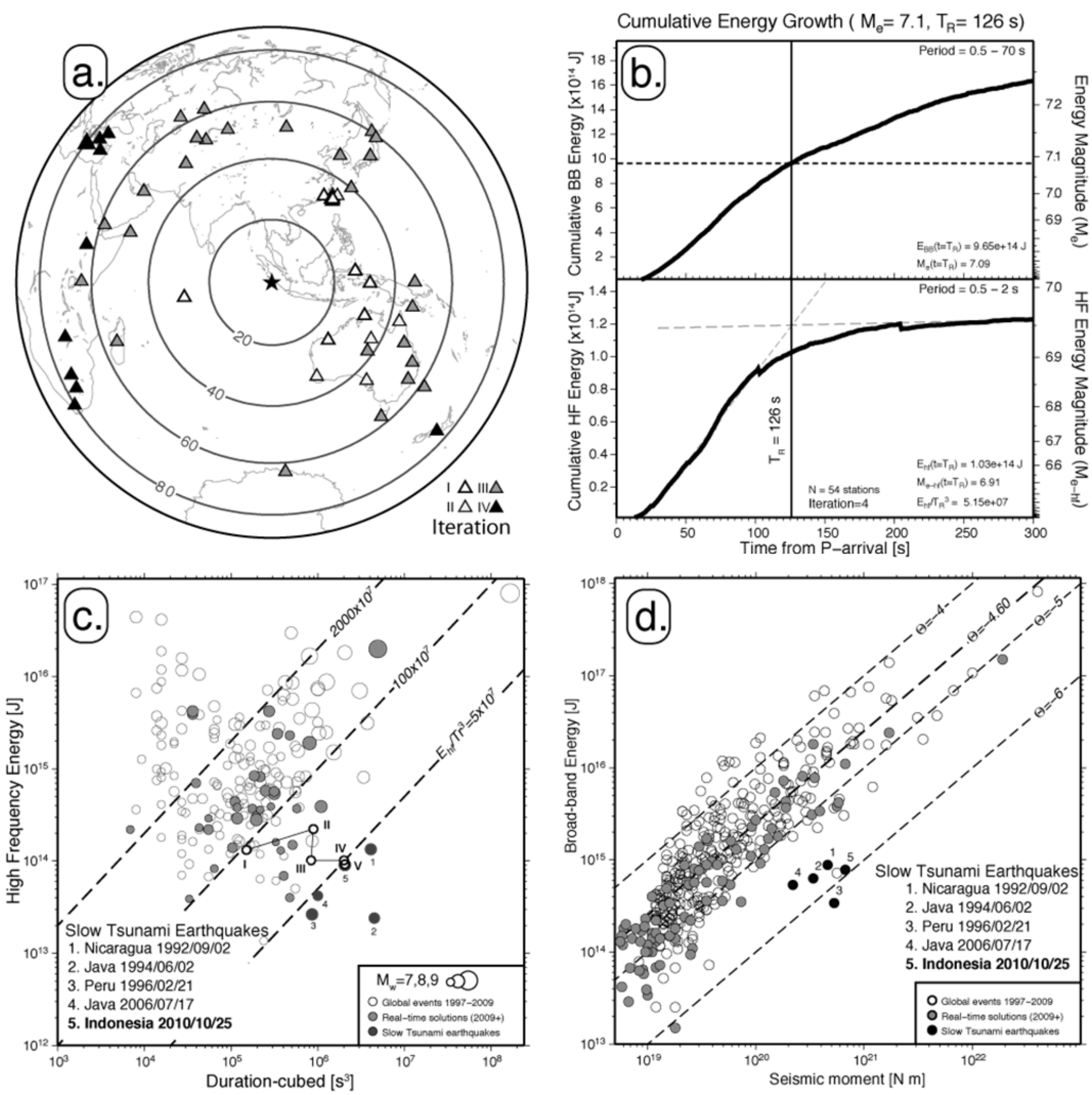

Figure 4.2: (a) Broadband seismic stations available for real time energy analysis (25°–80°; stations added in subsequent iterations are differentiated by shade). (b) The high-frequency energy growth identifies the approximate event duration T_R, while the total event energy E is determined using broadband energy at T_R (iteration 4 shown). (c) The

per-iteration (I-V) determinations of E/T_R^3 are shown relative to other real-time solutions since 2009 (gray circles), solutions with known mechanisms (open circles), and other TsE events (dark circles). By iteration 4 (IV) the result stabilized and was comparable to the final solution determined using the gCMT mechanism (5). (d) Like other TsE, E/M_0 for this event is significantly reduced ($\theta = -5.9$).

4.3 Evidence of the Mentawai 2010 as a Slow Source TsE

4.3.1 Long Rupture Duration

Two lines of evidence clearly denote excessive T_R for this event. First, we identified T_R = 127 s (124 in near-real time) using the termination of continued high-frequency energy growth (Figure 4.2b). Second, as a part of the finite-fault determination, the event source-time function was determined to be nearly identical (□120 - 125 s) [*Lay et al.*, 2011]. Such a long duration rupture would scale to an MW 8.5 earthquake following the relation found by *Houston* [2001].

4.3.2 Deficiency in Radiated Seismic Energy

Using the established E/M_0 [*Newman and Okal*, 1998], and newly tested E_{hf}/T_R^3 discriminant [e.g., *Lomax et al.*, 2007], we identify this event as a slow rupturing TsE. This event is more deficient than 99.5% of all E/M_0 recorded events since 2000 [*Convers and Newman*, 2011], and more deficient in E_{hf}/T_R^3 than any other event with $M_e \geq 6.5$ tested since the beginning of 2008, and similar to the four other slow-source TsE occurred since 1992 (Figure 4.2d).

4.3.3 Shallow, Near-Trench Rupture

The locations of early aftershocks, the W-phase and gCMT mechanisms, and the area of dominant slip distribution, all identify that the event ruptured up-dip of the point of nucleation and very near the trench [*Lay et al.*, 2011]. Such near-trench rupture is noted as an endemic feature of TsE [*Polet and Kanamori*, 2000], which is likely to control its enhanced tsunami excitation due to increased slip near the free surface [*Satake and Tanioka*, 1999], regardless of the rupture speed [*Newman et al.*, 2011b].

4.3.4 Tsunami Size Versus Magnitude

Large regional tsunamis are normally identified for earthquakes $M_W > 8$, however the 2010 Mentawai M_W 7.8 earthquake is reported to have up to 16 m of run-up [*Hill et al.*, 2012], and an observable cm-level open ocean tsunami 1600 km away. Kanamori's [1972] definition of TsE related the tsunami to higher-frequency body m_b and surface wave M_S magnitudes that are reduced due to slow rupture. This is comparable to the determination of $M_e = 7.03$, and $M_{e\text{-}hf} = 6.87$ found in this study, agreeing with $m_b = 6.5$ and $M_S = 7.3$ determined by the NEIC; values far too small to otherwise expect an earthquake generated tsunami.

4.4 Discussion

Because TsE are observed in the shallow near-trench region of the subduction interface [*Polet and Kanamori*, 2000], the relatively large distance to the coast, and slowing effect of shallowing ocean on tsunami waves frequently allows for considerable time between the earthquake rupture and tsunami inundation. In the case of the 2006 Java TsE, the initial tsunami waves reached the shore approximately 40 minutes after the earthquake, and a rapid TsE warning could have been valuable [*Fritz et al.*, 2007]. While, this was not the case for the very proximal Mentawai islands that were likely inundated within 15 minutes of rupture, RTerg detected the E_{hf}/T_R^3 discriminant could be useful for most coastal environments. Care should be used in determining an appropriate cut-off value for this discriminant, since an upward shift from the current value of 5 to a more sensitive 25 ($\times 10^7$) J/s^3 would have detected the event as a slow-source TsE as early as 9 minutes after rupture initiation, but with an increased expectation of false-positives (on □5–10% of events with M $\geq$ 6.5).

4.5 Conclusions

The M_W 7.8 Mentawai earthquake is a classic example of a rare slow-source tsunami earthquake, by exhibiting deficient radiated energy (M_e 7.0) and extended rupture duration (125 s), identifying the characteristically reduced rupture velocity (□1.25–1.5 km/s) [*Lay et al.*, 2011; *Newman et al.*, 2011a]. From the energy point of view, this earthquake behaved similar to other identified tsunami earthquakes by having a low energy-to-moment ratio and a low ratio of E/T_R^3, which was used for initial assessment since focal mechanism is not computed by RTerg, but was nevertheless obtained within 10 minutes from earthquake initiation.

CHAPTER 5

RAPID ESTIMATES OF EARTHQUAKE RUPTURE DURATION FROM TELESEISMIC ENERGY RATES, WITH APPLICATION TO EARLY WARNING.

5.1 Introduction

The duration of dynamic rupture plays an important role in describing earthquake source processes, most notably the lateral slip extent or rupture velocity in large earthquakes. Together with the total radiated seismic energy E the rupture duration T_R is a powerful tool for rapidly discriminating between normal and slow ruptures, such as those of tsunami earthquakes [e.g., *Convers and Newman*, 2011; *Newman et al.*, 2011a]. Detailed estimates of earthquake rupture duration can be obtained from inverted source-time functions [e.g., *Houston*, 2001]. Given its increasing importance in early tsunami warning or rapid damage assessments, it is important to accurately determine this parameter along with event location, magnitudes, and focal mechanism rapidly after an earthquake occurs.

Different approaches to rapidly evaluate T_R have been attempted. An estimate using the time at which 90% of the radiated energy was recorded was developed by *Lomax* [2005]. Another value was obtained from the 25% draw-down of energy from its maximum in the envelop of a velocity seismogram between 2 and 4 Hz [*Hara*, 2007]. Both of the above methods are relatively robust, but require an arbitrary cut-off that may fail with noisy data or for complex ruptures. *Convers and Newman* [2011] use the cross-over duration T_{XO}, marking the transition between near-linear cumulative energy growth and subsequent scattered energy, to asses the rupture termination, and the point where we calculate the radiated energy. While T_{XO} produces accurate results in most cases, it requires averaging results from numerous stations, and usually needs a minute or more of additional energy after the observation of the completed rupture before an accurate estimate can be made. In this chapter we propose a new method that works with individual teleseismic stations, and can be made immediately after the cessation of rupture is recorded.

As we discussed in chapter 4, both T_R and E can be independently useful for assessing an earthquake's size, but the combination of E and T_R^3 is also an effective real-time discriminator for tsunami earthquakes, such as the previously discussed 2010 Mentawai TsE. In addition, since it does not require knowledge of the exact value of M_0, it can be advantageously used for real-time evaluation.

For this chapter, we estimate the seismic rupture durations from global large earthquakes (moment magnitude ≥ 7.0) by characterizing changes in the radiated *P*-wave energy. By introducing the Time-Averaged Cumulative Energy Rate (TACER). We approximate rupture duration based on the peak first local maximum of an earthquake's high-frequency TACER measured at teleseismic broadband seismometers. This is particularly useful for real-time evaluations, including the identification of slow-rupturing tsunami earthquakes. In cases of long unilateral earthquake rupture and good azimuthal station distribution, the per-station behavior of TACER can identify the approximate rupture direction λ*, rupture velocity V_R, and length L due to directivity effects.

The dataset in this chapter is composed of earthquakes with moment magnitude $M_W \geq 7.0$ recorded at teleseismic distances since January 2000 and in real-time starting from 2009, using the set of algorithms collectively called "*RTerg*" (*http://geophysics.eas.gatech.edu/RTerg*). These algorithms automatically calculate both the duration and value of cumulative seismic energy release in increasing time-windows at two different bandwidths (0.5-70 s for broadband energy 'E' and 0.2-5 s for high frequency energy 'E_{hf}'). While broadband energy is used to calculate the total radiated energy (and energy magnitude, M_e), the high frequency energy, which helps characterize strong shaking, is used to approximate rupture duration due to its ability to filter out later body-wave arrivals [*Convers and Newman*, 2011].

5.2 Finding duration from TACER

We apply the methodology described in Chapter 2 to find the radiated seismic energy at teleseismic distances at both high frequency and broadband range. In the case were the only interest is the behavior of the cumulative energy to extract a proxy for rupture duration on each station, we can potentially discard some of the corrections that are routinely applied to obtain the energy at the source. Specifically, for source duration estimates only, there is no need to apply geometric, focal, or energy partitioning corrections, as they each linearly scale the time-history for any individual station-event pair, and consequently use only the station energy flux. However, because we routinely perform real-time and post-processed radiated energy calculations for these earthquakes, the energy results are included.

To evaluate the performance of proposed and existing methods for numerically evaluating the rupture duration based on energy signals in teleseismic P-waves, we compare results based on simple synthetic and complex measured source-time functions.

For each source-time function, we assume each second of rupture to equate an individual pulse of scaled energy whose individual pulses sum to the total radiated seismic energy (Figure 5.1). Each pulse exhibits an exponentially decaying tail representing the averaged scattered energy between source and receiver at teleseismic distances. The summation of pulses yields the cumulative energy growth as used by *Convers and Newman* [2011] for the determination of the crossover duration $T_{XO.}$ For each scenario of triangular, boxcar, and trapezoidal synthetic energy source-time function (**Figure 5.1**, cases a, b, and c), and moment source-time functions for two complex ruptures (case d and e), including the 2010 Mentawai tsunami earthquake [*Newman et al.*, 2011a], and the 2011 Tohoku-Oki earthquake [*Hayes et al.,* 2011], we illustrate the behavior of T_{XO} and two proposed methods for identifying the termination of rupture (**Figure 5.1**).

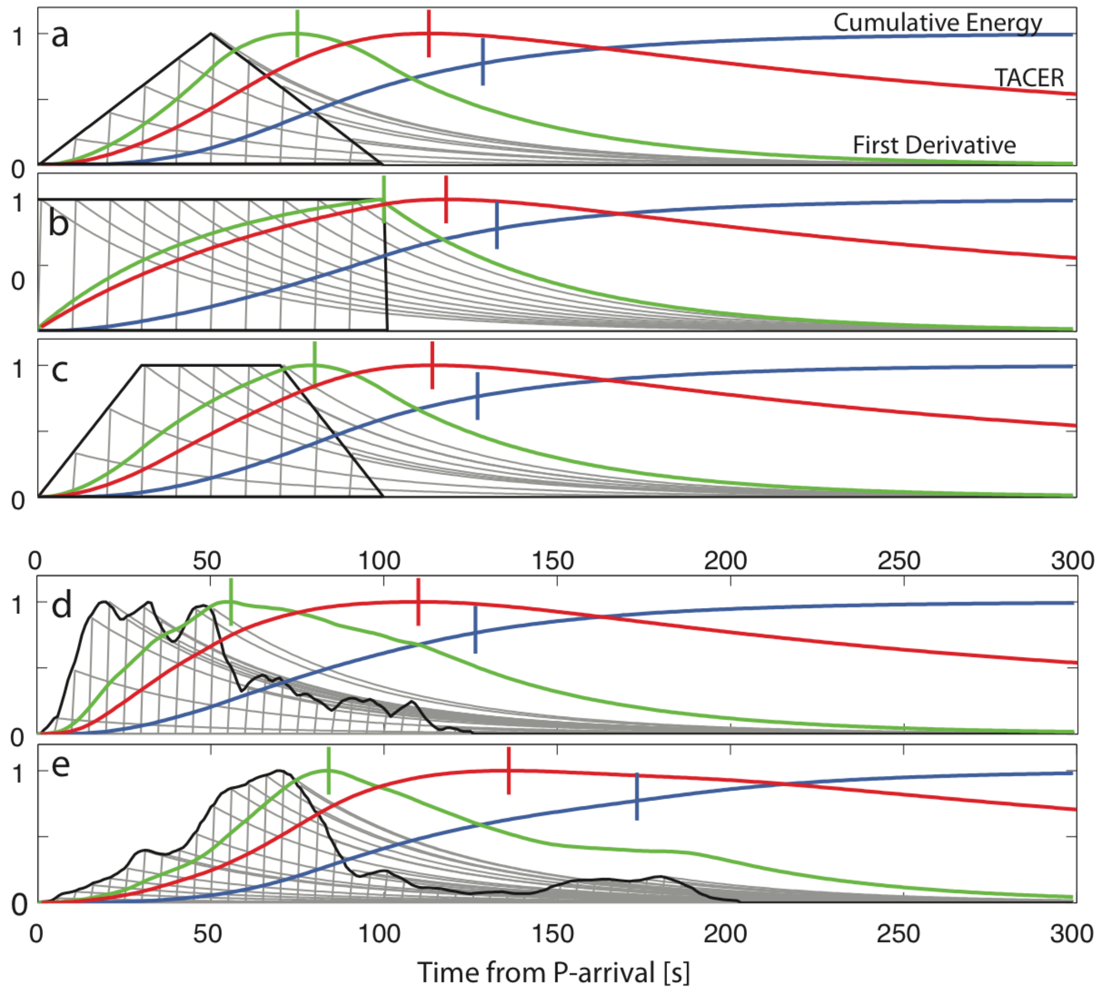

Figure 5.1: Source-time functions (black) are shown along with their predicted energy distribution at a teleseismic station using a simple exponential decay, mimicking scattering. The energy per time-step (gray) is combined to show the cumulative energy release (blue), the first-derivative of cumulative energy growth (green), and TACER (red). Three theoretical time-histories are shown; (a) triangular, (b) boxcar, and (c) trapezoidal functions as well as two event time-histories, (d) the M_W 7.8 2010 Mentawai tsunami earthquake [*Newman et al.*, 2011a] , and (e) the M_W 9.0 2011 Tohoku-Oki earthquake [*Hayes et al.*, 2011].

The maximum of the first derivative of the cumulative energy growth, representing the seismic energy release rate, is one potential rupture duration identifier that accurately identifies rupture duration in the case of a boxcar source (case b) (**Figure 5.1**). However, we find that peaks in the first-derivative energy tend to lag the peak moment-release, but occur before rupture terminates in each the synthetic triangle, and trapezoid sources (cases a, and c) and two test earthquakes (cases d, and e). In large and prolonged ruptures with complex source-time functions, the process of identifying duration is not straightforward. Indeed, an examination based on the first derivative becomes, in practice, a search for either a prominent decrease in the first derivative, or a search for a point where the first derivative falls to a certain value after a maximum, which again potentially becomes a subjective procedure.

A second and preferred method for estimating earthquake rupture duration is an adaptation of the energy growth, called the Time-Averaged Cumulative Energy Rate (TACER). With TACER we attempt to minimize the effect of small jumps in the cumulative energy growth while minimizing edge effects associated with short-window energy calculations in the frequency domain. In its discrete form TACER is:

$$TACER(t_n) = \frac{\sum_{i=1}^{n} \Delta E_i / \Delta t_i}{t_n}, \tag{5.1}$$

where the result is a function of time t from the first P-arrival, and it is determined as the summation of the time derivatives of the cumulative high-frequency (0.5 – 2 Hz) energy. The rupture duration T_{TACER} is calculated at the maximum TACER value, which is also the local maximum in most cases. In every test case T_{TACER} is longer than the first-derivative maximum, and is closer to the T_R in cases where the source diminishes before ceasing (cases a, c, d, and e). While no one method is ideal in all situations, T_{TACER} is closer than T_{XO} and the first derivative duration to the theoretical rupture termination in the two cases where there is regular energy fall-off (triangular and trapezoidal sources). In the two example long-duration earthquakes, T_{TACER} was similar but somewhat shorter than T_{XO}, which accurately estimated the rupture termination.

One advantage of T_{TACER} over T_{XO} is that TACER calculations can be routinely determined per-station, rather than from a stack of all waveforms as T_{XO} is normally done [*Convers and Newman*, 2011]. With the per-station solutions we are able to evaluate per-event duration and energy ranges based on the variance of the collected data. Using these data, we can report the optimal median solution, and the 75% range (Appendix Table B.1). This is chosen over a mean, since per-station solutions tend to include long tails with excessive duration due to later reflected waves or other local signals that would otherwise bias the mean.

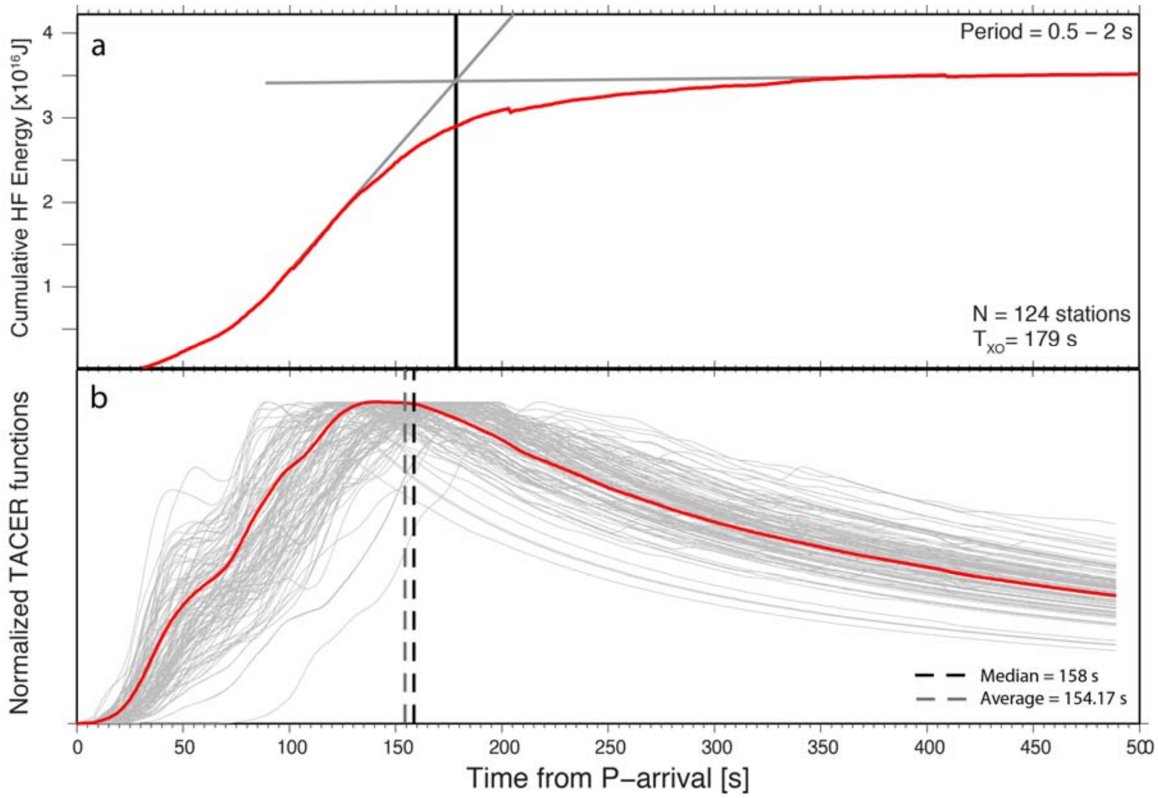

Figure 5.2: Duration estimates for the 2011 Tohoku-Oki M_W 9.0 earthquake. (a) The cumulative high-frequency energy is calculated from the average growth of 125 available broadband stations, yielding T_{XO} = 179 s. (b) The per-station (gray) and median (red) TACER solutions are shown for this event. T_{TACER} represented as the median (black dashed line; 158 s) or average (gray dashed line; 154 s) is somewhat earlier than T_{XO}.

5.3 Results and Discussion

5.3.1 Application to the Tohoku-Oki Earthquake

The application of this method to real-time situations aids in the rapid assessment of both the event rupture duration and total energy release. In **Figure 5.2**, we illustrate the application of T_{XO} and T_{TACER} for the recent 2011 Tohoku-Oki M_W 9.0 earthquake. Using the same stations for both methods we found comparable results (T_{XO} = 179 s, T_{TACER} = 158 s, 124 – 186 s 75% bounds). Though there is no definite directivity effect in duration, mostly due to its largely bilateral rupture, the seismic energy radiation was far stronger in the western hemisphere (Figure 5.3). Although the differential energy radiation for this earthquake is beyond the scope of this study, it is nevertheless intriguing and worth investigating in future studies.

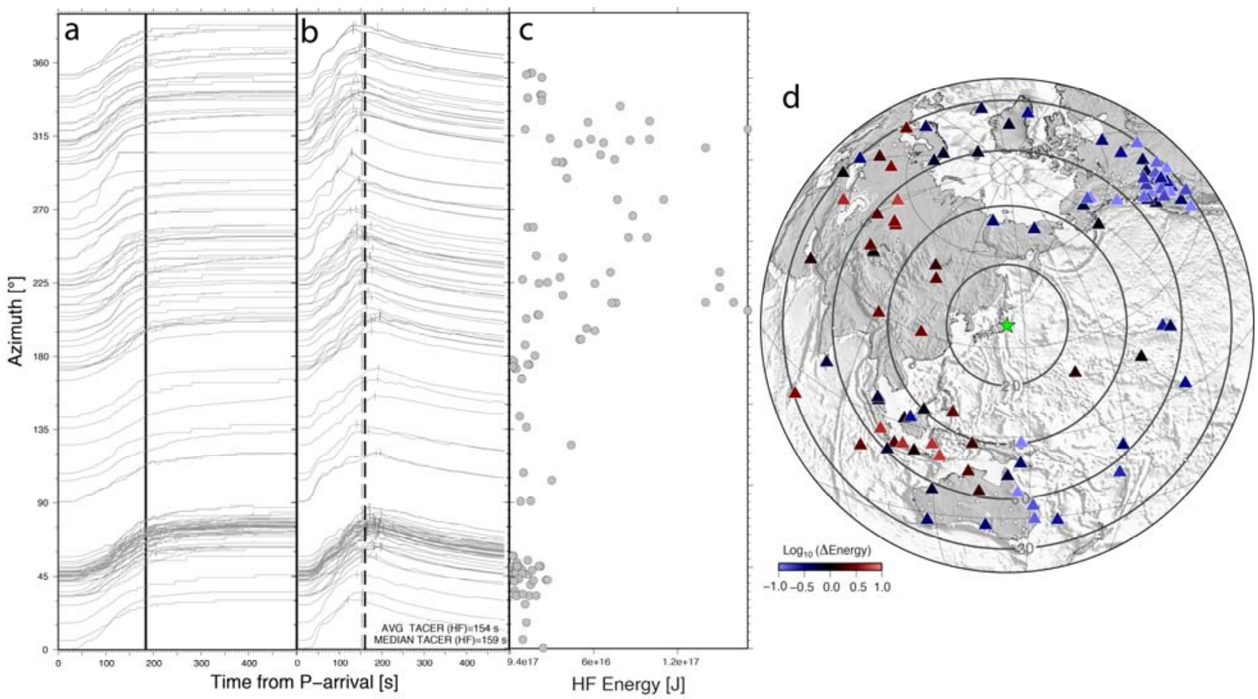

Figure 5.3: The azimuthal and spatial distribution of high-frequency energy is shown for the **2011** M_W 9.0 Tohoku-Oki earthquake. For each of the **stations used**, the normalized azimuthal distribution of (a) the cumulative energy, and (b) TACER are shown. Also shown are (c) the azimuthal and (d) spatial distribution of the per-station energy calculation (relative to the mean in (d)).

5.3.2 Directivity Effects and the 2007 Mw 8.1 Solomon Islands Earthquake

Because we evaluate T_R from stations that are azimuthally distributed, we can explore the applicability of the method to identify rupture directivity. Directivity manifests itself in shorter apparent durations in the direction of rupture propagation and longer durations in the opposite direction [*S Stein and Wysession*, 2003], similar to a Doppler shift but in duration rather than frequency. Such real-time estimates, when combined with the hypocenter, can be useful for evaluating the extent of the rupture area; valuable for evaluating damage and tsunami potential.

An earthquake's rupture is not a point source, but is a continuum of transient sources radiating across a fault over the event's duration [*Douglas et al.*, 1988]. Thus, directivity effects can be seen when a sufficiently long and unilateral rupture occurs causing changes in its apparent duration with azimuth [*Caldeira et al.*, 2010]. The rupture duration will appear shorter when the rupture is moving toward the observing station, and longer when it is moving away from it. This can also be used to differentiate the fault plane from the auxiliary plane in the case of strike-slip faults [e.g., *Warren and Silver*, 2006]. In a simplified way, the observed apparent duration T_{app} and its change with azimuth Φ can be expressed as [*S Stein and Wysession*, 2003]:

$$T_{app} = \frac{L}{V_r} - \frac{L}{V_{app}} \cos(\phi - \lambda^*), \tag{5.2}$$

where the fault length L over the rupture velocity V_r (the true rupture duration T_R), V_{app} is the apparent P-wave velocity, and λ^* is the rupture propagation direction.

For a long and largely unilaterally rupturing earthquake with good azimuthal station coverage, such as the 2007 M_W 8.1 Solomon Islands event [*Newman et al.*, 2011b], it is possible to extract important earthquake parameters from the directivity effects on T_{TACER}. We exemplify this by comparing the theoretical to best-fit estimates of the apparent rupture duration using known and predicted values for each rupture length L, orientation of rupture λ^*, and rupture velocity $V_{R.}$ The theoretical effect is estimated for an apparent velocity at 50° distance (V_{app} = 14.7 km/s), using geometric parameters from *Chen et al.* [2009] (L=294 km, and λ^*=-53°), and rupture velocity determined from the product of L over T_{TACER} (yielding V_R=2.88 km/s). We find that this theoretical result is equivalent to the best-fit directivity result solving simultaneously for orientation, rupture velocity, and rupture length (λ^{*}= -46°±10°, V_R = 2.5 ± 5 km/s, and L = 259 ± 56 km at one standard deviation) (Figure 5.4). While the results are remarkable for this near-ideal case, showing that it is possible to constrain the approximate direction, length of rupture and rupture velocity, such results may only be achieved when earthquakes have long unilateral rupture and good azimuthal coverage. Because there remains a strong trade-off between V_R and L, one or both parameters may need to be fixed for most attempts at constraining directivity.

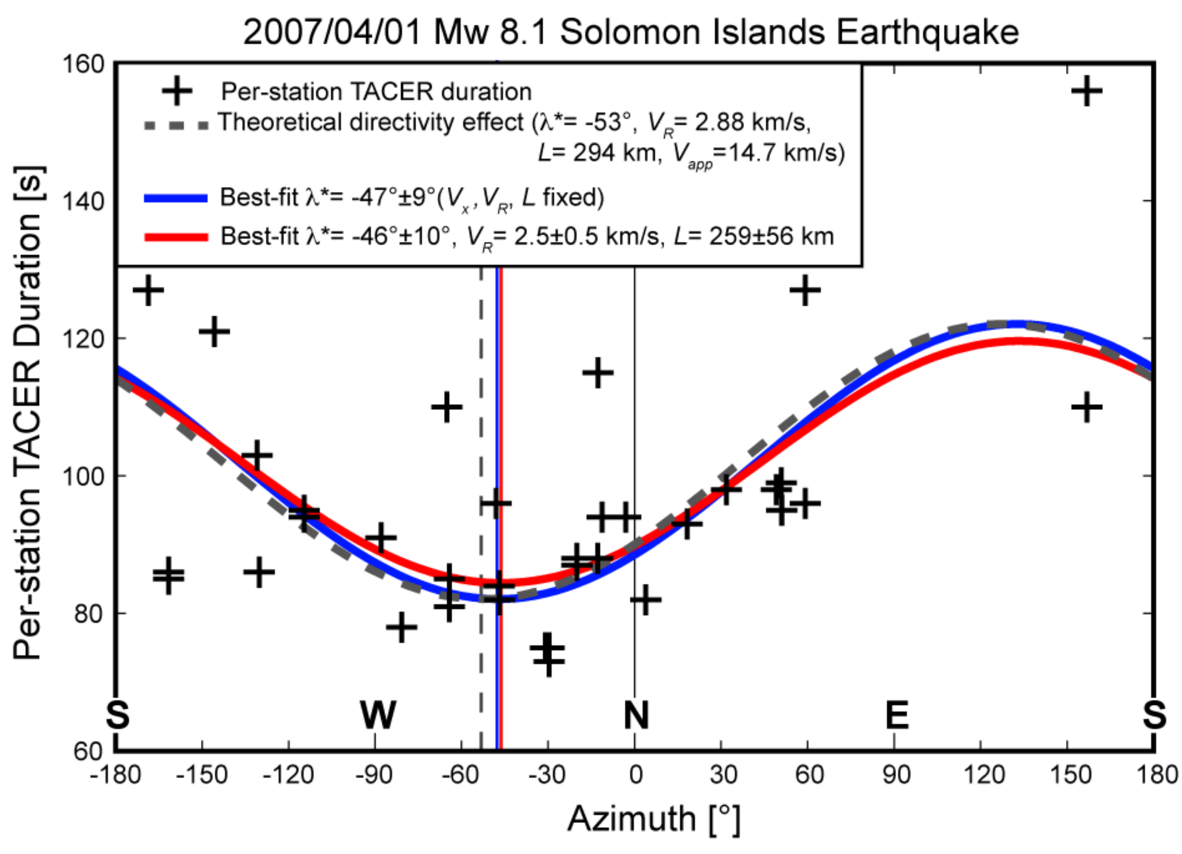

Figure 5.4 Azimuthal distribution of the per-station T_{TACER} for high frequency (0.5-2 s) stations recording the 1 April 2007 Solomon Islands earthquake (dark crosses). This event was chosen because it is known to be a large and unilateral rupture propagating from ESE to WNW. The theoretical directivity effect (gray dashed sinusoid) is

comparable to best-fit models solving for just orientation (λ*; blue sinusoid), or for each λ*, rupture velocity V_R, and rupture length L (red sinusoid).

5.3.3 Comparison with Other Results and TACER Stability

To test the robustness of median event T_{TACER} results, we compare it to each the duration estimates as calculated though the global CMT (gCMT) project [*Ekstrom et al.*, 2005], *W*-phase moment estimates [*Duputel et al.*, 2012], and our solutions for T_{XO} [*Convers and Newman*, 2011] (Figure 5.5). For the first two cases, duration is reported as twice the half-duration reported in each catalog, and is tied to $T_R^3 \propto M_0$ [*Houston*, 2001], for most smaller gCMT events. While there is no definite method for estimating durations from any of these robust catalogs, we view the W-phase catalog to be most representative, as solutions are dependent on the long-period elastic signal due to the displacement field created across the entire rupture area of the earthquake. The solutions are differentiated between those that were determined retrospectively between 2000 and 2009 and those between 2009 and 2012 determined using automated real-time solutions. Though large scatter remains for individual T_R determinations, there is little large-scale bias between the solutions. In comparing root mean square (rms) residuals between methods we find that T_{TACER} behaves comparably to T_R as determined by *W*-phase and gCMT methods (rms ~20 s), and performs about twice as well as T_{XO} (~40 s). A positive bias exists for T_{TACER} at small magnitudes. This lower bound bias, which is smaller than the one found with T_{XO}, likely comes from a combination of scattering within the earth, and the temporal separation between the direct *P* and the depth phases, which is approximately 16 s at teleseismic distances for an event at 40 km depth. For some larger earthquakes, half-durations which are based on regularly shaped moment release (e.g., triangular function in **Figure 5.1**a), will underestimate rupture duration as the methods best fit the largest moment release rather than the total slip over time.

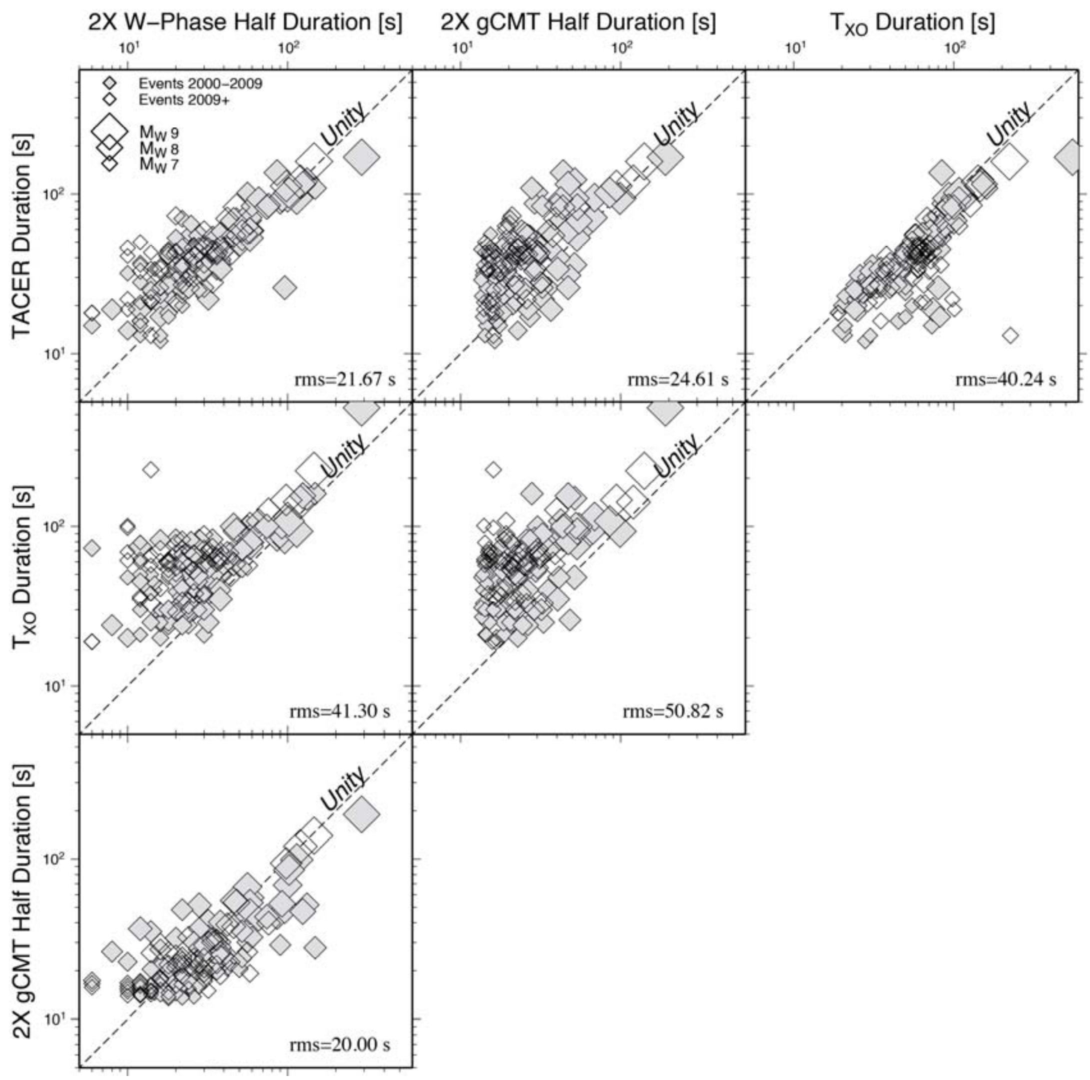

Figure 5.5 Comparison of the T_{TACER} with T_{XO} [Convers and Newman, 2011], gGMT [*Ekstrom et al.*, 2005], and W-Phase [*Duputel et al.*, 2012] durations. The W-phase and gCMT durations are reported as 2x the half duration of their catalogs. The rms differences for each comparison study are shown, and T_{XO} solutions are differentiated between retrospective (2000 – 2009) and real-time (after 2009).

The TACER method was implemented into our real-time assessment tool, "RTerg", in early 2009. Using these results we evaluate the performance of both median event solutions and per-station solutions over time (Figure 5.6). While 90% of median solutions are within 10% of the final median result within 6 minutes, 90% of the per-station solutions are within 20% of the final median result within 14 minutes. Thus, while individual TACER solutions may be reliable in some instances, more stations with good azimuthal coverage are preferable.

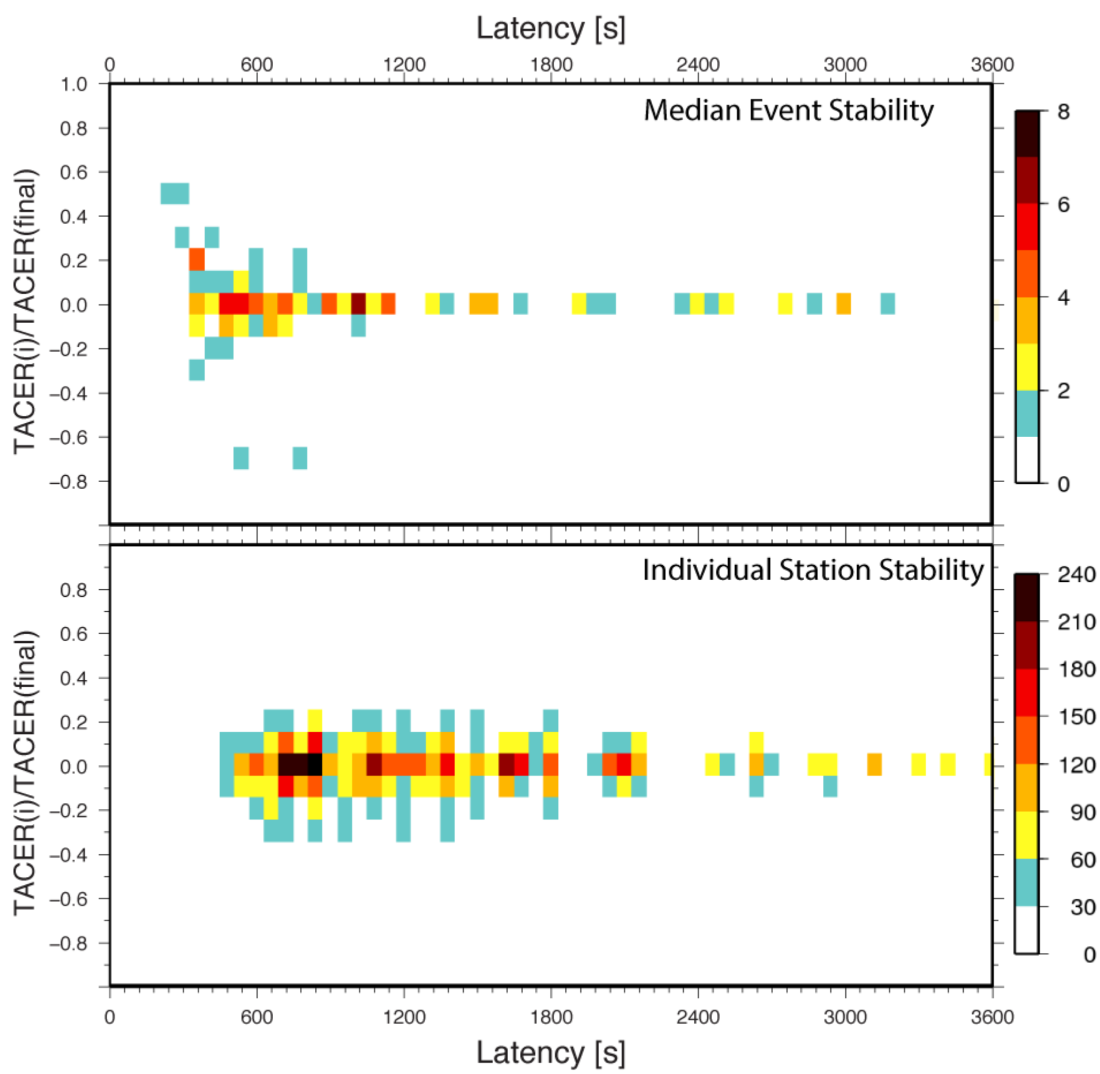

Figure 5.6: Stability and latency TACER(i) (iteration results), for events gathered by RTerg beginning in 2009. We plot the ratio of the median (top) and individual (bottom)

station TACER solutions relative to the final median TACER solution as a function of solution latency from event origin. Iterations in RTerg are typically from 1 to 5, with the fifth iteration taken as the final iteration.

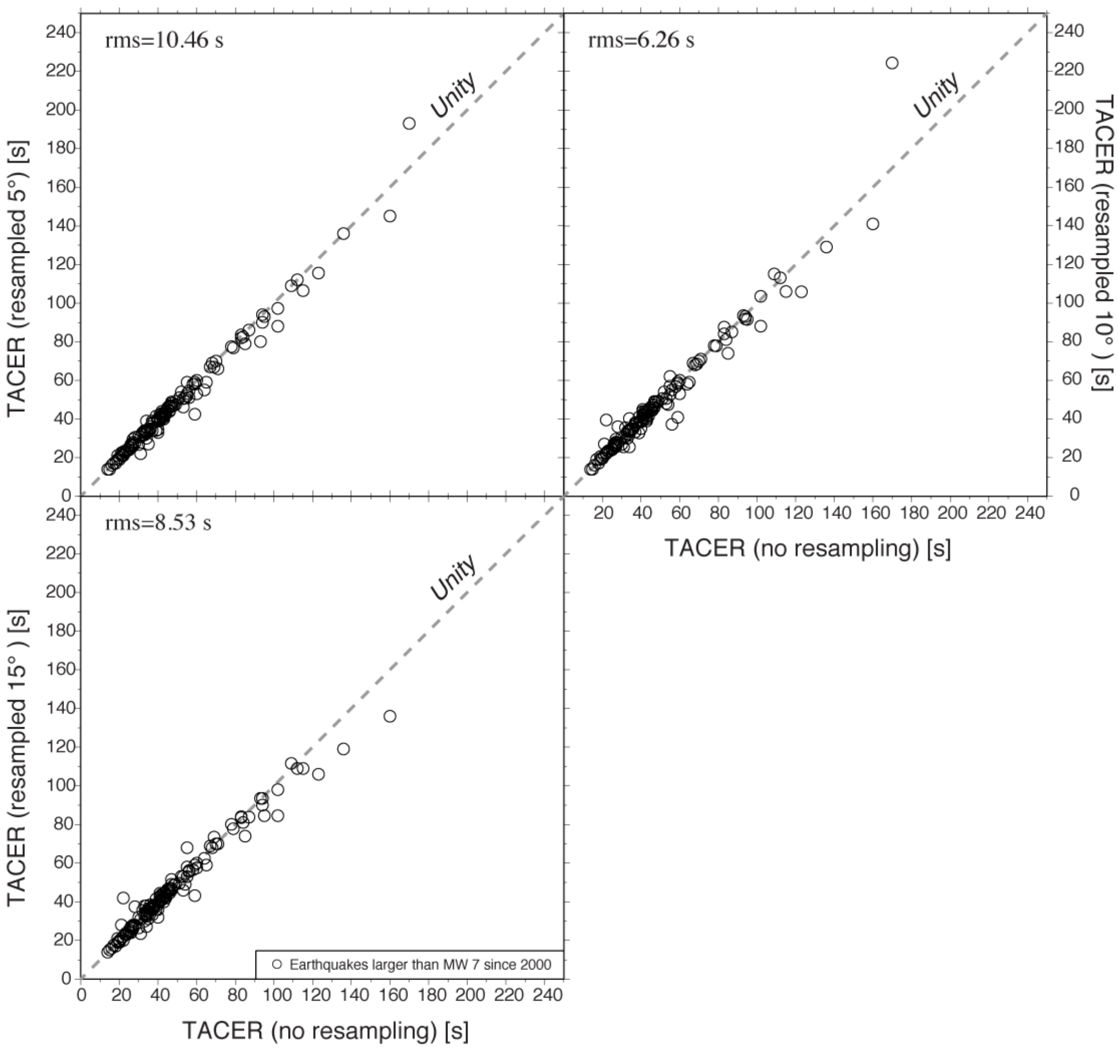

Figure 5.7 Because station spacing is uneven, and at times locally very dense (e.g., the U.S. Transportable Array), we evaluated the potential for biasing. To achieve this result, we choose a median solution every (a) 5°, (b) 10° and (c) 15° and use this as a new individual TACER solution to find a new event median. These results are all compared with the original results without resampling (*x*-axes). As sampling radius increases, solutions increasingly differ, however rms offsets remain small (~8, 6, and 10 s for 5°, 10°, and 15° respectively), indicating that azimuthal biasing is not a widespread issue.

Finally, we tested the effect azimuthal sampling has on the determination of median T_{TACER}, but found no substantial bias between total station medians, and medians taken including 5°, 10°, or 15° local median solutions (Figure 5.7). Regardless, to provide more rapid, and minimally biased solutions, one may avoid largely redundant data and consider similar spatial sub sampling of available stations.

5.4 Conclusions

Because TACER reliably estimates durations in real-time it is useful for early earthquake information, and potentially for tsunami warning in the case of very large and tsunami earthquakes. Some limitations beyond the geometric constrains remain, arising from the complexity of earthquake rupture, depth and direct P phase separation and differential ray path in deep earthquakes, and the occurrence of overlapping waveforms from multiple earthquakes. For complex ruptures, such as the case of two strong patches with some delay, the energy release can be biased towards the first rupture patch, giving a shortened duration estimate. For deeper earthquakes the depth phases are increasingly delayed, and depending on the orientation of the focal sphere, the delay may appear even larger than the direct *P*-arrival, and may appear excessively long. Finally, when two or more earthquakes rupture within a few minutes time, their energy can be superimposed at teleseismic distances. Normally this occurs when very large earthquakes have immediate aftershocks, but can also occur when a coincident event occurs elsewhere. Because of the contamination of energy, the later events are often ill-determined, and inaccurate results can be reported. Such cases are not surprising, and any analyst should be aware of this possible scenario.

Rupture duration is an important earthquake parameter that is otherwise obtained by modeling a source-time function or visually and sometimes subjectively examining seismograms. The Time-averaged Cumulative Energy Rate (TACER), provides a rapid and robust estimation of rupture duration. The latter, when combined with algorithms that routinely calculate earthquake energy in real-time, can be used for improved early earthquake information and tsunami warning [e.g., *Newman et al.*, 2011a]. Using the azimuthal variations in TACER, we show it is possible to provide an early determination of rupture directivity for some events, which combined with the hypocentral location, can quickly illuminate the geometry of rupture.

RTERG

6.1 Introduction

In this chapter we describe the procedure behind the group of programs and routines, collectively called RTerg, which stands for Real-Time erg (from the CGS units of energy). This is currently used to calculate radiated seismic energy from large earthquakes (we will leave however very specific code details for Appendix C). We revisit some steps from the methodology in Chapter 2 to describe how, starting from an initial location and origin time, we gather stations at distances between 25° and 80° from the event to find the cumulative earthquake radiated energy. For solutions at each station, we calculate the rupture duration using the growth of high frequency energy, and use the total energy observed by P-wave group though the rupture termination to determine the final radiated energy at that station. For each station, we apply distance, frequency and focal mechanism corrections to yield the cumulative radiated energy in broad (0.014 – 2 Hz) and high (0.5 – 2 Hz) frequency bands.

We do not limit our discussion to the currently operating RTerg, but we also discuss the implementation of the TACER function for per-station durations and other possible computational improvements that potentially seep up the calculation process. Final products and illustrations that have proven useful both for retrospective evaluations of earthquake behavior and for real-time indicators of strong-shaking and tsunami potential will be exemplified from an earthquake that we discussed previously, the slow source Mentawai 2010 tsunami earthquake (TsE).

6.2 Implementation

As described before, using velocity seismograms we obtain the *P*-wave group (*P*+*pP*+*sP*) at teleseismic distances to calculate energy flux at the station and then energy at the source [*Boatwright and Choy*, 1986; *Newman and Okal*, 1998]. These calculations are produced in increasing time windows [*Convers and Newman*, 2011]. Here we will review the important steps in the energy calculations performed by RTerg.

6.2.1 Data Selection

We select the vertical component of teleseismic broadband stations located between 25° and 80° of the source epicenter. Teleseismic waveforms are used to avoid triplication effects within the crust, and obtain near-vertical arrivals (thus only the vertical component is necessary). By excluding waveforms beyond 80° we avoid path contamination and heterogeneous attenuation near the core. Additionally, since this method utilizes the *P*-wave group at teleseismic distances, it is not necessary to wait for the arrival of later phases. This evidences an immediate advantage regarding timely calculations, since at these teleseismic distances, the fastest information is delivered by the *P*-wave group and arrives at seismic stations from 2 to 12 minutes, and the information necessary to perform calculations is ready from about 5 minutes after the origin time for the closest stations (25°) and 15 minutes for the more distant stations (80°).

6.2.2 Energy at the station

The vertical velocity records from seismograms are used to perform calculations. From these, the energy flux can be obtained in the time-domain at each station, and integrated over the duration of the generalized *P*-wave group. However, we carry out the per-station energy flux in the frequency domain, since it is possible to directly correct for frequency-dependent anelastic attenuation. The integration in the frequency domain over the angular frequency ω, leads to a new station energy flux corrected for ε^*_{gP} , and recalling equation 2.1 [*Boatwright and Choy*, 1986; *Newman and Okal*, 1998]:

$$\varepsilon_{gP}{}^* = \frac{\rho\alpha}{\pi}\int_{\omega_{\min}}^{\omega_{\max}} |\omega\cdot u(\omega)|^2 \exp[\omega t^*(\omega)]\,d\omega \ , \tag{6.1}$$

we approximate the near-source *P*-wave velocity α with 7 km/s and density and ρ with 3000 kg/m^3. In this equation, $u(\omega)$ is the ground displacement in the frequency domain after being corrected for instrument response [*Okal*, 1992]. The solution of ε^*_{gP} is determined in the frequency-domain and it is not the true station energy, because it is corrected for generalized frequency-dependent attenuation. This attenuation, t^*, is represented in seconds and is the reciprocal of the characteristic ω, that describes the frequency by which an exponential decay of energy is a factor of 1/e of its original value [*Der et al.*, 1982]. The values used for the attenuation factor follow *Choy and Boatwright* [1995], with the equation form of this factor after Newman and Okal [1998].

6.2.3 Energy at The Source

To scale results from the station back to the source we follow steps from *Newman and Okal* [1998]. Specifically, we correct for geometric spreading, partitioning of energy at the source between *P* and *S* waves and for the orientation of stations relative to the focal sphere. The radiated energy at the earthquake source *E* is then:

$$E = (1+q)4\pi(R)^2 \frac{\left\langle (F_P)^2 \right\rangle}{(F_{gP})^2}\varepsilon^*_{gP} \ , \tag{2}$$

where q (= 15.6) accounts for the relative partitioning between the S and P waves [*Boatwright and Fletcher*, 1984], R is the distance-dependent geometric spreading coefficient, $\langle (F_p)^2 \rangle$= 4/15) is the average squared radiation pattern of the direct P-wave [*Aki and Richards*, 1980] and F_{gP} is the mechanism-dependent radiation coefficient of the P-wave group including *pP* and *sP* [*Boatwright and Choy*]. Although F_{gP} is near 1 for dip-slip mechanisms, we require a lower bound of $F_{\mathrm{gP}} \geq 0.2$ in cases where a singularity might arise for strike-slip mechanisms with recordings at distal stations ($\Delta > 60^{\circ}$), and the take-off orientation is near-nodal for the direct-P and depth phase arrivals.

In order to obtain reliable energy determinations for real-time use without the knowledge of the final focal mechanism, it is necessary to estimate the focal correction for the P-wave group (F_{gP} in equation 2.2). While depth is usually poorly known initially, it has little effect on the final result, only affecting estimated E by less than 10% for shallow earthquakes (depth ≤ 70 km) [*Newman and Okal*, 1998]. To apply the estimation of focal mechanism correction for real-time solutions, we employ a generalized radiation coefficient following *Newman and Okal* [1998]. They evaluated the global distribution of gCMT focal mechanisms using existing and available seismic stations to determine a general distant-dependent correction for dip-slip earthquakes. This was chosen over a stochastically distributed event-station correction because the spatial occurrence of focal mechanism orientations is not random.

The use of this generalized radiation coefficient on strike-slip earthquakes will underestimate the true event energy by a factor of four or more, due to the increasingly near-vertical take-off occurring near the nodal axis of the source focal mechanism at greater teleseismic distances [*Choy and McGarr*, 2002; *Newman and Okal*, 1998; *Perez-*

Campos and Beroza, 2001]. Fortunately, less than 15% of all large earthquakes ($M_W \geq 7$) are strike-slip.

6.2.4 Earthquake Duration from Energy

One of the most important improvements that this algorithm has is the variable time-window for energy calculation and its automation in RTerg. While it is possible to calculate the energy at an fixed time after the *P*-arrival and be adequate for most large earthquakes [e.g., *Newman and Okal*, 1998], there are occasions where anomalous ruptures far exceed a 70 s time window duration, such as a typical TsE rupture, and very large ones, like the approximately 200 s of the Tohoku-Oki 2011 earthquake [*Hayes*, 2011], or most notably the ~540 s rupture of the Sumatra 2004 earthquake [*Ammon et al.*, 2005; *Ni et al.*, 2005; *Weinstein and Okal*, 2005].

Using the described methods for calculating energy, we perform 1 s increasing time-window calculations in each station to obtain the cumulative growth only at high-frequency (0.5 to 2 s) and broad-band (0.5 – 2 s), However, to approximate rupture duration, we use the high frequency cumulative energy, this frequency band helps to avoid significant contamination by later reflected phases which tend to have most energy at long-periods [*Convers and Newman*, 2011]. To determine the earthquake's approximate duration, two linear regression fits are calculated, one for each the near-constant growth period excited by finite rupture, and the near-constant die-off period excited by crustal scattering and some later arrivals.

These linear fits are performed for an interval that separates the total calculation time of the cumulative energy in two, and fits both halves in variable time windows. The first fit is performed at time windows that grow in 5-second intervals from a minimum value (greater than zero), up to half of the total calculation time. The second linear fit is performed in a similar manner, but starting at half of the total window of calculation up to the maximum time value for which the cumulative energy was calculated. The crossover point between the linear regressions, called the cross-over time T_{XO}, is approximated as the rupture duration T_r, and coincides with the maximum decay in energy growth (**Figure 2.1**), and is an good rapid approximation for rupture duration for large shallow earthquakes.

6.2.5 Cumulative Energy Results

Before obtaining T_r and calculating the final energy results, we perform an initial depuration of stations with cumulative energy that is either relatively too high or low. First, we take the value of each one of the cumulative energies and obtain the preliminary average of the stack of cumulative energies. Since routinely these calculations are carried out to 300 s, then the average of energies from all the stations at 300 s would be the first reference point. After this, any station with an energy value that deviates more than a predetermined tolerance factor (defined by the user) will be excluded from further calculations and final energy results.

Next, we exclude stations with initial energy values greater than the energy value at the maximum time (e.g., 300 s). This can occur for stations with a wrong *P*-arrival timing or for aftershocks that occur very rapidly after a large mainshock. Re-picking the *P*-arrivals would fix only the first of the previous two cases, however, in the automated scheme, it is assumed this cannot be checked prior to doing the calculations, and this measure is ensures that those stations with too large initial energies are not impeding accuracy from other stations.

We also impose a signal-to-noise (SNR) restriction for stations that could be too noisy or that might have not recorded a significant energy increase in their cumulative energy. This is achieved by assuming a fixed SNR value of 1.5, and using the pre-*P* energy rate. Given in *J/s*, this quantity is calculated from the cumulative energy contained in the 60 s prior to the P-arrival time and it serves as a reference value of the minimum cumulative energy increase per second of the signal. Assuming that prior to the P-arrival time we record only 'background noise', we expect that the last value of the cumulative energy (typically at 300 s), must be higher than the value recorded if there was no earthquake at all (pre-P energy rate multiplied by time). Ratio of these values must be higher than the SNR imposed. After initial discarding of potential stations with erroneous values is performed, we calculate the per-second energy average for the stations.

6.3 Results and Visualization

6.3.1 Cumulative Energy

For each earthquake, cumulative energy plots at high frequency (0.5 – 2 s) and broadband range (0.5 – 70 s) are generated for a stack of available stations aligned relative to the theoretical onset of the *P*-arrival. The inflection point as determined by the cross-over between a near constant growth and later high-frequency energy marks the approximate rupture duration (solid vertical black line at 127s in **Error! Reference source not found.**). At this point the cumulative energy is determined for both high frequency (E_{hf} = 9e13 J), and broadband (E_{BB} = 7.8e14 J). The energy can be converted into an energy magnitude following M_e=2/3 $\text{Log}_{10}(E_{BB})$-2.9 as described by *Choy and Boatwright* [1995]. The high-frequency energy magnitude $M_{\text{e-hf}}$ is calculated in a similar way and assumes only 1/5$^{\text{th}}$ the energy is available in that higher selected band pass.

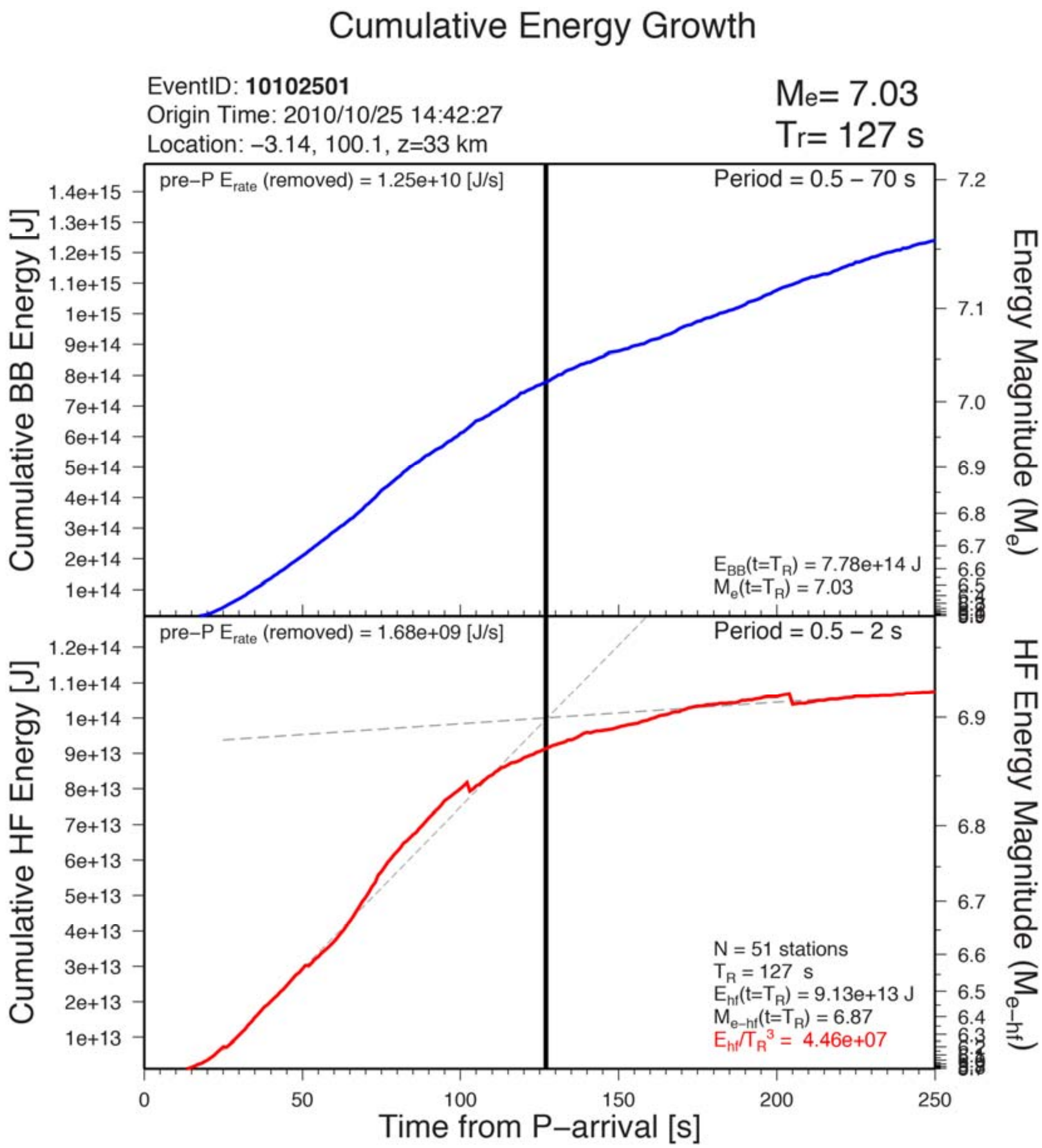

Figure 6.1: Example of final event cumulative energies for the Mentawai 2010 earthquake. High frequency (0.5 – 2 s) and broadband (0.5 – 70 s) cumulative energy plots of the stacked of available stations aligned relative to their theoretical *P*-arrival time. The approximated rupture duration is T_r (taken from T_{XO}, solid vertical black line). At T_r, the cumulative energy is determined for both high frequency and broadband ranges.

6.3.2 Station Used and Their Variation

Each event includes a hemispheric visualization of the stations used for the calculations along with each stations individual deviation from the stacked average energy, calculated as $\log_{10}(E_{station}/E_{average})$. This is prepared routinely for the high-frequency energy range, but can be done as well for the broadband range.

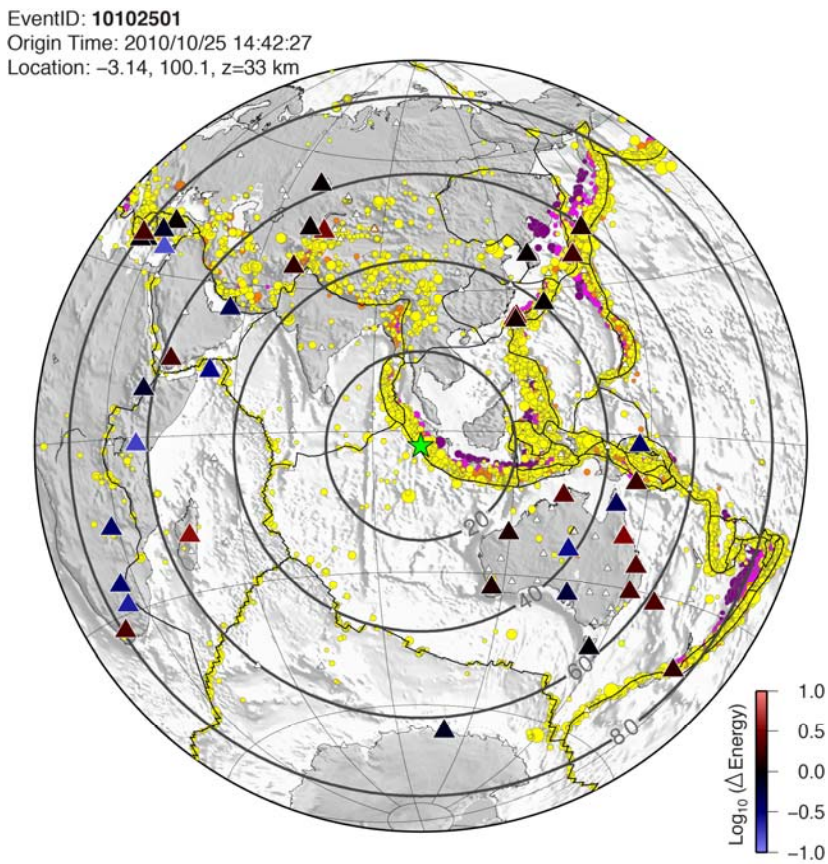

Figure 6.2: Stations used in final energy results for the Mentawai 2010 earthquake. They are colored by their deviation from the mean energy value for the event. The deviation is calculated as $\log_{10}(E_{station}/E_{average})$.

6.3.3 Per-Station Cumulative Energy

For each processed station, we plot its individual cumulative energy growth both for broadband and high frequency determinations normalized relative to each solutions maximum value (**Figure 6.3**). The data are distributed azimuthally and can be used to evaluate potential hemispheric or regional changes (e.g. such as strong directivity effects). Although, as we have examined in the previous chapter, when we assess possible directivity effects and we want to look at apparent *T*r at different azimuths, TACER is preferable, since it allows for easy processing of per-station durations.

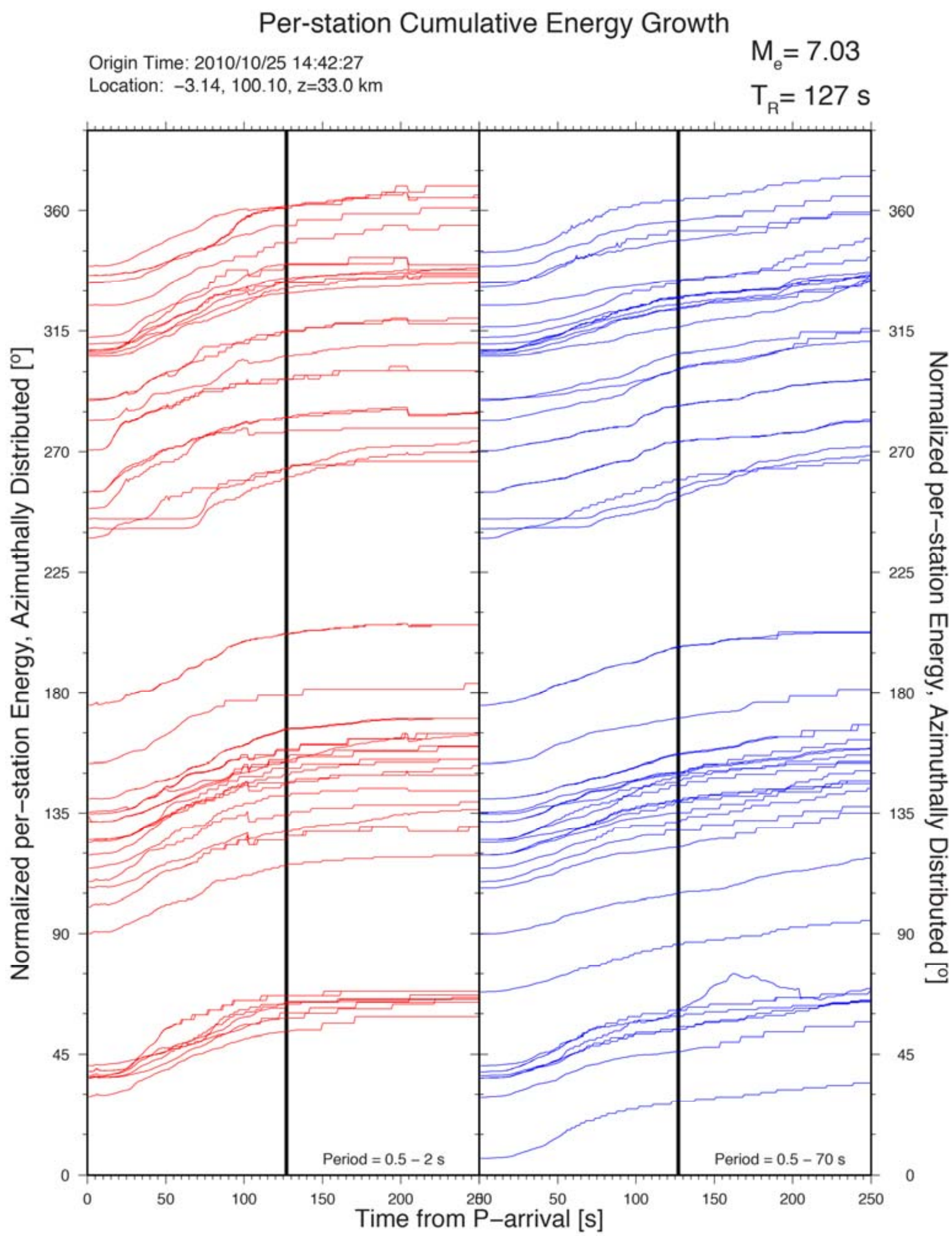

Figure 6.3: Per-station cumulative energy growth distributed azimuthally for the Mentawai 2010 earthquake in high frequency (0.5 – 2 s) and broadband energy (0.5 – 70 s). The cumulative energy for each station is normalized to the maximum per-station value.

6.4 A step forward

As we describe the currently working system we must also not forget that we can improve automated results. The first step fin this improvement is implementing the Time Averaged Cumulative Energy Rate (TACER) into calculations. In the previous chapter, we mentioned that if we are interested in duration estimates only (for which TACER was designed), we could look at the peak in TACER alone and work without the need of some of the corrections (i.e., geometric, focal or energy partitioning), since they are time-independent corrections, and will scale the time history of a station energy flux.

However, making only calculations of energy flux at stations to find the estimated duration at each station, only to later correct and do these calculations again to obtain the cumulative radiated energy seems impractical and time-inefficient. With this in mind, the step forward is, instead of calculating cumulative energy at each station (with all the corrections), we store only ε^* (equation 2.1), and store the geometrical spreading, S to P energy partitioning, and focal corrections separately, since they will vary according to the station, and most importantly, we can store the focal mechanism correction and the estimated focal correction [*Newman and Okal*, 1998]. This last can be especially useful if the focal mechanism is not know at the moment of calculation, and subsequent calculations are to be completed with a rapid focal mechanism (for example, w-phase [*Duputel et al.*, 2012]).

This allows not only obtain a final event T_{TACER}, but azimuthal TACER behavior as well, thus allowing for an examination of possible directivity. Moreover, future preliminary energy calculations can be done at T_{TACER} as well, and look at the energy and θ values, relative to others using the mechanism to calculate T_{TACER}.

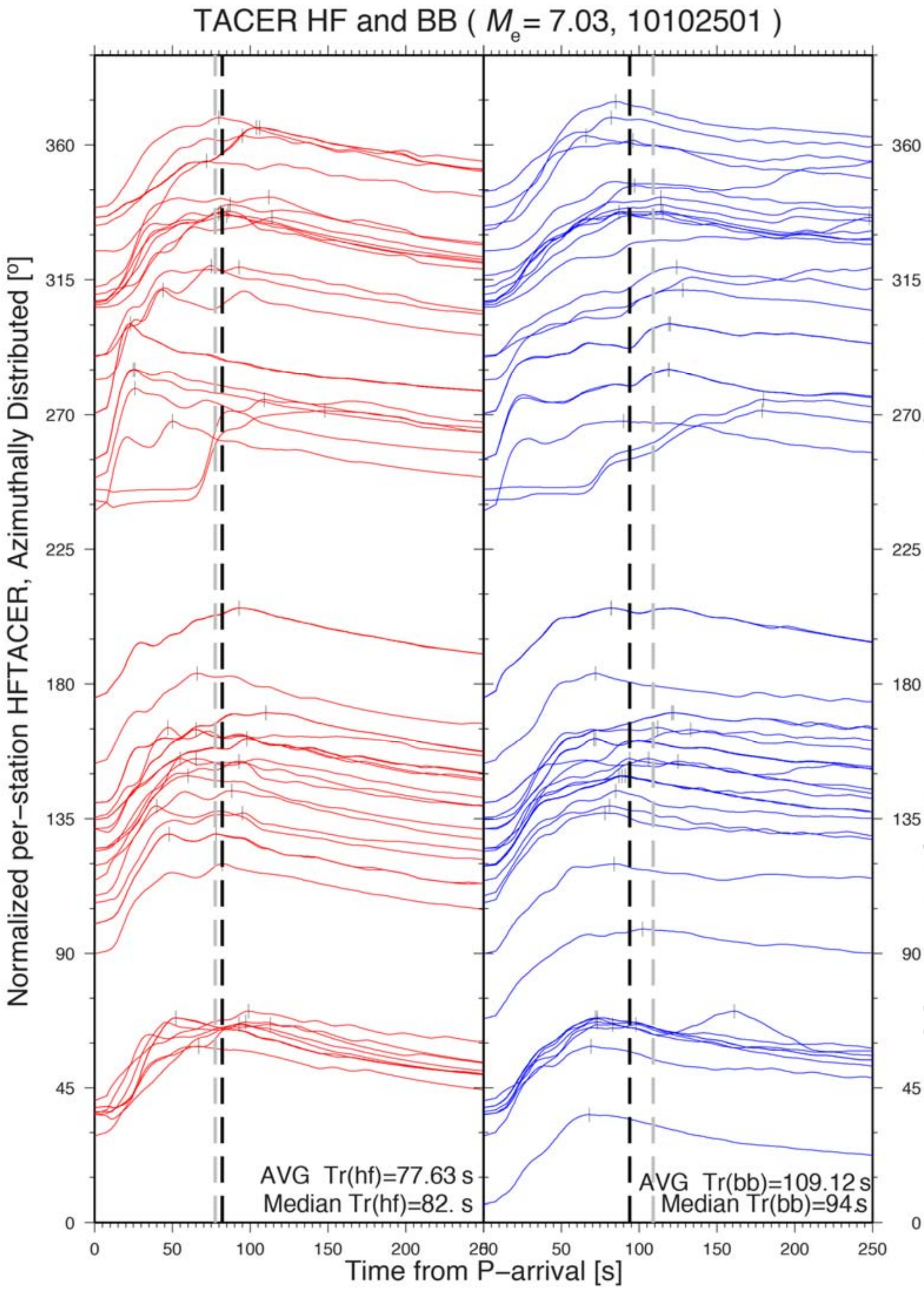

Figure 6.4: Azimuthal distribution of TACER calculated for the same stations used in **Figure 6.3**, TACER functions are calculated at broadband (0.5 – 2 s), and high (0.5 – 2 s) frequency ranges and average and median results are automatically calculated.

For example, for this particular case, with a value of $E(T_{\text{TACER}})$ of $4.83\text{x}10^{14}$ J the Mentawai event yields an energy-to-moment value of $\theta \approx$-6.1, similar to the value of -5.9 found in chapter 4. And with a $E_{\text{hf}}(T_{\text{TACER}})$=$6.43\text{x}10^{13}$ J, and a E_{hf}-T_{r} discriminant of $E_{\text{hf}}/T_{\text{r}}^3$=$1.17\text{x}10^8$ J/s^3, that even though places this event right above the $5\text{x}10^7$ J/s^3 discriminant, it still separates it from the general group trend, enough to trigger a warning.

Also, as we have pointed out the importance of rapid and reliable results, it is possible to make computational steps faster by integrating parallelization into the main scripts and programs. As a station energy result does not depend on the result found in other stations and duration estimates, we can further optimize ε^* results as well as duration estimates by doing multiple station calculations at once, and optimizing the algorithm to apply changes in the focal mechanism correction without recalculating ε^* at the station.

While the energy methods are more problematic at distances less than 25° due to triplication effects, a recent study by *Ebeling and Okal* [2012] suggests that energy calculations can be made at closer distances by applying a distance-based empirical correction that reduces the final energy calculation by up to an order of magnitude at distances less than 10° from the epicenter. Thus, the combination of such a correction with a systematic evaluation of near-field station duration estimates is expected to improve the rapid near-field duration result.

6.5 Special cases

This methodology can be applied to large shallow events with the corrections and approximations specified previously. However, there are some occasions where the depth of the earthquake or size can yield unexpected or unrealistic results. We specify them for reference and advise care must be taken when dealing with these.

6.5.1 Deep Earthquakes

The attenuation corrections used in these calculations are for shallow earthquakes where the direct (*P*) and depth phases (*pP* and *sP*) all travel twice through similar paths. However for deeper earthquakes, the depth phases become distinctly separated from the direct arrival, and are preferentially attenuated because those waves travel twice through the source-side crust, while the direct *P* takes no passes through the source-side crust.

Because the depth phases arrive much later than the direct *P* for deep earthquakes, the duration reported may be artificially lengthened. Alternatively, the algorithms may estimate duration based just on the direct *P*. This duration is more accurate, but again, the ultimate energy determination may be inaccurate as it may not take into account the *pP* and *sP* phases if the *T*r at which the energy is calculated only contains the *P* phase.

6.5.2 Early Aftershocks

While the energy algorithms work well for most events, there are instances where the calculations of energy from early aftershocks or doublets may yield unrealistically high energies due to the contribution of the first event's later arrivals [*Convers and Newman*, 2011], namely surface waves can alter the broadband results.

6.5.3 Complex Ruptures

Because the method relies on the cumulative development of energy through an earth that scatters energy, the energy results are comparable to highly smoothed integrated source-time functions. For events that start with a weaker initial sub-event that is separated significantly in time (e.g. the 2005 Kunlun China earthquake), the duration estimates may be blind to the pause and yield a seemingly excessive duration. Should an event start very strongly, but have a long tail with considerably less energetic rupture, the event may underestimate the true rupture duration. As a note however, in *post priori* tests of the 2004 M_W 9.15 Sumatran earthquake, this was not an issue [*Convers and Newman*, 2011].

6.6 Conclusions

RTerg has been operational since 2009 and two tsunami earthquakes have been identified since its implementation. This methodology and set of programs has proven useful for rapid earthquake energy determinations, rupture duration and possible slow-source identification for the recent Mentawai 2010 and El Salvador 2012 tsunami earthquakes. We show here the main steps of the automated system and provide assessment of potential problems from deep or small earthquakes, as well as complex ruptures, even though this has not been an issue for the largest recorded earthquakes using this method we advice caution when interpreting results from complex ruptures.

APPENDIX A

GLOBAL AND REGIONAL CATALOGS 1997 - 2010

Table A.1 Global Earthquakes with $M_0 \geq$ 1e19 Nm. Earthquakes are ordered by date, with letters identifying subsequent events occurring on the same date. Origin time, location, and focal mechanism information is taken from the gCMT catalog. E_{est} and θ_{est} are the estimated energy and energy-to-moment ratio, calculated without the knowledge of the true focal mechanism, instead with an averaged focal correction as suggested by *Newman and Okal* [1998]. High frequency results (0.5 Hz and 2 Hz), and broad-band results (14 mHz to 2Hz) are shown. σ_g is the $\log_{10}$ of the geometric standard deviation, calculated from all corrected station energies from their corrected average event energy.

General Information									BroabBand (0.5-70s)					High freq. (0.5-2s)	
Event YYDOY	Time hh:mm	Lat	Lon	Depth (km)	$\phi/\delta/\lambda$	$M_0(M_W)$ (Nm)	N	T_{XO} (s)	$E_{est}(M_e)$ (J)	$E(M_e)$ (J)	θ_{est}	θ	σ_g 10^X	$E(M_e)$ (J)	σ_g 10^X
92246a	0:16	11.2	-87.81	15	303/12/ 91	3.4e20(7.6)	13	165	5.5e14(6.9)	6.3e14(7.0)	-5.8	-5.7	0.68	2.4e13(6.0)	0.53
94153a	18:17	-11.03	113.04	15	278/ 7/ 89	5.3e20(7.8)	12	95	6.1e14(7.0)	3.4e14(6.8)	-5.9	-6.2	0.14	2.6e13(6.0)	0.34
96052a	12:51	-9.95	-80.23	15	335/14/ 88	2.2e20(7.5)	45	100	2.8e14(6.7)	5.4e14(6.9)	-5.9	-5.6	0.48	4.2e13(6.2)	0.59
97023a	2:15	-22.04	-65.92	281	85/ 4/185	5.8e19(7.1)	22	25	5.9e14(6.9)	1.2e15(7.2)	-5	-4.7	0.49	8.0e14(7.0)	0.61
97058a	21:08	29.74	68.13	15	298/15/122	5.2e19(7.1)	47	48	5.7e14(6.9)	4.0e14(6.8)	-5	-5.1	0.42	1.4e14(6.5)	0.5
97070a	19:22	7.64	127.63	15	351/38/267	2.2e19(6.8)	22	30	8.8e14(7.1)	9.4e14(7.1)	-4.4	-4.4	0.41	4.2e14(6.8)	0.61
97111a	12:02	-13.21	166.2	51	301/39/ 40	4.4e20(7.7)	11	85	1.3e16(7.8)	2.4e16(8.0)	-4.5	-4.3	0.31	3.5e15(7.5)	0.6
97118a	12:07	-42.03	42.75	15	279/88/ 1	1.5e19(6.7)	12	60	5.3e13(6.2)	2.4e14(6.7)	-5.4	-4.8	0.38	4.9e13(6.2)	0.59
97121a	11:37	18.96	-107.15	15	288/77/174	2.8e19(6.9)	17	30	2.2e14(6.7)	9.4e14(7.1)	-5.1	-4.5	0.52	8.9e13(6.4)	0.48
97123a	16:46	-31.7	-179.06	119	149/42/199	2.8e19(6.9)	12	80	1.8e15(7.3)	2.4e15(7.3)	-4.2	-4.1	0.51	5.8e14(6.9)	0.44
97130a	7:57	33.58	60.02	15	248/83/ 0	7.3e19(7.2)	36	63	9.4e14(7.1)	4.1e15(7.5)	-4.9	-4.2	0.42	1.0e15(7.1)	0.5
97141a	14:10	-20.34	169.03	64	268/47/ 3	1.4e19(6.7)	11	49	1.6e14(6.6)	3.6e14(6.8)	-4.9	-4.6	0.2	1.4e14(6.5)	0.34
97145a	23:22	-32.02	-179.95	345	236/44/158	5.2e19(7.1)	17	24	1.3e15(7.2)	2.0e15(7.3)	-4.6	-4.4	0.71	1.0e15(7.1)	0.71
97187a	9:54	-30.22	-72.21	15	0/21/ 92	1.9e19(6.8)	11	52	6.9e13(6.3)	1.1e14(6.5)	-5.4	-5.2	0.16	1.7e13(5.9)	0.57
97190a	19:24	10.7	-63.63	15	266/62/183	3.1e19(6.9)	34	48	1.2e14(6.5)	3.2e14(6.8)	-5.4	-5	0.45	8.2e13(6.4)	0.43
97200a	14:22	15.86	-98.26	15	282/14/ 78	1.2e19(6.7)	8	36	3.7e13(6.1)	2.5e13(6.0)	-5.5	-5.7	0.44	2.4e12(5.4)	0.29
97245a	12:13	4	-75.57	213	256/48/ 62	1.6e19(6.7)	26	22	4.4e14(6.9)	6.0e14(7.0)	-4.6	-4.4	0.46	4.2e14(6.8)	0.5
97247a	4:23	-26.45	178.52	621	235/12/296	2.1e19(6.8)	17	22	2.9e15(7.4)	3.4e15(7.4)	-3.9	-3.8	0.48	2.8e15(7.4)	0.6
97263a	16:11	-28.83	-176.99	46	195/29/ 90	3.5e19(7.0)	14	30	4.8e14(6.9)	2.9e14(6.7)	-4.9	-5.1	0.29	7.0e13(6.3)	0.63
97287a	9:53	-21.94	-176.15	165	257/17/330	4.5e20(7.7)	16	25	1.3e16(7.8)	1.5e16(7.9)	-4.5	-4.5	0.39	3.1e15(7.4)	0.68
97288a	1:03	-31.06	-71.42	69	315/12/232	4.9e19(7.1)	16	50	6.2e15(7.6)	1.2e16(7.8)	-3.9	-3.6	0.59	3.6e15(7.5)	0.46
97301a	6:15	-4.44	-76.55	118	339/38/271	7.2e19(7.2)	25	71	2.7e15(7.4)	2.4e15(7.4)	-4.4	-4.5	0.4	8.2e14(7.0)	0.48
97312a	10:02	35.33	86.96	16	79/69/ 2	2.2e20(7.5)	41	41	4.3e14(6.9)	1.8e15(7.3)	-5.7	-5.1	0.28	2.4e14(6.7)	0.51
97319a	18:59	-14.92	167.21	121	357/42/ 75	4.2e19(7.0)	24	83	2.7e15(7.4)	2.9e15(7.4)	-4.2	-4.2	0.3	5.8e14(6.9)	0.54
97329a	12:14	1.37	122.71	29	98/21/ 93	4.1e19(7.0)	23	46	1.0e15(7.1)	1.1e15(7.1)	-4.6	-4.6	0.5	1.2e14(6.5)	0.53
97339a	11:26	54.31	161.91	33	202/23/ 74	5.3e20(7.8)	38	62	4.8e15(7.6)	3.6e15(7.5)	-5	-5.2	0.39	9.4e14(7.1)	0.48
97356a	2:05	-5.56	148.05	196	318/67/196	6.2e19(7.1)	25	40	2.4e15(7.4)	6.9e15(7.7)	-4.4	-4	0.52	2.1e15(7.3)	0.68

Table A.1 (continued)

98004a	6:11	-22.31	171.08	114	348/47/160	1.8e20(7.4)	21	40	6.0e15(7.6)	1.1e16(7.8)	-4.5	-4.2	0.52	2.7e15(7.4)	0.78
98012a	16:36	-15.78	-179.19	15	165/88/180	1.2e19(6.7)	12	36	7.2e13(6.3)	3.3e14(6.8)	-5.2	-4.6	0.44	4.2e13(6.2)	0.73
98030a	12:16	-24.02	-70.62	41	8/17/105	4.4e19(7.0)	20	41	1.3e15(7.2)	2.3e15(7.3)	-4.5	-4.3	0.55	6.5e14(7.0)	0.55
98048a	00:-6	52.76	-33.78	15	184/70/349	1.5e19(6.7)	15	27	5.9e13(6.3)	2.2e14(6.7)	-5.4	-4.8	0.4	9.2e13(6.4)	0.45
98079a	21:08	-50.06	162.89	15	48/77/173	1.3e19(6.7)	7	40	7.0e13(6.3)	3.0e14(6.7)	-5.3	-4.6	0.21	1.3e14(6.5)	0.39
98084a	3:12	-62.99	148.64	28	189/73/174	1.7e21(8.1)	22	127	3.5e16(8.1)	1.4e17(8.5)	-4.7	-4.1	0.61	1.8e16(7.9)	0.53
98088a	19:48	-17.57	-178.85	553	359/53/156	6.4e19(7.1)	28	63	5.9e15(7.6)	1.2e16(7.8)	-4	-3.7	0.45	3.0e15(7.4)	0.68
98091a	17:56	-0.78	98.84	41	320/21/105	3.3e19(6.9)	37	34	4.7e14(6.9)	3.8e14(6.8)	-4.8	-4.9	0.31	1.3e14(6.5)	0.5
98091b	22:42	-40.64	-75.37	15	199/44/272	1.2e19(6.7)	15	24	2.7e14(6.7)	2.5e14(6.7)	-4.6	-4.7	0.52	5.2e13(6.2)	0.67
98123a	23:30	22.37	125.53	22	139/82/ 1	1.8e20(7.4)	29	50	2.4e15(7.3)	1.1e16(7.8)	-4.9	-4.2	0.44	3.0e15(7.4)	0.52
98136a	2:22	-22.27	-179.35	608	154/ 8/223	2.3e19(6.8)	27	22	2.5e15(7.4)	2.3e15(7.3)	-4	-4	0.51	1.7e15(7.3)	0.65
98190a	14:45	-30.51	-178.71	154	221/17/295	2.4e19(6.8)	17	23	5.8e14(6.9)	5.7e14(6.9)	-4.6	-4.6	0.39	3.5e14(6.8)	0.54
98197a	11:56	-10.91	166.09	100	37/38/105	4.1e19(7.0)	32	48	2.2e15(7.3)	2.7e15(7.4)	-4.3	-4.2	0.3	3.0e14(6.7)	0.59
98198a	8:49	-2.5	142.07	15	146/19/127	3.7e19(7.0)	7	62	1.1e14(6.5)	7.2e13(6.3)	-5.5	-5.7	0.33	1.4e13(5.9)	0.58
98210a	18:00	-2.72	138.99	25	53/ 6/ 24	1.2e19(6.7)	29	51	1.5e14(6.5)	2.3e14(6.7)	-4.9	-4.7	0.52	3.1e13(6.1)	0.77
98216a	18:59	-0.57	-80.48	25	27/15/124	6.4e19(7.1)	21	42	7.1e14(7.0)	1.8e15(7.3)	-5	-4.6	0.4	1.9e14(6.6)	0.57
98232a	6:40	28.99	139.47	425	83/27/198	4.7e19(7.0)	31	28	1.4e15(7.2)	2.8e15(7.4)	-4.5	-4.2	0.59	1.9e15(7.3)	0.71
98235a	13:57	11.58	-88.55	15	120/45/254	1.2e19(6.7)	27	47	4.4e14(6.9)	4.3e14(6.9)	-4.4	-4.4	0.63	4.0e13(6.2)	0.65
98245a	8:37	5.43	126.95	40	255/42/115	2.1e19(6.8)	28	37	1.0e15(7.1)	1.2e15(7.1)	-4.3	-4.2	0.55	2.8e14(6.7)	0.64
98313a	5:30	-7.05	128.75	15	134/56/141	1.4e19(6.7)	27	31	2.4e14(6.7)	4.4e14(6.9)	-4.8	-4.5	0.41	6.1e13(6.3)	0.63
98313b	5:38	-6.94	128.95	24	289/37/111	3.9e19(7.0)	26	38	1.5e15(7.2)	1.3e15(7.2)	-4.4	-4.5	0.34	1.3e14(6.5)	0.67
98333a	14:10	-2.03	125	16	92/63/332	4.5e20(7.7)	18	60	5.7e15(7.6)	1.4e16(7.9)	-4.9	-4.5	0.32	7.1e14(7.0)	0.57
98361a	0:38	-21.69	-175.86	159	274/22/342	2.0e19(6.8)	24	20	7.6e14(7.0)	8.6e14(7.1)	-4.4	-4.4	0.51	3.8e14(6.8)	0.72
99019a	3:35	-4.72	153.66	87	143/31/ 87	3.7e19(7.0)	17	54	3.8e14(6.8)	4.0e14(6.8)	-5	-5	0.43	1.3e14(6.5)	0.66
99037a	21:47	-12.78	166.58	98	304/33/ 41	1.1e20(7.3)	17	49	7.6e15(7.7)	1.3e16(7.8)	-4.2	-3.9	0.36	1.6e15(7.2)	0.51
99063a	8:52	5.38	122.03	18	340/37/ 84	4.9e19(7.1)	30	35	1.0e15(7.1)	1.0e15(7.1)	-4.7	-4.7	0.39	2.2e14(6.7)	0.65
99067a	12:25	51.75	159.87	15	242/28/101	2.6e19(6.9)	38	44	1.8e14(6.6)	1.4e14(6.5)	-5.2	-5.3	0.26	1.2e13(5.8)	0.57
99079a	10:47	51.67	-177.3	43	272/30/116	2.7e19(6.9)	52	47	3.7e14(6.8)	3.6e14(6.8)	-4.9	-4.9	0.57	9.5e13(6.4)	0.73
99093a	6:17	-16.38	-72.54	89	112/20/273	2.0e19(6.8)	32	51	8.3e14(7.0)	1.1e15(7.1)	-4.4	-4.3	0.5	3.2e14(6.8)	0.53
99095a	11:08	-5.65	149.71	149	248/17/ 65	1.5e20(7.4)	30	28	3.8e15(7.5)	3.4e15(7.5)	-4.6	-4.6	0.35	5.7e14(6.9)	0.68
99098a	13:10	43.66	130.47	575	81/25/160	5.1e19(7.1)	69	25	6.6e15(7.6)	1.1e16(7.8)	-3.9	-3.7	0.58	8.8e15(7.7)	0.65
99103a	10:38	-21.54	-175.89	172	272/15/346	1.9e19(6.8)	26	30	7.3e14(7.0)	8.2e14(7.0)	-4.4	-4.4	0.51	4.4e14(6.9)	0.71
99130a	20:33	-5.38	150.97	144	202/47/234	4.7e19(7.0)	33	54	2.9e15(7.4)	3.6e15(7.5)	-4.2	-4.1	0.39	6.4e14(7.0)	0.72
99136a	0:51	-4.99	152.76	42	262/28/ 96	4.5e19(7.0)	22	74	5.2e14(6.9)	4.4e14(6.9)	-4.9	-5	0.36	1.1e14(6.5)	0.43
99166a	20:42	18.44	-97.38	61	309/40/277	3.1e19(6.9)	32	65	9.1e14(7.1)	7.9e14(7.0)	-4.5	-4.6	0.55	2.8e14(6.7)	0.5
99192a	14:14	16.04	-88.53	15	347/79/190	1.2e19(6.7)	24	35	5.0e13(6.2)	2.2e14(6.7)	-5.4	-4.7	0.31	9.6e13(6.4)	0.36
99229a	0:01	41.01	29.97	17	182/74/ 3	2.9e20(7.6)	25	51	7.2e14(7.0)	3.3e15(7.4)	-5.6	-4.9	0.38	4.7e14(6.9)	0.56
99232a	10:02	9.28	-84.1	24	306/27/102	2.6e19(6.9)	30	86	2.4e14(6.7)	1.5e14(6.5)	-5	-5.2	0.23	1.2e13(5.8)	0.57
99263a	17:47	24.15	120.8	21	37/25/ 96	3.4e20(7.6)	38	45	5.3e15(7.6)	7.0e15(7.7)	-4.8	-4.7	0.45	5.4e14(6.9)	0.63
99273a	16:31	16.2	-96.96	46	102/42/257	1.7e20(7.4)	42	33	1.8e15(7.3)	1.8e15(7.3)	-5	-5	0.34	4.8e14(6.9)	0.53

Table A.1 (continued)

99289a	9:46	34.71	-116.27	15	336/80/174	6.0e19(7.1)	20	30	1.4e14(6.5)	6.8e14(7.0)	-5.6	-4.9	0.25	1.9e14(6.6)	0.44
99316a	16:57	40.93	31.25	18	268/54/193	6.7e19(7.2)	39	32	4.5e14(6.9)	1.2e15(7.1)	-5.2	-4.8	0.31	9.3e13(6.4)	0.58
99319a	5:42	-1.21	88.89	15	12/76/349	3.3e19(6.9)	74	36	4.1e14(6.8)	1.8e15(7.3)	-4.9	-4.3	0.42	5.1e14(6.9)	0.58
99321a	3:27	-6.27	149.03	38	279/35/103	2.9e19(6.9)	29	50	4.0e14(6.8)	3.7e14(6.8)	-4.9	-4.9	0.5	1.0e14(6.4)	0.63
99323a	13:56	-6.49	148.98	33	275/25/100	4.0e19(7.0)	28	69	3.7e14(6.8)	3.7e14(6.8)	-5	-5	0.58	6.1e13(6.3)	0.92
99330a	13:21	-16.08	168.31	15	174/30/ 67	1.7e20(7.4)	20	64	3.0e15(7.4)	2.4e15(7.3)	-4.8	-4.9	0.34	3.2e14(6.8)	0.4
99340a	23:12	57.35	-154.35	54	357/63/180	3.5e19(7.0)	32	41	2.3e15(7.3)	7.8e15(7.7)	-4.2	-3.7	0.51	3.4e15(7.5)	0.62
99345a	18:03	15.87	119.64	35	112/13/191	8.9e19(7.2)	67	46	2.9e15(7.4)	3.0e15(7.4)	-4.5	-4.5	0.41	4.2e14(6.8)	0.64
99363a	13:29	-11.14	165.19	15	347/23/120	2.3e19(6.8)	16	59	1.5e14(6.5)	1.9e14(6.6)	-5.2	-5.1	0.44	1.9e13(6.0)	0.75
00008a	16:47	-16.84	-173.81	162	79/ 8/347	6.9e19(7.2)	5	24	1.4e15(7.2)	1.8e15(7.3)	-4.7	-4.6	0.13	7.5e14(7.0)	0.18
00028a	14:21	43.08	146.81	50	163/38/ 15	2.0e19(6.8)	16	42	4.2e14(6.9)	1.5e15(7.2)	-4.7	-4.1	0.22	6.6e14(7.0)	0.34
00056a	1:43	-19.55	174.17	16	315/74/169	5.1e19(7.1)	22	33	3.6e14(6.8)	1.4e15(7.2)	-5.1	-4.5	0.29	1.6e14(6.6)	0.34
00088a	11:00	22.32	143.76	99	255/ 6/233	3.2e20(7.6)	40	40	1.1e16(7.8)	1.2e16(7.8)	-4.5	-4.4	0.45	4.8e15(7.5)	0.5
00114a	9:27	-28.41	-63.04	607	290/ 5/210	3.1e19(6.9)	59	21	2.2e15(7.3)	5.6e15(7.6)	-4.2	-3.7	0.41	4.8e15(7.6)	0.45
00125a	4:21	-1.29	123.59	18	225/64/172	2.4e20(7.5)	32	64	5.9e15(7.6)	2.0e16(8.0)	-4.6	-4.1	0.33	7.1e15(7.7)	0.45
00133a	18:43	-23.72	-66.85	226	214/12/298	6.6e19(7.1)	87	20	8.2e14(7.0)	9.4e14(7.1)	-4.9	-4.8	0.38	3.6e14(6.8)	0.56
00156a	16:28	-4.73	101.94	43	92/55/152	7.5e20(7.8)	33	79	3.3e16(8.1)	6.6e16(8.3)	-4.4	-4.1	0.47	3.0e16(8.1)	0.61
00159a	23:45	-4.63	101.82	16	358/34/ 78	1.3e19(6.7)	57	42	3.6e14(6.8)	4.7e14(6.9)	-4.6	-4.4	0.47	2.2e14(6.7)	0.59
00170a	14:44	-13.47	97.17	15	161/63/355	7.9e20(7.9)	39	48	5.5e15(7.6)	1.9e16(8.0)	-5.2	-4.6	0.28	3.0e15(7.4)	0.46
00217a	21:13	48.77	142.03	15	328/36/ 60	1.9e19(6.8)	122	31	1.7e14(6.6)	2.3e14(6.7)	-5	-4.9	0.41	3.4e13(6.1)	0.47
00219a	7:27	28.89	139.68	411	108/27/218	1.2e20(7.3)	68	24	2.8e15(7.4)	3.5e15(7.5)	-4.6	-4.5	0.52	2.6e15(7.4)	0.58
00241a	15:05	-4.18	127.59	15	292/31/116	1.7e19(6.8)	34	38	2.8e14(6.7)	2.6e14(6.7)	-4.8	-4.8	0.41	6.5e13(6.3)	0.41
00278a	16:58	-15.51	166.77	15	341/44/ 94	3.0e19(6.9)	31	30	2.2e14(6.7)	2.1e14(6.6)	-5.1	-5.2	0.31	6.0e13(6.3)	0.45
00280a	4:30	35.33	133.2	15	331/83/ 1	1.2e19(6.7)	56	39	5.7e13(6.3)	2.7e14(6.7)	-5.3	-4.7	0.45	8.2e13(6.4)	0.56
00303a	8:37	-5.21	153.95	92	142/27/ 90	3.0e19(6.9)	30	63	2.8e14(6.7)	3.2e14(6.8)	-5	-5	0.52	1.2e14(6.5)	0.57
00312a	0:18	-55.34	-29.24	16	113/24/103	1.6e19(6.7)	18	30	1.5e14(6.5)	2.3e14(6.7)	-5	-4.8	0.37	3.7e13(6.1)	0.65
00321a	4:54	-4.56	152.79	24	328/43/ 3	1.2e21(8.0)	25	84	5.1e15(7.6)	6.2e15(7.6)	-5.4	-5.3	0.39	1.6e15(7.2)	0.5
00321b	7:42	-5.03	153.17	31	253/15/ 93	6.5e20(7.8)	35	76	2.9e15(7.4)	3.0e15(7.4)	-5.3	-5.3	0.33	7.1e14(7.0)	0.52
00322a	21:01	-5.26	152.34	17	230/24/ 64	5.6e20(7.8)	38	95	1.1e15(7.1)	7.2e14(7.0)	-5.7	-5.9	0.28	1.6e14(6.6)	0.52
00323a	6:54	-5.43	151.85	50	243/37/ 75	1.6e19(6.7)	36	41	1.5e14(6.5)	1.5e14(6.5)	-5	-5	0.47	5.3e13(6.2)	0.57
00330a	18:09	40.24	49.95	15	93/ 2/215	1.8e19(6.8)	43	45	5.7e13(6.3)	6.8e13(6.3)	-5.5	-5.4	0.5	3.5e13(6.1)	0.61
00341a	17:11	39.6	54.87	33	319/33/136	3.9e19(7.0)	51	30	9.6e14(7.1)	1.2e15(7.2)	-4.6	-4.5	0.33	4.4e14(6.9)	0.51
01001a	6:57	6.73	127.07	44	171/45/ 60	1.7e20(7.4)	24	69	2.4e15(7.4)	2.5e15(7.4)	-4.8	-4.8	0.53	9.1e14(7.1)	0.62
01001b	8:54	7.12	127.13	44	34/34/147	1.8e19(6.8)	28	52	2.1e13(6.0)	2.5e13(6.0)	-5.9	-5.9	0.56	5.1e12(5.6)	0.65
01009a	16:49	-14.9	167.11	114	183/44/160	4.2e19(7.0)	20	55	2.1e15(7.3)	3.9e15(7.5)	-4.3	-4	0.31	1.2e15(7.2)	0.36
01010a	16:02	56.99	-153.56	21	224/ 8/ 74	3.3e19(6.9)	37	47	2.0e14(6.6)	3.1e14(6.8)	-5.2	-5	0.3	1.0e14(6.4)	0.55
01013a	17:33	12.97	-89.13	56	121/35/265	4.6e20(7.7)	15	48	1.7e16(7.9)	1.7e16(7.9)	-4.4	-4.4	0.17	1.3e15(7.2)	0.54
01016a	13:25	-4.38	101.42	20	321/14/111	2.0e19(6.8)	24	41	2.0e14(6.6)	2.1e14(6.6)	-5	-5	0.44	9.1e13(6.4)	0.6
01026a	3:16	23.63	70.24	19	298/39/136	3.4e20(7.6)	24	26	8.7e15(7.7)	9.1e15(7.7)	-4.6	-4.6	0.34	1.0e15(7.1)	0.65
01044a	19:28	-5.4	102.36	21	315/16/103	1.2e20(7.3)	26	63	1.0e15(7.1)	1.1e15(7.1)	-5.1	-5.1	0.42	4.3e14(6.9)	0.55

Table A.1 (continued)

01055a	7:23	1.55	126.42	42	197/42/ 78	4.5e19(7.0)	24	39	1.0e15(7.1)	9.4e14(7.1)	-4.6	-4.7	0.22	3.0e14(6.8)	0.45
01059a	18:54	47.14	-122.53	46	176/17/264	1.8e19(6.8)	36	31	3.2e14(6.8)	3.3e14(6.8)	-4.7	-4.7	0.36	1.7e14(6.6)	0.47
01083a	6:27	33.97	132.52	47	323/39/239	2.0e19(6.8)	27	47	2.9e14(6.7)	3.3e14(6.8)	-4.8	-4.8	0.49	1.8e14(6.6)	0.56
01118a	4:49	-18.07	-176.68	367	106/16/161	2.1e19(6.8)	20	15	8.5e14(7.1)	1.1e15(7.1)	-4.4	-4.3	0.61	8.2e14(7.0)	0.63
01145a	0:40	44.18	148.61	32	230/22/113	1.3e19(6.7)	30	47	8.9e13(6.4)	1.2e14(6.5)	-5.2	-5	0.37	3.0e13(6.1)	0.51
01154a	2:41	-29.37	-178.23	199	227/41/138	6.1e19(7.1)	21	21	2.0e15(7.3)	2.8e15(7.4)	-4.5	-4.3	0.55	1.3e15(7.2)	0.69
01174a	20:33	-17.28	-72.71	29	310/18/ 63	4.7e21(8.4)	16	145	2.0e16(8.0)	3.7e16(8.1)	-5.4	-5.1	0.37	7.0e15(7.7)	0.46
01177a	4:18	-17.87	-72.02	24	314/19/ 75	1.4e19(6.7)	17	45	1.6e14(6.6)	2.7e14(6.7)	-4.9	-4.7	0.25	5.9e13(6.3)	0.48
01188a	9:38	-17.45	-72.45	25	306/14/ 52	3.2e20(7.6)	16	66	1.9e15(7.3)	4.7e15(7.5)	-5.2	-4.8	0.29	5.9e14(6.9)	0.47
01218a	3:52	-55.67	-123.05	15	104/45/277	1.4e19(6.7)	18	24	5.3e13(6.2)	5.2e13(6.2)	-5.4	-5.4	0.31	1.0e13(5.8)	0.29
01233a	6:52	-36.7	-179.08	59	55/42/116	5.2e19(7.1)	9	72	2.9e15(7.4)	4.0e15(7.5)	-4.2	-4.1	0.2	1.4e15(7.2)	0.16
01285a	15:02	12.88	145.08	42	131/30/ 31	3.7e19(7.0)	36	48	2.2e15(7.3)	2.9e15(7.4)	-4.2	-4.1	0.38	3.9e14(6.8)	0.64
01292a	3:28	-4.31	124.11	18	358/77/176	1.9e20(7.5)	25	67	1.5e15(7.2)	6.7e15(7.7)	-5.1	-4.4	0.29	1.3e15(7.2)	0.52
01304a	9:10	-6.27	150.33	35	266/25/ 95	3.0e19(6.9)	30	40	2.2e14(6.7)	2.4e14(6.7)	-5.1	-5.1	0.55	3.1e13(6.1)	0.77
01318a	9:26	35.8	92.91	15	94/61/348	5.9e20(7.8)	40	150	1.4e15(7.2)	4.6e15(7.5)	-5.6	-5.1	0.27	8.1e14(7.0)	0.5
01346a	14:02	-42.69	124.67	16	349/82/ 6	4.7e19(7.0)	18	28	5.0e14(6.9)	2.2e15(7.3)	-5	-4.3	0.44	8.4e14(7.0)	0.5
01352a	4:02	24	122.79	16	329/47/225	2.1e19(6.8)	42	58	6.2e14(7.0)	9.2e14(7.1)	-4.5	-4.4	0.41	1.6e14(6.6)	0.56
01357a	22:52	-9.63	159.5	18	311/23/ 54	2.1e19(6.8)	21	53	4.1e14(6.8)	6.1e14(7.0)	-4.7	-4.5	0.24	9.7e13(6.4)	0.34
02002a	17:22	-17.78	167.85	40	299/18/ 22	7.7e19(7.2)	18	50	2.5e15(7.4)	3.8e15(7.5)	-4.5	-4.3	0.32	7.4e14(7.0)	0.43
02010a	11:14	-3.21	142.68	18	105/33/ 33	1.4e19(6.7)	32	53	1.9e14(6.6)	3.2e14(6.8)	-4.9	-4.6	0.37	7.7e13(6.4)	0.46
02062a	12:08	36.57	70.42	228	282/22/ 85	1.3e20(7.3)	44	60	7.7e15(7.7)	7.7e15(7.7)	-4.2	-4.2	0.43	2.9e15(7.4)	0.57
02064a	21:16	5.92	124.25	28	314/25/ 70	1.9e20(7.5)	29	83	2.1e15(7.3)	2.8e15(7.4)	-5	-4.8	0.27	7.2e14(7.0)	0.48
02090a	6:52	24.19	121.96	39	292/32/121	5.5e19(7.1)	52	49	9.2e14(7.1)	8.5e14(7.1)	-4.8	-4.8	0.41	1.5e14(6.5)	0.58
02108a	5:02	16.79	-101.22	15	291/ 9/ 89	1.5e19(6.7)	35	93	9.4e13(6.4)	9.6e13(6.4)	-5.2	-5.2	0.6	1.3e13(5.8)	0.77
02116a	16:06	13.15	144.67	69	172/ 3/ 11	4.3e19(7.0)	32	50	2.0e15(7.3)	1.8e15(7.3)	-4.3	-4.4	0.45	6.1e14(7.0)	0.61
02168a	21:26	-12.49	166.25	44	163/38/ 81	1.4e19(6.7)	30	55	2.2e14(6.7)	2.0e14(6.6)	-4.8	-4.8	0.36	7.0e13(6.3)	0.51
02179a	17:19	43.74	130.45	581	27/13/105	1.1e20(7.3)	55	25	1.5e16(7.9)	2.1e16(8.0)	-3.9	-3.7	0.61	1.9e16(7.9)	0.65
02231a	11:01	-21.74	-179.08	630	149/22/219	3.5e20(7.6)	36	25	6.8e16(8.3)	6.0e16(8.3)	-3.7	-3.8	0.39	4.1e16(8.2)	0.41
02231b	11:08	-24.16	178.49	699	50/ 3/ 83	4.3e20(7.7)	33	20	5.8e16(8.3)	6.9e16(8.3)	-3.9	-3.8	0.31	4.4e16(8.2)	0.39
02251a	18:44	-3.27	143.38	19	106/34/ 43	2.9e20(7.6)	37	82	5.3e15(7.6)	9.4e15(7.7)	-4.7	-4.5	0.31	5.6e14(6.9)	0.5
02283a	10:50	-1.79	134.3	15	60/83/ 4	2.6e20(7.5)	27	100	3.6e15(7.5)	1.7e16(7.9)	-4.9	-4.2	0.27	3.2e15(7.4)	0.6
02285a	20:09	-8.3	-71.66	539	353/40/285	2.4e19(6.8)	44	35	1.4e15(7.2)	1.3e15(7.2)	-4.2	-4.3	0.48	1.0e15(7.1)	0.55
02306a	1:26	2.65	95.99	23	297/16/ 73	9.0e19(7.2)	43	70	2.2e15(7.3)	2.0e15(7.3)	-4.6	-4.6	0.5	6.7e14(7.0)	0.77
02307a	22:12	63.23	-144.89	15	296/71/171	7.5e20(7.8)	72	80	4.9e15(7.6)	1.8e16(7.9)	-5.2	-4.6	0.37	5.7e15(7.6)	0.5
02321a	4:53	47.81	146.45	479	316/ 9/ 30	1.1e20(7.3)	71	20	7.9e15(7.7)	9.6e15(7.8)	-4.1	-4.1	0.49	6.7e15(7.6)	0.58
03022a	2:06	18.86	-103.9	26	308/12/110	2.0e20(7.5)	34	50	2.5e15(7.4)	2.4e15(7.4)	-4.9	-4.9	0.42	1.6e14(6.6)	0.63
03070a	7:27	-4.52	153.08	37	324/60/ 21	1.9e19(6.8)	35	63	1.9e14(6.6)	4.6e14(6.9)	-5	-4.6	0.49	2.2e14(6.7)	0.58
03076a	16:36	51.33	177.58	27	289/22/137	4.2e19(7.0)	47	60	2.2e14(6.7)	3.3e14(6.8)	-5.3	-5.1	0.33	1.2e14(6.5)	0.5
03124a	13:15	-30.65	-177.73	41	200/28/ 97	1.2e19(6.7)	37	38	3.6e14(6.8)	3.1e14(6.8)	-4.5	-4.6	0.65	1.2e14(6.5)	0.68
03146a	9:24	38.94	141.57	61	352/19/ 70	3.9e19(7.0)	48	55	3.5e15(7.5)	4.4e15(7.5)	-4	-4	0.5	1.4e15(7.2)	0.67

Table A.1 (continued)

03146b	19:23	2.61	128.88	34	326/36/ 60	3.1e19(6.9)	35	48	1.0e15(7.1)	1.2e15(7.1)	-4.5	-4.4	0.43	3.2e14(6.8)	0.65
03146c	23:13	6.9	123.85	579	227/24/342	2.3e19(6.8)	42	56	1.3e15(7.2)	2.1e15(7.3)	-4.2	-4	0.46	1.4e15(7.2)	0.53
03167a	22:08	55.48	160.25	180	123/32/199	2.4e19(6.8)	62	52	4.8e14(6.9)	7.1e14(7.0)	-4.7	-4.5	0.41	2.6e14(6.7)	0.61
03171a	6:19	-7.37	-71.89	556	353/47/295	4.4e19(7.0)	41	25	1.2e15(7.1)	1.1e15(7.1)	-4.6	-4.6	0.53	9.3e14(7.1)	0.56
03171b	13:30	-30.88	-71.97	35	1/27/ 93	1.8e19(6.8)	37	40	4.6e14(6.9)	6.2e14(7.0)	-4.6	-4.5	0.28	1.4e14(6.5)	0.46
03174a	12:12	51.55	176.6	28	298/25/142	2.6e19(6.9)	53	48	3.1e14(6.8)	5.3e14(6.9)	-4.9	-4.7	0.36	1.8e14(6.6)	0.5
03196a	20:27	-1.42	69.47	15	307/69/ 1	2.5e20(7.5)	49	85	1.3e15(7.2)	4.5e15(7.5)	-5.3	-4.7	0.25	8.3e14(7.0)	0.39
03216a	4:37	-60.8	-43.21	15	101/36/337	2.7e20(7.5)	20	52	2.6e15(7.4)	4.3e15(7.5)	-5	-4.8	0.29	1.1e15(7.1)	0.48
03233a	12:12	-45.01	166.87	31	35/23/ 95	7.5e19(7.2)	37	40	1.5e15(7.2)	2.2e15(7.3)	-4.7	-4.5	0.37	7.2e14(7.0)	0.51
03268a	19:50	42.21	143.84	28	250/11/132	3.1e21(8.3)	69	95	2.2e16(8.0)	3.5e16(8.1)	-5.2	-4.9	0.35	4.3e15(7.5)	0.55
03268b	21:08	41.75	143.62	47	208/18/ 86	1.3e20(7.3)	48	69	2.8e15(7.4)	3.0e15(7.4)	-4.7	-4.6	0.42	2.7e14(6.7)	0.55
03270a	11:33	50.02	87.86	15	228/70/ 20	9.4e19(7.2)	91	50	1.3e15(7.2)	3.6e15(7.5)	-4.9	-4.4	0.48	1.3e15(7.2)	0.65
03304a	1:06	37.89	142.68	15	196/ 9/ 80	3.5e19(7.0)	51	60	1.9e14(6.6)	2.9e14(6.7)	-5.3	-5.1	0.38	6.4e13(6.3)	0.55
03344a	4:38	22.94	121.43	25	221/44/113	2.0e19(6.8)	39	35	2.7e14(6.7)	2.8e14(6.7)	-4.9	-4.9	0.44	9.8e13(6.4)	0.71
03360a	21:26	-22.33	169.39	15	131/41/265	1.6e19(6.7)	15	35	2.7e14(6.7)	2.3e14(6.7)	-4.8	-4.8	0.26	3.6e13(6.1)	0.39
03361a	16:00	-21.99	169.81	23	324/29/ 95	9.5e19(7.2)	17	55	5.2e14(6.9)	8.4e14(7.0)	-5.3	-5.1	0.28	1.5e14(6.5)	0.47
03361b	22:38	-21.71	169.75	24	319/31/ 79	1.4e19(6.7)	26	50	1.2e14(6.5)	2.1e14(6.6)	-5	-4.8	0.25	4.8e13(6.2)	0.52
04003a	16:23	-22.41	169.72	15	314/39/283	5.9e19(7.1)	33	40	1.1e15(7.1)	1.0e15(7.1)	-4.7	-4.8	0.33	3.6e14(6.8)	0.48
04036a	21:05	-3.62	135.53	13	44/43/350	3.4e19(7.0)	21	62	4.5e14(6.9)	1.1e15(7.1)	-4.9	-4.5	0.37	3.0e14(6.7)	0.66
04038a	2:42	-4.03	134.78	12	261/68/353	9.8e19(7.3)	29	60	1.7e15(7.3)	6.6e15(7.6)	-4.8	-4.2	0.44	1.1e15(7.1)	0.66
04039a	8:58	-3.72	135.4	12	43/55/344	1.2e19(6.7)	19	50	9.2e13(6.4)	2.4e14(6.7)	-5.1	-4.7	0.34	5.2e13(6.2)	0.63
04162a	15:19	55.79	160.32	190	173/ 9/234	2.3e19(6.8)	29	55	7.8e14(7.0)	7.3e14(7.0)	-4.5	-4.5	0.4	2.9e14(6.7)	0.68
04180a	9:49	55.02	-134.46	12	333/51/179	1.9e19(6.8)	55	56	1.2e14(6.5)	1.7e14(6.6)	-5.2	-5.1	0.26	3.5e13(6.1)	0.41
04197a	4:27	-17.68	-178.52	577	345/44/137	4.8e19(7.0)	40	28	3.0e15(7.4)	3.1e15(7.4)	-4.2	-4.2	0.51	2.0e15(7.3)	0.63
04207a	14:35	-2.68	104.38	600	108/45/231	1.0e20(7.3)	58	25	1.4e16(7.9)	1.9e16(7.9)	-3.8	-3.7	0.63	1.2e16(7.8)	0.63
04249a	10:07	32.94	137	16	277/38/100	7.8e19(7.2)	69	48	4.7e15(7.5)	4.0e15(7.5)	-4.2	-4.3	0.26	4.6e14(6.9)	0.46
04249b	14:57	33.13	137.22	12	79/46/ 72	1.5e20(7.4)	59	55	4.1e15(7.5)	4.0e15(7.5)	-4.6	-4.6	0.33	7.1e14(7.0)	0.54
04250a	12:42	-55.43	-28.79	12	95/20/ 47	1.7e19(6.8)	29	48	2.1e14(6.6)	3.0e14(6.7)	-4.9	-4.8	0.28	8.7e13(6.4)	0.39
04282a	8:27	-10.87	162.27	40	108/51/ 23	1.6e19(6.7)	37	57	7.8e14(7.0)	1.5e15(7.2)	-4.3	-4	0.4	2.7e14(6.7)	0.56
04283a	21:26	11.25	-87.02	39	311/26/ 98	3.0e19(6.9)	39	40	3.3e14(6.8)	2.7e14(6.7)	-5	-5	0.45	9.2e13(6.4)	0.72
04315a	00:-1	-11.35	163.7	12	191/48/215	2.8e19(6.9)	47	33	5.3e14(6.9)	6.8e14(7.0)	-4.7	-4.6	0.38	2.6e14(6.7)	0.54
04316a	21:26	-7.87	125.12	17	67/27/ 72	2.1e20(7.5)	7	55	2.3e15(7.3)	5.4e15(7.6)	-5	-4.6	0.36	1.8e15(7.3)	0.44
04320a	9:06	4.72	-77.57	16	21/11/114	7.6e19(7.2)	91	85	2.0e15(7.3)	5.3e15(7.6)	-4.6	-4.2	0.39	3.8e14(6.8)	0.54
04327a	20:26	-46.36	164.91	40	43/36/103	5.6e19(7.1)	7	45	7.7e14(7.0)	7.5e14(7.0)	-4.9	-4.9	0.36	3.0e14(6.8)	0.44
04331a	2:25	-3.55	135.54	12	5/34/ 0	5.5e19(7.1)	11	67	7.8e14(7.0)	1.5e15(7.2)	-4.8	-4.6	0.42	5.6e14(6.9)	0.63
04333a	18:32	42.88	145.36	47	242/26/122	3.7e19(7.0)	45	50	1.7e15(7.3)	1.9e15(7.3)	-4.3	-4.3	0.35	4.0e14(6.8)	0.43
04341a	14:15	42.82	145.41	36	246/24/125	1.6e19(6.7)	69	45	4.7e14(6.9)	5.7e14(6.9)	-4.5	-4.4	0.44	1.8e14(6.6)	0.61
04349a	23:20	19.05	-81.52	12	258/84/358	1.8e19(6.8)	15	50	1.7e14(6.6)	7.3e14(7.0)	-5	-4.4	0.3	1.3e14(6.5)	0.4
04358a	14:59	-49.91	161.25	27	69/74/167	1.6e21(8.1)	16	75	1.4e16(7.9)	5.7e16(8.3)	-5.1	-4.4	0.29	8.6e15(7.7)	0.47
04361a	0:58	3.09	94.26	28	329/ 8/110	4.0e22(9.0)	71	540	5.1e17(8.9)	8.2e17(9.0)	-4.9	-4.7	0.38	8.0e16(8.4)	0.62

Table A.1 (continued)

05001a	6:25	4.97	92.22	12	111/68/187	1.2e19(6.7)	81	58	1.2e14(6.5)	4.2e14(6.8)	-5	-4.5	0.49	1.6e14(6.6)	0.64
05012a	8:40	-0.47	-20.53	12	261/85/180	1.9e19(6.8)	29	71	2.8e13(6.1)	1.3e14(6.5)	-5.8	-5.2	0.44	4.0e13(6.2)	0.45
05036a	12:23	5.47	123.67	530	158/14/246	5.2e19(7.1)	57	45	1.2e15(7.2)	1.8e15(7.3)	-4.6	-4.5	0.45	1.1e15(7.1)	0.57
05039a	14:48	-14.18	167.13	197	181/43/110	1.3e19(6.7)	40	68	4.0e14(6.8)	3.9e14(6.8)	-4.5	-4.5	0.32	1.9e14(6.6)	0.45
05057a	12:56	2.8	95.4	12	294/ 6/ 66	1.4e19(6.7)	58	50	1.2e14(6.5)	1.8e14(6.6)	-5.1	-4.9	0.56	6.3e13(6.3)	0.83
05061a	10:42	-6.54	129.99	196	308/35/176	5.7e19(7.1)	53	73	8.3e15(7.7)	1.2e16(7.8)	-3.8	-3.7	0.59	5.5e15(7.6)	0.64
05080a	12:23	-24.88	-63.54	572	64/18/352	2.3e19(6.8)	66	25	3.5e14(6.8)	1.0e15(7.1)	-4.8	-4.3	0.5	7.6e14(7.0)	0.55
05087a	16:09	1.67	97.07	25	333/ 8/118	1.0e22(8.6)	46	93	8.0e16(8.4)	1.1e17(8.5)	-5.1	-5	0.54	1.7e16(7.9)	0.79
05100a	10:29	-1.68	99.54	12	142/34/ 89	1.3e19(6.7)	63	27	3.4e14(6.8)	3.8e14(6.8)	-4.6	-4.5	0.44	1.8e14(6.6)	0.58
05101a	17:08	-22.01	170.5	78	351/37/210	1.5e19(6.7)	28	55	3.7e14(6.8)	6.6e14(7.0)	-4.6	-4.4	0.46	8.9e13(6.4)	0.43
05134a	5:05	0.42	98.24	39	326/22/ 88	1.5e19(6.7)	62	51	3.6e14(6.8)	3.9e14(6.8)	-4.6	-4.6	0.46	2.1e14(6.6)	0.59
05139a	1:54	1.88	96.74	12	290/ 8/ 65	2.4e19(6.8)	42	63	7.1e13(6.3)	1.3e14(6.5)	-5.5	-5.3	0.59	7.8e13(6.4)	0.67
05164a	22:44	-20.02	-69.23	94	182/23/279	5.3e20(7.8)	74	74	3.3e16(8.1)	3.9e16(8.2)	-4.2	-4.1	0.24	6.3e15(7.6)	0.55
05165a	17:10	51.15	179.52	18	268/20/115	1.8e19(6.8)	105	43	1.8e14(6.6)	3.3e14(6.8)	-5	-4.7	0.49	9.4e13(6.4)	0.7
05166a	2:50	41.15	-126.42	20	317/83/175	8.3e19(7.2)	40	42	3.9e14(6.8)	1.6e15(7.2)	-5.3	-4.7	0.41	3.3e14(6.8)	0.43
05205a	15:42	7.92	91.88	12	29/68/358	8.9e19(7.2)	85	46	1.2e15(7.2)	4.8e15(7.6)	-4.9	-4.3	0.4	1.9e15(7.3)	0.58
05228a	2:46	38.24	142.05	37	194/16/ 81	7.6e19(7.2)	73	56	8.0e14(7.0)	1.2e15(7.1)	-5	-4.8	0.37	3.5e14(6.8)	0.53
05252a	7:26	-5.2	153.95	83	140/30/ 91	3.7e20(7.6)	39	90	1.9e15(7.3)	2.2e15(7.3)	-5.3	-5.2	0.43	8.2e14(7.0)	0.63
05269a	1:55	-5.6	-76.2	108	347/39/268	2.2e20(7.5)	95	82	5.4e15(7.6)	5.6e15(7.6)	-4.6	-4.6	0.26	1.8e15(7.3)	0.45
05281a	3:50	34.38	73.47	12	334/40/123	2.9e20(7.6)	84	65	5.4e15(7.6)	4.9e15(7.6)	-4.7	-4.8	0.34	1.7e15(7.3)	0.51
05318a	21:38	38.22	144.97	18	181/43/256	3.7e19(7.0)	91	25	1.0e15(7.1)	8.9e14(7.1)	-4.6	-4.6	0.37	1.8e14(6.6)	0.49
05321a	19:26	-22.46	-68.13	155	126/26/211	1.9e19(6.8)	70	30	4.9e14(6.9)	6.2e14(7.0)	-4.6	-4.5	0.37	2.4e14(6.7)	0.57
05339a	12:19	-6.23	29.6	18	149/50/238	1.8e19(6.8)	52	45	2.4e14(6.7)	1.8e14(6.6)	-4.9	-5	0.38	8.4e13(6.4)	0.51
05347a	3:16	-15.04	-178.43	15	271/86/ 2	1.3e19(6.7)	34	42	7.7e13(6.4)	3.7e14(6.8)	-5.2	-4.5	0.41	2.7e13(6.1)	0.52
06002a	6:10	-61.12	-21.39	20	358/77/192	1.4e20(7.4)	23	36	1.1e15(7.1)	4.5e15(7.5)	-5.1	-4.5	0.35	4.8e14(6.9)	0.45
06002b	22:13	-19.8	-177.72	589	281/22/320	6.9e19(7.2)	74	25	2.7e15(7.4)	4.1e15(7.5)	-4.4	-4.2	0.36	2.3e15(7.3)	0.46
06008a	11:34	35.93	23.29	64	201/44/ 55	1.5e19(6.7)	47	65	1.1e15(7.1)	1.1e15(7.1)	-4.1	-4.1	0.42	5.7e14(6.9)	0.53
06027a	16:58	-5.61	128.2	397	43/42/316	3.5e20(7.6)	42	30	1.9e16(7.9)	2.4e16(8.0)	-4.3	-4.2	0.55	1.6e16(7.9)	0.66
06033a	12:48	-17.77	-178.13	611	244/37/321	1.5e19(6.7)	68	20	3.0e14(6.8)	3.2e14(6.8)	-4.7	-4.7	0.49	2.3e14(6.7)	0.56
06053a	22:19	-21.2	33.33	12	325/27/246	4.2e19(7.0)	58	30	8.0e14(7.0)	1.0e15(7.1)	-4.7	-4.6	0.25	1.2e14(6.5)	0.51
06073a	6:57	-3.35	127.31	13	284/69/ 11	1.5e19(6.7)	30	30	3.0e14(6.8)	1.0e15(7.1)	-4.7	-4.2	0.39	3.4e14(6.8)	0.52
06110a	23:25	60.89	167.05	12	207/40/ 76	3.0e20(7.6)	215	55	2.8e15(7.4)	2.7e15(7.4)	-5	-5	0.28	6.0e14(7.0)	0.43
06123a	15:26	-20.39	-173.47	67	226/22/123	1.1e21(8.0)	108	80	5.9e16(8.3)	7.6e16(8.3)	-4.3	-4.2	0.36	8.6e15(7.7)	0.58
06136a	10:39	-31.41	-178.91	151	129/19/ 58	1.8e20(7.4)	40	35	1.0e16(7.8)	1.1e16(7.8)	-4.2	-4.2	0.65	3.9e15(7.5)	0.76
06136b	15:28	0.01	96.98	13	92/60/189	2.1e19(6.8)	63	42	1.2e15(7.1)	3.4e15(7.4)	-4.2	-3.8	0.5	8.7e14(7.1)	0.7
06198a	8:19	-10.28	107.78	20	290/10/102	4.6e20(7.7)	64	160	1.2e15(7.1)	8.8e14(7.1)	-5.6	-5.7	0.34	1.3e14(6.5)	0.52
06219a	22:18	-15.76	167.63	157	275/43/326	2.0e19(6.8)	38	18	6.8e14(7.0)	7.1e14(7.0)	-4.5	-4.5	0.39	5.2e14(6.9)	0.43
06232a	3:41	-61.27	-34.52	17	4/82/184	3.7e19(7.0)	29	25	3.4e14(6.8)	1.7e15(7.3)	-5	-4.3	0.22	4.1e14(6.8)	0.33
06244a	10:18	-7.01	155.42	45	301/42/ 78	1.6e19(6.7)	34	53	3.6e14(6.8)	4.2e14(6.8)	-4.6	-4.6	0.41	2.3e14(6.7)	0.41
06271a	6:22	-16.63	-171.66	15	6/40/260	2.7e19(6.9)	82	27	7.3e14(7.0)	6.8e14(7.0)	-4.6	-4.6	0.4	1.3e14(6.5)	0.48

Table A.1 (continued)

06274a	9:06	46.38	153.64	12	224/29/100	8.3e18(6.5)	48	46	6.5e13(6.3)	7.8e13(6.4)	-5.1	-5	0.38	2.3e13(6.0)	0.54
06288a	17:07	19.83	-155.94	48	88/45/214	1.5e19(6.7)	54	40	2.1e14(6.6)	5.4e14(6.9)	-4.9	-4.4	0.51	1.6e14(6.6)	0.59
06290a	1:25	-6.09	151.26	31	43/36/105	1.4e19(6.7)	31	36	5.1e14(6.9)	8.1e14(7.0)	-4.4	-4.2	0.62	3.9e14(6.8)	0.72
06293a	10:48	-13.46	-76.98	22	327/16/ 73	1.4e19(6.7)	158	36	7.8e13(6.4)	2.4e14(6.7)	-5.3	-4.8	0.24	4.5e13(6.2)	0.41
06317a	1:26	-26.1	-63.47	573	344/ 7/273	2.3e19(6.8)	97	25	8.5e14(7.0)	3.1e15(7.4)	-4.4	-3.9	0.36	2.2e15(7.3)	0.41
06319a	11:14	46.71	154.33	13	215/15/ 92	3.5e21(8.3)	183	115	9.0e15(7.7)	2.0e16(8.0)	-5.6	-5.2	0.22	1.5e15(7.2)	0.4
06319b	11:40	46.47	154.83	23	54/45/284	1.4e19(6.7)	11	70	9.6e16(8.4)	6.9e16(8.3)	-2.2	-2.3	0.46	4.6e13(6.2)	0.45
07013a	4:23	46.17	154.8	12	266/39/306	1.8e21(8.1)	181	100	3.8e16(8.2)	5.4e16(8.3)	-4.7	-4.5	0.26	7.4e15(7.7)	0.46
07021a	11:27	1.1	126.21	22	34/35/108	2.0e20(7.5)	67	40	3.6e15(7.5)	4.4e15(7.5)	-4.7	-4.7	0.44	2.4e15(7.4)	0.59
07030a	4:54	-55.12	146.26	13	171/77/358	2.4e19(6.8)	17	20	1.6e14(6.6)	6.6e14(7.0)	-5.2	-4.6	0.46	1.6e14(6.6)	0.39
07051a	8:04	-0.91	127.17	12	276/49/340	1.5e19(6.7)	36	33	2.4e14(6.7)	6.5e14(7.0)	-4.8	-4.4	0.48	3.7e14(6.8)	0.68
07084a	0:40	-20.6	169.12	41	333/36/ 89	6.2e19(7.1)	25	31	1.5e15(7.2)	1.9e15(7.3)	-4.6	-4.5	0.48	3.3e14(6.8)	0.41
07084b	0:41	37.28	136.61	12	34/40/108	1.3e19(6.7)	21	26	1.9e14(6.6)	2.2e14(6.7)	-4.8	-4.8	0.56	3.9e13(6.2)	0.57
07084c	1:08	-20.89	168.99	31	331/31/ 83	2.7e19(6.9)	9	73	3.1e15(7.4)	3.5e15(7.5)	-3.9	-3.9	0.44	6.1e13(6.3)	0.37
07091a	20:39	-7.79	156.34	14	333/37/121	1.6e21(8.1)	41	101	1.6e16(7.9)	1.8e16(7.9)	-5	-5	0.42	2.4e15(7.4)	0.53
07091b	21:11	-7.46	155.8	29	291/40/ 49	2.6e19(6.9)	59	65	2.9e16(8.1)	5.3e16(8.2)	-2.9	-2.7	0.59	2.2e14(6.7)	0.46
07119a	12:41	51.89	-179.81	121	175/16/295	2.8e18(6.2)	194	13	1.5e14(6.6)	1.6e14(6.6)	-4.3	-4.2	0.58	1.2e14(6.5)	0.61
07164a	19:29	13.43	-91.22	31	286/31/ 75	1.3e19(6.7)	127	38	1.1e14(6.5)	1.2e14(6.5)	-5.1	-5.1	0.45	3.4e13(6.1)	0.65
07179a	2:52	-7.95	154.7	18	40/60/179	1.3e19(6.7)	44	34	1.3e14(6.5)	4.1e14(6.8)	-5	-4.5	0.47	1.7e14(6.6)	0.49
07197a	1:13	37.5	138.47	12	37/30/ 83	1.1e19(6.6)	126	28	2.3e14(6.7)	2.5e14(6.7)	-4.7	-4.6	0.31	6.4e13(6.3)	0.4
07197b	14:17	36.84	135.03	373	289/48/349	2.0e19(6.8)	133	21	2.3e14(6.7)	6.9e14(7.0)	-4.9	-4.5	0.43	5.5e14(6.9)	0.47
07207a	5:40	2.95	127.47	41	16/37/ 72	3.2e19(6.9)	43	50	6.2e14(7.0)	6.4e14(7.0)	-4.7	-4.7	0.43	2.6e14(6.7)	0.45
07213a	17:08	-15.41	167.41	126	356/29/ 79	7.4e19(7.2)	45	45	9.5e14(7.1)	1.5e15(7.2)	-4.9	-4.7	0.32	4.8e14(6.9)	0.48
07214a	3:21	51.1	-179.73	31	271/27/123	1.6e19(6.7)	149	37	2.1e14(6.7)	5.0e14(6.9)	-4.9	-4.5	0.54	3.8e14(6.8)	0.6
07220a	17:04	-6.03	107.58	304	330/30/155	2.6e20(7.5)	23	30	6.1e15(7.6)	7.2e15(7.7)	-4.6	-4.6	0.58	2.7e15(7.4)	0.61
07227a	23:40	-13.73	-77.04	33	321/28/ 63	1.1e21(8.0)	159	155	1.1e16(7.8)	1.8e16(7.9)	-5	-4.8	0.2	3.1e15(7.4)	0.38
07245a	1:05	-11.74	165.68	18	338/23/101	9.0e19(7.2)	38	82	7.5e14(7.0)	1.4e15(7.2)	-5.1	-4.8	0.34	5.0e13(6.2)	0.51
07253a	1:49	3.08	-78.12	18	54/23/265	1.7e19(6.8)	163	42	1.5e14(6.6)	2.8e14(6.7)	-5	-4.8	0.2	2.9e13(6.1)	0.44
07255a	11:10	-3.78	100.99	24	328/ 9/114	6.7e21(8.5)	41	108	6.1e16(8.3)	6.9e16(8.3)	-5	-5	0.51	8.8e15(7.7)	0.8
07255b	23:48	-2.46	100.13	43	317/19/102	8.1e20(7.9)	31	108	1.8e16(7.9)	1.8e16(7.9)	-4.6	-4.7	0.48	2.5e15(7.4)	0.71
07256a	3:35	-2.31	99.39	17	312/10/ 90	4.7e19(7.0)	42	55	9.6e14(7.1)	1.0e15(7.1)	-4.7	-4.7	0.49	2.5e14(6.7)	0.66
07263a	8:31	-2.24	99.85	32	313/19/ 99	1.3e19(6.7)	35	43	3.2e14(6.8)	2.2e14(6.7)	-4.6	-4.8	0.5	1.0e14(6.4)	0.63
07269a	12:36	-5.2	153.52	47	138/44/ 86	1.7e19(6.8)	47	58	2.0e14(6.6)	2.0e14(6.6)	-4.9	-4.9	0.48	1.1e14(6.5)	0.56
07271a	13:38	21.94	143.07	275	73/49/ 50	2.0e20(7.5)	89	24	4.5e15(7.5)	6.6e15(7.6)	-4.6	-4.5	0.44	3.7e15(7.5)	0.54
07273a	2:08	10.51	145.68	14	16/76/167	3.3e19(6.9)	45	44	5.0e14(6.9)	2.0e15(7.3)	-4.8	-4.2	0.43	8.5e14(7.1)	0.55
07273b	5:23	-49.26	164.1	12	29/36/123	1.6e20(7.4)	27	57	1.6e15(7.2)	2.9e15(7.4)	-5	-4.7	0.4	1.5e14(6.5)	0.53
07288a	12:29	-44.71	167.24	18	54/30/132	2.0e19(6.8)	39	38	2.7e14(6.7)	5.4e14(6.9)	-4.9	-4.6	0.35	7.8e13(6.4)	0.51
07297a	21:02	-4.4	100.81	20	321/12/107	2.3e19(6.8)	51	52	2.5e14(6.7)	3.2e14(6.8)	-5	-4.9	0.47	1.3e14(6.5)	0.66
07304a	3:30	18.83	145.59	211	196/60/152	9.3e19(7.2)	80	25	1.5e15(7.2)	3.0e15(7.4)	-4.8	-4.5	0.48	1.8e15(7.3)	0.59
07318a	15:40	-22.64	-70.62	37	358/20/ 98	4.8e20(7.7)	113	71	5.9e15(7.6)	1.2e16(7.8)	-4.9	-4.6	0.2	2.8e15(7.4)	0.37

Table A.1 (continued)

07319a	15:05	-22.98	-70.94	20	360/16/ 98	2.0e19(6.8)	63	42	1.7e14(6.6)	4.3e14(6.9)	-5.1	-4.7	0.22	1.1e14(6.5)	0.37
07320a	3:13	-2.5	-78	114	177/29/316	1.8e19(6.8)	122	20	6.0e13(6.3)	1.3e14(6.5)	-5.5	-5.1	0.44	9.6e13(6.4)	0.5
07326a	8:48	-5.96	147.05	56	102/43/ 86	1.7e19(6.8)	30	61	4.2e14(6.8)	4.3e14(6.9)	-4.6	-4.6	0.36	2.0e14(6.6)	0.49
07333a	19:00	15.06	-61.41	147	109/58/328	1.6e20(7.4)	136	24	3.8e15(7.5)	1.4e16(7.9)	-4.6	-4.1	0.52	7.5e15(7.7)	0.61
07343a	7:28	-25.75	-177.22	149	34/25/ 38	7.1e20(7.8)	61	35	1.7e16(7.9)	2.7e16(8.1)	-4.6	-4.4	0.5	1.1e16(7.8)	0.63
07350a	8:09	-23.02	-70.41	30	246/ 6/159	1.5e19(6.7)	121	65	2.6e14(6.7)	6.1e14(7.0)	-4.8	-4.4	0.3	1.3e14(6.5)	0.55
07353a	9:30	51.02	-179.27	27	274/21/118	7.2e19(7.2)	146	41	5.3e14(6.9)	1.4e15(7.2)	-5.1	-4.7	0.52	6.8e14(7.0)	0.66
08039a	9:38	10.85	-41.71	16	274/78/180	3.2e19(6.9)	153	21	2.6e14(6.7)	1.0e15(7.1)	-5.1	-4.5	0.32	3.1e14(6.8)	0.5
08045a	10:09	36.24	21.79	20	332/ 6/120	2.4e19(6.8)	39	66	4.5e14(6.9)	5.3e14(6.9)	-4.7	-4.7	0.43	1.6e14(6.6)	0.54
08051a	8:08	2.69	95.98	14	299/11/ 80	1.1e20(7.3)	60	64	1.1e15(7.1)	1.6e15(7.2)	-5	-4.8	0.47	6.2e14(7.0)	0.69
08054a	15:57	-57.12	-23.13	12	25/53/331	1.7e19(6.8)	31	52	5.3e14(6.9)	9.6e14(7.1)	-4.5	-4.2	0.39	4.1e14(6.8)	0.57
08056a	8:36	-2.66	99.95	14	317/ 6/102	7.8e19(7.2)	55	52	1.2e15(7.2)	1.7e15(7.2)	-4.8	-4.7	0.51	4.2e14(6.8)	0.73
08063a	14:11	13.52	125.59	17	290/44/245	2.6e19(6.9)	53	31	4.6e14(6.9)	4.8e14(6.9)	-4.8	-4.7	0.51	2.8e14(6.7)	0.59
08080a	22:33	35.43	81.37	12	358/41/250	5.4e19(7.1)	36	38	3.9e14(6.8)	5.2e14(6.9)	-5.1	-5	0.39	6.7e13(6.3)	0.6
08100a	12:46	-20.12	168.8	35	340/30/101	1.1e20(7.3)	47	49	9.9e14(7.1)	1.2e15(7.1)	-5	-5	0.26	1.7e14(6.6)	0.46
08103a	0:30	-55.56	158.49	22	3/43/102	5.5e19(7.1)	44	30	1.3e15(7.2)	1.2e15(7.1)	-4.6	-4.7	0.25	1.7e14(6.6)	0.37
08128a	16:45	36.18	141.61	26	204/15/ 91	2.4e19(6.8)	88	52	2.1e14(6.7)	4.1e14(6.8)	-5	-4.8	0.36	1.2e14(6.5)	0.47
08130a	21:51	12.36	143.28	83	325/59/213	1.7e19(6.8)	44	33	1.9e14(6.6)	2.5e14(6.7)	-5	-4.8	0.38	6.6e13(6.3)	0.53
08133a	6:28	31.44	104.1	12	231/35/138	9.0e20(7.9)	79	100	1.7e16(7.9)	2.7e16(8.1)	-4.7	-4.5	0.41	7.2e15(7.7)	0.58
08165a	23:43	39.03	140.85	12	17/42/ 87	2.6e19(6.9)	131	32	3.7e14(6.8)	3.4e14(6.8)	-4.8	-4.9	0.35	7.7e13(6.4)	0.53
08182a	6:17	-58.33	-21.77	26	143/83/181	3.4e19(7.0)	18	52	1.9e14(6.6)	9.3e14(7.1)	-5.2	-4.6	0.45	3.2e14(6.8)	0.71
08187a	2:12	54.12	153.37	610	143/48/226	4.5e20(7.7)	197	30	9.7e15(7.8)	1.5e16(7.9)	-4.7	-4.5	0.56	1.2e16(7.8)	0.59
08201a	2:39	37.47	142.42	21	200/16/ 88	2.9e19(6.9)	150	60	2.0e14(6.6)	3.9e14(6.8)	-5.2	-4.9	0.32	7.3e13(6.3)	0.52
08205a	15:26	39.73	141.51	98	14/18/285	1.9e19(6.8)	153	25	6.9e14(7.0)	5.8e14(6.9)	-4.4	-4.5	0.39	2.9e14(6.7)	0.5
08238a	13:22	30.61	83.51	17	30/48/312	1.4e19(6.7)	110	30	1.5e14(6.6)	1.8e14(6.6)	-5	-4.9	0.44	5.0e13(6.2)	0.63
08252a	18:52	-13.37	166.75	125	1/40/ 87	3.0e19(6.9)	82	30	2.4e15(7.3)	2.6e15(7.4)	-4.1	-4.1	0.57	9.2e14(7.1)	0.69
08255a	0:20	41.79	144.11	20	235/15/116	1.8e19(6.8)	143	60	1.9e14(6.6)	4.0e14(6.8)	-5	-4.7	0.32	9.2e13(6.4)	0.53
08273a	15:19	-29.85	-177.46	51	197/32/ 92	4.5e19(7.0)	53	30	9.3e14(7.1)	6.0e14(6.9)	-4.7	-4.9	0.46	3.5e14(6.8)	0.57
08279a	15:52	39.5	73.64	12	246/38/ 78	1.4e19(6.7)	96	32	1.8e14(6.6)	1.7e14(6.6)	-4.9	-4.9	0.4	6.3e13(6.3)	0.5
08293a	5:10	-21.82	-173.56	43	189/44/ 81	2.9e19(6.9)	76	50	1.4e15(7.2)	1.2e15(7.2)	-4.3	-4.4	0.35	4.2e14(6.8)	0.59
08321a	17:02	1.5	122.05	29	92/20/ 84	1.3e20(7.3)	76	60	1.8e15(7.3)	2.3e15(7.3)	-4.9	-4.7	0.39	5.1e14(6.9)	0.61
08329a	9:02	54.27	154.71	502	276/19/331	1.1e20(7.3)	58	30	3.0e15(7.4)	6.0e15(7.6)	-4.6	-4.3	0.5	4.3e15(7.5)	0.57
08344a	6:23	-31.03	-176.54	18	174/38/256	1.5e19(6.7)	48	50	2.7e14(6.7)	2.1e14(6.6)	-4.7	-4.8	0.43	6.8e13(6.3)	0.56
09003a	19:43	-0.38	132.83	15	99/23/ 47	3.9e20(7.7)	53	50	4.2e15(7.5)	8.4e15(7.7)	-5	-4.7	0.28	1.1e15(7.1)	0.52
09003b	22:33	-0.58	133.48	18	101/26/ 72	1.4e20(7.4)	72	42	2.0e15(7.3)	2.9e15(7.4)	-4.8	-4.7	0.35	3.5e14(6.8)	0.58
09015a	17:49	46.97	155.39	45	11/44/ 84	1.5e20(7.4)	125	65	6.2e15(7.6)	6.2e15(7.6)	-4.4	-4.4	0.35	8.2e14(7.0)	0.54
09042a	17:34	3.92	126.81	23	177/38/ 83	5.9e19(7.1)	77	40	1.9e15(7.3)	1.9e15(7.3)	-4.5	-4.5	0.41	6.3e14(7.0)	0.55
09049a	21:53	-27.27	-175.9	36	274/38/179	3.5e19(7.0)	56	50	1.6e15(7.2)	2.0e15(7.3)	-4.3	-4.2	0.52	5.3e14(6.9)	0.59
09078a	18:17	-23.08	-174.23	49	205/44/ 98	3.4e20(7.6)	76	45	1.4e16(7.9)	1.2e16(7.8)	-4.4	-4.4	0.26	1.8e15(7.3)	0.54
09097a	4:23	46	151.99	43	231/31/110	2.5e19(6.9)	113	50	2.9e14(6.7)	3.1e14(6.8)	-4.9	-4.9	0.41	4.4e13(6.2)	0.52

Table A.1 (continued)

09106a	14:57	-60.71	-26.55	24	226/33/113	1.3e19(6.7)	28	31	2.0e14(6.6)	2.3e14(6.7)	-4.8	-4.7	0.38	6.4e13(6.3)	0.48
09148a	8:24	16.5	-87.17	12	63/60/353	1.3e20(7.3)	80	71	2.2e15(7.3)	9.7e15(7.8)	-4.8	-4.1	0.41	2.4e15(7.4)	0.49
09174a	14:19	-5.17	153.79	72	138/34/ 84	1.4e19(6.7)	35	53	4.4e14(6.9)	4.0e14(6.8)	-4.5	-4.5	0.36	1.8e14(6.6)	0.49
09196a	9:22	-45.81	166.28	22	26/24/140	6.0e20(7.8)	26	65	3.4e15(7.5)	9.1e15(7.7)	-5.2	-4.8	0.29	8.1e14(7.0)	0.43
09215a	17:59	29.27	-113.5	15	221/84/357	2.5e19(6.9)	28	30	6.4e13(6.3)	2.9e14(6.7)	-5.6	-4.9	0.28	7.3e13(6.3)	0.43
09221a	10:55	33.07	138.2	303	85/17/167	5.0e19(7.1)	117	29	1.4e15(7.2)	2.3e15(7.3)	-4.5	-4.3	0.45	1.4e15(7.2)	0.56
09222a	19:55	14.15	92.91	21	49/34/284	2.1e20(7.5)	74	65	5.8e15(7.6)	6.6e15(7.6)	-4.6	-4.5	0.51	2.3e15(7.3)	0.61
09228a	7:38	-1.56	99.45	12	175/34/107	1.2e19(6.7)	51	38	2.7e14(6.7)	4.4e14(6.9)	-4.6	-4.4	0.43	1.5e14(6.5)	0.61
09229a	0:05	23.33	123.61	25	136/67/ 12	1.3e19(6.7)	57	40	2.0e14(6.6)	7.0e14(7.0)	-4.8	-4.3	0.47	4.7e14(6.9)	0.58
09240a	1:51	-7.08	123.52	632	262/35/221	2.6e19(6.9)	52	30	1.4e15(7.2)	1.7e15(7.2)	-4.3	-4.2	0.6	1.4e15(7.2)	0.65
09245a	7:55	-8.08	107.34	52	51/45/117	3.6e19(7.0)	75	65	2.3e15(7.3)	2.1e15(7.3)	-4.2	-4.2	0.44	6.8e14(7.0)	0.58
09272a	17:48	-15.19	-171.91	12	129/31/216	1.8e21(8.1)	67	75	2.0e16(8.0)	3.6e16(8.1)	-4.9	-4.7	0.5	3.2e15(7.4)	0.6
09273a	10:16	-0.74	99.69	75	72/51/136	2.6e20(7.5)	75	60	1.3e16(7.8)	1.6e16(7.9)	-4.3	-4.2	0.41	6.5e15(7.6)	0.63
09280a	21:41	4.14	122.53	583	191/11/260	1.7e19(6.8)	57	20	8.2e14(7.0)	7.6e14(7.0)	-4.3	-4.3	0.53	7.0e14(7.0)	0.58
09280b	22:03	-12.64	166.27	46	346/40/ 90	3.2e20(7.6)	31	50	3.2e15(7.4)	3.4e15(7.5)	-5	-5	0.27	8.7e14(7.1)	0.45
09280c	22:18	-11.84	166.05	43	339/36/ 82	6.5e20(7.8)	12	105	1.2e16(7.8)	1.5e16(7.9)	-4.7	-4.6	0.48	9.6e14(7.1)	0.34
09280d	23:13	-13	166.42	46	341/41/ 83	1.5e20(7.4)	49	55	4.4e15(7.5)	5.0e15(7.6)	-4.5	-4.5	0.36	4.7e14(6.9)	0.41
09281a	8:28	-13.07	166.11	12	354/26/103	1.5e19(6.7)	22	50	1.4e14(6.5)	2.8e14(6.7)	-5	-4.7	0.23	2.7e13(6.1)	0.3
09297a	14:40	-6.09	130.59	155	315/45/167	2.9e19(6.9)	68	25	1.4e15(7.2)	1.7e15(7.3)	-4.3	-4.2	0.61	1.3e15(7.2)	0.67
09303a	7:03	28.99	130.26	37	208/29/ 80	1.9e19(6.8)	76	53	1.4e14(6.5)	1.3e14(6.5)	-5.1	-5.2	0.42	2.9e13(6.1)	0.6
09313a	10:44	-17.1	178.53	604	172/42/ 32	1.0e20(7.3)	83	30	3.8e15(7.5)	5.2e15(7.6)	-4.4	-4.3	0.38	4.3e15(7.5)	0.43
09328a	12:47	-20.83	-173.54	22	99/54/355	1.4e19(6.7)	35	25	3.5e14(6.8)	7.1e14(7.0)	-4.6	-4.3	0.58	3.9e14(6.8)	0.66
10003a	22:36	-8.83	157.23	12	322/22/101	5.3e19(7.1)	68	65	5.3e14(6.9)	7.7e14(7.0)	-5	-4.8	0.36	5.8e13(6.3)	0.45
10005a	4:55	-58.47	-14.82	15	354/76/181	1.8e19(6.8)	38	60	9.2e13(6.4)	4.1e14(6.8)	-5.3	-4.6	0.4	9.2e13(6.4)	0.55
10005b	12:15	-9.05	157.79	12	292/27/ 60	2.0e19(6.8)	41	60	1.3e14(6.5)	2.1e14(6.6)	-5.2	-5	0.31	5.4e13(6.3)	0.41
10012a	21:53	18.62	-72.59	12	151/64/158	4.7e19(7.0)	156	60	1.9e15(7.3)	4.6e15(7.5)	-4.4	-4	0.37	5.4e14(6.9)	0.64
10049a	1:13	42.52	130.71	580	70/15/164	2.6e19(6.9)	196	20	6.4e14(7.0)	8.7e14(7.1)	-4.6	-4.5	0.5	7.1e14(7.0)	0.56
10057a	20:31	25.86	128.65	17	91/72/ 3	3.6e19(7.0)	125	45	1.2e15(7.1)	5.1e15(7.6)	-4.5	-3.8	0.46	2.1e15(7.3)	0.59
10058a	6:34	-35.95	-73.15	24	18/18/112	1.8e22(8.8)	78	170	1.2e17(8.5)	2.6e17(8.7)	-5.2	-4.8	0.34	3.3e16(8.1)	0.49
10064a	16:07	-3.96	100.57	12	326/ 9/111	1.6e19(6.7)	72	55	1.2e14(6.5)	1.4e14(6.5)	-5.1	-5.1	0.42	6.8e13(6.3)	0.57
10070a	14:39	-34.53	-72.09	15	324/37/268	2.5e19(6.9)	117	35	1.2e15(7.2)	1.0e15(7.1)	-4.3	-4.4	0.27	2.5e14(6.7)	0.43
10094a	22:40	32.35	-115.37	12	221/83/354	7.3e19(7.2)	59	60	3.6e14(6.8)	1.6e15(7.2)	-5.3	-4.7	0.3	3.1e14(6.8)	0.41
10096a	22:15	2.05	96.71	19	308/ 9/ 87	5.6e20(7.8)	80	68	6.8e15(7.7)	9.0e15(7.7)	-4.9	-4.8	0.44	2.1e15(7.3)	0.6
10101a	9:40	-11.02	161.24	36	291/40/ 82	2.2e19(6.8)	91	40	9.4e14(7.1)	9.9e14(7.1)	-4.4	-4.3	0.4	4.5e14(6.9)	0.53
10103a	23:49	33.1	96.82	20	210/77/180	2.5e19(6.9)	92	30	1.2e14(6.5)	5.4e14(6.9)	-5.3	-4.7	0.49	3.4e14(6.8)	0.58
10129a	5:59	3.38	95.79	37	308/15/ 86	9.0e19(7.2)	89	66	1.7e15(7.3)	2.0e15(7.3)	-4.7	-4.7	0.52	8.1e14(7.0)	0.65
10147a	17:14	-13.78	166.67	42	162/45/ 85	6.6e19(7.1)	73	35	7.2e14(7.0)	6.4e14(7.0)	-5	-5	0.37	2.0e14(6.6)	0.49
10163a	19:26	7.83	91.63	36	116/61/152	1.9e20(7.5)	98	50	6.6e15(7.6)	1.5e16(7.9)	-4.5	-4.1	0.51	3.5e15(7.5)	0.63
10167a	3:16	-1.84	136.39	12	332/82/186	3.9e19(7.0)	42	40	7.5e14(7.0)	3.3e15(7.4)	-4.7	-4.1	0.38	4.7e14(6.9)	0.51
10177a	5:30	-10.52	161.47	40	180/48/128	1.4e19(6.7)	67	42	2.3e14(6.7)	3.4e14(6.8)	-4.8	-4.6	0.44	2.1e14(6.6)	0.53

Table A.2 Mean deviation $\sigma_g^{\pm}$ and locations of stations with 10 or more recorded events computed as described in Equation 2.4. '*N*' is the number of recorded events, and the stations with the * symbol are those for which we applied corrections.

Name	*	NTWK	LOC	Lon	Lat	Mean $\sigma^{\pm}$	N
ATKA		AK		-174.2	52.2	-0.033	14
BESE		AK		-134.85	58.58	-0.496	11
CHUM		AK		-152.31	63.88	0.083	14
COLD		AK		-150.2	67.23	-0.14	11
DOT		AK		-144.06	63.65	0.234	14
EYAK		AK		-145.75	60.55	0.032	12
FALS		AK		-163.42	54.86	-0.179	11
GAMB		AK		-171.7	63.78	-0.121	16
MCK		AK		-148.93	63.73	0.054	15
RC01		AK		-149.74	61.09	0.058	11
SAW	*	AK		-148.33	61.81	-0.772	11
SPIA		AK		-170.25	57.18	0.286	17
TNA		AK		-167.92	65.56	-0.136	23
TRF		AK		-150.29	63.45	0.075	14
UNV		AK		-166.5	53.85	-0.219	22
AKUT		AT		-165.77	54.13	-0.241	13
CRAG		AT		-133.12	55.47	-0.14	12
OHAK		AT		-153.29	57.22	0.03	20
PMR		AT		-149.13	61.59	-0.031	16
SDPT		AT		-160.48	55.35	0.222	15
SIT		AT		-135.32	57.06	0.012	13
SKAG		AT		-135.33	59.46	-0.074	14
SMY		AT		174.1	52.73	0.22	20
ARMA		AU		151.63	-30.42	-0.299	31
BBOO		AU		136.06	-32.81	0.089	71
BLDU		AU		116.71	-30.61	0.25	60
CMSA		AU		145.69	-31.54	0.085	28
CNB		AU		149.36	-35.31	-0.272	30
COEN		AU		143.18	-13.96	-0.423	63
CTA		AU		146.25	-20.09	-0.061	27
EIDS		AU		151.08	-25.37	-0.22	60
FITZ		AU		125.64	-18.1	-0.246	32
FORT		AU		128.06	-30.78	0.064	69
KMBL		AU		121.88	-31.37	-0.334	68
LHI		AU		159.06	-31.52	-0.027	14
MAW	*	AU		62.87	-67.6	-1.264	12
MOO		AU		147.19	-42.44	-0.166	27
MTN		AU		131.13	-12.84	-0.032	31
STKA	*	AU		141.6	-31.88	-1.248	24
TOO		AU		145.49	-37.57	-0.287	50
XMIS		AU		105.65	-10.48	0.186	24
YNG		AU		148.4	-34.3	0.187	51
AKRB		AV		-166.07	54.13	0.231	12
CMB		BK		-120.39	38.03	-0.235	10
GLA		CI		-114.83	33.05	-0.07	10
ATD		G		42.85	11.53	-0.414	10
CAN	*	G		149	-35.32	1.144	29
CAN		G	00	149	-35.32	-0.022	39
DRV	*	G		140.01	-66.67	1.181	20
DRV		G	SB	140	-66.67	0.024	19
APE		GE		25.53	37.07	-0.197	10
ECH		G	10	7.16	48.22	-0.367	10
CSS		GE		33.33	34.96	-0.086	16
DAG		GE		-18.66	76.77	-0.328	16
DSB		GE		-6.38	53.24	-0.54	13
EIL		GE		34.95	29.67	-0.13	24

Table A.2 (continued)

GVD		GE		24.09	34.84	0.091	10
IBBN		GE		7.76	52.31	0.057	12
ISP		GE		30.51	37.84	-0.205	17
KBS		GE	00	11.94	78.93	-0.285	16
KSDI		GE		35.66	33.19	0.106	12
KWP		GE		22.71	49.63	0.298	22
LAST		GE		25.48	35.16	-0.023	11
MALT		GE		38.43	38.31	-0.231	21
MAUI		GE		-156.24	20.77	0.201	15
MHV		GE		37.77	54.96	0.199	14
MORC		GE		17.54	49.78	-0.27	23
MTE		GE		-7.54	40.4	-0.219	11
PSZ		GE		19.89	47.92	-0.084	25
RGN		GE		13.32	54.55	0.252	15
RUE		GE		13.78	52.48	0.257	10
SANT		GE		25.46	36.37	-0.083	10
SNAA		GE		-2.84	-71.67	0.023	35
STU		GE		9.2	48.77	-0.131	10
SUMG		GE		-38.45	72.58	0.26	33
SUW		GE		23.18	54.01	0.223	62
TIRR		GE		28.41	44.46	-0.189	43
UGM	*	GE		110.52	-7.91	0.577	52
VSU		GE		26.73	58.46	0.226	54
WLF		GE		6.15	49.66	-0.282	12
ZKR		GE		26.22	35.12	0.09	10
FDF		G	00	-61.14	14.73	0.272	10
HYB	*	G		78.55	17.42	1.143	19
INU	*	G		137.03	35.35	1.142	41
INU		G	00	137.03	35.35	-0.275	10
KIP	*	G		-158.01	21.42	1.084	13
KIP		G	00	-158.01	21.42	-0.05	10
NOUC	*	G		166.3	-22.1	0.973	13
PPT		G		-149.58	-17.57	0.154	29
RER		G	00	55.75	-21.16	0.286	16
SCZ	*	G		-121.4	36.6	1.114	12
SSB		G	00	4.54	45.28	0.004	12
WUS	*	G		79.22	41.2	1.135	12
BJT		IC	00	116.17	40.02	0.048	22
ENH		IC	00	109.49	30.28	0.064	25
ENH		IC	10	109.49	30.28	-0.202	21
HIA		IC	00	119.74	49.27	-0.286	30
KMI		IC	00	102.74	25.12	-0.078	19
LSA		IC	00	91.13	29.7	0.064	23
LSA		IC	10	91.13	29.7	-0.079	23
MDJ		IC	00	129.59	44.62	-0.248	31
SSE		IC	00	121.19	31.09	-0.287	14
SSE	*	IC	10	121.19	31.09	-0.551	12
WMQ		IC	00	87.7	43.81	0.169	15
WMQ		IC	10	87.7	43.81	-0.042	15
AAK		II	00	74.49	42.64	-0.027	40
ABKT		II	00	58.12	37.93	0.094	51
ALE		II	00	-62.35	82.5	-0.265	59
ALE		II	10	-62.35	82.5	-0.233	29
ARU		II	00	58.56	56.43	0.308	101
ASCN	*	II	00	-14.36	-7.93	0.884	16
ASCN	*	II	10	-14.36	-7.93	0.4	13
BFO		II	00	8.33	48.33	-0.32	35
BORG		II	00	-21.33	64.75	0.35	25
BORG		II	10	-21.33	64.75	-0.051	27
BRVK		II	00	70.28	53.06	0.228	90
CMLA	*	II	00	-25.52	37.76	1.007	12
CMLA		II	10	-25.52	37.76	0.291	12

Table A.2 (continued)

COCO	*	II	00	96.83	-12.19	0.764	73
COCO		II	10	96.83	-12.19	0.287	40
COCO		II	20	96.83	-12.19	0.334	50
DGAR		II	00	72.45	-7.41	0.425	19
DGAR		II	10	72.45	-7.41	0.421	18
EFI	*	II	00	-58.06	-51.67	0.602	13
EFI		II	10	-58.06	-51.67	-0.12	17
ERM		II	0	143.16	42.02	-0.057	37
ESK		II	00	-3.21	55.32	-0.121	53
FFC		II	00	-101.98	54.73	0.122	57
HOPE		II	00	-36.49	-54.28	0.276	15
HOPE		II	10	-36.49	-54.28	-0.209	18
JTS		II	00	-84.95	10.29	0.06	10
JTS		II	10	-84.95	10.29	-0.038	10
KAPI	*	II	00	119.75	-5.01	0.804	56
KAPI		II	10	119.75	-5.01	0.054	66
KDAK		II	00	-152.58	57.78	0.645	71
KDAK		II	10	-152.58	57.78	0.026	78
KIV		II	00	42.69	43.95	0.432	81
KIV		II	10	42.69	43.95	0.299	15
KURK		II	00	78.62	50.72	0.441	103
KWAJ	*	II	00	167.61	8.8	0.486	32
KWAJ		II	10	167.61	8.8	0.102	39
LVZ		II	00	34.65	67.9	0.046	52
MBAR		II	00	30.74	-0.6	0.095	17
MBAR		II	10	30.74	-0.6	-0.351	24
MSEY		II	00	55.48	-4.67	0.225	45
MSEY	*	II	10	55.48	-4.67	-0.405	46
MSVF		II	00	178.05	-17.73	0.227	25
NIL		II	10	73.27	33.65	0.306	50
NNA		II	00	-76.84	-11.99	0.007	17
OBN		II	00	36.57	55.12	0.484	79
OBN		II	10	36.57	55.12	0.175	53
PALK	*	II	00	80.7	7.27	0.643	65
PALK		II	10	80.7	7.27	-0.326	68
PFO		II	00	-116.46	33.61	-0.367	25
PFO	*	II	10	-116.46	33.61	-0.392	22
RAYN		II	00	45.5	23.52	0.197	39
RAYN		II	10	45.5	23.52	-0.279	29
RPN		II	00	-109.33	-27.13	-0.008	35
RPN		II	10	-109.33	-27.13	-0.052	23
SACV		II	00	-23.61	14.97	0.536	12
SACV		II	10	-23.61	14.97	-0.304	13
SHEL	*	II	00	-5.75	-15.96	1.106	17
SHEL		II	10	-5.75	-15.96	0.054	31
SUR		II	00	20.81	-32.38	0.043	37
SUR		II	10	20.81	-32.38	-0.152	31
TAU		II	00	147.32	-42.91	-0.049	115
TLY		II	00	103.64	51.68	-0.223	115
WRAB	*	II	00	134.36	-19.93	0.868	96
WRAB		II	10	134.36	-19.93	0.082	117
ADK		IU		-176.68	51.88	-0.106	14
ADK		IU	00	-176.68	51.88	-0.042	66
AFI		IU	00	-171.78	-13.91	-0.285	58
AFI		IU	10	-171.78	-13.91	-0.27	55
ANMO		IU		-106.46	34.95	-0.107	10
ANMO		IU	00	-106.46	34.95	-0.305	40
ANMO		IU	10	-106.46	34.95	-0.218	40

Table A.2 (continued)

ANTO		IU	00	32.79	39.87	-0.154	44
BBSR		IU	00	-64.7	32.37	-0.231	26
BBSR		IU	01	-64.7	32.37	-0.224	19
BILL		IU		166.45	68.06	-0.451	16
BILL		IU	00	166.45	68.06	-0.263	98
CASY		IU		110.54	-66.28	-0.202	18
CASY		IU	00	110.54	-66.28	-0.235	98
CASY		IU	10	110.54	-66.28	-0.223	78
CCM		IU		-91.25	38.06	0.126	11
CCM		IU	00	-91.25	38.06	-0.042	24
CHTO		IU		98.98	18.79	-0.276	18
CHTO		IU	00	98.98	18.79	-0.302	116
CHTO		IU	10	98.98	18.79	-0.28	31
COLA		IU	00	-147.85	64.87	0.012	62
COLA		IU	10	-147.85	64.87	0.188	49
COR		IU	00	-123.3	44.59	0.225	35
CTAO		IU		146.25	-20.09	-0.296	17
CTAO		IU	00	146.25	-20.09	-0.153	106
DAV		IU	00	125.58	7.07	0.167	41
DWPF		IU	00	-81.43	28.11	0.044	28
FUNA		IU	00	179.2	-8.53	-0.009	14
FUNA		IU	10	179.2	-8.53	0.208	21
FURI		IU	00	38.69	8.9	0.099	17
FURI		IU	10	38.69	8.9	0.157	17
GNI		IU	00	44.74	40.15	0.201	68
GRFO		IU		11.22	49.69	-0.031	35
GUMO		IU		144.87	13.59	-0.036	14
GUMO		IU	00	144.87	13.59	0.089	76
GUMO		IU	10	144.87	13.59	0.192	62
HKT		IU	00	-95.84	29.96	-0.009	26
HNR		IU	00	159.95	-9.43	0.045	53
HNR		IU	10	159.95	-9.43	0.478	26
HRV	*	IU		-71.56	42.51	-0.315	31
INCN		IU		126.63	37.48	-0.294	13
INCN		IU	00	126.63	37.48	-0.245	98
INCN		IU	10	126.63	37.48	-0.232	78
JOHN		IU	00	-169.53	16.73	0.146	45
JOHN		IU	10	-169.53	16.73	0.212	41
KBL		IU		69.04	34.54	-0.045	38
KBS		IU	00	11.94	78.93	-0.292	54
KBS		IU	10	11.94	78.92	-0.273	46
KEV		IU	00	27.01	69.75	-0.224	64
KEV		IU	10	27.01	69.75	-0.225	66
KIEV		IU	00	29.21	50.69	-0.151	56
KIP		IU		-158.01	21.42	-0.075	13
KIP		IU	00	-158.01	21.42	0.032	95
KIP		IU	10	-158.01	21.42	0.061	80
KMBO		IU	00	37.25	-1.13	-0.26	26
KMBO		IU	10	37.25	-1.13	-0.258	22
KONO		IU	00	9.6	59.65	-0.277	41
KONO		IU	10	9.6	59.65	-0.253	42
LCO		IU		-70.7	-29.01	-0.096	13
LSZ		IU	00	28.19	-15.28	-0.411	39
LSZ		IU	10	28.19	-15.28	-0.406	37

Table A.2 (continued)

LVC	IU	00	-68.91	-22.61	0.155	13
LVC	IU	10	-68.91	-22.61	0.151	11
MA2	IU		150.77	59.58	-0.292	17
MA2	IU	00	150.77	59.58	-0.165	69
MAJO	IU		138.21	36.54	-0.543	25
MAJO	IU	00	138.21	36.54	-0.314	141
MAJO	IU	10	138.21	36.54	-0.323	40
MAKZ	IU		81.98	46.81	-0.153	13
MAKZ	IU	00	81.98	46.81	-0.161	33
MAKZ	IU	10	81.98	46.81	-0.151	33
MBWA	IU	00	119.73	-21.16	-0.107	81
MBWA	IU	10	119.73	-21.16	-0.064	89
MIDW	IU	00	-177.37	28.22	-0.154	48
NWAO	IU		117.23	-32.93	-0.285	30
NWAO	IU	00	117.23	-32.93	-0.215	124
NWAO	IU	10	117.23	-32.93	-0.073	41
OTAV	IU	00	-78.45	0.24	0.065	11
PAB	IU	00	-4.35	39.55	-0.256	24
PAYG	IU	00	-90.29	-0.67	-0.146	19
PAYG	IU	10	-90.29	-0.67	-0.038	13
PET	IU		158.65	53.02	-0.357	22
PET	IU	00	158.65	53.02	-0.146	119
PMG	IU		147.15	-9.41	-0.385	11
PMG	IU	00	147.15	-9.41	-0.036	83
PMG	IU	10	147.15	-9.41	0.026	61
PMSA	IU		-64.05	-64.77	-0.186	14
PMSA	IU	00	-64.05	-64.77	-0.158	32
POHA	IU	00	-155.53	19.76	0.002	98
POHA	IU	10	-155.53	19.76	0.039	30
PTCN	IU	00	-130.1	-25.07	0.044	33
PTCN	IU	01	-130.1	-25.07	0.095	14
QSPA	IU	00	145	-89.93	0.211	44
QSPA	IU	10	145	-89.93	0.283	44
QSPA	IU	20	145	-89.93	0.381	23
QSPA	IU	30	145	-89.93	0.257	44
QSPA	IU	50	145	-89.93	0.233	24
RAR	IU		-159.77	-21.21	-0.535	11
RAR	IU	00	-159.77	-21.21	-0.248	51
RAR	IU	10	-159.77	-21.21	-0.329	19
RCBR	IU	00	-35.9	-5.83	-0.251	36
RCBR	IU	10	-35.9	-5.83	-0.196	32
RSSD	IU	00	-104.04	44.12	-0.185	29
RSSD	IU	10	-104.04	44.12	-0.093	15
SBA	IU	00	166.76	-77.85	0.121	107
SDV	IU	00	-70.63	8.88	-0.061	21
SDV	IU	10	-70.63	8.88	-0.036	13
SFJ	IU	00	-50.62	67	-0.178	27
SFJD	IU	00	-50.62	67	-0.298	22
SFJD	IU	10	-50.62	67	-0.298	17
SJG	IU	00	-66.15	18.11	0.134	19
SNZO	IU	00	174.7	-41.31	-0.043	63
SNZO	IU	10	174.7	-41.31	0.001	67
SSPA	IU	00	-77.89	40.64	-0.145	27
TARA	IU	00	172.92	1.35	0.219	10

Table A.2 (continued)

TATO		IU		121.5	24.97	-0.201	13
TATO		IU	00	121.5	24.97	0.017	88
TATO		IU	10	121.5	24.97	0.089	54
TEIG		IU	00	-88.28	20.23	0.03	12
TEIG		IU	10	-88.28	20.23	0.096	10
TIXI		IU	00	128.87	71.65	-0.198	101
TRQA		IU	00	-61.98	-38.06	-0.042	12
TRQA		IU	10	-61.98	-38.06	-0.073	14
TSUM	*	IU	00	17.58	-19.2	-0.427	24
TSUM	*	IU	10	17.58	-19.2	-0.424	22
TUC	*	IU	00	-110.78	32.31	-0.395	40
ULN		IU		107.05	47.87	-0.273	12
ULN		IU	00	107.05	47.87	-0.288	100
WAKE		IU		166.65	19.28	0.02	16
WAKE		IU	00	166.65	19.28	0.179	70
WAKE		IU	01	166.65	19.28	0.15	43
WAKE		IU	20	166.65	19.28	0.195	24
WCI		IU	00	-86.29	38.23	-0.017	15
WVT		IU		-87.83	36.13	0.039	23
XMAS		IU		-157.45	2.04	-0.185	12
XMAS		IU	00	-157.45	2.04	0.058	48
XMAS		IU	01	-157.45	2.04	0.103	12
XMAS		IU	10	-157.45	2.04	0.015	33
YAK		IU		129.68	62.03	0.111	14
YAK		IU	00	129.68	62.03	0.249	107
YSS		IU		142.76	46.96	-0.286	19
YSS		IU	00	142.76	46.96	-0.089	124
ASAJ		JP		142.59	44.12	0.021	27
CBIJ		JP		142.18	27.1	0.314	20
JHJ2		JP		139.81	33.12	0.468	12
JNU		JP		130.88	33.12	-0.022	30
JOW		JP		128.27	26.84	-0.015	23
YOJ		JP		123.01	24.47	0.018	18
AAK		KN		74.49	42.63	-0.088	16
AML		KN		73.69	42.13	0.047	23
CHM		KN		74.75	43	-0.157	27
EKS2		KN		73.78	42.66	-0.021	25
KBK		KN		74.95	42.66	0.144	21
KZA		KN		75.25	42.08	0.146	28
TKM2		KN		75.6	42.92	0.098	27
UCH		KN		74.51	42.23	-0.217	23
ULHL		KN		76.24	42.25	-0.217	28
USP		KN		74.5	43.27	0.047	23
ABKAR		KZ		59.94	49.26	0.078	19
KKAR		KZ		70.51	43.1	-0.164	18
MKAR		KZ		82.29	46.79	-0.007	20
AQU		MN		13.4	42.35	0.072	21
BNI		MN		6.68	45.05	-0.043	23
CEL		MN		15.89	38.26	0.158	14
CII		MN		14.3	41.72	0.239	10
CUC		MN		15.81	39.99	-0.06	11
DIVS		MN		19.99	44.1	-0.198	15
IDI		MN		24.89	35.29	0.026	23
TIP		MN		16.76	39.18	-0.167	17
TIR		MN		19.86	41.35	0.083	10
TRI		MN		13.76	45.71	-0.238	19
TUE		MN		9.35	46.47	-0.128	17
VLC		MN		10.39	44.16	-0.03	19

Table A.2 (continued)

VSL		MN	9.38	39.5	-0.19	12
VTS		MN	23.23	42.62	-0.138	31
WDD		MN	14.52	35.84	0.139	18
IPM		MY	101.03	4.48	-0.062	19
KKM		MY	116.21	6.04	0.093	19
KOM		MY	103.85	1.79	-0.149	19
KSM		MY	110.31	1.47	-0.056	25
KUM		MY	100.65	5.29	-0.179	21
LDM		MY	118.5	5.18	0.28	17
SBM		MY	112.21	2.45	-0.111	22
BLO		NM	-86.52	39.17	0.21	30
FVM		NM	-90.43	37.98	0.177	17
MPH	*	NM	-89.93	35.12	0.652	21
PLAL		NM	-88.08	34.98	-0.016	10
PVMO	*	NM	-89.7	36.41	0.736	13
SIUC		NM	-89.22	37.72	0.136	10
SLM		NM	-90.24	38.64	0.092	28
UALR		NM	-92.34	34.77	-0.089	29
USIN		NM	-87.67	37.97	0.23	15
UTMT		NM	-88.86	36.34	0.481	19
PATS		PS	158.32	6.84	0.034	18
PSI		PS	98.92	2.69	-0.156	25
113A		TA	-113.77	32.77	-0.376	10
115A		TA	-112.23	32.7	0.095	11
116A		TA	-111.7	32.56	-0.093	10
319A		TA	-109.28	31.38	0.058	12
A04A		TA	-122.71	48.72	0.145	12
A05A		TA	-122.09	49	0.061	13
A12A		TA	-115.65	48.93	-0.093	11
A13A		TA	-114.41	48.93	0.132	11
B04A		TA	-123.5	48.06	-0.1	11
B05A		TA	-122.1	48.26	-0.308	11
B06A		TA	-121.48	48.52	-0.209	12
B07A		TA	-120.12	48.46	-0.145	12
B08A		TA	-119.33	48.36	-0.09	10
B13A		TA	-114.47	48.37	-0.004	12
BNLO		TA	-122.17	37.13	-0.152	11
C07A		TA	-120.06	47.69	-0.153	10
C14A		TA	-113.75	47.77	-0.095	10
D03A		TA	-123.77	47.12	0.527	11
D05A		TA	-121.99	47.19	0.291	20
D15A		TA	-112.52	47.04	0.021	13
E06A		TA	-120.98	46.54	-0.119	10
E07A		TA	-119.85	46.56	0.008	17
E13A		TA	-114.19	46.44	-0.196	12
ELFS		TA	-120.73	40.62	0.222	11
F03A		TA	-123.56	45.93	0.373	16
F04A		TA	-122.42	45.93	0.029	12
F10A		TA	-117.23	45.97	-0.107	10
G04A		TA	-122.48	45.21	0.199	12
G05A		TA	-121.32	45.24	0.498	10
G08A		TA	-118.96	45.29	-0.313	15
H04A		TA	-122.19	44.68	0.046	17
H06A		TA	-120.33	44.73	-0.06	10
HAST		TA	-121.55	36.39	-0.058	19
HATC		TA	-121.46	40.82	0.313	13
HELL		TA	-119.02	36.68	-0.214	11
I05A		TA	-121.27	44.16	0.251	14
I07A		TA	-119.5	44.08	-0.157	11
J06A		TA	-120.15	43.25	-0.085	11
K05A		TA	-120.89	42.73	0.429	10
K14A		TA	-113.18	42.55	-0.174	10

Table A.2 (continued)

L10A	TA		-116.47	42.08	0.01	10
M02C	TA		-122.85	41.39	-0.121	12
M03C	TA		-122.12	41.27	0.116	13
M04C	TA		-121.84	41.78	0.114	14
M05C	TA		-121.15	41.36	0.158	11
M06C	TA		-120.48	41.2	0.084	11
N02C	TA		-123.31	40.82	-0.634	13
N13A	TA		-114.2	40.86	0.121	10
O03C	TA		-122.03	40	0.156	10
O04C	TA		-121.09	40.32	0.095	12
O05C	TA		-120.92	39.96	-0.138	10
O11A	TA		-115.66	40.13	-0.003	10
P01C	TA		-123.34	39.47	-0.213	11
P05C	TA		-120.61	39.3	-0.213	13
Q03C	TA		-122.01	38.63	0.343	13
Q04C	TA		-121.38	38.84	0.085	11
R04C	TA		-120.94	38.26	-0.205	12
R05C	TA		-120.08	38.7	-0.347	14
R06C	TA		-119.45	38.52	-0.141	21
S04C	TA		-121.33	37.51	-0.211	13
S05C	TA		-120.33	37.35	0.134	16
S08C	TA		-118.17	37.5	-0.215	11
T06C	TA		-119.71	37.01	-0.274	10
U04C	TA		-120.78	36.36	0.117	16
V03C	TA		-121.24	36.02	0.243	13
V04C	TA		-120.87	35.64	0.278	10
W13A	TA		-113.89	35.1	-0.149	15
X13A	TA		-113.83	34.59	-0.257	11
X15A	TA		-112.24	34.49	-0.175	10
Y12C	TA		-114.52	33.75	-0.114	17
Y14A	TA		-113	33.94	-0.206	17
ANPB	TW		121.52	25.19	0.046	10
KMNB	TW		118.39	24.46	-0.037	74
NACB	TW		121.59	24.17	-0.078	91
SSLB	TW		120.95	23.79	-0.225	100
TPUB	TW		120.63	23.3	-0.007	95
TWGB	TW		121.08	22.82	-0.07	72
TWKB	TW		120.81	21.94	0.324	23
YHNB	TW		121.37	24.67	-0.041	67
YULB	TW		121.3	23.39	-0.138	82
DBO	UO		-123.24	43.12	-0.173	10
AAM	US		-83.66	42.3	-0.111	10
ACSO	US		-82.98	40.23	0.026	18
AHID	US		-111.1	42.77	-0.24	30
AMTX	US		-101.68	34.88	0.026	16
BINY	US		-75.99	42.2	0.094	24
BLA	US		-80.42	37.21	0.104	26
BMO	US		-117.31	44.85	-0.144	17
BOZ	US		-111.63	45.65	0.021	15
BW06	US		-109.56	42.77	-0.156	19
CBKS	US		-99.74	38.81	0.353	21
CBN	US		-77.37	38.2	0.122	11
CMB	US		-120.39	38.03	-0.224	17
DGMT	US		-104.2	48.47	0.477	14
DUG	US		-112.81	40.2	-0.059	21
EGAK	US		-141.16	64.78	-0.085	28
EGMT	US		-109.75	48.02	0.154	13
ERPA	US		-79.99	42.12	0.349	12
EYMN	US		-91.5	47.95	-0.127	26
EYMN	US	HR	-91.5	47.95	-0.101	12
GOGA	US		-83.47	33.41	-0.203	15
GOGA	US	HR	-83.47	33.41	-0.204	10

Table A.2 (continued)

HAWA	US		-119.53	46.39	-0.137	22
HLID	US		-114.41	43.56	-0.155	30
HWUT	US		-111.57	41.61	0.028	23
ISCO	US		-105.61	39.8	-0.179	22
JCT	US		-99.8	30.48	0.057	21
JFWS	US		-90.25	42.91	0.205	23
JFWS	US	HR	-90.25	42.91	0.119	13
KSU1	US		-96.61	39.1	0.132	18
KSU1	US	HR	-96.61	39.1	0.096	10
KVTX	US		-97.89	27.55	0.518	10
LAO	US		-106.22	46.69	0.216	13
LBNH	US		-71.93	44.24	-0.147	19
LONY	US		-74.58	44.62	-0.331	11
LRAL	US		-87	33.03	-0.17	16
LTX	US		-103.67	29.33	-0.186	10
MCWV	US		-79.85	39.66	0.15	19
MIAR	US		-93.58	34.55	-0.07	20
MNTX	US		-105.38	31.7	-0.24	14
MSO	US		-113.94	46.83	-0.528	24
NATX	US		-94.66	31.76	0.348	14
NCB	US		-74.22	43.97	-0.26	36
NEW	US		-117.12	48.26	-0.205	34
NEW	US	HR	-117.12	48.26	-0.205	15
NHSC	US		-80.18	33.11	0.512	11
NLWA	US		-123.87	47.39	0.035	21
OCWA	US		-124.18	47.75	0.228	12
OXF	US		-89.41	34.51	0.302	21
SAO	US		-121.44	36.77	-0.238	19
SCIA	US		-93.22	41.91	0.243	11
SDCO	US		-105.5	37.75	0.039	23
TPNV	US		-116.25	36.95	-0.039	15
WDC	US		-122.54	40.58	-0.274	21
WMOK	US		-98.78	34.74	-0.19	19
WMOK	US	HR	-98.78	34.74	-0.196	15
WRAK	US		-132.35	56.42	-0.18	14
WRAK	US	HR	-132.35	56.42	-0.184	14
WUAZ	US		-111.37	35.52	-0.022	21
WVOR	US		-118.64	42.43	-0.097	29
GNW	UW		-122.83	47.56	-0.292	23
HEBO	UW		-123.76	45.21	0.234	18
HOOD	UW		-121.65	45.32	0.374	13
LON	UW		-121.81	46.75	-0.38	19
LTY	UW		-120.67	47.26	-0.155	14
OFR	UW		-124.4	47.93	0.332	19
SQM	UW		-123.05	48.08	0.311	15
TAKO	UW		-124.08	43.74	0.118	13
TOLO	UW		-123.92	44.62	0.36	12
TTW	UW		-121.69	47.69	-0.043	16

Table A.3 Middle America Trench earthquakes with $M_0 \geq$ 5e17 Nm. Earthquakes are ordered by date, with letters identifying subsequent events occurring on the same date. Origin time, location, and focal mechanism information is taken from the gCMT catalog. E_{est} and θ_{est} are the estimated energy and energy-to-moment ratio, calculated without the knowledge of the true focal mechanism, instead with an averaged focal correction as suggested by *Newman and Okal* [1998]. High frequency results (0.5 Hz and 2 Hz), and broad-band results (14 mHz to 2Hz) are shown. σ_g is the $\log_{10}$ of the geometric standard deviation. Last two columns are the EHB/NEIC depths

General Information									BroadBand (0.5-70s)					High Freq.(0.5-2s)			
Event YYDOY	Time HH:MM	Lat	Lon	Depth (km)	$\phi/\delta/\lambda$	$M_0(M_W)$	N (#)	T_{XO} (s)	$E_{est}(M_e)$ (J)	$E(M_e)$ (J)	θ_{est}	θ	σ_g 10^X	E(Me) (J)	σ_g 10^X	Depth (km)	src
92246a	0:16	11.2	-87.81	15	303/12/ 91	3.40E+20	13	165	5.50E+14	6.30E+14	-5.8	-5.7	0.68	2.40E+13	0.53	45	EHB
97200a	14:22	15.86	-98.26	15	282/14/ 78	1.20E+19	13	60	9.00E+13	6.90E+13	-5.1	-5.2	0.29	6.30E+12	0.35	31.4	EHB
97338a	14:56	13.56	-91.25	36	292/27/ 80	9.90E+17	6	65	4.30E+13	5.40E+13	-4.4	-4.3	0.8	4.50E+12	0.48	35	EHB
97350a	11:48	16.43	-98.73	16	260/18/ 64	1.00E+18	6	67	1.20E+13	1.20E+13	-4.9	-4.9	0.72	1.40E+12	0.68	15.8	EHB
97356a	10:03	13.62	-90.84	55	251/24/ 34	1.40E+18	17	60	2.00E+13	3.00E+13	-4.8	-4.7	0.83	5.70E+12	0.61	81.6	EHB
97359a	22:16	14.15	-92.71	33	284/26/ 78	6.30E+17	8	50	8.90E+12	8.10E+12	-4.8	-4.9	0.46	3.30E+12	0.67	51.3	EHB
98034a	3:02	15.92	-96.22	24	288/42/104	3.70E+18	20	50	7.80E+13	7.10E+13	-4.7	-4.7	0.71	2.10E+13	0.51	24	EHB
98130a	6:05	13.59	-91.35	25	283/22/ 73	3.70E+18	11	31	1.00E+14	1.10E+14	-4.6	-4.5	1.03	1.70E+13	0.64	18	EHB
98282a	11:54	11.08	-86.93	32	302/21/ 89	1.20E+18	18	50	1.00E+13	6.80E+12	-5.1	-5.2	0.37	3.50E+12	0.49	16	EHB
99128a	22:12	14.19	-92.38	32	285/29/ 76	1.40E+18	20	40	5.10E+12	3.80E+12	-5.4	-5.6	0.46	1.70E+12	0.54	32.1	EHB
99232a	10:02	9.28	-84.1	24	306/27/102	2.60E+19	33	69	2.60E+14	1.60E+14	-5	-5.2	0.38	1.30E+13	0.65	19	EHB
99233a	10:49	9.07	-83.97	15	295/24/ 93	5.50E+17	21	50	3.20E+12	1.80E+12	-5.2	-5.5	0.58	6.80E+11	0.63	37.9	EHB
00072a	22:21	14.84	-93.02	66	254/19/ 32	3.10E+18	36	61	7.10E+13	1.10E+14	-4.6	-4.4	0.73	2.50E+13	0.66	53	EHB
00339a	4:43	14.86	-94	36	296/19/ 70	1.10E+18	21	35	2.50E+13	3.90E+13	-4.6	-4.4	0.52	6.20E+12	0.39	28.1	EHB
01015a	12:20	12.95	-89.06	56	274/16/ 50	5.90E+17	8	45	2.40E+12	4.00E+12	-5.4	-5.2	0.3	1.80E+12	0.44	56	EHB
01075a	0:01	12.84	-89.43	36	271/19/ 53	8.80E+17	18	52	4.60E+12	4.10E+12	-5.3	-5.3	0.5	2.80E+12	0.58	36	EHB
02108a	5:02	16.79	-101.22	15	291/ 9/ 89	1.50E+19	33	80	4.80E+13	3.00E+13	-5.5	-5.7	0.38	3.10E+12	0.54	11	EHB
02108b	17:57	17.45	-100.92	44	273/17/ 81	8.80E+17	17	60	2.80E+12	2.10E+12	-5.5	-5.6	0.53	2.60E+11	0.5	44.2	EHB
02158a	17:00	16.23	-96.74	22	269/18/ 69	2.50E+17	12	20	1.50E+12	8.90E+11	-5.2	-5.4	0.34	5.60E+11	0.34	36.8	EHB
02284a	14:41	15.49	-95.99	15	260/16/ 60	2.30E+17	14	30	1.60E+12	1.10E+12	-5.1	-5.3	0.46	1.10E+11	0.5	15	EHB
02313a	0:14	13.76	-91.64	19	286/24/ 76	1.10E+18	30	50	1.50E+13	1.30E+13	-4.9	-4.9	0.53	4.20E+12	0.55	18	EHB
03021a	2:46	13.53	-91.31	41	290/33/ 80	5.40E+18	45	55	7.20E+13	6.50E+13	-4.9	-4.9	0.59	1.10E+13	0.69	24	EHB
04001a	23:31	17.45	-101.4	15	299/13/ 92	1.50E+18	37	35	2.00E+13	1.50E+13	-4.9	-5	0.51	2.40E+12	0.57	17	EHB
04056a	18:22	13.65	-92.63	12	293/17/ 82	5.00E+17	24	38	7.00E+12	6.20E+12	-4.9	-4.9	0.59	4.90E+11	0.68	12	EHB
04062a	3:47	11.45	-87.25	26	307/16/ 96	2.30E+18	17	32	9.80E+12	1.20E+13	-5.4	-5.3	0.48	3.60E+12	0.66	28	EHB
04119a	4:09	11.81	-87.9	34	296/28/ 84	2.50E+17	31	25	3.40E+12	3.00E+12	-4.9	-4.9	0.57	2.30E+12	0.7	65.2	EHB
04120a	0:57	10.32	-86.38	19	309/15/ 97	2.40E+18	45	30	1.70E+13	1.80E+13	-5.1	-5.1	0.64	5.40E+12	0.69	18	EHB
04166a	22:54	16.46	-97.92	18	277/11/ 70	8.70E+17	34	25	5.10E+12	4.70E+12	-5.2	-5.3	0.46	1.90E+12	0.51	18	EHB

Table A.3 (continued)

04283a	21:26	11.25	-87.02	39	311/26/ 98	3.00E+19	14	56	3.80E+14	3.40E+14	-4.9	-4.9	0.56	1.30E+14	0.79	35	EHB
04325a	22:01	13.13	-90.61	34	285/27/ 71	3.40E+18	40	40	3.00E+13	3.60E+13	-5.1	-5	0.6	1.30E+13	0.78	34.4	EHB
04348a	15:23	13.3	-89.81	60	314/ 6/105	9.60E+17	30	53	1.20E+13	1.90E+13	-4.9	-4.7	0.67	8.70E+12	0.87	60	EHB
05074a	0:15	10.71	-86.61	32	310/25/ 94	6.40E+17	56	40	8.80E+12	8.10E+12	-4.9	-4.9	0.42	2.00E+12	0.57	32.9	EHB
05181a	21:26	8.43	-82.82	26	334/38/111	9.20E+17	43	25	4.30E+12	3.20E+12	-5.3	-5.5	0.53	1.30E+12	0.68	34	EHB
05183a	2:16	11.06	-86.7	28	311/22/ 96	1.00E+19	63	45	7.60E+13	8.80E+13	-5.1	-5.1	0.57	3.70E+13	0.67	27	EHB
05183b	4:11	10.86	-86.92	35	308/29/ 95	5.60E+17	29	55	3.80E+12	3.40E+12	-5.2	-5.2	0.44	1.40E+12	0.62	35.7	EHB
06121a	7:47	8.11	-82.88	12	326/39/121	9.10E+17	54	55	4.70E+12	3.00E+12	-5.3	-5.5	0.31	2.90E+11	0.51	13	EHB
06178a	13:03	14.95	-94.53	12	305/20/ 87	6.60E+17	47	45	4.10E+12	4.50E+12	-5.2	-5.2	0.36	5.90E+11	0.53	9	EHB
06231a	5:41	16.26	-97.27	26	277/16/ 72	2.80E+17	44	56	2.00E+12	1.40E+12	-5.2	-5.3	0.45	5.10E+11	0.56	26.4	EHB
07103a	5:42	17.37	-100.14	42	98/17/ 84	1.10E+18	53	50	2.40E+13	4.60E+13	-4.7	-4.4	0.44	1.60E+13	0.55	34	EHB
07159a	13:32	13.51	-91.32	39	292/34/ 84	6.70E+17	85	50	4.10E+12	3.90E+12	-5.2	-5.2	0.54	1.90E+12	0.65	65	EHB
07164a	19:29	13.43	-91.22	31	286/31/ 75	1.30E+19	123	48	1.30E+14	1.30E+14	-5	-5	0.47	4.00E+13	0.67	65	EHB
08023a	5:49	14.54	-93.99	12	292/18/ 76	2.20E+17	54	25	1.40E+12	1.60E+12	-5.2	-5.1	0.27	4.80E+11	0.45	--	EHB
08148a	11:28	13.45	-91.39	29	287/27/ 77	3.90E+17	49	32	1.30E+12	1.30E+12	-5.5	-5.5	0.42	6.90E+11	0.5	26	NEIC
08290a	19:41	14.28	-92.9	29	289/26/ 74	1.20E+19	75	62	1.60E+14	1.50E+14	-4.9	-4.9	0.44	3.70E+13	0.61	24	NEIC
08320a	23:03	12.97	-89.08	64	245/ 7/ 30	6.40E+17	36	55	4.80E+12	7.00E+12	-5.1	-5	0.45	2.80E+12	0.62	48	NEIC
09070a	17:24	8.55	-83.18	18	291/25/ 86	9.40E+17	66	35	8.40E+12	6.10E+12	-5.1	-5.2	0.48	1.50E+12	0.65	14	NEIC
09070b	21:03	8.52	-83.22	22	150/44/115	7.90E+17	50	25	4.10E+12	7.00E+12	-5.3	-5	0.53	3.10E+12	0.66	17	NEIC
09117a	16:46	17.06	-99.41	32	69/23/ 62	6.90E+17	61	35	8.90E+12	1.90E+13	-4.9	-4.6	0.45	9.20E+12	0.56	35	NEIC
10018a	15:40	13.76	-90.57	75	256/14/ 41	8.20E+17	7	60	7.20E+12	1.90E+13	-5.1	-4.6	0.33	7.60E+12	0.51	55	NEIC
10054a	15:16	16.25	-91.31	21	142/27/110	2.50E+17	9	48	1.40E+12	1.80E+12	-5.3	-5.1	0.57	4.90E+11	0.56	10	NEIC
10056a	3:15	10.67	-86.64	32	307/26/ 90	3.60E+17	26	28	1.80E+12	1.80E+12	-5.3	-5.3	0.48	7.60E+11	0.66	--	--
10140a	22:16	9.23	-84.24	24	307/26/ 99	1.00E+18	82	50	4.90E+12	3.10E+12	-5.3	-5.5	0.47	1.20E+12	0.61	--	--
10152a	3:26	9.18	-84.29	26	300/24/ 96	1.20E+18	95	52	7.00E+12	4.40E+12	-5.2	-5.4	0.49	1.60E+12	0.61	--	--
10181a	7:22	16.52	-97.87	20	294/13/ 77	2.60E+18	81	65	3.00E+13	2.70E+13	-4.9	-5	0.5	9.10E+12	0.61	--	--

Table A.4 Java trench earthquakes with $M_0 \geq 5e17$ Nm. Earthquakes are ordered by date, with letters identifying subsequent events occurring on the same date. Origin time, location, and focal mechanism information is taken from the gCMT catalog. E_{est} and θ_{est} are the estimated energy and energy-to-moment ratio, calculated without the knowledge of the true focal mechanism, instead with an averaged focal correction as suggested by *Newman and Okal* [1998]. High frequency results (0.5 Hz and 2 Hz), and broad-band results (14 mHz to 2Hz) are shown. The value σ_g is $\log_{10}$ of the geometric standard deviation. Last two columns are the EHB/NEIC depths.

General Information									BroadBand (0.5-70s)					High Freq.(0.5-2s)			
Event YYDOY	Time HH:MM	Lat	Lon	Depth (km)	$\phi/\delta/\lambda$	$M_0(M_W)$	N (#)	T_{XO} (s)	$E_{est}(M_e)$ (J)	$E(M_e)$ (J)	θ_{est}	θ	σ_g 10^X	E(Me) (J)	σ_g 10^X	Depth (km)	src
94153a	18:17	-11.03	113.04	15	278/ 7/ 89	5.30E+20	12	95	6.10E+14	3.40E+14	-5.9	-6.2	0.14	2.60E+13	0.34	35.5	EHB
97271a	1:38	-3.92	119.77	34	13/40/110	7.10E+17	26	50	1.00E+13	9.00E+12	-4.8	-4.9	0.37	4.10E+12	0.51	13	EHB
98341a	23:37	-8.28	121.8	22	109/32/117	5.40E+17	28	38	4.70E+12	8.80E+12	-5.1	-4.8	0.51	4.00E+12	0.55	25	EHB
00005a	18:26	-9.39	109.59	22	294/20/104	5.40E+17	44	45	5.70E+12	3.10E+12	-5	-5.2	0.5	2.30E+12	0.54	34.7	EHB
00023a	6:08	-7.77	120.99	15	228/48/ 61	5.00E+17	44	40	1.60E+13	1.90E+13	-4.5	-4.4	0.36	1.30E+13	0.46	11	EHB
00135a	20:08	-4.31	123.56	16	235/32/125	2.90E+18	48	32	2.70E+13	3.10E+13	-5	-5	0.44	1.40E+13	0.56	14	EHB
00281a	11:57	-10.2	119.38	27	277/30/ 97	7.00E+17	44	52	2.30E+13	1.20E+13	-4.5	-4.7	0.39	5.80E+12	0.45	21	EHB
00299a	9:32	-7.28	105.43	45	299/27/102	1.70E+19	63	65	5.00E+14	3.00E+14	-4.5	-4.7	0.53	1.10E+14	0.61	38	EHB
01071a	23:35	-7.87	106.03	37	293/23/ 98	6.50E+17	54	41	1.20E+13	7.70E+12	-4.7	-4.9	0.7	5.30E+12	0.78	44.7	EHB
02238a	14:55	-7.19	105.6	56	281/36/ 93	5.00E+17	50	45	6.10E+12	4.40E+12	-4.9	-5.1	0.64	3.10E+12	0.69	65.6	EHB
02279a	15:46	-8.08	118.63	20	78/21/ 90	2.70E+18	28	71	4.00E+13	5.50E+13	-4.8	-4.7	0.37	2.20E+13	0.53	14	EHB
03134a	7:40	-8.56	107.22	27	257/11/109	1.10E+18	51	74	5.50E+12	3.40E+12	-5.3	-5.5	0.53	1.40E+12	0.61	51.8	EHB
03200a	21:20	-9.16	111.23	43	283/25/ 97	6.70E+17	64	40	2.30E+13	1.40E+13	-4.5	-4.7	0.53	1.00E+13	0.57	54.1	EHB
03251a	6:26	-8.98	110.62	44	272/28/120	7.20E+17	33	69	8.00E+12	5.20E+12	-5	-5.1	0.56	2.50E+12	0.55	56.6	EHB
03324a	12:24	-10.69	110.99	15	286/20/106	7.80E+17	24	58	4.70E+12	1.90E+12	-5.2	-5.6	0.22	6.60E+11	0.35	17.7	EHB
05015a	13:47	-6.63	105.25	14	309/ 3/100	1.00E+18	43	35	4.10E+12	5.00E+12	-5.4	-5.3	0.68	2.90E+12	0.69	58.3	EHB
05050a	0:04	-5.52	122.23	12	41/49/121	5.60E+18	16	55	2.80E+14	3.10E+14	-4.3	-4.3	0.48	1.00E+14	0.56	16	EHB
06076a	14:21	-4.88	123.27	12	210/42/156	2.90E+17	33	48	5.40E+12	1.40E+13	-4.7	-4.3	0.61	4.80E+12	0.62	16.3	EHB
06198a	8:19	-10.28	107.78	20	290/10/102	4.60E+20	61	160	1.20E+15	1.00E+15	-5.6	-5.7	0.38	1.50E+14	0.59	24.3	EHB
06200a	10:57	-7.18	105.21	46	311/35/116	2.00E+18	69	52	2.20E+13	1.90E+13	-5	-5	0.65	1.20E+13	0.67	45	EHB
06264a	18:54	-9.49	110.57	34	276/24/ 85	1.10E+18	64	50	1.40E+13	1.10E+13	-4.9	-5	0.54	5.40E+12	0.59	25	EHB
06335a	14:01	-8.16	118.8	27	89/24/104	4.00E+18	55	56	3.40E+13	4.00E+13	-5.1	-5	0.53	2.00E+13	0.61	19	EHB
07031a	20:31	-8.14	107.25	72	183/44/ 48	2.30E+17	52	30	4.70E+12	4.90E+12	-4.7	-4.7	0.67	3.70E+12	0.7	53	EHB
07277a	14:28	-8.4	116.82	21	96/32/112	3.30E+17	37	30	3.80E+12	5.20E+12	-4.9	-4.8	0.56	1.80E+12	0.69	23.9	EHB
07329b	16:02	-8.21	118.47	25	88/23/103	6.10E+18	67	52	1.40E+14	1.70E+14	-4.6	-4.5	0.47	3.90E+13	0.64	35	EHB
07329c	19:53	-8.2	118.53	19	87/25/100	6.10E+18	60	60	9.20E+13	1.10E+14	-4.8	-4.8	0.5	3.20E+13	0.58	35	EHB
08036a	5:56	-3.44	118.12	18	28/51/ 51	5.70E+17	54	24	8.90E+12	1.50E+13	-4.8	-4.6	0.6	1.10E+13	0.72	13	EHB

Table A.4 (continued)

08155a	17:31	-8.09	120.32	20	93/26/100	8.40E+17	50	34	4.70E+12	6.30E+12	-5.3	-5.1	0.47	2.60E+12	0.54	14.4	NEIC
08155b	21:03	-8.09	120.3	18	88/23/ 93	5.50E+17	41	45	4.40E+12	5.70E+12	-5.1	-5	0.39	2.30E+12	0.52	7	NEIC
08155c	22:04	-8.07	120.25	18	88/23/ 97	1.20E+18	47	57	1.30E+13	1.50E+13	-5	-4.9	0.43	4.50E+12	0.6	14	NEIC
09245a	7:55	-8.08	107.34	52	51/45/117	3.60E+19	83	65	2.00E+15	2.00E+15	-4.2	-4.3	0.45	6.20E+14	0.59	46	EHB
09261a	23:06	-9.43	115.56	66	21/41/ 65	5.20E+17	40	55	2.00E+13	3.20E+13	-4.4	-4.2	0.46	2.80E+13	0.5	74	NEIC
09289a	9:52	-7.03	105.11	44	304/33/107	1.70E+18	46	65	2.90E+13	2.40E+13	-4.8	-4.8	0.54	1.30E+13	0.61	38	NEIC
09297a	20:54	-10.24	118.81	31	257/23/ 91	3.30E+17	31	32	5.50E+12	2.80E+12	-4.8	-5.1	0.46	1.90E+12	0.52	10	NEIC
09312a	19:41	-8.21	118.76	20	86/23/103	1.10E+19	50	49	1.80E+14	2.40E+14	-4.8	-4.7	0.55	5.60E+13	0.59	33	NEIC
10128a	3:22	-8.07	118.29	12	86/22/ 99	8.70E+17	30	51	7.90E+12	1.10E+13	-5	-4.9	0.44	1.70E+12	0.62	--	--

Figure A.1 Performance of individual vertical broadband seismic stations consistently over- or under-reported earthquake energies in the 1997 – 2010 catalog.

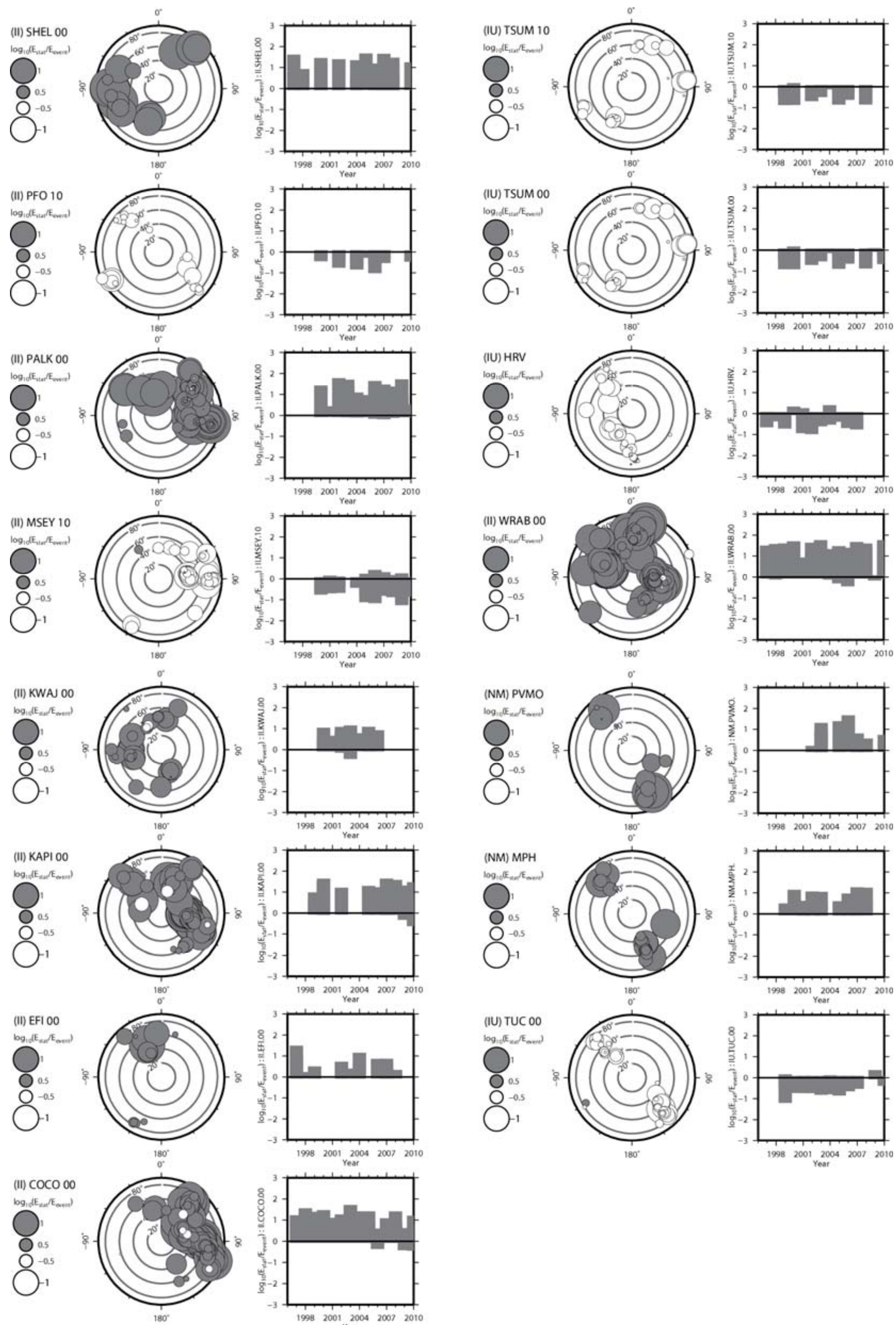

Figure A.1 continued

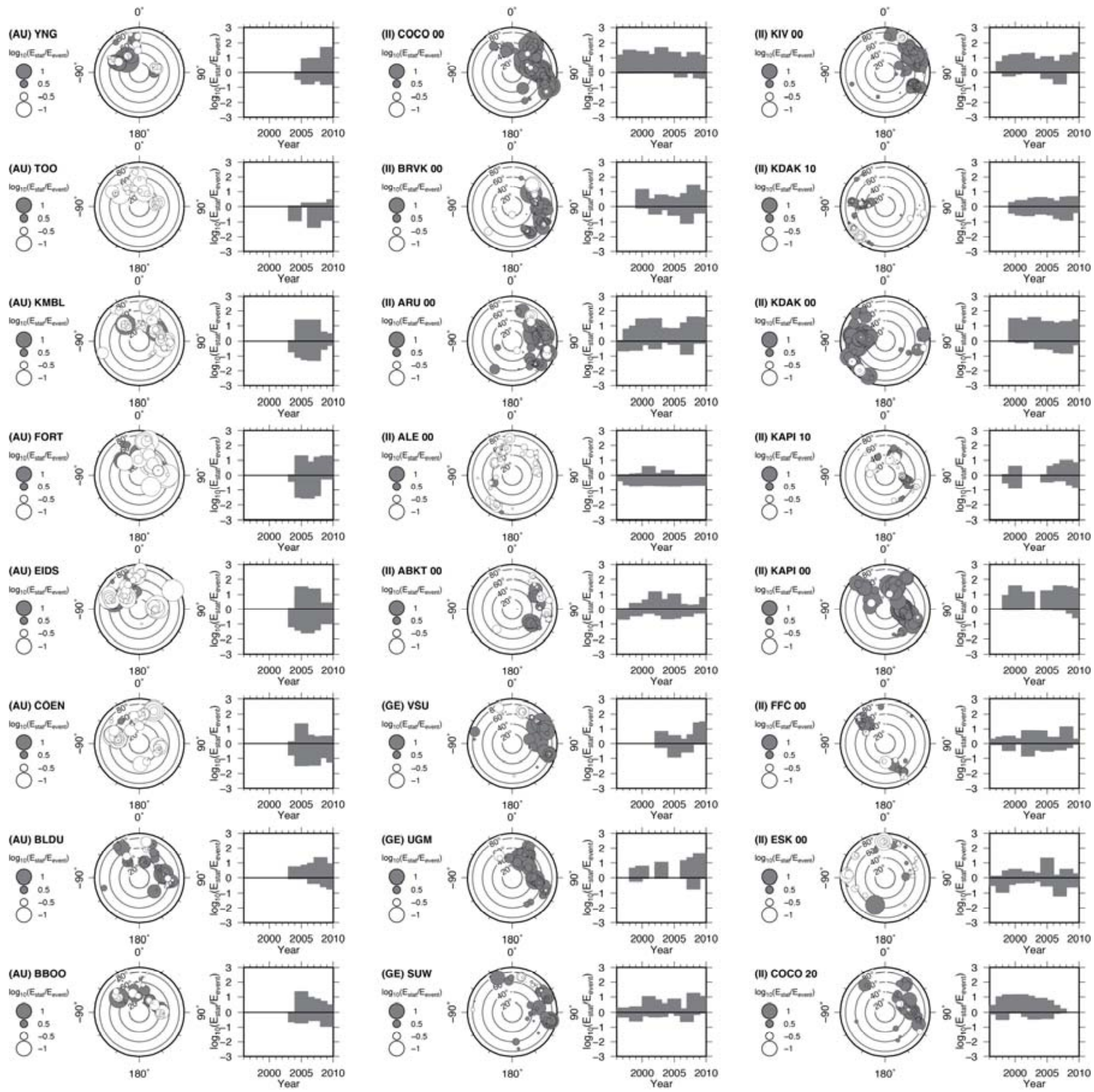

Figure A.2 Azimuthal and temporal deviations in energy calculations shown for all stations with 50 or more recorded events in this study.

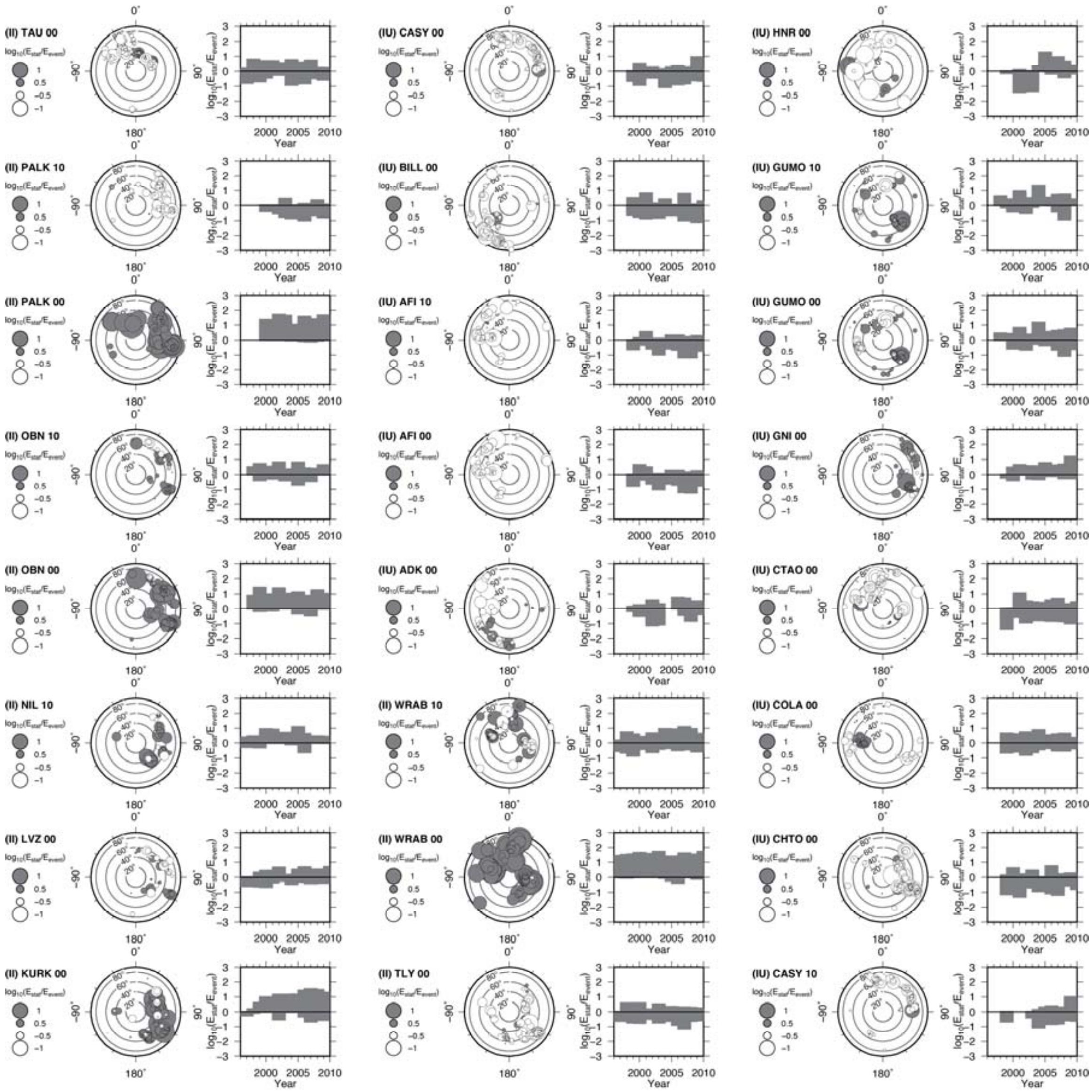

Figure A.2 continued

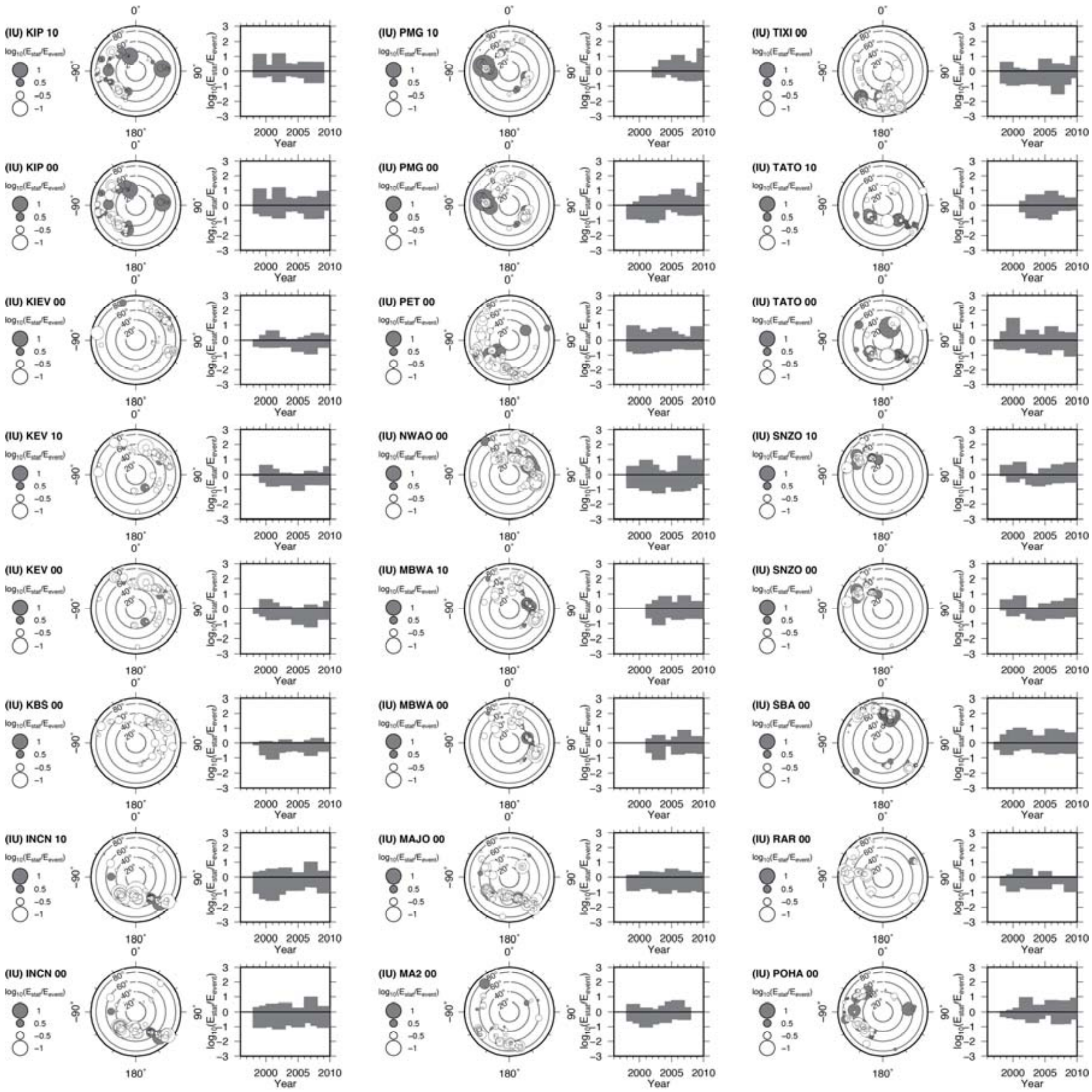

Figure A.2 continued

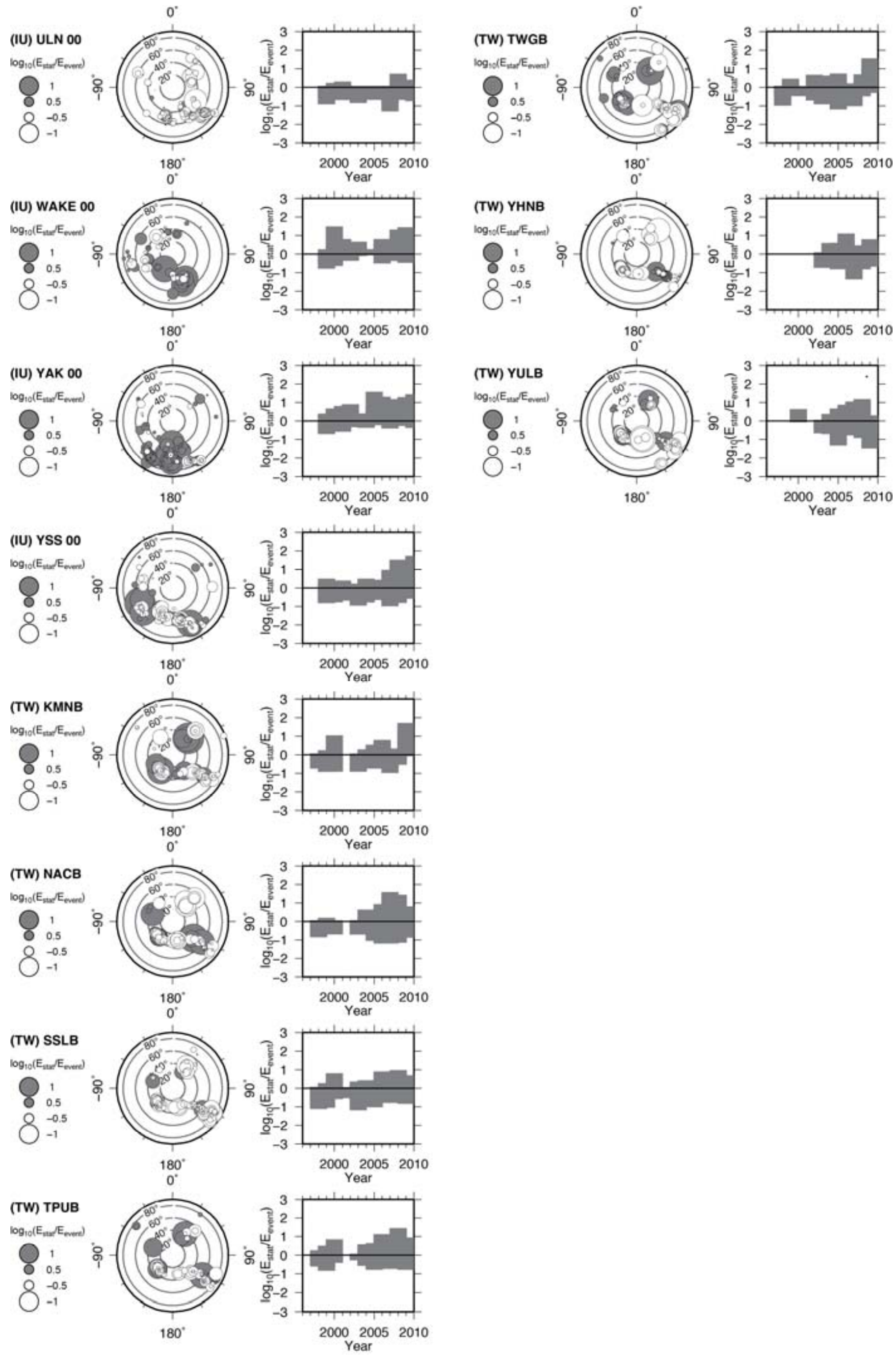

Figure A.4 continued

Table A.5 Linear regressions for the relation between energy-to-moment ratio and depth for different regions. The regressions are done for two different depth information sources (CMT and EHB)using both hypocentral and gCMT depths.

Region	**source**	**intercept**	**slope**
MAT	CMT	59 ± 43.9 km	3.37 ± 8.55 km
MAT	EHB	53.6 ± 36.3 km	4.86 ± 7.01 km
Java	CMT	171 ± 31.2 km	25.8 ± 6.1 km
Java	EHB	111 ± 38.3 km	14.2 ± 7.52 km
Global	CMT	95.9 ± 20.7 km	13.7 ± 4.36 km

APPENDIX B

TACER RESULTS AND STABILITY

Table B.1: Events with their TACER and T-crossover. Estimated durations. For TACER durations we include the upper and lower 75%

Date	HH:MM	M_w	M_r	$\phi/\delta/\lambda$	T_{TACER} (s)	T_{TACER} Lower 75% (s)	T_{TACER} Upper 75% (s)	T_{XO} (s)
2000/01/08	16:47	7.2	7.24	79/8/347	27	23	30	24
2000/03/28	11:00	7.6	7.97	255/6/233	26	22	30	40
2000/05/04	04:21	7.5	7.87	225/64/172	49	33	94	64
2000/05/12	18:43	7.1	7.00	214/12/298	20	16	26	20
2000/06/04	16:28	7.8	8.24	92/55/152	59	38	115	79
2000/06/18	14:44	7.9	7.82	161/63/355	36	24	49	48
2000/08/06	07:27	7.3	7.40	108/27/218	23	17	28	24
2000/11/16	04:54	8.0	7.99	328/43/3	136	78	159	84
2000/11/16	07:42	7.8	7.42	253/15/93	79	36	112	76
2000/11/17	21:01	7.8	6.90	230/24/64	69	38	93	95
2001/01/01	06:57	7.4	7.27	171/45/60	60	41	80	69
2001/01/13	17:33	7.7	7.87	121/35/265	40	25	51	48
2001/01/26	03:16	7.6	7.71	298/39/136	31	26	36	26
2001/02/13	19:28	7.3	7.07	315/16/103	47	39	63	63
2001/06/03	02:41	7.1	7.33	227/41/138	23	20	28	21
2001/08/21	06:52	7.1	7.46	55/42/116	70	51	111	72
2001/10/19	03:28	7.5	7.63	358/77/176	55	44	77	67
2001/11/14	09:26	7.8	7.58	94/61/348	123	62	181	150
2002/01/02	17:22	7.2	7.42	299/18/22	43	28	59	50
2002/03/05	21:16	7.5	7.27	314/25/70	54	39	71	83
2002/03/31	06:52	7.1	7.03	292/32/121	39	20	52	49
2002/06/28	17:19	7.3	7.72	27/13/105	24	19	31	25
2002/08/19	11:01	7.6	8.23	149/22/219	22	19	26	25
2002/09/08	18:44	7.6	7.54	106/34/43	45	37	57	82
2002/10/10	10:50	7.5	7.82	60/83/4	102	33	148	100
2002/11/02	01:26	7.2	7.27	297/16/73	49	39	60	70
2002/11/03	22:12	7.8	7.75	296/71/171	26	22	73	80
2002/11/17	04:53	7.3	7.59	316/9/30	14	13	24	20
2003/01/22	02:06	7.5	7.27	308/12/110	39	20	63	50
2003/07/15	20:27	7.5	7.56	307/69/1	87	73	101	85
2003/08/04	04:37	7.5	7.49	101/36/337	43	34	51	52
2003/08/21	12:12	7.2	7.27	35/23/95	30	19	42	40
2003/09/25	19:50	8.3	8.04	250/11/132	71	53	96	95
2003/09/25	21:08	7.3	7.43	208/18/86	64	44	76	69
2003/09/27	11:33	7.2	7.39	228/70/20	38	28	144	50
2003/12/27	16:00	7.2	7.10	324/29/95	46	37	54	55
2004/01/03	16:23	7.1	7.09	314/39/283	34	23	44	40
2004/02/07	02:42	7.3	7.53	261/68/353	41	26	50	60

Table B.1 (continued)

2004/07/25	14:35	7.3	7.85	108/45/231	20	14	25	25
2004/09/05	10:07	7.2	7.41	277/38/100	34	22	47	48
2004/09/05	14:57	7.4	7.51	79/46/72	51	46	64	55
2004/11/11	21:26	7.5	7.89	67/27/72	46	39	55	55
2004/11/15	09:06	7.2	7.44	21/11/114	53	12	87	85
2004/11/22	20:26	7.1	7.09	43/36/103	40	22	66	45
2004/11/26	02:25	7.1	7.14	5/34/0	40	30	89	67
2004/12/23	14:59	8.1	8.23	69/74/167	53	39	71	75
2004/12/26	00:58	9.0	8.71	329/8/110	170	131	271	540
2005/02/05	12:23	7.1	7.14	158/14/246	16	13	24	45
2005/03/02	10:42	7.1	7.60	308/35/176	15	11	33	73
2005/03/28	16:09	8.6	8.43	333/8/118	94	78	104	93
2005/06/13	22:44	7.8	7.83	182/23/279	19	17	26	74
2005/06/15	02:50	7.2	7.14	317/83/175	33	25	47	42
2005/07/24	15:42	7.2	7.49	29/68/358	36	29	45	46
2005/08/16	02:46	7.2	7.09	194/16/81	45	25	72	56
2005/09/09	07:26	7.6	7.31	140/30/91	84	64	155	90
2005/09/26	01:55	7.5	7.33	347/39/268	17	14	55	82
2005/10/08	03:50	7.6	7.41	334/40/123	40	33	56	65
2006/01/02	06:10	7.4	7.44	358/77/192	27	23	35	36
2006/01/02	22:13	7.2	7.39	281/22/320	18	12	23	25
2006/01/27	16:58	7.6	8.01	43/42/316	28	25	35	30
2006/04/20	23:25	7.6	7.26	207/40/76	41	28	53	55
2006/05/03	15:26	8.0	8.26	226/22/123	59	36	82	80
2006/05/16	10:39	7.4	7.69	129/19/58	26	21	32	35
2006/07/17	08:19	7.7	7.05	290/10/102	109	72	155	160
2006/11/15	11:14	8.3	7.93	215/15/92	95	73	111	115
2007/01/13	04:23	8.1	8.18	266/39/306	68	54	87	100
2007/01/21	11:27	7.5	7.53	34/35/108	37	30	44	40
2007/03/25	00:40	7.1	7.15	333/36/89	37	27	43	31
2007/04/01	20:39	8.1	7.91	333/37/121	94	81	115	101
2007/08/01	17:08	7.2	7.46	356/29/79	27	23	84	45
2007/08/08	17:04	7.5	7.64	330/30/155	33	24	40	30
2007/08/15	23:40	8.0	7.89	321/28/63	115	62	138	155
2007/09/02	01:05	7.2	7.19	338/23/101	65	42	76	82
2007/09/12	11:10	8.5	8.26	328/9/114	102	89	125	108
2007/09/12	23:48	7.9	7.64	317/19/102	93	46	107	108
2007/09/28	13:38	7.5	7.56	73/49/50	19	15	29	24
2007/09/30	05:23	7.4	7.41	29/36/123	44	39	55	57
2007/10/31	03:30	7.2	7.37	196/60/152	25	12	85	25
2007/11/14	15:40	7.7	7.77	358/20/98	59	50	73	71
2007/11/29	19:00	7.4	7.83	109/58/328	25	22	29	24
2007/12/09	07:28	7.8	7.98	34/25/38	34	25	46	35
2007/12/19	09:30	7.2	7.09	274/21/118	35	27	49	41
2008/02/20	08:08	7.3	7.17	299/11/80	58	40	72	64
2008/02/25	08:36	7.2	7.12	317/6/102	47	22	58	52
2008/03/20	22:33	7.1	6.89	358/41/250	36	33	46	38

Table B.1 (continued)

2008/04/09	12:46	7.3	7.08	340/30/101	43	18	52	49
2008/04/12	00:30	7.1	7.14	3/43/102	25	19	42	30
2008/05/12	06:28	7.9	7.95	231/35/138	83	50	123	100
2008/11/16	17:02	7.3	7.21	92/20/84	46	33	74	60
2008/11/24	09:02	7.3	7.55	276/19/331	27	25	30	30
2009/03/19	18:17	7.8	7.62	205/44/98	28	23	57	65
2009/05/28	08:24	7.5	7.34	63/60/353	41	26	73	48
2009/07/15	09:22	7.6	7.77	25/26/138	55	44	122	58
2009/08/09	10:55	7.0	7.06	86/17/168	18	12	22	19
2009/08/10	19:55	7.4	7.46	39/36/268	56	44	69	57
2009/09/29	17:48	8.1	8.08	119/38/229	83	61	114	93
2009/09/30	10:16	7.7	7.55	74/52/139	34	20	65	70
2009/10/07	22:03	7.5	7.61	344/41/87	43	31	75	63
2009/10/07	22:18	8.1	7.81	337/36/82	78	52	98	103
2009/10/07	23:13	7.9	7.41	341/43/83	37	28	74	38
2009/11/09	10:44	7.2	7.26	172/42/33	38	22	42	29
2009/11/09	10:44	7.5	7.26	172/42/33	73	67	88	78
2010/01/03	22:36	6.9	7.10	321/21/102	44	32	84	78
2010/01/12	21:53	7.3	7.03	152/69/159	33	25	50	36
2010/02/27	06:34	8.6	8.78	19/18/116	119	97	146	142
2010/02/27	08:01	8.0	7.35	3/46/258	32	21	52	35
2010/04/04	22:40	6.7	7.17	221/83/254	63	53	77	108
2010/04/06	22:15	7.5	7.76	308/9/87	70	59	85	68
2010/05/09	05:59	7.1	7.23	308/15/86	47	39	63	58
2010/05/27	17:14	7.1	7.14	162/45/85	36	20	74	83
2010/06/12	19:26	7.5	7.44	116/61/152	42	29	48	60
2010/07/18	13:35	7.2	7.31	259/29/87	52	27	112	80
2010/07/23	22:08	7.1	7.29	259/18/324	27	17	40	34
2010/07/23	22:51	7.7	7.63	235/18/324	26	21	34	33
2010/07/23	23:15	7.6	7.43	257/24/309	22	16	45	33
2010/08/10	05:23	7.4	7.24	355/32/126	30	21	48	56
2010/08/12	11:54	7.0	7.06	151/20/289	16	12	35	35
2010/10/25	14:42	7.1	7.81	319/7/98	85	44	109	127
2010/12/21	17:19	7.7	7.37	115/42/233	42	23	62	56
2010/12/25	13:16	7.5	7.25	150/45/249	41	28	51	59
2011/01/01	09:56	7.3	7.03	1/20/299	13	12	25	226
2011/01/02	20:20	6.9	7.10	2/15/94	32	19	44	37
2011/01/18	20:23	7.1	7.22	78/31/300	44	19	73	54
2011/03/09	02:45	7.2	7.36	189/10/77	46	36	67	67
2011/03/11	05:46	8.5	9.08	203/10/88	158	124	186	179
2011/04/07	14:32	7.4	7.11	19/37/82	34	17	50	60
2011/06/24	03:09	7.4	7.25	15/10/200	37	29	49	53
2011/07/06	19:03	7.6	7.58	163/36/246	44	32	61	72
2011/08/20	18:19	7.0	7.04	343/33/94	44	30	67	49
2011/08/24	17:46	7.2	7.02	197/40/303	18	11	63	19
2011/09/03	22:55	7.0	7.02	19/29/160	22	16	47	98
2011/09/15	19:31	7.7	7.31	312/38/353	21	18	25	29

Table B.1 (continued)

2011/10/21	17:57	7.5	7.38	202/37/83	48	38	69	71
2011/10/23	10:41	7.0	7.13	246/38/60	26	17	45	41
2012/01/10	18:37	6.3	7.17	105/76/192	60	35	92	89
2012/02/02	13:34	7.2	7.03	53/52/319	44	33	63	68
2012/03/20	18:02	7.9	7.38	295/13/91	41	27	82	38
2012/03/25	22:37	7.1	7.18	21/11/114	48	36	76	61
2012/04/11	08:38	8.1	8.56	20/64/1	112	75	185	146
2012/04/12	07:15	6.6	7.02	41/89/0	51	38	81	76
2012/08/14	02:59	7.9	7.72	25/33/58	27	24	34	70
2012/08/27	04:37	6.5	7.31	287/15/81	55	43	81	72
2012/08/31	12:47	7.7	7.61	345/45/63	34	17	61	51
2012/09/05	14:42	7.3	7.59	317/19/118	42	37	58	60
2012/09/30	16:31	7.4	7.23	228/41/243	27	24	31	32
2012/10/28	03:04	7.3	7.74	320/29/111	67	50	146	69
2012/11/07	16:35	7.1	7.34	296/26/87	35	21	84	37
2012/12/07	08:18	7.6	7.19	18/40/270	52	36	74	75
2012/12/10	16:53	7.4	7.09	310/47/167	56	13	85	138

APPENDIX C

RTERG PROGRAMS AND ROUTINES

Since the beginning of this project we had in mind leaving the set of programs and routines for the continuation of research of radiated seismic energy. The set of programs and routines found here are a combination of Python scripts, FORTRAN code, and GMT scripts for Bash shell that were developed for a Linux/Unix operating system. Directory paths follow Unix directory structure, and external calls of other programs and scripts were designed to work under the bash shell environment.

C.1. Main structure

The two initial parameters that the program must contain are earthquake location and origin time. In the past, at the system implemented at Georgia Tech, these were obtained from the NEIC as a trigger for our routines. However, code implementation for different places may not necessarily contain the same trigger. Nevertheless, the initial input from the user must be a location, origin time and an estimation of magnitude. This last does not have to be the final magnitude, but is kept as record for comparison of results. Additionally, user must choose a unique identification number for that event; it should have the same name of the folder where the event is going to be processed.

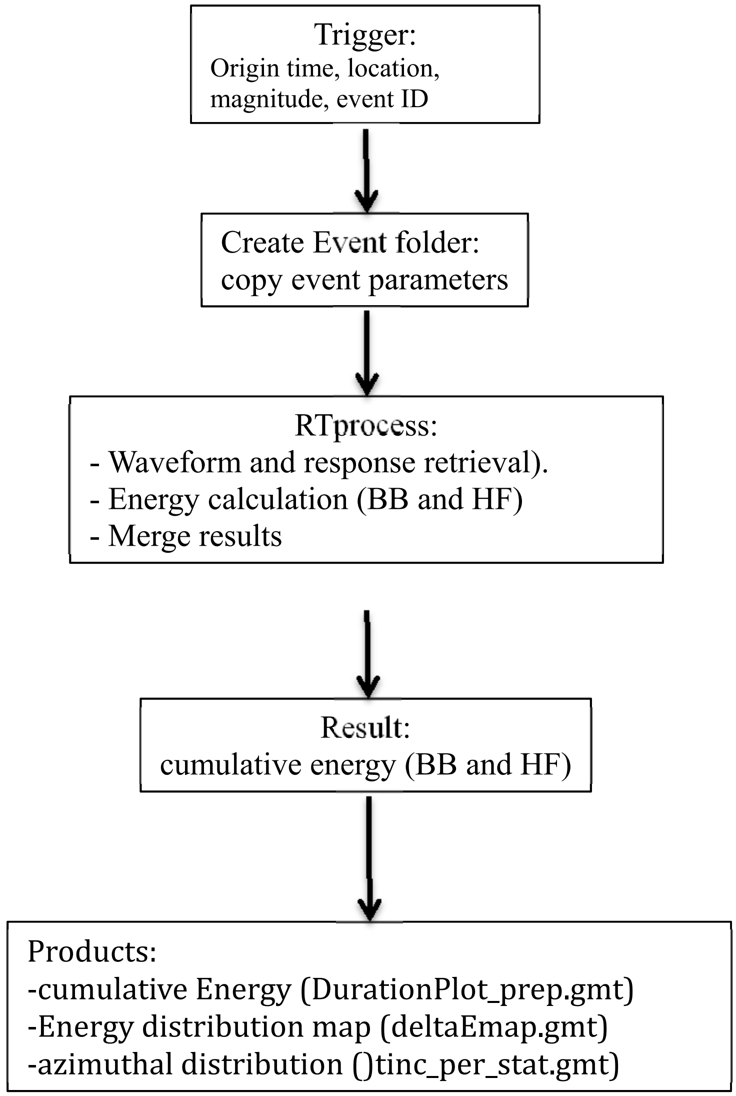

Figure C.1 Main structure of RTerg

C.2 RTprocess

This python script can be considered a wrapper for all other scripts that, as a group, select data, retrieve waveforms, calculate radiated seismic energy for each waveform, and produce final results and figures.

C.2.1 Information of Available Stations

The program will first find, among all the stations, which ones contain data at the time of the earthquake. This is implemented to avoid data transfer errors that could result in empty waveform files or a possible halt of the whole process. The program '*AvailableStationsXMLIRIS.py*' finds this information from the IRIS website and gets information about network and station names as well as location codes. Also, information about location of the stations is retrieved for subsequent discrimination of those stations found at teleseismic distances from the earthquake.

C.2.2 Discrimination of Stations Based on Distance

We use stations at teleseismic distances (25° to 80°), and before downloading stations we exclude stations found outside of that distance range. To do this, we use a FORTRAN program called '*NRT_teleseism*' that not only achieves this distance range discrimination, but also calls travel-time routines that evaluate the travel time of the *P*-wave from the earthquake location to the station. This serves to further minimize the amount of requested data and will aid in the storage of *P*-time information in the retrieved SAC files. After the list of available stations at the time of the earthquake goes through the distance discrimination and a P-travel time is added we request the waveforms.

C.2.3 Data.

Data retrieval is performed by '*triggeredERG*.py'. It is optimized to retrieve waveforms at stations one minute before the P-arrival time at the station up to a default of 300 s after the P-arrival time. The time after the P-arrival to download data can be varied to accommodate to large or extended ruptures. SAC files and metadata for each station is retrieved together with the pole-zero response information.

C.2.4 Waveform Processing and Energy Calculations

After waveforms have header information CWBerg.py calls the FORTRAN program that calculates the cumulative energy per-station and then results are merged with the script mergeergs.py.

C.3 Figures and Products

Finalized products include the cumulative energy at broadband and high frequency, the energy deviation of the stations used and the azimuthal distribution of the per-station cumulative energy. These are all done in bash scripts that rely on the GMT routines.

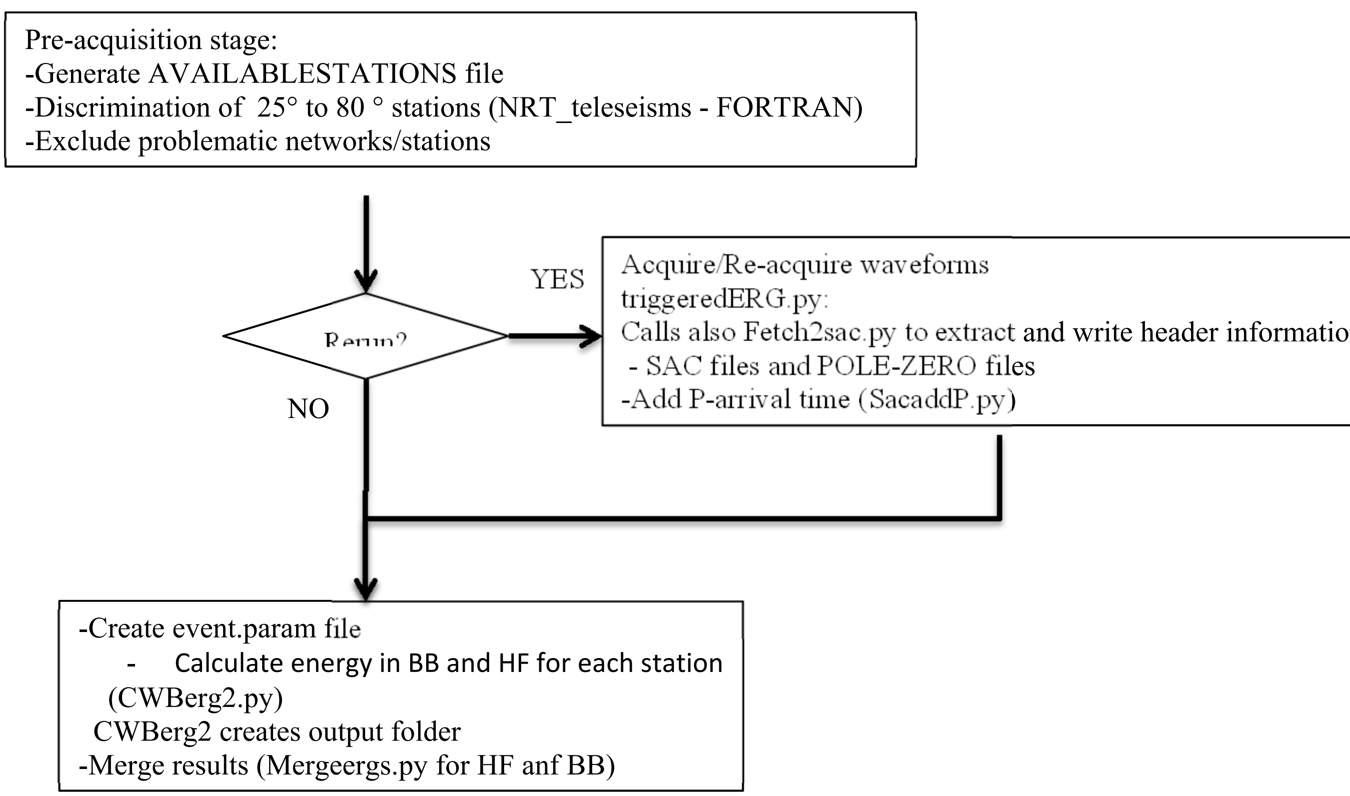

Figure C.2 RTprocess structure

C.4 Code

```
#!/usr/bin/python3.2
# given an epoch, this will retrieve the available stations at that time
# (the restrictions about data availability will be apparent here)

import xml.etree.ElementTree as ET

import time
from optparse import OptionParser
import urllib.request
import datetime
import os

parser = OptionParser()
parser.add_option("-s",nargs=1,dest="sepoch",help="Epoch Time of the Start of the Earth
quake (GMT)")
(options, args) = parser.parse_args()

SEPOCH = float(options.sepoch)

SEPOCH_post = SEPOCH + 1000

t = datetime.datetime.fromtimestamp(SEPOCH)
t_p = datetime.datetime.fromtimestamp(SEPOCH_post)

if t.month < 10:
   month = ’0’ + str(t.month)
else:
   month = str(t.month)

if t.day < 10:
   day = ’0’ + str(t.day)
else:
   day = str(t.day)

if t.hour < 10:
   hour = ’0’ + str(t.hour)
else:
   hour = str(t.hour)

if t.minute < 10:
   minute = ’0’ + str(t.minute)
else:
   minute = str(t.minute)

if t.second < 10:
   second = ’0’ + str(t.second)
else:
   second = str(t.second)

if t_p.month < 10:
   month_p = ’0’ + str(t_p.month)
else:
   month_p = str(t_p.month)

if t_p.day < 10:
   day_p = ’0’ + str(t_p.day)
else:
   day_p = str(t_p.day)

if t_p.hour < 10:
   hour_p = ’0’ + str(t_p.hour)
else:
   hour_p = str(t_p.hour)
```



```
if t_p.minute < 10:
   minute_p = ’0’ + str(t_p.minute)
else:
   minute_p = str(t_p.minute)

if t_p.second < 10:
   second_p = ’0’ + str(t_p.second)
else:
   second_p = str(t_p.second)

stime = str(t.year) + ’-’ + month + ’-’ + day + ’T’ + hour + ’:’ + minute
+ ’:’ + second
etime = str(t_p.year) + ’-’ + month_p + ’-’ + day_p + ’T’ + hour_p + ’:’ +
 minute_p + ’:’ + second_p

url_xml = ’http://www.iris.edu/ws/availability/query?net=II,IU,US&sta=*&loc=*&cha=BHZ&start=’
+ stime + ’&end=’ + etime + ’&output=xml’

xmlfile = urllib.request.urlopen(url_xml)

tree = ET.parse( xmlfile )
root = tree.getroot() # root node
DUMMYPART=’:   0.0 -90.0   0.0:’
OUTPUTFILE=’AVAILABLESTATIONS’
f = open(OUTPUTFILE, ’w’)

for child in root:
        if (child.tag == ’Station’):
                statname=child.attrib[’sta_code’]
                ntwk=child.attrib[’net_code’]
                lat=child.find(’Lat’).text
                lat_f= ’{0:3.4f}’.format(float(lat)) # formatted
                lon=child.find(’Lon’).text
                lon_f=’{0:3.4f}’.format(float(lon))
                elevation=child.find(’Elevation’).text
                for channel in child.iter(’Channel’):
                        if ( channel.attrib[’chan_code’] == ’BHZ’ ):
                                component=channel.attrib[’chan_code’]
                                loc=channel.attrib[’loc_code’]
                                for availability in channel.iter(’Extent’):
                                        starttime=availability.attrib[’start
’].split(’T’)
                                        endtime=availability.attrib[’end’]
.split(’T’)
                                        # Print the whole thing:
                                        AVAILABLES = ’{0:2} {1:5} {2:2} {3:3}{4} {
5:8} {6:9} {7} {8} {9} to {10} {11} \n’.format( ntwk,statname,loc,component,DUMMYPART
,lat_f.rjust(8),lon_f.rjust(9),elevation.rjust(6),starttime[0],starttime[1
][0:5],endtime[0],endtime[1][0:5]  )
                                        f.write(AVAILABLES)



# close the file
f.close()





exit()
```

```
#!/usr/bin/python3.2
# last modified by jconvers on Fri Apr 27 15:38:38 EDT 2012 from triggered
ERGz.py

import os
import time
from optparse import OptionParser
import subprocess
import shlex
from subprocess import Popen, PIPE, STDOUT
from datetime import datetime
import urllib.request

# First: export Environmental variables, this is so it runs properly from
crontab
CONFIGFILE = '/home/gterg/GTerg/bin/GTerg_config.sh'
SOURCE_CMD = 'source /home/gterg/GTerg/bin/GTerg_config.sh'
print('Sourcing environmental variables needed')
os.system(SOURCE_CMD)

  # triggeredERG gets coordinates and initial EQ time and  acquires
  # waveforms in SAC format and response files with zero and pole informat
ion (.pz)

  # The input is the pre-P time before the estimated arrival time at stati
ons, to begin
  # acquiring the waveforms, it aquires information for 600 seconds (10min
)
  # the information needed for the station name and time of estimated p-ar
rival is found
  # on the STATIONSREADY (AVAILABLESTATIONS.teles), it takes information f
rom there to use as
  # parameteres to request the waveform and the SAC file from CWBquery.
  # Please check documentation by IRIS for detailed information on how to
request data


# Input basic event information
parser = OptionParser()
parser.add_option("-E",nargs=1,dest="eepoch",help="Number of seconds after 1970")
parser.add_option("-N",nargs=1,dest="event_name", help="Format is YYMMDDNN")
parser.add_option("-P",nargs=1,dest="pre_p", help="Seconds recorded before P-wave")
parser.add_option("-A",nargs=1,dest="after_p", help="Seconds recorded after P-wave")
parser.add_option("-D",nargs=1,dest="path", help="Location of STATIONSREADY file
")
parser.add_option("-S",nargs=1,dest="STATIONSREADY", help="Available Stations Fi
le")
(options, args) = parser.parse_args()

# Necessary Files
STATIONSREADY2 = options.path + options.STATIONSREADY + ".teles"
      # Should be in folder


datafolder = "data"

# Check Length of Inputs
l_eepoch = len(options.eepoch)
l_event_name = len(options.event_name)
l_pre_p = len(options.pre_p);
l_after_p = len(options.after_p);

if l_eepoch!=10:
  print ("EEPOCH is number of seconds after 1970")
```



```
  print ("-E requires a 10 digit argument")
  exit(1)
if l_event_name!=8:
  print ("EVENT_NAME format is YYMMDDNN")
  print ("-N requires an 8 digit argument")
  exit(1)
if l_pre_p!=2:
  print ("PRE_P is seconds recorded before P-wave")
  print ("-P requires a 2 digit argument")
  exit(1)
if l_after_p!=3:
  print ("AFTER_P is seconds recorded after P-wave")
  print ("-A requires a 3 digit argument")
  exit(1)

# Change to appropriate directory
yr = options.event_name[0:2];
GTerg = '/home/gterg/GTerg'
EDIR = GTerg + '/events/' + '20' + yr + '/' + options.event_name
DDIR = EDIR + '/data'
GTERGBIN = GTerg+'/bin'
print("event directory:\n",EDIR)
print("destination directory:\n",DDIR)


if not os.path.exists(EDIR):
   print("creating folder ",EDIR)
   os.makedirs(EDIR)

os.chdir(EDIR)

if not os.path.exists(DDIR):
    print("creating folder ",DDIR)
    os.makedirs(DDIR)
if os.path.exists(BATCH_QUERY):
    print("removing file ",BATCH_QUERY)
    os.remove(BATCH_QUERY)

# Aquire sac files and response files
openfile = open(STATIONSREADY2)

line = openfile.readline()

NET = line[0:2]
STAT = line[3:8]
STAT = STAT.replace(' ', '')
LOC = line[9:11]
CHAN = line[12:15]
PTIME = line[102:110]

PTIME = float(PTIME)
eepoch = float(options.eepoch)
pre_p = float(options.pre_p)
after_p = float(options.after_p)

SEPOCH = eepoch + PTIME - pre_p
TTOTAL = after_p + pre_p
STIME = time.gmtime(SEPOCH)
STIMEJAVA = time.strftime("%Y/%m/%d %H:%M:%S", STIME)
WAVEFORM = NET + STAT + CHAN + LOC


lines = ['-s ' + WAVEFORM + ' -nodups -b ' + '"' + STIMEJAVA + '"' + ' -d ' + st
r(TTOTAL) + ' -q -sacpz nm -nogaps -sactrim -t sac -o data/%n.%s.%l.%c.SAC']
```

```
i = 1;
openfile.seek(109*i,0)
line = openfile.readline()

while len(line)==109:
  i = i + 1

  NET = line[0:2]
  STAT = line[3:8]
  STAT = STAT.replace(' ', '')
  LOC = line[9:11]
  CHAN = line[12:15]
  PTIME = line[102:110]

  PTIME = float(PTIME)
  eepoch = float(options.eepoch)
  pre_p = float(options.pre_p)
  after_p = float(options.after_p)

  SEPOCH = eepoch + PTIME - pre_p
  TTOTAL = after_p + pre_p
  STIME = time.gmtime(SEPOCH)
  STIMEJAVA = time.strftime("%Y/%m/%d %H:%M:%S", STIME)
  WAVEFORM = NET + STAT + CHAN + LOC


# time format conversions
  SEPOCH_post = SEPOCH + 600
  t = datetime.utcfromtimestamp(SEPOCH)
  t_p = datetime.utcfromtimestamp(SEPOCH_post)

  if t.month < 10:
     month = '0' + str(t.month)
  else:
     month = str(t.month)

  if t.day < 10:
     day = '0' + str(t.day)
  else:
     day = str(t.day)

  if t.hour < 10:
     hour = '0' + str(t.hour)
  else:
     hour = str(t.hour)

  if t.minute < 10:
     minute = '0' + str(t.minute)
  else:
     minute = str(t.minute)

  if t.second < 10:
     second = '0' + str(t.second)
  else:
     second = str(t.second)

  if t_p.month < 10:
     month_p = '0' + str(t_p.month)
  else:
     month_p = str(t_p.month)

  if t_p.day < 10:
```



```
     day_p = '0' + str(t_p.day)
  else:
     day_p = str(t_p.day)

  if t_p.hour < 10:
     hour_p = '0' + str(t_p.hour)
  else:
     hour_p = str(t_p.hour)

  if t_p.minute < 10:
     minute_p = '0' + str(t_p.minute)
  else:
     minute_p = str(t_p.minute)

  if t_p.second < 10:
     second_p = '0' + str(t_p.second)
  else:
     second_p = str(t_p.second)


  stime = str(t.year) + '-' + month + '-' + day + 'T' + hour + ':' + minut
e + ':' + second
  etime = str(t_p.year) + '-' + month_p + '-' + day_p + 'T' + hour_p + ':'
 + minute_p + ':' + second_p


#  print(stime, etime)
  print('\n ----------- calling Fetch2sac.py -------- \n')
  FB_call = GTERGBIN+'/Fetch2sac.py -N ' + NET + ' -S ' + STAT + ' -L ' + LOC + '
-C ' + CHAN + ' -s ' + stime + ' -e ' + etime + ' -n ' + options.event_name
  print(FB_call)
  os.system(FB_call)
  RM3_call = 'rm *.mSEED'
  os.system(RM3_call)
  openfile.seek(109*i,0)
  line = openfile.readline()


eepoch_str = str(options.event_name)
```

```
#!/usr/bin/python3.2

import os
import time
from optparse import OptionParser
import subprocess
import shlex
from subprocess import Popen, PIPE, STDOUT
import warnings
import sys

# First: export Environmental variables, this is so it runs properly from
crontab
CONFIGFILE = '/home/gterg/GTerg/bin/GTerg_config.sh'
SOURCE_CMD = 'source /home/gterg/GTerg/bin/GTerg_config.sh'
print('Sourcing environmental variables needed')
os.system(SOURCE_CMD)

# Added for the full path to GTerg bin folder
GTerg = '/home/gterg/GTerg'
GTERGBIN = GTerg+'/bin'
EVENTSFOLDER = GTerg+'/events'

# Input basic event information
parser = OptionParser()
parser.add_option("-N",type="str",nargs=1,dest="network", help="Network (II, IU, et
c.)")
parser.add_option("-S",type="str",nargs=1,dest="station", help="Station")
parser.add_option("-L",type="str",nargs=1,dest="location", help="Location (00, 10, e
tc.)")
parser.add_option("-C",type="str",nargs=1,dest="channel", help="Channel (BHZ, etc.
)")
parser.add_option("-s",type="str",nargs=1,dest="stime", help="Starting time of the ev
ent (YYYY-MM-ddThh:mm:ss)")
parser.add_option("-e",type="str",nargs=1,dest="etime", help="Ending time of the ev
ent (YYYY-MM-ddThh:mm:ss)")
parser.add_option("-n",type="str",nargs=1,dest="event_name", help="Event name")
parser.add_option("-k",type="str",nargs=1,dest="latlon", help="Latitude and Longitu
de")
(options, args) = parser.parse_args()

len_stat = len(options.station)
stat_name = options.station

if len_stat == 3:
   options.station = options.station + '__'
if len_stat ==4:
   options.station = options.station + '_'

# print(options.station) # for log purposes
output = options.network + '.' + options.station + '.' + options.location +
 '.' + options.channel + '.mSEED'
metaout = options.network + '.' + options.station + '.' + options.location
+ '.' + options.channel + '.meta'
pzdir = 'data'

# Call to FetchBulkData with -sd option for PZ response files
print('\n\n ----- Call FetchBulkdata ----- \n\n')
FBD_input = GTERGBIN+"/FetchBulkData -N " +  options.network + " -S " +  stat_n
ame + " -L " + options.location + " -C " + options.channel + " -s " +  option
s.stime + " -e " + options.etime + " -o " + output + " -m " + metaout + " -sd "
 + pzdir
print(FBD_input) # for log purposes
os.system(FBD_input)
```



```
print('\n\n ----- Finished Call to FetchBulkdata ----- \n\n')

# warning, this makes it hardwired to work only on events from 2000 only
YR = 2000 + int( options.event_name[0:2] )
out_conv = EVENTSFOLDER +'/'+ str(YR) +'/' + options.event_name + '/' + out
put
# print(out_conv)
print("send order to mseed2sac")
MSS_input = GTERGBIN+"/mseed2sac -v -m " + metaout + ' ' + out_conv
#MSS_input = 'mseed2sac -v -k ' + options.latlon + ' -m ' + metaout + ' '
+ output
print(MSS_input)
os.system(MSS_input)


conv = options.network + '.' + stat_name + '.' + options.location + '.' + o
ptions.channel + '.M.*'
# print(conv)

import glob
conv_name = str(glob.glob(conv))
conv_name = conv_name[2:-2]
# print(conv_name)

output_sac = options.network + '.' + options.station + '.' + options.locati
on + '.' + options.channel + '.SAC'
CP_input = "cp " + conv_name + ' ' + output_sac
# print(CP_input)
os.system(CP_input)

conv_pz = 'SACPZ.' + options.network + '.' + stat_name + '.' + options.loca
tion + '.' + options.channel
output_pz = options.network + '.' + options.station + '.' + options.locatio
n + '.' + options.channel + '.SAC.pz'
CP2_input = 'cd data; cp ' + conv_pz + ' ' + output_pz + '; cd ..'
# print(CP2_input)
os.system(CP2_input)

pzname = pzdir + '/SACPZ.' + options.network + '.' + stat_name + '.' + optio
ns.location + '.' + options.channel
# print(pzname)
pz_len = os.path.getsize(pzname)
# print(pz_len)

if pz_len == 0:
   warnings.warn('PZ file is empty')
   sys.exit(0)

# print(lat_val, lon_val)

MV_input = 'mv ' + output_sac + ' data'
os.system(MV_input)
# print(MV_input)

RM_input = 'rm ' + options.network + '.' + stat_name + '*'
os.system(RM_input)
# print(RM_input)

RM2_input = 'cd data; rm ' + conv_pz + ' ; cd ..'
os.system(RM2_input)
# print(RM2_input)
```

```
#!/usr/bin/python3.2
# this program (or routine) adds the theoretical P-times for sac data usin
g
# information within the AVAILABLESTATIONS.teles file
# las modified Wed Feb 22 20:03:19 EST 2012
# sac calls are taken as seen in: http://www.iris.edu/software/sac/manual/
sac_script.html
# importing things I need:
import os # for external orders
import argparse
import time # this will help me convert from DOY 2 Cal and also to EPOCH a
nd vice versa
import subprocess # this will allow me to call sac :)
import re # regular expressions (I use it to separate the freaking date I
get from the sac header)
from glob import glob # not sure what this is.. got it from the sac tutori
al for python
from datetime import datetime
from calendar import timegm

# First: export Environmental variables, this is so it runs properly fron
crontab
CONFIGFILE = '/home/gterg/GTerg/bin/GTerg_config.sh'
SOURCE_CMD = 'source /home/gterg/GTerg/bin/GTerg_config.sh'
print('Sourcing environmental variables needed')
os.system(SOURCE_CMD)

# programs needed:
SAC='/usr/local/sac/sac/bin/sac' # sac
SACHDR='/home/gterg/GTerg/bin/sachdr' # sac header (for reading and writting)
# constants:
PNAME='A'
#SACLIST=[]
# Parsing options and setting help
parser = argparse.ArgumentParser(description="adds the teoretical P-arrival time for SA
C data using:\n The event EPOCH, the file AVAILABLESTATIONS.teles and\n the name or list of names of
sac files")
parser.add_argument("-F",nargs=1,type=str,dest="TELESESIMICSTATIONS",
                    help="-F Ptimingfile\n is created before and is just a list of station,\n location, code,
 and other station information with the relative P-time\n the 14th (last) column.")
parser.add_argument("-E",nargs=1,dest="EEPOCH",
                    help="'EEPOCH' is the timing of the event in integer time from jan 1 1970.")
parser.add_argument("-S",dest="SACLIST",nargs='+',help="SAC file(s) are the files wh
ose p-arrival header information will be added or updated")
#parser.disable_interspersed_args() # Set parsing to stop on the first non
-option
args = parser.parse_args() # read the options
# check if options are actually added
if not args.TELESESIMICSTATIONS and not args.EEPOCH and not args.SACLIST:
        print("No options selected, please use the -h option for help")
        exit(1)

TELESESIMICSTATIONS=str(args.TELESESIMICSTATIONS[0])
if not os.path.exists(TELESESIMICSTATIONS):
        print("file ",TELESESIMICSTATIONS," does not exist, quitting...\n")
        exit(1)
if not args.SACLIST:
        print("no sac files specified, please select at least one sac file to add\n")
        exit(1)
EEPOCH=args.EEPOCH[0]
#print(args.SACLIST)
with open(TELESESIMICSTATIONS,'r') as TTIMESFILE:
        ttimeslines=TTIMESFILE.readlines()
# now for each sac file:
```



```
PTIME=60 # default p-time, just for testing
print('------ Adding theoretical P-time arrival markers ro SAC files:')
for SACFILE in args.SACLIST:
        if os.path.exists(SACFILE):
                #print(SACFILE) # just a check
                # acquiring network, station name and location code from s
achdr (this is an external call)
                NTWK,STAT=subprocess.getoutput(SACHDR+' '+SACFILE+' -c KNET
WK KSTNM').splitlines() # takes network and stat name at the same time
                # I can't get LOC with the other ones because sometimes KH
OLE might be an empty field
                LOC=subprocess.getoutput(SACHDR+' '+SACFILE+' -c KHOLE')
                if not LOC : LOC="--" # this is to put "__" if there is no
 LOC info on the SAC header
                # Convert the starting date and time to epoch
                WFYRDOY=subprocess.getoutput(SACHDR+' '+SACFILE+' -c KZDATE
') # get date of sac file
                SACFILETIME=subprocess.getoutput(SACHDR+' '+SACFILE+' -c KZ
TIME') # get time from sacfile
                MON,DD,DOY,YY=WFYRDOY.split() # parsing
                HOUR=SACFILETIME.split('.')[0]
                FULLTIME=YY+" "+MON+" "+DD+" "+HOUR
                #print('testing inside sacaccP.py: '+FULLTIME)
                #time.strptime(FULLTIME, '%Y %b %d %H:%M:%S')
                #SACFILESEPOCH=int(time.mktime(time.strptime(FULLTIME, '%Y
 %b %d %H:%M:%S'))) - time.timezone # this one was 3600s off
                SACFILESEPOCH=timegm(datetime.strptime(FULLTIME, '%Y %b %d
 %H:%M:%S').utctimetuple())
                for line in ttimeslines:
                        if [NTWK,STAT,LOC] == line.split()[0:3]:
                                #print(line.split()[0],line.split()[1],lin
e.split()[2],line.split()[13])
                                PTIME=(line.split()[13])
                                T9TIME=int(EEPOCH)-int(SACFILESEPOCH)+floa
t(PTIME)-1
                                #print(PTIME,SACFILESEPOCH,EEPOCH)
                                orderforsac='printf \"read '+SACFILE+'\n chnhdr '+
PNAME+' '+str(T9TIME)+'\n wh\nquit\n\" | '+SAC+' '
                                #print(orderforsac) # done as a check
                                subprocess.Popen(orderforsac,stdout=open('
/dev/null', 'w'),shell=True) # send order to sac
                                print('Theor. P-time '+PNAME+' at '+str(T9TIME)
+' from start of file added for '+SACFILE )
                #print(NTWK,STAT,LOC,PTIME,T9TIME)
        else:
                print(SACFILE+' Could not be found... Skipping this file')


print("sacaddP.py routine finished\n") # this is for me to know the program finishe
d and for log purposes
```

```
#!/usr/bin/python3.2
# Version 2 is modified to add origin time and event ID to nergy.sac.in in
 order to pass it to
# the energy calculation program so it can save it in the header of the ti
nc files.

# this script whould produce a single output folder where all the .tinc fi
les are stored
# It takes the sac files and calls the energy processing FORTRAN code to c
alculate
# energy growth with time to produce .tinc files

# external programs and folders needed:
ERGLIB='/home/gterg/GTerg/lib' # where the RESP (not .pz) files are located
SACHDR='/home/gterg/GTerg/bin/sachdr' # sac header reads header information from
sac files
NERGY='/home/gterg/GTerg/bin/E_star_wprep.cwb.IRISpz_V2' # the energy calculation FOR
TRAN routine
TMPDIR='/home/scratch'

# name of control file:
CONTROL='nergy.sac.in'

# directories that will be either created or used by the program:
BADDIR='not_used' # folder where we copy the .SAC and .pz files not used
DATA='data' # the sac files and response files are here
OUTDIRDEFAULT='output' # default output folder

# default values for processing
TTOTALDEFAULT=300 # seconds (process for a maximum of X seconds after p-ar
rival)
TSTEPDEFAULT=1   # seconds, interval between time steps (its going to do i
t in increasing time windows)
DIFF=50   # used to remove data outside of tolerance range and improve the
 result, but might not be used

# default values for the CONTROL file:
TTABLES=ERGLIB
RHO=3000.
ALPHA=7000.
QFACT=15.6
DEFAULT_SP1=0.5 # lower range of period for spectral period range
DEFAULT_SP2=70  # upper limit of period for spectral period to work over
D1=-2   # '-' means seconds before p-arrival time for window width in seco
nds
D2=70   # window for duration of data use for calculation (in seconds)

# importing modules
import argparse # used for menu, usage and flag options
import os       # used to find out for existence of folders and some files
import shutil
import glob

# First: export Environmental variables, this is so it runs properly from
crontab
CONFIGFILE = '/home/gterg/GTerg/bin/GTerg_config.sh'
SOURCE_CMD = 'source /home/gterg/GTerg/bin/GTerg_config.sh'
print('Sourcing environmental variables needed')
os.system(SOURCE_CMD)


# Parsing options and setting help
parser =  argparse.ArgumentParser(description='Function: Calculates energy for all usab
le sac data either in the '+DATA+'/ or local directory.')
```



```
parser.add_argument("-C",nargs=1,dest="PARAMETERS",required=True,
                help="build Control file ("+CONTROL+"), from input parameters in the form:\nEL
AT/ELON/DEPTH/STRIKE/DIP/RAKE/MOMENT[dyne-cm]")
parser.add_argument("-O",nargs=1,dest="OUTDIR",metavar=OUTDIRDEFAULT,
                help="Output directory [default="+OUTDIRDEFAULT+"]")
parser.add_argument("-P",nargs=1,dest="PRANGE",
                help="Period range over which to do processing [default="+str(DEFAULT_SP1
)+"/"+str(DEFAULT_SP2)+"]")
parser.add_argument("-T",nargs=1,dest="TTOTSTEP",
                help='''Define the window over which event will be processed using TTOTAL,
                and the increment by which to step calculations using TSTEP [defaults='''+str(T
TOTALDEFAULT)+'''/'''+str(TSTEPDEFAULT)+''']''' )
parser.add_argument("-D",nargs=1,dest="ORIGINTIME",
                help="add the event date YYYY/MM/DDTHH:MM:SS")
parser.add_argument("-I",nargs=1,dest="EVENTID",
                help="add the event ID for the nergy.sac.in file and the result .thin files")
args = parser.parse_args() # read the options

# PARAMETERS CHECK
# Checking that at least we have the right number of options
if len(args.PARAMETERS[0].split('/')) == 7 and all(args.PARAMETERS[0].spli
t('/')) :
        # extract and convert to float
        [ELAT,ELON,DEPTH,MOMENT] = [ float(i) for i in [args.PARAMETERS[0]
.split('/')[j] for j in (0,1,2,6)] ] # separate by '/' and asign values to
 variables
        STRIKE,DIP,RAKE=[ int(i) for i in [args.PARAMETERS[0].split('/')[j
] for j in (3,4,5)] ]
        # Now, nergy will crash for depths <0.1, change to 0.1 depth if th
at is the case.
        if DEPTH < 0.1: DEPTH=0.1; print("input depth was less than 0.1, changed to",DE
PTH)
else:
        print("-C option requires 7 arguments: ELAT/ELON/DEPTH/STRIKE/DIP/RAKE/MOMEN
T[dyne-cm]\nTry -h option for help")
        exit(1)

# TIME RANGE: Checking TTOT and TSTEP:
if not args.TTOTSTEP:
        print('no -T flag selected, using default values: -T'+str(TTOTALDEFAULT)+'/'+str(
TSTEPDEFAULT))
        TTOT,TSTEP = TTOTALDEFAULT,TSTEPDEFAULT
else:
        if len(args.TTOTSTEP[0].split('/')) != 2:
                print("ERROR: -T flag requires 2 arguments: TOTAL/TSTEP, one is missing\n"
)
                exit(1)
        else:
                TTOT,TSTEP = args.TTOTSTEP[0].split('/')
                if TSTEP >= TTOT:
                        print('ERROR: Maximum time must be at least larger than time step'
)
                        exit(1)
print( 'running to '+str(TTOT)+'s in steps of '+str(TSTEP)+'s' )

# PERIOD RANGE: CHECKING FOR SPRECTRAL PERIOD RANGE:
if not args.PRANGE:
        print('no -P  flag selected, using default values: -P'+str(DEFAULT_SP1)+'/'+str(DE
FAULT_SP2) )
        SP1,SP2=DEFAULT_SP1,DEFAULT_SP2
else:
        if len(args.PRANGE[0].split('/')) != 2:
                print("ERROR: -P flag requires 2 arguments: SP1/SP2, one is missing\n")
                exit(1)
```

```
        else:
                SP1,SP2 = args.PRANGE[0].split('/')
                if SP1 > SP2:
                        print('ERROR: -P option requires SP1 to be lower than SP2')
                        exit(1)
print(  'Calculating in spectral period range from '+str(SP1)+'s to '+str(SP2)+'s'  )


# asign the output directory, had to do it like this because easier method
s were not that effective
if not args.OUTDIR: OUTDIR=OUTDIRDEFAULT
else: OUTDIR=args.OUTDIR[0]

# Check OUTDIR: output folder, if it exists, move it to .old
if os.path.isfile(OUTDIR):
                os.remove(OUTDIR)
                print(OUTDIR,'name is used by a file, will remove before making folder')

if os.path.isdir(OUTDIR):
        print("Folder",OUTDIR,"exists. Moving to",OUTDIR+".old")
        if os.path.isdir(OUTDIR+".old"):

                shutil.rmtree(OUTDIR+".old")
        shutil.move(OUTDIR,OUTDIR+".old")

elif os.path.isfile(OUTDIR+".old"):
        shutil.move(OUTDIR,OUTDIR+".old")

print("Creating folder:",OUTDIR)
os.mkdir(OUTDIR)
# CHECKING ORIGIN TIME:
if not args.ORIGINTIME:
        print("no origin time specified, setting to UNKNOWN")
        ORIGINTIME='UNKNOWN'
else:
        ORIGINTIME=args.ORIGINTIME[0]
        print("origin time: ",ORIGINTIME)
# CHECKING EVENT ID:
if not args.EVENTID:
        print("No event ID specified, setting to UNKNOWN")
        EVENTID='UNKNOWN'
else:
        EVENTID=args.EVENTID[0]
        print("eventID: ",EVENTID)

# moving BADDIR folder to .old and creating BADDIR (all info in .old folde
r will be erased)
if os.path.isdir(BADDIR):
        if os.path.isdir(BADDIR+".old"): shutil.rmtree(BADDIR+".old")
        shutil.move(BADDIR,BADDIR+".old")
else:
        os.mkdir(BADDIR)


# put together lines for control file:
control=TTABLES+' \n'
control=control+str(ELAT)+' '+str(ELON)+'           Lat Long Coordinates of event \n'
control=control+str(DEPTH)+'           Depth of earthquake source \n'
control=control+str(STRIKE)+' '+str(DIP)+' '+str(RAKE)+'        Focal mechanism (ph
i, delta, lambda) \n'
control=control+str(MOMENT)+'          Seismic Moment [dyne-cm] \n'
control=control+str(RHO)+'             Density (of Upper Mantle) \n'
control=control+str(ALPHA)+'             P wave Velocity \n'
control=control+str(QFACT)+'             q factor (Boatwright & Choy use 15.6) \n'
```



```
control=control+str(SP2)+' '+str(SP1)+'              Spectral period range (Pmax Pmin)\n
'
control=control+str(-2)+' '+str(TTOT)+'              Start time relative to P for processing
 and duration \n'
control=control+str(ORIGINTIME)+'  Origin time  \n'
control=control+str(EVENTID)+'    Event ID \n'

# exit if no .SAC files in DATA folder or folder doesn't exists
SACFILELIST=glob.glob( os.path.join(DATA,'*.[Ss][Aa][Cc]') )
if SACFILELIST:
        print('Running on '+str(len(SACFILELIST))+' waveforms...')

else:
        print(DATA,' folder does not contain .SAC files or doesn\'t exists, exit...')
        exit(1)
# Run nergy to get energy from event
for sacfile in SACFILELIST:
        #print(sacfile)
        NTWK,STAT,LOC,CHNL,EXT = sacfile.split('/')[1].split('.')
        # deal with naming problems when location code is empty in the SAc
 file name
        if not LOC:
                LOC='__'
        RESP=DATA+'/'+NTWK+'.'+STAT+'.'+LOC+'.'+CHNL+'.'+EXT+'.pz'
        # Run nergy if there is a response file and it is not empty
        if  os.path.isfile(RESP) and  os.path.getsize(RESP) >0:
                # will calculate energy...
                nergyorder=sacfile+'\\n'+RESP+'\\n'+str(TTOT)+'\\n'+str(TSTEP
)+'\\n' # build input for nergy
                # build nergy.sac.in file that will be used by nergy
                with open(CONTROL,'w') as controlfile:
                        controlfile.write(sacfile+' \n'+RESP+' \n')
                        controlfile.write(control)
                # write the whole nergy order as a variable
                EXT_CALL=('printf \"'+nergyorder+'\" | '+NERGY)
                #print(EXT_CALL)  # for log purposes
                os.system(EXT_CALL) # external call to nergy FORTRAN progr
am
                # Moving the output files to output directory...
        else:
                print(RESP+' file for '+sacfile+' seems to be empty or nonexistent, skipping
...')
        # once it is finished, move the result files (.tin and summary fil
es ), to the output folder
        tinclist = glob.glob(STAT[0:3]+'*.tinc')
        for file in tinclist: ##+summfilelist :
                #print(file)
                shutil.move(file,OUTDIR) # moving summary file to output d
irectory
                #shutil.move(tincfile,OUTDIR)
print('moved summary files and .tinc files to',OUTDIR)

print("done processing files")
exit()
```

```
#!/usr/bin/python3.2
# This script  takes the .tinc format (t Ebb* Ehf*) and computes the geopm
etrical
# mean for all the tinc files. but before it does that it has to compute t
he energy by multtiplying
# by the focal mechanism correction, both for the "real" and the "averaged
" focal correction
# each correction can be found in the corresponding station tinc file.
# Then merges the results from the .tinc files within a tolerance range fr
om the user and creates the files
# HF.out and BB.out containing: time (s). Eest_avg, Etrue_avg
# this will make a conversion to Joules (1E7)

# libraries with functions that I need:
import argparse # for flag options parsing
import os       # check for existence of folders and such
import linecache # allows to use getline
from numpy import *

# parsing options and setting help
parser = argparse.ArgumentParser(description="merges the results from the .tinc files wit
hin a tolerance range and\n creates the files HF.out and BB.out containing: time (s). Eest_avg, Etrue_avg")
parser.add_argument("-O",nargs=1,dest="TINCDIR",type=str,help="The directory th
at contains the .tinc files.")
parser.add_argument("-A",nargs=1,dest="TOLE",type=float,help="The tolerance of
data to use outside the bulk average measured at TTOT")
parser.add_argument("-T",dest="TTOTAL",help="-T TTOT/TSTEP. total and Time increme
nt")
parser.add_argument("-F",nargs=1,dest='FREQBAND',type=str,help="-F BB or -F
HF \nChoose either Broad-Band or High frequency bands\n")
#parser.disable_interspred_args() # sets the pasing to stop on the first n
on-option
args = parser.parse_args()

# exit if any of the mandatory flags are missing
if not args.TINCDIR and not args.TOLE and not args.TTOTAL:
        print("one or more of the mandatory flags is not set, try -h for help\n")
        exit(1)
# checking TTOT and TSTEP:
if len(args.TTOTAL.split('/')) != 2:
        print("-T flag requires 2 arguments: TOTAL/TSTEP, you have ",len(args.TTOTAL.sp
lit('/')),"\n")
        exit(1)
else:
        TTOT,TSTEP = args.TTOTAL.split('/')
        if not TTOT or not TSTEP:
                print("-T flag requires 2 arguments: TOTAL/TSTEP, one is missing\n")
                exit(1)
# check for existence of TINCDIR folder:
TINCDIR = args.TINCDIR[0]
if not os.path.isdir(TINCDIR):
        print("error: ",TINCDIR," folder does not exist, quitting...\n")
        exit(1)
TOLE=args.TOLE[0]
TINCOUTPUT=TINCDIR+".out"
#print(args.FREQBAND[0])
if not args.FREQBAND:
        print("please use the -F flag and use either BB or HF\n")
        exit(1)
elif args.FREQBAND[0] == 'BB':
        TINCOUTPUT=args.FREQBAND[0]+".out"
        print("Broadband selected, output will be in ",TINCOUTPUT)
        freqcolumn=1
elif args.FREQBAND[0] == 'HF':
```



```
        TINCOUTPUT=args.FREQBAND[0]+".out"
        print("High frequency selected, output will be in ",TINCOUTPUT)
        freqcolumn=2
else:
        print("Please select either BB or HF in the -F flag")
        exit(1)


outofrangetincs=[]
inrangetincs=[]

# get the names of the files with the termination ".tinc"
tincfiles = [f for f in os.listdir(TINCDIR) if f.endswith('.tinc')]

SNR=1.5 # signal-to-noise ratio, will help discard stations where the last
 value of the energy
        # is below SNR times the vaule that is calculated using the pre-P
Erate(Tmax)

Eest = [ [] for i in range(int(TTOT)) ]
Etrue = [ [] for i in range(int(TTOT)) ]

# initalize lists to store last lines (to avoid need to read file twice)
Emaxstat=[[],[]]

# Take all the tinc files, then do intial discrimination
print("- taking all tinc files in folder ",TINCDIR," for initial discrimination")
for tincfile in tincfiles:
        tincfile=TINCDIR+'/'+tincfile

        (time2, Eest2, Etrue2) = loadtxt(tincfile,unpack=True, usecols=[0,
freqcolumn,freqcolumn])
        if isnan(Eest2).any() or isnan(Etrue2).any() or 0 in Eest2 or 0 in
 Etrue2 or isinf(Eest2).any() or isinf(Etrue2).any() : # exclude non-numbe
rs
                print(tincfile,"contains nan or zero values for energy")
                outofrangetincs=outofrangetincs+[tincfile] # Populating li
st of bad .tinc files (that contain nan)
        else:
                # Get Fp2 TrueFgp2 EstFgp2 and Pre-P Energy
                Fp2 = float(linecache.getline(tincfile,9).split()[3])
                trueFgp2 = float(linecache.getline(tincfile,10).split()[4]
)
                EstFgp2 = float(linecache.getline(tincfile,11).split()[3])

                PREPEestRATE=float(linecache.getline(tincfile,14).split()[
6]) # get the pre-P estimated Erate

                if Eest2[0] > Eest2[-1]: # exclude when initial value is b
igger than las value
                        print(tincfile,"has too much energy at beginning")
                        outofrangetincs=outofrangetincs+[tincfile]
                elif PREPEestRATE * time2[-1] * SNR > Eest2[-1]: # exclude
 those below SNR
                        print(tincfile,"last value is below SNR")
                        outofrangetincs=outofrangetincs+[tincfile]

                else:
                        # store energy values to be used in initial averag
e calculation
                        Eest = column_stack(( Eest, Eest2*Fp2/EstFgp2) )
                        Etrue = column_stack(( Etrue, Etrue2*Fp2/trueFgp2)
 )
                        # store last values of energy:
```

```
#!/bin/bash
# GMT script for cumulative enrgy plots for HF and BB energy
# needs HF_energy and BB_energy files (HF.out BB.out) containing HF and BB
 energy information
# Created by Jaime Convers
# Last modification: Tue Apr 30 19:52:21 PDT 2013

# EXTERNAL PROGRAMS
#ERG=/products/eqenergy
ERG=/home/gterg/GTerg
TMPDIR=$ERG/scratchfolder
source $ERG/bin/GTerg_config.sh
CONVERT=convert
FITXY=$ERG/bin/fitxy

#################################
## DECLARE YOUR VARIABLES HERE ##
HFENERGY=HF.out
BBENERGY=BB.out
USAGE=$TMPDIR/'basename $0'.usage

printf "
USAGE: 'basename $0' -T'TMIN'/'TMAX' -E'EVENTNAME' [-R]

FUNCTION:
    Calculates and creates a plot of the energy growth with time for High Frequencies (HF)
    and Broad-band frequencies (BB) from files '$HFENERGY' and '$BBENERGY' over the relative
    time window from 'tmin' to 'tmax' from the p-arrivals. The program assumes certain information
    created by RTprocess exists in the eventname directory.

MANDATORY FLAGS:
  -T fit limits for begining of 1st and end of second slopes (tmin and tmax)
  -E EVENTNAME
OPTIONS (arguments for graph output):
  -h Show this help and exit
New option:
  -R Use the ''True'' energy to plot the cumulative energy at BB and HF. Default is use the result from
    Estimated energy [this option takes 3rd column of '$BBENERGY' and '$HFENERGY' file instead of col
umn 2].
    Use ONLY when real CMT focal mechanism is used.

 Example: create plot for event 09040600 fitting from 5s to 200s and use the value of energy from True_Erg
   %% 'basename $0' -T5/200 -E09040600 -R \n\n"> $USAGE
#### FLAG OPTIONS ########

while getopts "T:E:Rh:" OPT
do
   case ${OPT} in
       T) XMIN='echo $OPTARG | awk -F"/" '{print $1}''      # tmin
          XMAX='echo $OPTARG | awk -F"/" '{print $2}''      # tmax
        ;;
       E) EVENTNAME=$OPTARG
        ;;
       R) RFLAG=1 # sets a value for the flag to plot TrueErg instead of E
stErg
        ;;
       h) cat $USAGE  # display usage
          rm $USAGE
          exit 1 # exit with error after removing temp file
        ;;
   esac
done

if [[ ! "$XMIN" ]] ; then
```



```
        echo "ERROR: Mandatory parameters not set.  Exiting !!"
        cat $USAGE
        rm $USAGE
        exit 1
fi
rm $USAGE

#  Checking HF energy file "HFENERGY"
 if [[ ! -s $HFENERGY || ! -s $BBENERGY ]] ; then
         echo "ERROR: File $HFENERGY, or $BBENERGY  doesn't exist or is empty....Exiting"
         exit 1
 fi
## done for the REal-time system. not used for IRIS
#EIDSTR_OUT=event.eids_triggerrun
# if [[ ! -s $EIDSTR_OUT ]] ; then
#          echo "WARNING: File $EIDSTR_OUT doesn't exist or is empty....Con
tinuing"
# fi
#
EVPARAMS=$EVENTNAME.params
 if [[ ! -s $EVPARAMS ]] ; then
         echo "WARNING: File $EVPARAMS doesn't exist or is empty....Continuing"
 fi


#output pertinent information to file
 OSRC='__'
 OMTP='M_'
## from EIDSTR_OUT file:
#  if [[ -s $EIDSTR_OUT ]] ; then
#       EEPOCH='awk 'NR==2{print $9}'  $EIDSTR_OUT'
#          OLAT='awk 'NR==2{print $4}'  $EIDSTR_OUT'
#          OLON='awk 'NR==2{print $5}'  $EIDSTR_OUT'
#          ODEP='awk 'NR==2{print $6}'  $EIDSTR_OUT'
#          OSRC='awk 'NR==2{print $10}' $EIDSTR_OUT'
#          OMAG='awk 'NR==2{printf "%3.1f", $2}'  $EIDSTR_OUT'
#          OMTP='awk 'NR==2{print $1}'  $EIDSTR_OUT'
#  fi

# From EVPARAMS file:
  if [[ -s $EVPARAMS ]] ; then
        EEPOCH='awk 'NR==2{print $7}' $EVPARAMS'
          OLAT='awk 'NR==2{print $1}' $EVPARAMS'
          OLON='awk 'NR==2{print $2}' $EVPARAMS'
          ODEP='awk 'NR==2{print $3}' $EVPARAMS'
          OMAG='awk 'NR==2{printf "%3.1f", $4}'  $EVPARAMS'
          ODATE='date -u -d @$EEPOCH +%Y/%m/%d'
          OTIME='date -u -d @$EEPOCH +%H:%M:%S'
  fi
#ODATE='date -u -d @$EEPOCH +%Y/%m/%d'
#OTIME='date -u -d @$EEPOCH +%H:%M:%S'
EVENTLINE="$ODATE $OTIME ($EVENTNAME) at $OLAT, $OLON, z=$ODEP"

###########################################################################
################################
### Gathering pre-p Erates, averaging them and sbtracting them from the BB
 and HF cumulatibve energies ###
USEDSTATIONSHF=BBHF/HFTINC.inrange
HFSTATIONSINRANGE='awk '{print $1}' $USEDSTATIONSHF'
HFRATESFILE=HFRATES.temp
USEDSTATIONSBB=BBHF/BBTINC.inrange
BBSTATIONSINRANGE='awk '{print $1}' $USEDSTATIONSBB'
BBRATESFILE=BBRATES.temp
# cleaning temporary files for Erate, both BB and HF
```

```
                        Emaxstat=append(Emaxstat,[ [tincfile],[Eest2[-1]]]
 ,1) # ONLY append that worked
                        # populating list of inrange stations
                        inrangetincs=inrangetincs+[tincfile]

print("- stations in range:",len(inrangetincs),"Stations out of range:",len(outofrangeti
ncs) )

# Find INITIAL AVERAGES: more specifically the geometric mean
print("- finding preliminary geometric mean")
time=time2
EtrueGeomean=exp(mean(log(Etrue),axis=1)) # preliminary True Energy
geometric mean

EestGeomean=exp(mean(log(Eest),axis=1))   # preliminary Estimated Energy
geometric mean
averages=column_stack((time,EestGeomean,EtrueGeomean))


# Now ELIMINATE THOSE STATIONS OUTSIDE OF TOLERANCE RANGE:
print("- eliminate those stations outside of tolerance range")

# resetting the Eest and Etrue lists, this time they will be the final one
s.
Eest = [ [] for i in range(int(TTOT)) ]
Etrue = [ [] for i in range(int(TTOT)) ]


for station1 in inrangetincs:

        (time3,Eest3,Etrue3) = loadtxt(station1,unpack=True, usecols=[0,fr
eqcolumn,freqcolumn])

        if Eest3[-1] > TOLE*EestGeomean[-1] or Eest3[-1] < EestGeomean[-1]
/TOLE:
                #print(station1,"is greater than tolerance range, with",Ee
st3[-1],"compared to ",TOLE*EestGeomean[-1])
                print(station1,"is outside of tolerance range")
                outofrangetincs=outofrangetincs+[station1]
                inrangetincs.remove(station1)
        else:
                # Get Fp2 TrueFgp2 EstFgp2
                Fp2 = float(linecache.getline(station1,9).split()[3])
                trueFgp2 = float(linecache.getline(station1,10).split()[4]
)
                EstFgp2 = float(linecache.getline(station1,11).split()[3])
                # store energy values
                Eest = column_stack(( Eest, Eest3*Fp2/EstFgp2) )
                #print(Etrue3)
                Etrue = column_stack(( Etrue, Etrue3*Fp2/trueFgp2) )

print("- final number of stations used:",len(inrangetincs),"Stations not used:",len(outofr
angetincs) )
print("- finding final average")
EtrueGeomean=exp(mean(log(Etrue),axis=1)) # preliminary True Energy
geometric mean

EestGeomean=exp(mean(log(Eest),axis=1))   # preliminary Estimated Energy
geometric mean
averages=column_stack((time,EestGeomean/1e7,EtrueGeomean/1e7))

# WRITTING RESULTS:
# AVERAGE ENERGY VALUES
```



```
header="#t  Eest   Etrue \n"
f=open(TINCOUTPUT,'w')
f.write(header)
for line in averages:
        f.write('{0:3.0f} {1:5.2e} {2:5.2e}'.format(line[0],line[1],line[2])+"\n"
)
f.close()
print("- Results saved in ",TINCOUTPUT)
# WRITING THE FILE WITH TINCS USED
f=open(TINCDIR+'/'+str(args.FREQBAND[0])+'TINC.inrange','w')
f.writelines( "%s\n" % item for item in inrangetincs )
f.close()
# WRITING THE FILE WITH TINCS NOT USED
f=open(TINCDIR+'/'+str(args.FREQBAND[0])+'TINC.outofrange','w')
f.writelines( "%s\n" % item for item in outofrangetincs )
f.close()

# END
exit()
```

```
if [ -e $HFRATESFILE ] ; then
        rm $HFRATESFILE
fi
if [ -e $BBRATESFILE ] ; then
        rm $BBRATESFILE
fi
########## HF AND BB PRE-P ENERGY RATE
# acquiring average HF E-rate
for stationfile in $HFSTATIONSINRANGE
do
        Fp2=‘awk 'NR==9 {print $4} ' $stationfile‘      # (F_p)^2 this is equa
l to 4/15
        EstFgp2=‘awk 'NR==11 {print $4}' $stationfile‘  # from the tinc file
Estimated = (Fgp)^2
        TrueFgp2=‘awk 'NR==10 {print $5}' $stationfile‘ # From ,tinc file. (F
gp)^2 from the True focal mechanism
        # Energy = (E*) X (F_p)^2/<Fgp>^2
        # Store the pre-P energy rate (J/s): Pre-P Erate = E(hr)* X Fp2 /
(Fgp)^2
        if [ $RFLAG ] ; then
           # RFLAG = True focal mechanism
           awk 'NR==14 {print $8* '$Fp2'/'$TrueFgp2'}' $stationfile >> $HFRATES
FILE # if -R flag is chosen: takes preP E-rate from Etrue/t
        else
           # NO FLAG: estimated focal mechanism
           awk 'NR==14 {print $8* '$Fp2'/'$EstFgp2'}' $stationfile >> $HFRATESF
ILE # is the default, from preP Eest/t
        fi
done
HFRATE=‘awk 'BEGIN{HFEratesum=0;count=0} {HFEratesum+=log($1);count+=1}END{printf "%5.2e"
,exp(HFEratesum/count)/1e7}' $HFRATESFILE‘

# calculating average BB E-rate
for stationfile in $BBSTATIONSINRANGE
do
        Fp2=‘awk 'NR==9 {print $4} ' $stationfile‘      # this is equal to 4/1
5
        EstFgp2=‘awk 'NR==11 {print $4}' $stationfile‘  # from the tinc file
Estimated = (Fgp)^2
        TrueFgp2=‘awk 'NR==10 {print $5}' $stationfile‘ # From ,tinc file. (F
gp)^2 from the True focal mechanism
        if [ $RFLAG ] ; then
           # RFLAG = True focal mechanism
           awk 'NR==14 {print $7 * '$Fp2' / '$TrueFgp2'}' $stationfile >> $BBRAT
ESFILE # if -R flag is chosen: takes preP E-rate from Etrue/t
        else
           # NO FLAG: estimated focal mechanism
           awk 'NR==14 {print $7 * '$Fp2' / '$EstFgp2' }' $stationfile >> $BBRATE
SFILE # is the default, from preP Eest/t
        fi
done
BBRATE=‘awk 'BEGIN{BBEratesum=0;count=0} {BBEratesum+=log($1);count+=1}END{printf "%5.2e
",exp(BBEratesum/count)/1e7}' $BBRATESFILE‘
#echo $HFRATE $BBRATE
# cleaning temp files:
rm $HFRATESFILE $BBRATESFILE

# files to be used for plotting:
CORRHFENERGY=correctedHF.out
CORRBBENERGY=correctedBB.out
########## MAKE PRE_P CORRECTED ENERGY VALUES #############
#echo $HFRATE $BBRATE Will change according to -R flag option
if [ $RFLAG ] ; then
     # if flag is chose, use third column instead of second column of $HFE
```



```
NERGY and $BBENERGY:
     # making corrected HF file with True Energy values:
      awk '{print $1,$3-('$HFRATE'*$1)}' $HFENERGY > $CORRHFENERGY
     # making corrected BB file with "True energy" values
      awk '{print $1,$3-('$BBRATE'*$1)}' $BBENERGY > $CORRBBENERGY
     echo "Using values from True_Erg instead of Est_Erg"
else
     # If no flag is chosen then this will be the default
     # making corrected HF file
       awk '{print $1,$2-('$HFRATE'*$1)}' $HFENERGY > $CORRHFENERGY
     # making corrected BB file
       awk '{print $1,$2-('$BBRATE'*$1)}' $BBENERGY > $CORRBBENERGY
fi
########## PLOTTING ###########
################################
  XSCALE=14                   # scale of overall plot
  YSCALE=8                    # scale of overall plot
#  XMIN=$3  XMAX=$4  # Longitude range of plots
  XHALF=‘echo $XMIN $XMAX | awk '{print ($1+$2)/2}' ‘
  #YMIN=‘awk '$1==XMIN{printf "%10.5e",$2}' XMIN=$XMIN  $CORRHFENERGY‘
  #YMIN=‘awk '$1!~"#"{print $2}' $CORRHFENERGY | minmax -C | awk '{print $
1}'‘
  # Defines the YMAX for plot according to the value corresponding to XMAX
 in Estimated Energy
  YMAX=‘awk '$1==XMAX{printf "%7.1e",$2*1.2}' XMAX=$XMAX $CORRHFENERGY‘
  YMIN=‘echo $YMAX | awk '{printf "%10.5e",$1/100}'‘
#  YMAX=8.0e13 # Latitude range of plots
  YMIN2=‘echo $YMIN|awk '{printf"%.2f", 2/3*log($1*5)/2.303-2.9}' ‘
  YMAX2=‘echo $YMAX|awk '{printf"%.2f", 2/3*log($1*5)/2.303-2.9}' ‘
  RANGE="-R0/$XMAX/$YMIN/$YMAX"
  PROJ="-JX${XSCALE}/$YSCALE"
  BGN="$RANGE $PROJ -K"
  MID="$RANGE $PROJ -O -K"
  END="$RANGE $PROJ -O"
  OUTFILE=$EVENTNAME.ps                # Output file
#################################
# CREATE A BOUNDING BOX
 # gmtset PAPER_MEDIA letter+ DEGREE_FORMAT 5  # pre 4
  gmtset ANNOT_FONT_SIZE_PRIMARY 10 PAPER_MEDIA letter+ PLOT_DEGREE_FORMAT
 D # GMT 4

###########################################################

# FIRST PLOT: HF CUMULATIVE ENERGY (Bottom plot)

  # get a well scaled Y axis with tics
    EXPm1=‘echo $YMAX | awk -F"+" '{print $2-1}' ‘
    MANT=‘echo $YMAX | awk -F"e|E" '{print $1}' ‘
    if [[ $MANT > 4 ]] ; then
              YTIC=5
    elif [[ $MANT > 3 ]] ; then
              YTIC=2
    else
              YTIC=1
    fi
  # get a well scaled x axis with tics
    if [[ $XMAX -ge 200 ]] ; then
              XTIC=50
      else
              XTIC=20
    fi
# changed: draw each xis separately to get%7.1e formatting in Y-AXIS
  psbasemap -B5a$XTIC/Sn -Y4 -X4 $BGN -P > $OUTFILE
  psbasemap -B/${YTIC}e${EXPm1}W --D_FORMAT=%7.1e $MID  >> $OUTFILE
```

```
# plot Magnitude scale on right
    YMINTICK2='echo $YMIN2 $YMAX2 | awk '{print $1+0.6*($2-$1)}''
   #  echo $YMINTICK2
      # there is a problem with the scaling because we have not determined
 the correct power
      psbasemap -B1000/0.05a0.1E -R$XMIN/$XMAX/$YMIN2/$YMAX2 ${PROJ}P25 -O
 -K >> $OUTFILE
 msftlow=1e+35
 x0=$XMIN
 XMINp20='echo $XMIN | awk '{print $1+10}''
 x0=$XMIN;x1=$XMAX
 x1=$XMAX
 XMAXm20='echo $XMAX | awk '{print $1-10}''

 # earlier
     msftlow=1e+35
     x0=$XMIN
     for x1 in 'seq $XMINp20 5 $XHALF'
     do
         FITS='awk '$1>=x0 && $1 <= x1 {print $1,$2}' x0=$x0 x1=$x1 $CORRHFENERGY
  | $FITXY'
         msft='echo $FITS | awk '{print $7}''
         if [[ 'echo $msft $msftlow|awk '$1<$2{print 1}'' == "1" ]]
         then
                 c='echo $FITS | awk '{print $2}''
                 d='echo $FITS | awk '{print $3}''
                 msftlow=$msft
         fi
     done
     x0=$XMIN;x1=$XMAX
     echo $x0 $x1 $c $d | awk '{printf "%f %f\n%f %f\n", $1,$3+$4*$1,$2,$3+$4*$2}' |\
         psxy $MID -W2t-/150 >>$OUTFILE
     #echo "slope of HFerate: $d  and Intercept: $c"
 #  later
     msftlow=1e+35
     x1=$XMAX
     for x0 in 'seq $XHALF 5 $XMAXm20'
     do
         FITS='awk '$1>=x0 && $1 <= x1 {print $1,$2}' x0=$x0 x1=$x1 $CORRHFENERGY
  | $FITXY'
         msft='echo $FITS | awk '{print $7}''
         if [[ 'echo $msft $msftlow|awk '$1<$2{print 1}'' == "1" ]]
         then
                 c1='echo $FITS | awk '{print $2}''
                 d1='echo $FITS | awk '{print $3}''
                 msftlow=$msft
         fi
     done
     x0=$XMIN;x1=$XMAX
     echo $x0 $x1 $c1 $d1 | awk '{printf "%f %f\n%f %f\n", $1,$3+$4*$1,$2,$3+$4*$2}' |
\
         psxy $MID -W3t-/150 >>$OUTFILE
     #  crossover From Estimated HF energy
      XoverE='echo $c $d $c1 $d1 | awk '{printf "%d", ($1-$3)/($4-$2)}''
      Tr=$XoverE
     echo $XoverE | awk '{printf "%f %f\n%f %f\n",$1,YMIN,$1,YMAX}' YMIN=$YMIN YMA
X=$YMAX |\
         psxy $MID -W10/black >>$OUTFILE
 #echo Printing: XoverE=$XoverE

# ESTIMATED ENERGY lINE
  awk '$1!~"#" {print $1,$2}' $CORRHFENERGY | psxy $MID -W7/red >>$OUTFILE

# Calculate the HF energy and Hf energy magnitude (Mehf):
```



```
#echo calculate Mehf
  #echo $Tr
  #awk '$1=='"$XoverE"' {print $0}' $CORRHFENERGY
   EHFxover='awk '$1=='"$XoverE"' {printf "%4.2e",$2}' $CORRHFENERGY' # HF energy
 at XoverE
   Mehf='echo $EHFxover | awk '{printf "%4.2f", 2/3*(log($1*5))/2.303-2.9}''
   EhfTr3='echo $EHFxover $Tr | awk '{printf "%9.2e\n", $1/($2**3)}''
   #echo done with Me=$Mehf and EhfTr3=$EhfTr3
#number of stations used
# NSTATS='awk 'NR==1{print $3}' $CORRHFENERGY'
NSTATS='awk 'END{print NR}' $USEDSTATIONSHF'

# write data and titles
 pstext $MID -N <<...END >>$OUTFILE
 'echo $RANGE | cut -c 3- | awk -F"/" '{print $1-0.16*($2-$1), ($3+$4)/2}' ' 16 90
0 6  Cumulative HF Energy [J]
 'echo $RANGE | cut -c 3- | awk -F"/" '{print $2+0.12*($2-$1), ($3+$4)/2}' ' 16 -90
 0 6 HF Energy Magnitude (M@-e-hf@-)
 'echo $RANGE | cut -c 3- | awk -F"/" '{print ($1+$2)/2, $3-1.2*($4-$3)/10}' ' 16 0
0 6 Time from P-arrival [s]
# 'echo $RANGE | cut -c 3- | awk -F"/" ' {print $2-0.08*($2-$1), $3-1.3*($
4-$3)/10}' ' 12 0 0 6 Iteration=$ITER
...END

RANGE=0/1/0/1
 pstext $MID -R$RANGE -N <<...END >>$OUTFILE
 0.72 .95 12 0 0 0 Period = 0.5 - 2 s
 0.02 .95 10 0 0 0 pre-P E@-rate@- (removed) = $HFRATE [J/s]
 0.72 .25 10 0 0 0 N = $NSTATS stations
 0.72 .20 10 0 0 0 T@-R@- = $Tr  s
 0.72 .15 10 0 0 0 E@-hf@-(t=T@-R@-) = $EHFxover J
 0.72 .10 10 0 0 0 M@-e-hf@-(t=T@-R@-) = $Mehf
...END
# plot red if it is a tsunami earthquake

IsTsE='echo $EhfTr3 | awk '$1<5e7{print 1}''

if [ $IsTsE ]  ; then
    echo TsE
    echo "0.72 .05 10 0 0 0 E@-hf@-/T@-R@-@+3@+ = $EhfTr3"|pstext $MID -R$RANGE -
N -Gred >>$OUTFILE
 else
    echo "0.72 .05 10 0 0 0 E@-hf@-/T@-R@-@+3@+ = $EhfTr3"|pstext $MID -R$RANGE -
N  >>$OUTFILE
fi


# END OF FIRST PLOT (HF energy)

##########################################################################
########################
# SECOND PLOT: broadband Duration plot

################################
  YMAX='awk '$1==XMAX{printf "%.2e",$2*1.2}' XMAX=$XMAX $CORRBBENERGY'
  YMIN='echo $YMAX | awk '{print $1/100}''
  YMIN2='echo $YMIN|awk '{printf"%.2f", 2/3*log($1)/2.303-2.9}' '
  YMAX2='echo $YMAX|awk '{printf"%.2f", 2/3*log($1)/2.303-2.9}' '
  RANGE="-R0/$XMAX/$YMIN/$YMAX"
  BGN="$RANGE $PROJ -K"
  MID="$RANGE $PROJ -O -K"
  END="$RANGE $PROJ -O"
#################################
```

```
  # get a well scaled Y axis with tics
    EXPm1='echo $YMAX | awk -F"+" '{print $2-1}' '
    MANT='echo $YMAX | awk -F"eE" '{print $1}' '
    if [[ $MANT > 4 ]] ; then
              YTIC=5
    elif [[ $MANT > 3 ]] ; then
              YTIC=2
    else
              YTIC=1
    fi
  # get a well scaled x axis with tics
    if [[ $XMAX -ge 200 ]] ; then
              XTIC=50
      else
              XTIC=20
    fi

  psbasemap -B/${YTIC}e${EXPm1}WSn --D_FORMAT=%7.1e  -Y$YSCALE $MID -P >>
$OUTFILE

  # plot Magnitude scale on right
        YMINTICK2='echo $YMIN2 $YMAX2 | awk '{print $1+0.6*($2-$1)}''
        # starts the scale from a larger minimum
          psbasemap -B1000/0.05a0.1E -R$XMIN/$XMAX/$YMIN2/$YMAX2 ${PROJ}P2
5 -O -K >> $OUTFILE

 # Crossover HF energy redraw for the BB cumulative energy plot (Calculate
d before)
     echo $XoverE | awk '{printf "%f %f\n%f %f\n",$1,YMIN,$1,YMAX}' YMIN=$YMIN YMA
X=$YMAX |\
         psxy $MID -W10/black >>$OUTFILE

# Estimated Energy SOLID line
 awk '$1!~"#"{print $1,$2}' $CORRBBENERGY | psxy $MID -W7/blue >>$OUTFILE
# True Energy line
# awk '{print $1,$3}' $CORRBBENERGY | psxy $MID -W7/red >>$OUTFILE

  msftlow=1e+35
  x0=$XMIN
  XMINp20='echo $XMIN | awk '{print $1+20}''
  x1=$XMA
  XMAXm20='echo $XMAX | awk '{print $1-20}''


# Calculate the Broad-Band energy and BB energy magnitude (Mebb):
   EBBxover='awk '$1=="'$XoverE'"{printf "%4.2e",$2}' $CORRBBENERGY' # HF energy
 at XoverE
   Mebb='echo $EBBxover | awk '{printf "%4.2f", 2/3*(log($1))/2.303-2.9}''
#  echo "XoverE= $XoverE ; Mehf= $Mehf"


pstext $MID -N <<...END >>$OUTFILE
 'echo $RANGE | cut -c 3- | awk -F"/" '{print $1-0.16*($2-$1), ($3+$4)/2}' ' 16 90
0 6 Cumulative BB Energy [J]
 'echo $RANGE | cut -c 3- | awk -F"/" '{print $2+0.12*($2-$1), ($3+$4)/2}' ' 16 -90
 0 6 Energy Magnitude (M@-e@-)
...END

RANGE=0/1/0/1
 pstext $MID -R$RANGE -N <<...END >>$OUTFILE
 0.72 .95 12 0 0 0 Period = 0.5 - 70 s
 0.02 .95 10 0 0 0 pre-P E@-rate@- (removed) = $BBRATE [J/s]
 0.72 .10 10 0 0 0 E@-BB@-(t=T@-R@-) = $EBBxover J
 0.72 .05 10 0 0 0 M@-e@-(t=T@-R@-) = $Mebb
```



```
...END
 pstext $END -R$RANGE -N -Y2.2 <<...END >>$OUTFILE
# 'echo $RANGE | awk -F"/" ' {print ($1+$2)/2, $4}' ' 18 0 0 TC Cumulative
 Energy Growth ( M@-e@-= $Mebb, T@-R@-= $Tr )
'echo $RANGE | awk -F"/" '{print ($1+$2)/2, $4}' ' 18 0 0 TC Cumulative Energy G
rowth
#'echo $RANGE | awk -F"/" ' {print ($1+$2)/2, $4-($4-$3)/7}' ' 12 0 0 6 $E
VENTLINE
'echo $RANGE | awk -F"/" '{print ($1) , $4-0.9*($4-$3)/7}' ' 12 0 0 BL EventID: $EV
ENTNAME
'echo $RANGE | awk -F"/" '{print ($1) , $4-1.3*($4-$3)/7}' ' 12 0 0 BL Origin Time:
 $ODATE $OTIME
'echo $RANGE | awk -F"/" '{print ($1) , $4-1.7*($4-$3)/7}' ' 12 0 0 BL Location: $O
LAT, $OLON, z=$ODEP km
'echo $RANGE | awk -F"/" '{print ($2) , $4-0.9*($4-$3)/7}' ' 16 0 0 BR M@-e@-= $Meb
b
'echo $RANGE | awk -F"/" '{print ($2) , $4-1.5*($4-$3)/7}' ' 16 0 0 BR T@-R@-= $Tr
s
...END

########### END OF PLOT ##################################
COMMENTS="(SRC=$OSRC, $OMTP=$OMAG); $COMMENTS"
if [ -e $EVENTNAME.results ] ; then
       mv $EVENTNAME.results $EVENTNAME.results.old.$$
fi
 echo  "#Eventname   Date  Otime  Lat.  Long.  Depth  Me  Tr   Ehf   Ebb  Mehf  Ehf/Tr^3  Nstat
s : Comments" > $EVENTNAME.results
 printf " $EVENTNAME $ODATE $OTIME %6.2f %7.2f %6.1f %5.2f %4d %8.1e %8.1e %5.2f %8.1
e  %4d : $COMMENTS\n" \
                         $OLAT $OLON $ODEP $Mebb $Tr  $EHFxover $EBBxover
$Mehf $EhfTr3 $NSTATS >> $EVENTNAME.results
cat $EVENTNAME.results

# want to change the scale?
#  perl -pi.bak -e 's/0\.24\ 0\.24\ scale/0\.22\ 0\.22\ scale/g' $OUTFILE
# put hidden stamp in file that will denote its source
  echo " %% created by ${USER} using ${HOST}:${PWD}/$0 $* " >>$OUTFILE

  $CONVERT $OUTFILE 'basename $OUTFILE .ps'.png
# bring up plot
#  gs $OUTFILE

exit 0
```

```
#!/bin/bash
# GMT plot showing stations colored by deviation from the mean value at th
e estimated
# rupture duration.
# THIS srcipt NEEDS the .results file
# example: 'stationsperevent.gmt -O BB -E09022000'
# Created by jconvers
# last modified on Tue Jan 20 09:19:45 EST 2009
##################################################
# external programs and files
CONVERT=convert
#############################
## LOCAL FIXED PATHS (may need to change if changing location of main fold
er) ##
CONTROLFILE="nergy.sac.in" # the nergy control file. I will assume this scrip
t will be run in the event folder
ERG=/products/eqenergy
ERG=/home/gterg/GTerg # main folder where events, bin folder and libraries
 are organized
GMTLIB=$ERG/lib/GMTlib
TMPDIR=$ERG/scratchfolder
## USAGE ##
USAGE=$TMPDIR/usage.'basename $0'
ITER=0
printf "
USAGE: 'basename $0' -O'tinc_files_folder' -E'Eventname' -F'BB' or 'HF'

Function:
   Plots stations with a color according to the deviation from the mean with respect
   to the average value at the estimated rupture duration

MANDATORY FLAGS:
   -E Name of event (needed to locate the .results file)
   -O folder where the data is stored (specifically looks for BBTINC.inrange, or
      HFTINC.inrange, they contain information of the stations used for the final average).
   -F Frequency band ('BB' or 'HF')
New option:
   -R use the ''True'' focal mechanism (the one in nergy.sac.in) to calculate the energy at each
      station to get the deviation. default will use the Estimated focal correction.
      !! important: the use of this flag must be consistent with the -R flag used to plot the
         cumulative energy. (use true focal mechanism in both plots or estimated in both) !!

   Example:
%% 'basename $0' -E09011800 -O BBHF -FBB -R \n\n"> $USAGE

##### FLAG OPTIONS #####
while getopts "O:E:F:Rh" OPT
do
   case ${OPT} in
        O) DATAFOLDER=$OPTARG
       ;;
        E) EVENTNAME=$OPTARG
       ;;
        F) FREQBAND=$OPTARG
       ;;
        R) RFLAG=1 # sets a value for the flag to plot TrueErg instead of
EstErg
       ;;
        h) cat $USAGE  # display usage
           rm $USAGE
            exit 1 # exit with error after removing temp file
       ;;
        *) cat $USAGE
           rm $USAGE
```



```
           exit 1
        ;;
    esac
done

if [[  ! "$DATAFOLDER"   || ! "$EVENTNAME" || ! "$FREQBAND"  ]] ; then
        printf "\n ERROR: Mandatory parameters not set!!\n"
        cat $USAGE
        rm $USAGE
        exit 1
fi

####### NECESSARY FILES ######
STATIONSFILE=AVAILABLESTATIONS.teles # file produced after MDGET and NRT_t
eleseisms CAREFUL I MIGHT NOT HAVE THIS FILE
USEDSTATIONS="$DATAFOLDER/${FREQBAND}TINC.inrange" # files used for the fin
al tinc calculation
STATIONSNOTUSED="$DATAFOLDER/${FREQBAND}TINC.outofrange" # stations discarde
d
#echo $USEDSTATIONS
RESULTSFILE=$EVENTNAME.results
OUTFILE=E_Distr_map_$EVENTNAME.ps # output file
PLATES=$GMTLIB/PB2002_plates.dig
EQS=$GMTLIB/EQM4plus.data
EQSCPT=$GMTLIB/EQCOLOR.cpt
CPT=$GMTLIB/gray.cpt
TOPO=$GMTLIB/topo.grd
Edist=Edist_bylocation.llE
STATCPT=Edist.cpt
#######################################################################

if [[  ! "$DATAFOLDER"   || ! "$EVENTNAME" || ! "$FREQBAND" ]] ; then
        printf "\n \033[5;31mERROR: Mandatory parameters not set!!\033[5;0m Here is how to use t
his program:\n"
        cat $USAGE
        rm $USAGE
        exit 1
fi

# verify data folder exists
if [ ! -e $DATAFOLDER ] ; then
        printf "\nfolder $DATAFOLDER NOT found, verify name of folder in -O option\n\n"
        exit 1
fi
# verify results file exists
if [ ! -e $RESULTSFILE ] ; then
        printf "\nresults file $RESULTSFILE NOT found, verify name of file in the -E option\n\n"
        exit 1
fi

rm $USAGE # "clear" usage file
# DECLARE VARIABLES
SCALE=18.65 # scale of overall plots
#CENTERLONG='awk 'NR==2 {print $6}' $STATIONSFILE'
RANGE="-Rd"
EQLON='awk 'NR==2 {print $5}' $RESULTSFILE' # earthquake longitude
EQLAT='awk 'NR==2 {print $4}' $RESULTSFILE' # earthquake latitude
EQDEPTH='awk 'NR==2 {print $6}' $RESULTSFILE' # earthquake depth
ODATE='awk 'NR==2 {print $2}' $RESULTSFILE' # Origin date
OTIME='awk 'NR==2 {print $3}' $RESULTSFILE' # Origin time
PROJ="-JA${EQLON}/${EQLAT}/${SCALE}"   #"-JH$CENTERLONG/${SCALE}"
BGN="$RANGE $PROJ -K -P"
MID="$RANGE $PROJ -O -K -P"
END="$RANGE $PROJ -O -P"
```

```
GRIDFILE=dist_jaime.grd # temporary grid file
STATIONSINRANGE='awk '{print $1}' $USEDSTATIONS' # Stations used within toler
ance range
STATIONSOUTOFRANGE='awk '{print $1}' $STATIONSNOTUSED' # stations not used
#echo $STATIONSINRANGE
TRUPTURE='awk '$1!~"#"&&NR==2 {print $8}' $RESULTSFILE'
EHFAVG='awk '$1!~"#"&&NR==2 {print $9}' $RESULTSFILE'
EBBAVG='awk '$1!~"#"&&NR==2 {print $10}' $RESULTSFILE'
#echo $EHFAVG
#### BOUNDING BOX ####
gmtset ANNOT_FONT_SIZE_PRIMARY 10 PAPER_MEDIA letter+ PLOT_DEGREE_FORMAT D
 # GMT 4
# create grid
grdmath -Rd  -I1 $EQLON $EQLAT SDIST = $GRIDFILE
pscoast -B10a20g30wsen  -Dc -A1000 -G220 -S255 -W0/0 -X1 -Y4 $BGN > $OUTFI
LE
#echo passed grdmath and pscoast
# create grid
    #grdraster 2 -R-180/180/-90/90 -G$TOPO -I20m
    #grdgradient $TOPO -G$TOPO.ill -A45/80 -Ne.45
grdimage $TOPO $MID  -I$TOPO.ill -C$CPT -E100 >>$OUTFILE
pscoast -B10a20g30wsen -Di -A10000 -W1/0 $MID >> $OUTFILE
#echo passed grdimage pscoast
# PLOT PREVIOUS SEISMICITY
   # sorted by depth
   #  awk '$4>=MMIN{print $1,$2,$3,($4-MMIN+1)/10 }' MMIN=5.5 $EQS | sort
-g -r +2 > $EQS.sorted
      psxy $EQS.sorted $MID -Sc -C$EQSCPT -W1/100  >>$OUTFILE
#echo passed $EQS.sorted
# PLOT PLATE BOUNDARIES
   awk -F"," '$1!="#"{if (NF==1) print ">"; else print $1,$2 }' $PLATES | psxy -W3/0 -M $M
ID >>$OUTFILE

grdcontour $GRIDFILE -A+v+a5+s16+k070 -Glz-/z+ -C20 -L20/80 -O -K $PROJ -W
8/070 >> $OUTFILE
### plot available stations for this event:
##awk '{print $9,$8}' $STATIONSFILE | psxy $MID -St0.2 -W1/0 -Gwhite -N >>
 $OUTFILE
# STATIONSNOTUSED
for stationtincfile in $STATIONSOUTOFRANGE
do
        stationlat='awk 'NR==2 {print $4}' $stationtincfile'
        stationlong='awk 'NR==2 {print $5}' $stationtincfile'
        echo $stationlong $stationlat | psxy $MID -St0.5 -W2/0 -Gwhite -N
>> $OUTFILE
        #echo $stationlong $stationlat
done

# plot stations used
#echo plotting stations...
for stationtincfile in $STATIONSINRANGE
do
        stationlat='awk 'NR==2 {print $4}' $stationtincfile'
        stationlong='awk 'NR==2 {print $5}' $stationtincfile'
        Fp2='awk 'NR==9 {print $4} ' $stationtincfile'      # (F_p)^2 this is
equal to 4/15
        EstFgp2='awk 'NR==11 {print $4}' $stationtincfile'  # from the tinc f
ile Estimated = (Fgp)^2
        TrueFgp2='awk 'NR==10 {print $5}' $stationtincfile' # From ,tinc file
. (Fgp)^2 from the True focal mechanism
        # Energy = (E*) X (F_p)^2/<Fgp>^2
        if [ $RFLAG ] ; then
                # RFLAG: true mechanism
                focalfactor='echo $Fp2 $TrueFgp2  | awk '{print $1/$2}' '
```



```
                #echo "selected true focal correction"
        else
                # No flag: estimated focal mechanism:
                focalfactor='echo $Fp2 $EstFgp2  | awk '{print $1/$2}' '
                #echo "did not select true focal correction"
        fi
        # selecting the right frequency band
        if [[ $FREQBAND == "HF" ]] ; then
                awk '$1=='$TRUPTURE'{ print '$stationlong','$stationlat',log($3*
'$focalfactor'/1e7/'$EHFAVG')/2.303 }' $stationtincfile >> $Edist
        elif [[ $FREQBAND == "BB" ]]; then
                awk '$1=='$TRUPTURE'{ print '$stationlong','$stationlat',log($2*
'$focalfactor'/1e7/'$EBBAVG')/2.303 }' $stationtincfile >> $Edist
        else
                echo  "neither BB or HF?? check the arguments for the -F flag"
                exit 1
        fi

        #echo adding result from $stationtincfile
done
#echo file $Edist
#cat $Edist
        makecpt -T-1./1./.5 -Z -D -Csplit >$STATCPT

psxy $Edist $MID -St0.65 -W2/255 -C$STATCPT>> $OUTFILE
# plot epicenter of Earthquake
awk 'NR==2 {print $5,$4}'  $RESULTSFILE | psxy $MID -Sa0.65 -W2/0 -Ggreen -N >
> $OUTFILE
#echo passed plotting epicenter

## Plot focal mechanism:
#EQMAG=7.5
#awk 'NR==6{print '$EQLON','$EQLAT',30,$1,$2,$3,'$EQMAG',0,0}' $CONTROLFIL
E | psmeca -W4/0 -Sa1/0 -G255/0/0 $MID >>$OUTFILE


psscale -D17.4/2.3/3/.2 -C$STATCPT -O -K >>$OUTFILE
# write title
RANGE2=0/1/0/1
PROJ2="-JX${SCALE}"
# psxy -R$RANGE2 $PROJ2 -O -K -P -N >>$OUTFILE
#echo $RANGE2 | awk -F"/" '{print 0.76*$2, $4/5-0.144*$4}' | psxy -R$RANGE
2 $PROJ2 -St0.2 -W1/0 -Gwhite -O -K -P -N >>$OUTFILE
# Title and conventions
 pstext -R$RANGE2 $PROJ2 -Y2 -O -P -N <<..END >>$OUTFILE
  0.01 1.00 12 0 0 TL Event: $EVENTNAME
  0.01 0.97 12 0 0 TL Origin time: $ODATE $OTIME
  0.01 0.94 12 0 0 TL Location: $EQLAT, $EQLON , z=$EQDEPTH km
#  0.78 0.99 12 0 0 TL Iteration: $ITER
#  0.78 .10  10 0 0 0 Stations Reporting
  0.91  .08  10 90 0 BR Log@-10@- (@~D@~ Energy)
..END

# put hidden stamp at end of  file that will denote its source
echo " %% created by ${USER} using ${HOST}:${PWD}/$0 $* " >>$OUTFILE

rm $GRIDFILE $Edist $STATCPT
  $CONVERT -antialias  $OUTFILE 'basename $OUTFILE .ps'.png

  #$CONVERT -antialias -scale 541x541 $OUTFILE 'basename $OUTFILE .ps'.png
echo "Plot $OUTFILE created"
# DECLARE VARIABLES
# bring up plot
# gs $OUTFILE
```

```
exit 0
```

```
#!/bin/bash
# GMT script for cumulative enrgy plots per station
# Last modified  Tue Apr  7 13:47:32 EDT 2009

# EXTERNAL PROGRAMS
CONVERT=convert
FITXY=fitxy

################################
CONTROLFILE="nergy.sac.in" # the nergy control file. I will assume this scrip
t will be run in the event folder
## DECLARE YOUR VARIABLES HERE ##
ERG=/home/gterg/GTerg
TMPDIR=$ERG/scratchfolder
#source GTerg_config.sh
ITER=0
USAGE=$TMPDIR/'basename $0'.usage
XMIN=0

printf "
USAGE: 'basename $0' -Ttmin/tmax -Eeventname  -Iiter
   Function:
     Calculates and creates a plot of the energy growth with time for High Frequencies (HF)
     and Broad-band frequencies (BB) from files 'stationfile'.timc  over  the relative
     time window 'tmin' to 'tmax' from the p-arrivals. The program assumes certain information
     created by RTprocess exists in the eventname directory.
     plots are per station.

MANDATORY FLAGS:
   -O Folder where the .tinc files are
   -T fit limits for begining of 1st and end of second slopes (tmin and tmax)
   -E Name of event in final plot
OPTIONS (arguments for graph output):
   -I iteration number
   -h Show this help and exit

   Example:
     %% 'basename $0' -E09010306 -T20/200 -OBBHF \n\n"> $USAGE
#### FLAG OPTIONS ########
while getopts "T:E:O:I:h" OPT
do
   case ${OPT} in
        T) TARG=$OPTARG
           XMIN='echo $OPTARG | awk -F"/" '{print $1}''      # tmin
           XMAX='echo $OPTARG | awk -F"/" '{print $2}''      # tmax
         ;;
        E) EVENTNAME=$OPTARG
         ;;
        O) DATAFOLDER=$OPTARG
         ;;
        I) ITER=$OPTARG
         ;;
        h) cat $USAGE  # display usage
           rm $USAGE
           exit 1 # exit with error after removing temp file
   esac
done

if [[ ! "$XMAX"  || ! "$EVENTNAME" ]] ; then
        echo "ERROR: Mandatory parameters not set.  Exiting !!"
        cat $USAGE
        rm $USAGE
        exit 1
fi
```



```
rm $USAGE

####### NECESSARY FILES ######
HFSTATS=$DATAFOLDER"/HFTINC.inrange" # files used for the final tinc calculat
ion
BBSTATS=$DATAFOLDER"/BBTINC.inrange" # files used for the final tinc calculat
ion
#######################################################################

#  Checking HF energy file "HFENERGY"
 if [[ ! -s $HFSTATS || ! -s $BBSTATS ]] ; then
         echo  "ERROR: File $HFSTATS, or $BBSTATS doesn't exist or is empty,"
         echo  "check the folder names and/or file names.... Exiting"
         exit 1
 fi
 ERESULTS=$EVENTNAME.results
 if [[ -s $ERESULTS ]] ; then
          ODATE='awk 'NR==2{print $2}'  $ERESULTS'
          OTIME='awk 'NR==2{print $3}'  $ERESULTS'
          OLAT='awk 'NR==2{print $4}'   $ERESULTS'
          OLON='awk 'NR==2{print $5}'   $ERESULTS'
          ODEP='awk 'NR==2{print $6}'   $ERESULTS'
            Me='awk 'NR==2{print $7}'   $ERESULTS'
            Tr='awk 'NR==2{print $8}'   $ERESULTS'
          OEhf='awk 'NR==2{print $9}'   $ERESULTS'
          OEbb='awk 'NR==2{print $10}'  $ERESULTS'
 else
         echo  "WARNING: File $EVPARAMS doesn't exist or is empty....Continuing"
 fi

EVENTLINE="$ODATE $OTIME ($EVENTNAME) at $OLAT, $OLON, z=$ODEP"

################################
  XSCALE=9                    # scale of overall plot
  YSCALE=24                    # scale of overall plot
  YMIN=0 ;YMAX=390
#  YMAX=8.0e13 # Latitude range of plots
  RANGE="-R0/$XMAX/$YMIN/$YMAX"
  PROJ="-JX${XSCALE}/$YSCALE"
  BGN="$RANGE $PROJ -K"
  MID="$RANGE $PROJ -O -K"
  END="$RANGE $PROJ -O"
OUTFILE=Tdist_$EVENTNAME.ps # output file
################################
# CREATE A BOUNDING BOX
 # gmtset PAPER_MEDIA letter+ DEGREE_FORMAT 5  # pre 4
  gmtset ANNOT_FONT_SIZE_PRIMARY 10 PAPER_MEDIA letter+ PLOT_DEGREE_FORMAT
 D # GMT 4
############################################################
# get a well scaled x axis with tics
    if [[ $XMAX -ge 200 ]] ; then
              XTIC=50
      else
              XTIC=20
    fi
# FIRST PLOT: HF ENERGY (left plot)
    psbasemap -B5a$XTIC/15a45WeSn -Y2 -X2.5 $BGN -P > $OUTFILE
    # Draw Tr solution
          printf "$Tr $YMIN \n$Tr $YMAX" | psxy $MID -W10/black >>$OUTFILE

    # ITERATE OVER STATIONS
    for file in 'cat $HFSTATS'
    do
        #SLNFILE=HF/'basename $file .tinc'.*.*.*
```

```
        #DIST='awk '$1~"Distance,"{print $5}' $SLNFILE'
        #AZ='awk '$1~"Distance,"{print $6}' $SLNFILE'
        #BAZ='awk '$1~"Distance,"{print $7}' $SLNFILE'
        AZ='awk 'NR==5{print $4}' $file'
        EMAX='awk 'END{print $3}' $file'
        awk '$1!~"#" {print $1,'$AZ'+($3/'$EMAX')*30}' $file | psxy $MID -W2/red >
>$OUTFILE
    done
 pstext $MID -N <<...END >>$OUTFILE
 'echo $RANGE | cut -c 3- | awk -F"/" '{print $1-0.18*($2-$1), 190}' ' 16 90 0 6
Normalized per-station Energy, Azimuthally Distributed [@+o@+]
 'echo $RANGE | cut -c 3- | awk -F"/" '{print $2,-15}' ' 16 0 0 6 Time from P-
arrival [s]
...END

# SECOND PLOT: BB ENERGY (right plot)
    psbasemap -B5a$XTIC/15a45wESn -X$XSCALE $MID >> $OUTFILE
    # Draw Tr solution
          printf "$Tr $YMIN \n$Tr $YMAX" | psxy $MID -W10/black >>$OUTFILE

    # ITERATE OVER STATIONS
    for file in 'cat $BBSTATS'
    do
        #SLNFILE=BB/'basename $file .tinc'.*.*.*
        #DIST='awk '$1~"Distance,"{print $5}' $SLNFILE'
        #AZ='awk '$1~"Distance,"{print $6}' $SLNFILE'
        #BAZ='awk '$1~"Distance,"{print $7}' $SLNFILE'
        AZ='awk 'NR==5{print $4}' $file'
        EMAX='awk 'END{print $2}' $file'
        awk '$1!~"#" {print $1,'$AZ'+($3/'$EMAX')*30}' $file | psxy $MID -W2/blue
>>$OUTFILE
    done
 pstext $MID -N <<...END >>$OUTFILE
 'echo $RANGE | cut -c 3- | awk -F"/" '{print $2+0.18*($2-$1), 190}' ' 16 -90 0 6
 Normalized per-station Energy, Azimuthally Distributed [@+o@+]
...END

  XSCALE=9                   # scale of overall plot
  YSCALE=26                   # scale of overall plot
  PROJ="-JX${XSCALE}/$YSCALE"
  RANGE="-R0/0.5/0/1.5"
  BGN="$RANGE $PROJ -K"
  MID="$RANGE $PROJ -O -K"
  END="$RANGE $PROJ -O"

 pstext $MID -N -X-$XSCALE <<...END >>$OUTFILE
 0.49   .01 14 0 0 BR Period = 0.5 - 2 s
 0.99   .01 14 0 0 BR Period = 0.5 - 70 s
...END
# 0.88  1.03 10 0 0 0 Iteration: $ITER
# END OF SECOND PLOT (HF energy)
 pstext $END -N <<...END >>$OUTFILE
       0.5 1.49 18 0 0 TC Per-Station Cumulative Energy Growth
       0.01 1.45 12 0 0 TL Origin time $ODATE $OTIME
       0.01 1.42 12 0 0 TL Location $OLAT, $OLON, z=$ODEP km
       0.99 1.45 14 0 0 TR M@-e@-= $Me
       0.99 1.42 14 0 0 TR T@-R@-= $Tr s
...END
# ( M@-e@-= $Me, T@-R@-= $Tr )
# 0.5 1.05 12 0 0 TC $EVENTLINE
########### END OF PLOT #################################

#output pertinent information to file
```



```
# want to change the scale?
#  perl -pi.bak -e 's/0\.24\ 0\.24\ scale/0\.22\ 0\.22\ scale/g' $OUTFILE
# put hidden stamp in file that will denote its source
  echo " %% created by ${USER} using ${HOST}:${PWD}/$0 $* " >>$OUTFILE

  $CONVERT $OUTFILE 'basename $OUTFILE .ps'.png
# bring up plot
#  gs $OUTFILE

exit 0
```

C.3 Fortran programs


```
c -- E_star_wprep.cwb.IRISpz_.f is the Energy program to rapidly calculate
 E_star
c    of an earthquake at teleseismic distances using the P-wave train
c    including P, sP and pP BUT WITHOUT FOCAL MECHANISM.
c    THIS PROGRAM ALSO CALCULATES THE PRE-P E_STAR RATE before the
c    p-arrival
c    Please see Newman and Okal (1998) and
c    Boatright and Choy (1986) for details.
c    Authors: Andrew Newman and Emile Okal
C    HEAVILY modified by Jaime Convers to produce a sequence of energy
C    calculations in increasing time windows
C    last modified in Mon Mon Feb 25 21:03:57 EST 2013 adding comments to
C    compile the 64bit version in terremoto with the new sacio
C    ** IMPORTANT MODIFICATION: **
C    This is designed to use a new response Routine to accomodate for the
IRIS pole-zero
C     file (it has different formatting and no  explicit CONSTANT)
C -------------------------------------------------------
C  Reference
C -------------------------------------------------------
C     Newman, A. V. & E. A. Okal, Teleseismic Estimates of Radiated
C     Seismic Energy: The E/M0 Discriminant for Tsunami Earthquakes, Jour.
 of
C     Geoph. Res., 103 (11), 26,885-98, 1998.
C -------------------------------------------------------
C  Compilation
C -------------------------------------------------------
c     Read in binary sac data using sacio library...
C     Make sure you put the right path to the sacio.a file!
C
C     must compile as 32-bit (since this is the only sacio.a library that
works at present)
C     using :
C     g77 -o E_star_wprep.cwb.IRISpz_.f E_star_wprep.cwb.IRISpz_.f  /usr/l
ocal/sac/sac/lib/sacio.a -m32 -lm
C     g77 -o nergy_wprep.cwb.IRISpz nergy_wprep.cwb.IRISpz.f  /usr/local/s
ac/sac/lib/sacio.a -m32 -lm -static
c     or
C     gfortran -o E_star_wprep.cwb.IRISpz E_star_wprep.cwb.IRISpz_.f /usr/
local/sac/sac/lib/sacio.a -m32 -lm -static
C
C     NEW!!: In terremoto, f77 can be used to compile with f77 and 64-bit
sacio version form sac sac-101.3b:
C     FOR EXAMPLE:
C     f77 -o E_star_wprep.cwb.IRISpz E_star_wprep.cwb.IRISpz_.f /usr/local
/sac/sac/lib/sacio.a -m64 -lm
C     f77 -o E_star_wprep.cwb.IRISpz E_star_wprep.cwb.IRISpz_.f /usr/local
/sac/sac/lib/sacio.a -m64 -lm -static
C -------------------------------------------------------
C  necessary files
C -------------------------------------------------------
c    The program will read in the sac file looking for the AMARKER ('a' va
riable using
c    getnhv from the sacio.a).  This marker should be the initial arrival
of the p-wave
c    and can be added using r 'sacfile' ; plotpk ; p (at location of initi
al arrival); writehdr;
c
c    If it is not defined the program will send out a non-fatal error and
warning and
c    will process from the start-time of the input file.

c    Three files are required and need to be in the current directory for
any run.
```



```
c         nergy.sac.in       --  input file
c         'sac file'         --  seismic data file in sac format
c         'response file'    --  .pz file "ploes and zeros file" from CWBq
uery
c
c     As well, three tables need to be readable.  By default, these files
c     are in  /usr/local/geophysics/lib/
c     The files are d2tdd2.p, d2tdd2.pcp, jfbup.dat
c     LOCATION OF THESE WILL VARY, PAY ATTENTION TO THIS
c
C -------------------------------------------------------
C  input 'control' file
C -------------------------------------------------------
C  nergy.sac.in  (example file without leading C-comment -- only reads in
12 lines)

C  2006.360.12.33.46.8495.II.BRVK.00.BHZ.R.SAC  (or emty)             Used
 to have SACfile (1st 72 chars.)
C  RESP.II.BRVK.00.BHZ                          (or empty)            Used
 to have Response file (1st 72 chars.)
C  /usr/local/geophysics/lib
    Location of JB and geometric spreading tables (1st 72 chars.) CAREFUL
WITH LOCATION
C  21.83  120.39                     Coordinates of event (lat,lon)
C  22.5                              Depth of earthquake source [km]
C  155. 032. 274.                    Focal mechanism (phi, delta, lambda) m
ust be positive
C  3.32e26                           MOment (in dyne-cm)
C  3000.                             Density of Upper Mantle [kg/m^3]

C  7000.                             P wave Velocity [m/s]

C  15.6                              q factor (Boatwright & Choy use 15.6)

C  70. .5                            Max and Min Period to passed though fi
lter [s]
C  -1. 70.                           Time relative to P-arrival to start, a
nd duration of measure [s]

C---------------------------------------------------------
C      RUNNING THE PROGRAM
C ---------------------------------------------------------
C When running program needs input in screen of:
C      - name of sac file
C      - name of .pz file
C      - tdur time up to which energy is calculated
C      - tinc time increment between energy calculations
C -------------------------------------------------------
C  output files: summary file and .tinc file
C -------------------------------------------------------
C  Program will create 2 output files:
C
C  for the above example, it will be named 'BRV.00.II.155.032.274' which i
s the 3-char truncated name of
C  the station, its relative gain, the network, phi, delta, and lambda.  T
he naming was meant to test
C  different mechanisms on the solution. Most all information within outpu
t file is self explanatory.
C  The last lin is a summary of information that can be used with other st
ation outputs for an average
C  energy calculation using either the focal mechanism corrected (aka 'tru
e energy') or the estimated
C  energy using distance averaged corrections (aka 'estimated energy').
C
```

```
C  ".tinc" file: file with information of energy in time increasing window
s, first column will the the time relative
C   to the p-wave arrival, and the two following columns will be
C   estimated energy and corrected energy

C  to run you can write:
C  printf "filein\nrespfilepz\nttotal\ntstep\n" | nergy_wprep.cwb

c ***********************************************************************
************
C +++++++++++++++++++++++++   MAIN PROGRAM  ++++++++++++++++++++++++++++
++++++++++++
c ***********************************************************************
************
      implicit complex (z)
c      parameter (max=131072)
      parameter (max=65536)
c      parameter (max=32768)
      dimension x(max),xin(max)
      dimension y3(132000)
      complex z(132768)
      dimension zero (50),zpole (50)
      character*72 filein,responsefile,tdir,respfilepz
      character*72 jfbup,d2tdd2p,d2tdd2pcp
      character*5 csta
      character*2 loc
      character*1 ntwk1,ntwk2
      character*5 ntwk
      character*25 tempname
      character*25 outfile
      character*25 tincsumfile ! summary file for cumulatice energy clacul
ations
      character*20 origintime  ! origin time as read from nergy control fi
le
      character*10 eventid     ! event ID (variable length, that is why it
 can be long)
      integer ifaif,idelta,ialamda,ilen,itdur
      integer nstart,ndur,nend,WFnend,i,k ! k is dummy for indexing in cle
aning array.
      integer*4 nerr
      real gain,tp,tstart,starttime,version
      integer tstep,tdur,ttotal
      real bpts,btime,epts,etime
      real tduroriginal,tstartoriginal,ergenergy_rate,ergenergyz_rate ! en
ergy rate for Estimated and true energy: E/tdur
      real ergenergyHF,ergenergyzHF
C      common z,x(max),xin(max),y3(132000),z(132768),zero (50)
C     * ,zpole(50)
C     * ,filein,responsefile,tdir,respfilepz,jfbup,d2tdd2p,d2tdd2pcp,csta
C     * ,csta,loc,ntwk1,ntwk2,ntwk,tempname,outfile,tincsumfile
C     * ,ifaif,idelta,ialamda,ilen,itdur
C     * ,nstart,ndur,nend,WFnend,i,k,nerr
C     * ,gain,tp,tstart,tdur,starttime,ttotal, tstep
C     * ,bpts,btime,epts,etime,slat,slon,reth,rethkm,pi
C
      version=1.5
      slat=-1000.
      slon=-1000.
      reth=6371.e3
      rethkm=6371.
      pi=4.*atan(1.)


c *********************************************************************
```



```
c  use location in nergy.sac.in
c  these need to reflect the absolulte location of these tables
c      d2tdd2p='/usr/local/geophysics/lib/d2tdd2.p'
c      d2tdd2pcp='/usr/local/geophysics/lib/d2tdd2.pcp'
C      jfbup='/usr/local/geophysics/lib/jfbup.dat'

c -- qbc is the parameter q in Boatwright and Choy [1986]
      aob=sqrt(3.)
c      qbc=aob**5.
c      qbc=15.6

c -- Regression parameters for distance correction
      a0=1.171
      a1=-7.271e-3
      a2=6.009e-5

c --  Crustal paramters (density of upper mantle and Vp)
c      rho=3.0e3
c      vel=7.0e3
c --  Band-Pass range (max and min periods)
C      tmax = 1000.
C      tmin = 0.5
c --  time window to taper from  (note we cannot process less data than
c       is tapered)
      btime=5  ! length of taper in seconds on front
      etime=10.  ! and on back
C **********************************************************************
c    READING SAC RESP and tdur FROM SCREEN INSTEAD OF NERGY FILE
C **********************************************************************
      read(5,2) filein,respfilepz  ! read from screen
      read(5,*) ttotal, tstep ! read tdur from screen: for increasing wind
ows
c      read(5,*) elat,elon,edepth ! lat,long,depth input from EIDS trigger
c *********************************************************************
c -- OPEN AND READ IN THE INPUT CONTROL FILE
c *********************************************************************
      open(unit=4,file='nergy.sac.in',status='old',err=2344 )
c  changed to skip the first two lines from the control file by JCONVERS
      read(4,2,err=9998)  ! used to read sacfilename from controlfile
      read(4,2,err=9998)  ! used to read respfilename from controlfile
c -- Sac file  reading originally
c      read(4,2,err=9998) filein
c -- Response file name read originally
c      read(4,2,err=9998) responsefile
c -- tables location
      read(4,2,err=9998) tdir
2     format(a)
c -- Event latitude longitude and depth red from control file
      read(4,*,err=9998)  elat,elon
      read(4,*,err=9998)  edepth
c -- Event Focal Mechanism in degrees (strike, dip, rake)
      read(4,*,err=9998) faif,delta,alamda
c -- Event Moment (dyne-cm)
      read(4,*,err=9998) amom
c -- Crustal parameters (density of upper mantle, Vp, Q-factor)
      read(4,*,err=9998) rho
      read(4,*,err=9998) vel
      read(4,*,err=9998) qbc
c -- Band-Pass range (max and min periods)
      read(4,*,err=9998) tmax,tmin
c -- Change: now it is doing both BB (0.5 - 70s) amd HF (0.5 -2s)
      tmaxBB=70
      tminBB=0.5
      tmaxHF=2
```

```
      tminHF=0.5
c -- start time and duration... relative to p-arrival
      read(4,*,err=9998) tstart ! ,tdur varies now!
c -- Read Origin time and event ID
      read(4,2,err=9998) origintime ! origin time
      read(4,2,err=9998) eventid    ! event ID can be our event ID or IRIS
 ID
c       write(6,*)origintime,eventID
c *********************************************************************
c -- FINISHED OPEN AND READ IN THE INPUT FILE
c *********************************************************************
       ilen = INDEX(tdir,' ') -1
      write(d2tdd2p,2)tdir(1:ilen)//'/d2tdd2.p'
      write(d2tdd2pcp,2)tdir(1:ilen)//'/d2tdd2.pcp'
      write(jfbup,2)tdir(1:ilen)//'/jfbup.dat'
c *********************************************************************
c -- OPEN THE SEISMIC DATAFILE AND GET RESPONSE FROM POLE-ZEROS FILE
c *********************************************************************
c   Read in sac datafile to memory
      call rsac1(filein,xin,nx,beg,dt,max,nerr)
c   Get station name
      call getkhv('kstnm',csta,nerr)
      call getkhv('knetwk',ntwk,nerr)
        read(ntwk,2001) ntwk1,ntwk2
2001   format (a1,a1)
       if (ntwk2.eq." ") ntwk2="_"
c         print *, "ntwk, ntwk1,2 =", ntwk,",", ntwk1,",",ntwk2

c     read in the record zero time
       call getnhv('nzyear',izyear,nerr)
       call getnhv('nzjday',izjday,nerr)
       call getnhv('nzhour',izhour,nerr)
       call getnhv('nzmin',izmin ,nerr)
       call getnhv('nzsec',izsec ,nerr)
       call getnhv('nzmsec',izmsec,nerr)
c     read in relative P-time
c     will set to 60 seconds if an a-marker does not exist or have bad tim
ing
      tp=0.
      call getfhv('a',tp,nerr)
      if (tp.eq.-12345.) then
            tp=60.
            write(6,*)  "WARNING: P-pick does not exist."
            write(6,*)  "   Setting P-time to 60s after start of file."
      endif
C     Reading response from .pz IRIS response file
      call irispzersp(respfilepz,izyear,izjday,npole,nzero,zpole,
     *            zero,amp0,ivacc,loc)

c     Subroutine to read in Instrument resonse from RESP file (using
c       only data for the correct time) THIS IS FROM OLD nergy.sac program
.
C      call rresp2(responsefile,izyear,izjday,npole,nzero,zpole,zero,
C     *    amp0,ivacc)

c     get location information from response file: new irispzersp does thi
s already
c      call rresploc(responsefile,loc)

      call getfhv('stla',slat,nerr)
      call getfhv('stlo',slon,nerr)


c *********************************************************************
```



```
c -- FINISHED READING IN DATA
c *********************************************************************

c Find distance, take-off and back- azimuths,and length of great circle
c     azes=take-off azimuth, azse=back-azimuth, ggc=greatcircle length
      call mygrt(elat,elon,slat,slon,disd,azes,azse,ggc)
      fai=faif-azes

c -- Express Boatwright & Choy (10) p.2097
c    'Equivilent' radiation pattern coefficient
c     first lines are read in.. second line are determined within
c     the subroutine
      call bc10(disd,edepth,fai,delta,alamda,rho,vel,
     * p,g,rpz,fp,fpp,fsp,PP,SP,jfbup,d2tdd2p,d2tdd2pcp)

      FgP2=fp**2+(fpp*PP)**2+(2./(3.*aob))*qbc*((SP*fsp)**2)

c -- Compute estimated value of above for given distance
        estgp2=disd*disd*a2+disd*a1+a0
      pskm=p*pi*rethkm/180.


c --------- If response is in m/s or m/ss, corrected by adding zero(es)
      if(ivacc.gt.0) then
              do j=1,ivacc
              nzero=nzero+1
              zero(nzero)=cmplx(0.,0.)
              enddo
      end if

C       if(ivacc.eq.0) go to 22901
C         nzero=nzero+1
C         zero(nzero)=cmplx(0.,0.)
C       if(ivacc.eq.1) go to 22901
C       nzero=nzero+1
C       zero(nzero)=cmplx(0.,0.)
C22901 continue
c *********************************************************************
***
c  Begin writting tincsummfile - the time increment cumulative energy file

c *********************************************************************
***
      write(tincsumfile,2004)csta,loc,ntwk1,ntwk2
2004  format(a3,'.',a2,'.',a1,a1,'.tinc')

      open(unit=8,file=tincsumfile)
c      write(8,*)'# ptime = ',tp
C *********************************************************************
**
C ************ PRE-P ENERGY CALCULATION ************************
C ** Resetting tstart and tdur for pre_p energy calculation. 'beg' is
      tduroriginal=tdur      ! Just saving the original parameters for
      tstartoriginal=tstart  ! later use in the tinc calculation
C the initial time
      if(tp.ge.70.) then
              tstart=-65
              tdur=60
      else
              tstart=beg-tp+5
              tdur=tp-beg-10
      endif
      !write(6,*)'tstart=',tstart,' tdur=',tdur
C *********************************************************************
```

```
c      Uses only data for tdur from tstart relative to tp

c -- Broadband range of periods:
      tmax=tmaxBB
      tmin=tminBB

      j=1
      nstart=0
      ndur=0
      nend=0
      nstart=int((tp+tstart)/dt)
      ndur=int(tdur/dt)
      nend=nstart+ndur
      WFnend=0
      do j=1,ndur
         x(j)=xin(nstart+j)
      enddo
       nx=j
C     find next smaller n^2 for FFT
       nfft=0
       jfft=0
      call myfnd(nx,nfft,jfft)
C     Detrend data (remove mean...not really detrend)
      call mydtr(x,nx)
C     apply a simple cosine filter to smooth data for fft
      bpts=btime/dt
      epts=etime/dt
      if (bpts.gt.tdur/dt/2) bpts=tdur/dt/2
      if (epts.gt.tdur/dt/2) epts=tdur/dt/2
      call mytpr2(x,nx,bpts,epts)  ! uses a fixed number of points rather
than a fraction
C     convert to f-domain
      afft=nfft
      df=1./(afft*dt)

      fmax=1./tmin
      fmin=1./tmax
      nfmin=fmin/df+0.5
      if(nfmin.lt.2) nfmin=2
      nfmax=fmax/df+1.5
      nff=nfmax+1-nfmin
      lcent=nfft/2+1
C     clean z:
      do j=1,132768
        z(j)=cmplx(0.,0.)
      enddo
C   add a complex component to data
      do j=1,nx
        z(j)=cmplx((x(j)*dt),0.)
      enddo

      call coolb(jfft,z,-1.0)
      do 71 j=1,lcent
        if(j.ge.nfmin.and.j.le.nfmax) go to 81
        z(j)=cmplx(0.,0.)
        go to 71
81       f = df * float(j-1)
        omega=2.*pi*f
        gain=amp0
        call instrument(f,zero,zpole,nzero,npole,gain,zres)
        zres=zres/cmplx(0.,omega)
c --   z(j) is velocity spectrum
        z(j)=z(j)/zres
        y3(j)=alog10(cabs(z(j)))
```



```
71      continue
c --- Get ready for Integration
      sinu=0.
      energy=0. ! test for clearing the value of variable energy
      dom=2.*pi*df
c ---- Integrate
      do j=nfmin,lcent
        f=df*float(j-1)
        omega=2.*pi*f
c ---   Computing Tstar from Boatwright and Choy
        tstar=1.
        if(j.eq.1)tstar=1.
        tstar=tst(f)
C ----   Sum over the integral
        sinu=sinu+(cabs(z(j))**2)*dom*exp(omega*tstar)
      enddo
      energy=sinu*rho*vel/pi
c      write(*,*)'BB pre-P energy1 ',energy
      epsilongp=energy ! this is the value of the integral
c -- energy is now the value of the integral (17) p. 2100 of Boatwright an
d Choy.

c -- At this point, we take care of the geometrical spreading. I believe
c       one should also correct for the surface response (rpz)
      geomsp=g*rpz
      energy=energy*((reth/geomsp)**2.)
c********************Important Change.
c-- this average value is given on p. 2096 of BC and corresp. to <FP>**2
c-- comes from eqn. (9) of B &C taking into account that Rp=reth/g

      avfpsq=(4./15.)

c-- this is the energy corrected for the True Focal Mechanism
c---This next section is to correct for energies that tend to blow up
      FgP2_old=1.
      if(FgP2.lt.0.2)then
        Fgp2_old=FgP2
        FgP2=0.2
      endif
      energyz=energy*4.*pi*(avfpsq/FgP2)

c-This is the energy Corrected for the Estimated Value
      energy=energy*4. *pi *(avfpsq/estgp2)

c-- Add in the S wave factor and convert to dyne-cm instead of Joules
      ergenergy=1.0e7*energy*(1.+qbc)
      ergenergyz=1.0e7*energyz*(1.+qbc)
c      estrain=ergenergy/amom
c      tstrain=ergenergyz/amom

c-This is epsilon star, the value of energy WITHOUT any focal correction
c- the focal correction would have to be multiplied by: <FP>**2/FgP2
      epsilonstar=1.0e7*(1.+qbc)*4*((reth/geomsp)**2.)*rho*vel*sinu

      itdur=tdur ! to write it as integer in the output file
      ergenergy_rate=ergenergy/tdur
      ergenergyz_rate=ergenergyz/tdur

CCCCCCCC PRE-P HIGH FREQUENCY CALCULATION CCCCCCC
C reset the tmin and tmax:
      tmax=tmaxHF
      tmin=tminHF

c      Uses only data for tdur from tstart relative to tp
```

```
      j=1
      nstart=0
      ndur=0
      nend=0
      nstart=int((tp+tstart)/dt)
      ndur=int(tdur/dt)
      nend=nstart+ndur
      WFnend=0
      do j=1,ndur
         x(j)=xin(nstart+j)
      enddo
       nx=j
C     find next smaller n^2 for FFT
       nfft=0
       jfft=0
      call myfnd(nx,nfft,jfft)
C     Detrend data (remove mean...not really detrend)
      call mydtr(x,nx)
C     apply a simple cosine filter to smooth data for fft
      bpts=btime/dt
      epts=etime/dt
      if (bpts.gt.tdur/dt/2) bpts=tdur/dt/2
      if (epts.gt.tdur/dt/2) epts=tdur/dt/2
      call mytpr2(x,nx,bpts,epts)  ! uses a fixed number of points rather
than a fraction
C     convert to f-domain
      afft=nfft
      df=1./(afft*dt)

      fmax=1./tmin
      fmin=1./tmax
      nfmin=fmin/df+0.5
      if(nfmin.lt.2) nfmin=2
      nfmax=fmax/df+1.5
      nff=nfmax+1-nfmin
      lcent=nfft/2+1
C     clean z:
      do j=1,132768
        z(j)=cmplx(0.,0.)
      enddo
C   add a complex component to data
      do j=1,nx
        z(j)=cmplx((x(j)*dt),0.)
      enddo

      call coolb(jfft,z,-1.0)
      do 710 j=1,lcent
        if(j.ge.nfmin.and.j.le.nfmax) go to 810
        z(j)=cmplx(0.,0.)
        go to 710
810       f = df * float(j-1)
        omega=2.*pi*f
        gain=amp0
        call instrument(f,zero,zpole,nzero,npole,gain,zres)
        zres=zres/cmplx(0.,omega)
c --    z(j) is velocity spectrum
        z(j)=z(j)/zres
        y3(j)=alog10(cabs(z(j)))
710      continue
c --- Get ready for Integration
      sinu=0.
      energy=0. ! test for clearing the value of variable energy
      dom=2.*pi*df
c ---- Integrate
```



```
      do j=nfmin,lcent
        f=df*float(j-1)
        omega=2.*pi*f
c ---   Computing Tstar from Boatwright and Choy
        tstar=1.
        if(j.eq.1)tstar=1.
        tstar=tst(f)
C ----    Sum over the integral
        sinu=sinu+(cabs(z(j))**2)*dom*exp(omega*tstar)
      enddo
      energy=sinu*rho*vel/pi
c      write(*,*)'BB pre-P HF energy1 ',energy
      !epsilongp=energy ! this is the value of the integral
c -- energy is now the value of the integral (17) p. 2100 of Boatwright an
d Choy.

c -- At this point, we take care of the geometrical spreading. I believe
c       one should also correct for the surface response (rpz)
      geomsp=g*rpz
      energy=energy*((reth/geomsp)**2.)
c*********************Important Change.
c-- this average value is given on p. 2096 of BC and corresp. to <FP>**2
c-- comes from eqn. (9) of B &C taking into account that Rp=reth/g

      avfpsq=(4./15.)

c-- this is the energy corrected for the True Focal Mechanism
c---This next section is to correct for energies that tend to blow up
      FgP2_old=1.
      if(FgP2.lt.0.2)then
        Fgp2_old=FgP2
        FgP2=0.2
      endif
      energyzHF=energy*4.*pi*(avfpsq/FgP2)

c-This is the energy Corrected for the Estimated Value
      energyHF=energy*4. *pi *(avfpsq/estgp2)

c-- Add in the S wave factor and convert to dyne-cm instead of Joules
      ergenergyHF=1.0e7*energyHF*(1.+qbc)
      ergenergyzHF=1.0e7*energyzHF*(1.+qbc)

c-This is epsilon star, the value of energy WITHOUT any focal correction
c- the focal correction would have to be multiplied by: <FP>**2/FgP2
      epsilonstarHF=1.0e7*(1.+qbc)*4*((reth/geomsp)**2.)*rho*vel*sinu

      itdur=tdur ! to write it as integer in the output file
      ! HF energy pre-P rate:
      ergenergy_rateHF=ergenergyHF/tdur
      ergenergyz_rateHF=ergenergyzHF/tdur


C-- Write Header for the output .tinc file:
      write(8,2011)ntwk1,ntwk2,csta,loc
2011  format(' # Station NTWK,STAT,LOC:  ',a1,a1,3X,a4,5X,a2)
      write(8,2012)slat,slon
2012  format(' # Station lat,long: ',2(1X,f8.2))
      write(8,2013)elat,elon,edepth
2013  format(' # Epicenter lat,long,depth: ',3(1X,f8.2))
      write(8,2017)faif,delta,alamda
      write(8,117) disd,azes,azse
117   format(' # Distance,azimuth,back-azimuths(deg):', 3f9.3)
2017  format(' # Focal mechanism (Phi, Delta, Lambda): ',3f6.0)
      write(8,2024)origintime,eventID
```

```
2024  format(' # Origin Time:,'a,/,
     * ' # EventID: ',a)
      write(8,2014) ((reth/geomsp)**2.)  ! Distance dependent Geometrical
spreading coefficient
2014  format(' # R^2: ',e9.2)
      write(8,2015)avfpsq   ! <FP>**2 = 4/15
2015  format(' # (F_p)^2 (4/15):',f8.5)
      write(8,2016)FgP2 ! for the true focal mechanism
2016  format(' # FOCAL MECHANISM (FgP)^2: ',e9.2)
      write(8,2023)estgp2
2023  format(' # Estimated (FgP)^2:',e9.2)
      write(8,*)'# (1+q): ',(1.+qbc)
      write(8,*)"# Energy = (E*) X (F_p)^2/<Fgp>^2"
C      write(8,*)'# pre-P Estar(estimated)/t Estar(FM)/t',
C2017  format(' # ',2(1X,e9.2))
C      write(8,*)'# NTWK   STAT    LOC      tdur    Eest/t   Etrue/t'
C      write(8,2010)ntwk1,ntwk2,csta,loc,itdur,ergenergy_rate
C     *           ,ergenergyz_rate
2010  format(' #  ',a1,a1,3X,a4,5X,a2,6X,i4,2(1X,e9.2))
C      write(8,2019)ergenergy_rate,ergenergyz_rate
C2019  format(' # Broad-Band Pre-P E rate[J/s] Eest/t,Etrue/t',
C     * 2(1X,e9.2))
C      write(8,2020)ergenergy_rateHF,ergenergyz_rateHF
C2020  format(' # High-Freq Pre-P E rate[J/s] Eest/t,Etrue/t',
C     * 2(1X,e9.2))
      write(8,2022)epsilonstar/tdur,epsilonstarHF/tdur
2022  format(' # Pre-P E* rate [J/s] BB,HF: ',2(1X,e9.2))

C ****** END PRE-P ENERGY CALCULATION ***************************
C ************************************************************************
**

C ** Resetting tstart and tdur to original values for time incrementing en
ergy calculation
      tdur=tduroriginal      ! going back to the original values
      tstart=tstartoriginal  !
      !write(6,*)tstart
      write(8,*)'#----------------------------------------------------'
C      write(8,*)'# tdur   slat    slon       EVlat  EVlon   Sugg_Erg',
C     *  '  True_Erg'
C      write(8,*)'# tdur Sugg_ErgBB  True_ErgBB  Sugg_ErgHF   True_ErgHF'
      write(8,*)'# tdur[s]  E(bb)*[J]    E(hf)*[J]  '


c ************************************************************************
*
c ****  "DO" loop to calculate energy in  time increasing windows  *******
*
c ************************************************************************
*
      do tdur =tstep,ttotal,tstep
c     Uses only data for tdur from tstart relative to tp
c --- BROADBAND RANGE
      tmax=tmaxBB
      tmin=tminBB
c      write(*,*)tmax,tmin
      j=1
      nstart=0
      ndur=0
      nend=0
      nstart=int((tp+tstart)/dt)
      ndur=int(tdur/dt)
      nend=nstart+ndur
      WFnend=0
```



```
      do j=1,ndur
         x(j)=xin(nstart+j)
      enddo
       nx=j
C     find next smaller n^2 for FFT
       nfft=0
       jfft=0
      call myfnd(nx,nfft,jfft)
C     Detrend data (remove mean...not really detrend)
      call mydtr(x,nx)
C     apply a simple cosine filter to smooth data for fft
      bpts=btime/dt
      epts=etime/dt
      if (bpts.gt.tdur/dt/2) bpts=tdur/dt/2
      if (epts.gt.tdur/dt/2) epts=tdur/dt/2
      call mytpr2(x,nx,bpts,epts)  ! uses a fixed number of points rather
than a fraction
C     convert to f-domain
      afft=nfft
      df=1./(afft*dt)

      fmax=1./tmin
      fmin=1./tmax
      nfmin=fmin/df+0.5
      if(nfmin.lt.2) nfmin=2
      nfmax=fmax/df+1.5
      nff=nfmax+1-nfmin
      lcent=nfft/2+1
c      write(*,*)fmin,fmax
C     clean z:
      do j=1,132768
        z(j)=cmplx(0.,0.)
      enddo
C   add a complex component to data
      do j=1,nx
        z(j)=cmplx((x(j)*dt),0.)
      enddo

      call coolb(jfft,z,-1.0)
      do 7 j=1,lcent
        if(j.ge.nfmin.and.j.le.nfmax) go to 8
        z(j)=cmplx(0.,0.)
        go to 7
8       f = df * float(j-1)
        omega=2.*pi*f
        gain=amp0
        call instrument(f,zero,zpole,nzero,npole,gain,zres)
        zres=zres/cmplx(0.,omega)
c --   z(j) is velocity spectrum
        z(j)=z(j)/zres
        y3(j)=alog10(cabs(z(j)))
7      continue
c --- Get ready for Integration
      sinu=0.
      energy=0. ! test for clearing the value of variable energy
      dom=2.*pi*df
c ---- Integrate
      do j=nfmin,lcent
        f=df*float(j-1)
        omega=2.*pi*f
c ---   Computing Tstar from Boatwright and Choy
        tstar=1.
        if(j.eq.1)tstar=1.
        tstar=tst(f)
```

```
C ----   Sum over the integral
        sinu=sinu+(cabs(z(j))**2)*dom*exp(omega*tstar)
      enddo
      energy=sinu*rho*vel/pi
c -- energy is now the value of the integral (17) p. 2100 of Boatwright an
d Choy.

c -- At this point, we take care of the geometrical spreading. I believe
c       one should also correct for the surface response (rpz)
      geomsp=g*rpz
      energy=energy*((reth/geomsp)**2.)
c*********************Important Change.
c-- this average value is given on p. 2096 of BC and corresp. to <FP>**2
c-- comes from eqn. (9) of B &C taking into account that Rp=reth/g

      avfpsq=(4./15.)

c-- this is the energy corrected for the True Focal Mechanism
c---This next section is to correct for energies that tend to blow up
      FgP2_old=1.
      if(FgP2.lt.0.2)then
        Fgp2_old=FgP2
        FgP2=0.2
      endif
      energyz=energy*4.*pi*(avfpsq/FgP2)

c-This is the energy Corrected for the Estimated Value
      energy=energy*4. *pi *(avfpsq/estgp2)

c-- Add in the S wave factor and convert to dyne-cm instead of Joules
      ergenergy=1.0e7*energy*(1.+qbc)
      ergenergyz=1.0e7*energyz*(1.+qbc)
c      estrain=ergenergy/amom
c      tstrain=ergenergyz/amom

c-This is epsilon star, the value of energy WITHOUT any focal correction
c- the focal correction would have to be multiplied by: <FP>**2/FgP2
      epsilonstar=1.0e7*(1.+qbc)*4*((reth/geomsp)**2.)*rho*vel*sinu

      itdur=tdur ! to write it as integer in the output file

C      write(*,*)tdur,ergenergy,ergenergyz ! test jconvers
C       write(8,*)tdur,slat,slon,elat,elon,ergenergy,ergenergyz

c      write(8,2008)itdur,slat,slon,elat,elon,ergenergy,ergenergyz
c2008  format(3X,i3,4(1X,f8.2),2(1X,e9.2))

CCCCCCC HIGH FREQUENCY LOOP 0.5 - 2s
C reset the tmin and tmax:
      tmax=tmaxHF
      tmin=tminHF
c      write(*,*)tmax,tmin
C now re-do the loop with these new periods, the idea is to replace all
C this for a fuunction, but since I am having NEW probolems I decided to
C do this for now. this is just a copy opf the previous part...
c     Uses only data for tdur from tstart relative to tp

      j=1
      nstart=0
      ndur=0
      nend=0
      nstart=int((tp+tstart)/dt)
      ndur=int(tdur/dt)
      nend=nstart+ndur
```



```
      WFnend=0
      do j=1,ndur
         x(j)=xin(nstart+j)
      enddo
       nx=j
C     find next smaller n^2 for FFT

       nfft=0
       jfft=0
      call myfnd(nx,nfft,jfft)
C     Detrend data (remove mean...not really detrend)

      call mydtr(x,nx)
C     apply a simple cosine filter to smooth data for fft

      bpts=btime/dt
       am epts=etime/dt
      if (bpts.gt.tdur/dt/2) bpts=tdur/dt/2
      if (epts.gt.tdur/dt/2) epts=tdur/dt/2
      call mytpr2(x,nx,bpts,epts)  ! uses a fixed number of points rather
than a fraction
C     convert to f-domain
      afft=nfft
      df=1./(afft*dt)

      fmax=1./tmin
      fmin=1./tmax
      nfmin=fmin/df+0.5
      if(nfmin.lt.2) nfmin=2
      nfmax=fmax/df+1.5
      nff=nfmax+1-nfmin
      lcent=nfft/2+1
c      write(*,*)fmin,fmax
C     clean z:
      do j=1,132768
        z(j)=cmplx(0.,0.)
      enddo
C   add a complex component to data
      do j=1,nx
        z(j)=cmplx((x(j)*dt),0.)
      enddo

      call coolb(jfft,z,-1.0)
      do 711 j=1,lcent
        if(j.ge.nfmin.and.j.le.nfmax) go to 811
        z(j)=cmplx(0.,0.)
        go to 711
811     f = df * float(j-1)
        omega=2.*pi*f
        gain=amp0
        call instrument(f,zero,zpole,nzero,npole,gain,zres)
        zres=zres/cmplx(0.,omega)
c --   z(j) is velocity spectrum
        z(j)=z(j)/zres
        y3(j)=alog10(cabs(z(j)))
711    continue
c --- Get ready for Integration
      sinu=0.
      energy=0. ! test for clearing the value of variable energy
      energyHF=0. ! added, the HF range
      dom=2.*pi*df
c ---- Integrate
      do j=nfmin,lcent
        f=df*float(j-1)
```

```
      omega=2.*pi*f
c ---   Computing Tstar from Boatwright and Choy
        tstar=1.
        if(j.eq.1)tstar=1.
        tstar=tst(f)
C ----   Sum over the integral
        sinu=sinu+(cabs(z(j))**2)*dom*exp(omega*tstar)
      enddo
      energyHF=sinu*rho*vel/pi
c -- energy is now the value of the integral (17) p. 2100 of Boatwright an
d Choy.

c -- At this point, we take care of the geometrical spreading. I believe
c       one should also correct for the surface response (rpz)
      geomsp=g*rpz
      energyHF=energyHF*((reth/geomsp)**2.)
c*********************Important Change.
c-- this average value is given on p. 2096 of BC and corresp. to <FP>**2
c-- comes from eqn. (9) of B &C taking into account that Rp=reth/g

      avfpsq=(4./15.)

c-- this is the energy corrected for the True Focal Mechanism
c---This next section is to correct for energies that tend to blow up
      FgP2_old=1.
      if(FgP2.lt.0.2)then
        Fgp2_old=FgP2
        FgP2=0.2
      endif
      energyzHF=energyHF*4.*pi*(avfpsq/FgP2)

c-This is the energy Corrected for the Estimated Value
      energyHF=energyHF*4. *pi *(avfpsq/estgp2)

c-- Add in the S wave factor and convert to dyne-cm instead of Joules
      ergenergyHF=1.0e7*energyHF*(1.+qbc)
      ergenergyzHF=1.0e7*energyzHF*(1.+qbc)

c-This is epsilon star, the value of energy WITHOUT any focal correction
c- the focal correction would have to be multiplied by: <FP>**2/FgP2
      epsilonstarHF=1.0e7*(1.+qbc)*4*((reth/geomsp)**2.)*rho*vel*sinu

      itdur=tdur ! to write it as integer in the output file

C      write(8,2018)itdur,ergenergy,ergenergyz,ergenergyHF,ergenergyzHF
C2018  format(3X,i3,4(3X,e9.2))
      write(8,2021)itdur,epsilonstar,epsilonstarHF
2021  format(3X,i3,1X,2(4X,e9.2))

      enddo ! end of loop over tinc
c *******************************************************************
c      big energy "DO" loop ends
c ******************************************************************

c ----- Closing files used for reading
        close(1)       ! response file
        close(2)
        close(4)       ! close nergy.sac.in (input file)
        close(21)
        close(78)
        close(8)       ! close tincsumfile

CCc *********************************************************************
CCc --  START OUTPUT TO OLD SUMMARY FILE
```



```
CCc *********************************************************************
CCc  Create an output file name that is taken from the station name,
CCc  network,strike, dip and rake
CCc  get network from responsefile name
CCc  create integer versions of strike dip and rake for tempfile
CC         ifaif = faif
CC         idelta =delta
CC         ialamda =alamda
CC      write(outfile,2002)csta,loc,ntwk1,ntwk2,ifaif,idelta,ialamda
CC2002    format(a3,'.',a2,'.',a,a,'.',i3.3,'.',i3.3,'.',i3.3)
CC
CCc        itdur = tdur ! included by jconvers to write tdur inside filen
ame also
CCC Modified naming of output file to include tdur at the end of filename

CCc      write(outfile,2002)csta,loc,ntwk1,ntwk2,ifaif,idelta,ialamda,itdu
r
CCc2002    format(a3,'.',a2,'.',a,a,'.',i3.3,'.',i3.3,'.',i3.3,'.',i3.3)
CC
CC
CC      open(unit=7,file=outfile)
CCc ****************************************************************
CCc ****************************************************************
CCc     start time of processing in seconds from the beginning of day
CC      starttime=real(izsec)+real(izmsec)/1000+tp+tstart+real(izmin)*60
CC     * + real(izhour)*3600
CC
CC      write(7,31099) csta,izyear,izjday,starttime
CC31099  format(a4,' ',i4,' ',i3,' ',f9.3,
CC     * ' :Processing start time (Year,Jday,sec_of_day)')
CC      write(7,31100) float(nx)*dt
CC31100    format('Time duration of window processed: ',f8.2,' seconds')
CC
CC      write(7,31102) elat,elon,amom,faif,delta,alamda
CC31102   format('Epicentral coordinates: ',2f8.2,/,
CC     * 'Published seismic moment: ',e15.4,' dyn-cm',/,
CC     * 'Focal mechanism (Phi, Delta, Lambda): ',3f6.0)
CC
CC      write(7,31103)
CC31103  format('INSTRUMENT INFORMATION RETRIEVED-----')
CC      if(ivacc.eq.1) then
CCc              write(6,31104)
CC             write(7,31104)
CC             write(7,10182) ivacc,nzero
CC31104 format('This response for VELOCITY in m/s')
CC10182 format('IVACC = ',i2,' One zero [0., 0.] added,',
CC     * '  now ',i2,' zeroes')
CC      else if(ivacc.eq.2) then
CCc              write(6,31106)
CC             write(7,31106)
CC             write(7,10182) ivacc,nzero
CC             write(7,10183) ivacc,nzero
CC31106 format('This response for ACCELERATION in m/s**2')
CC10183 format('IVACC = ',i2,' Second zero [0., 0.] added,',
CC     * '  now ',i2,' zeroes')
CC      endif
CC
CC      write(7,31105) amp0,nzero,npole
CC      write(7, *) (zero(j),j=1,nzero)
CC      write(7, *) (zpole(j),j=1,npole)
CC31105  format('AMP 0 = ', e16.6,/,i5,' Zeros; ',i5,' Poles')
CC
CC        write(7,22907) csta,slat,slon
CC22907 format('Coordinates for ',a3,' obtained from data file:',2f10.3)
```

```
CC
CC      write(7,117) disd,azes,azse
CC117   format('Distance, takeoff & back-azimuths(deg):', 3f9.3)
CC
CC      write(7,22915) rpz,g
CC22915 format('Receiver function : ',f8.3,
CC     * /,' Geometrical spreading : ',f8.3)
CC
CC      write(7,118) p,pskm
CC118   format('Ray Parameter p = ',f7.2,' s/deg = ',f10.2,' s/km')
CC      write(7,1109) fp,fpp,fsp
CC1109  format('F-P = ',f7.3,' ;  F-pP = ',f7.3,' ; F-sP = ',f7.3)
CC      write(7,22900) PP,SP
CC22900 format('Reflection coefficients : PP = ',f7.3,
CC     * ' ;  SP (corrected) = ',f7.3)
CC      write(7,*) '(FgP)**2 = ',FgP2
CC      write(7,*) 'Estimated (FgP)**2 = ',estgp2
CC
CCC   after switching to f-domain
CC      write(7,10) jfft
CC10    format('FFT (order ',i5,') carried out')
CC      write(7,17) tmax,tmin
CC17    format('Band-pass filtering between ',f10.2,' and',
CC     * f10.2, ' seconds')
CC
CC
CC      do 21700 j=1,11
CC        write(7,21701) j,f,zres,z(j),cabs(z(j))
CC21700 continue
CC21701  format(i5,6e16.6)
CC
CC
CC      write(7,*)'dom =',dom
CC      write(7,*) 'Energy out of integral',sinu
CC      write(7,*) 'Preliminary energy in P waves use',
CC     * ' TRUE mechanism = ',energyz,' Joules'
CC      write(7,*)'Preliminary ESTIMATED energy in P waves = ',
CC     * energy, ' Joules'
CC
CC
CC      if (FgP2_old.lt.0.2)then
CC        write(7,*)"FgP2 Corrected; Orig. = ",FgP2_old
CC      else
CC        Write(7,*)"FgP2 good; = ",FgP2
CC      endif
CCc      write(7,*) 'Suggested total energy = ',ergenergy,' dyne-cm'
CCc      write(7,*) 'Suggested strain  (E/Mo)  = ',estrain
CCc      write(7,*) 'True Mech. total energy = ',ergenergyz,' dyne-cm'
CCc      write(7,*) 'True Mech. strain (E/Mo) = ',tstrain
CC
CC      write(7,21704)
CC21704 format("# ST NTWK  dist  tkoff  b_az  secOday  Sugg_ERG ",
CC     * " True_ERG    Moment TF datafile") ! original
CCc     * " True_ERG    Moment TF  Tdur   datafile")  ! modified, includes
 tdur
CC      write(7,21705)
CC21705 format("#------------------------------------------------",
CC     * "------------------------------------------------------------")
CC
CCC ORIGINAL WRITTING OF LAST LINE OF OUTPUTFILE
CC      write(7,21702)csta,ntwk1,ntwk2,disd,azes,azse,
CC     *   starttime,ergenergy,ergenergyz,amom,WFnend,filein
CC21702 format(" ",a4," ",2a1," ",f5.1," ",f6.1," ",f6.1," ",
CC     * f9.2," ",e9.2," ",e9.2," ",e9.2,"  ",i1," ",a60)
```



```
CC
CC      close(7)
CCc *** END WRITTING TO OLD SUMMARY FILE ***
c ------------------------------------------------------------------
      write(6,*)'Energy calculated for:',filein,'using ',respfilepz
      goto 2350
9998  write(6,*)"ERROR:  with 'nergy.sac.in'. Be certain to use"
      write(6,*)"Version",version," of control file... Exiting"
      goto 2350
2344  write(6,*)"ERROR: File 'nergy.sac.in' does not exist... Exiting"
      goto 2350
2345  write(6,*)"ERROR: File '",filein,"' does not exist... Exiting"
2350  stop
      end
c #####################################################################

c ######################  END OF MAIN PROGRAM  ########################
C #####################################################################

C+++++++++++++++++++++++++++++++++++++++++++++++++++++++++++++++++++++++
C++++++++  S U B R O U T I N E S   A N D   F U N C T I O N S  ++++++++
C+++++++++++++++++++++++++++++++++++++++++++++++++++++++++++++++++++++++

      SUBROUTINE instrument(f,zero,zpole,nzero,npole,gain,zres)

      implicit complex (z)
      dimension zero(50), zpole(50)
      pi=4.*atan(1.0)
      w=2 *pi * f
      zw=cmplx(0.,w)
      znum =cmplx(1,1)
      zdenom = cmplx(1,1)

      do 10 j=1,nzero
        znum=znum*(zw-zero(j))
10    continue
      j=0
      do 20 j=1,npole
        zdenom=zdenom*(zw-zpole(j))
20    continue

      zres = gain *znum / zdenom
      return
      end
c-------------------------------------------------------------------
      SUBROUTINE georpz(del,depth,psd,alphar,betar,rhor,
     *  ilayer,iray,g,rpz,d2tdd2p,d2tdd2pcp)
c      computes geometric spreading and receiver functions
c      g=geometric spreading factor (see Kanamori and Stewart, 1976)
c      rpz=receiver function (see Helmberger, 1974)
c      (mult by alpha for displacement)
c      alphar,betar,rhor = parameters at the receiver
c      p = ray parameter
c      del = delta

      double precision etaa,etab
      dimension der2(15,113),deps(15)
      character*72 d2tdd2p,d2tdd2pcp
      pi=4.*atan(1.0)
      rade=6371.
      reth=rade
      xonst=pi/180.
      p=psd*180./pi
      p=p/reth
```

```
      rh=2.9
      alph=6.5
      bet=alph/sqrt(3.)
      ilayer=n
10      continue
      reth=6371.
      error=reth/(reth-depth)
      angih=asin(p*alph)
      degih=180*angih/pi
C      write(7,90600) degih
C90600 format('Entering Geometrical Spreading routine; i h = ',
C     * f7.2,' degrees')
c      d(ih)/d(delta) from pre-tabulated values
      if(iray.eq.1) open(unit=78,file=d2tdd2p
     * ,status='old',err=2343)
      if(iray.eq.2) open(unit=78,file=d2tdd2pcp
     *    ,status='old',err=2344)
      rewind 78
      read(78,12001) (deps(kdep),kdep=1,15)
12001  format(/,5x,15f5.1)
      do 12002 kdep=1,15
      read(78,*) (der2(kdep,j),j=1,113)
12002 continue
      close (78)
c -- compute depth index for interpolation
      do 12003 kdep=1,14
      if(depth.gt.deps(kdep).and.depth.le.deps(kdep+1)) go to 12004
12003 continue
      write(6,12005) depth
12005 format('ERROR inserting depth ',e15.5,
     *   ' into d2T/dDELTA2 array...ABORTING')
      stop
12004 bdep=depth-deps(kdep)
      adep=deps(kdep+1)-depth
      cdep=adep+bdep
      adep=adep/cdep
      bdep=bdep/cdep
c -- compute distance index for interpolation
      idel=del
      jdel=idel+11
      adel=float(idel+1)-del
      bdel=del-float(idel)
      if(jdel.ge.21) go to 12008
      idel=2.*del
      jdel=idel+1
      adel=float(idel+1)-2.*del
      bdel=2.*del-float(idel)
12008 d2tda=der2(kdep,jdel)*adel+der2(kdep,jdel+1)*bdel
      d2tdb=der2(kdep+1,jdel)*adel+der2(kdep+1,jdel+1)*bdel
      d2tdd2=d2tda*adep+d2tdb*bdep
C      write(7,12006) depth,del,d2tdd2
C12006 format('d2t/d[DELTA]2 at depth ', f5.1,
C     *  '; Distance ',f7.2,' = ',e15.5)
      d2tdd2=d2tdd2*(180./pi)*(180./pi)
      cosih=cos(angih)
      dihdel=(d2tdd2/cosih)*alph/(reth-depth)
C      write(7,12007) dihdel
C12007 format('New dihdel = ',e15.5)
      dihdel=abs(dihdel)
c      calculate geometrical spreading factor
c      angi0=asin(p*alphar)
      angi0=asin(p*alphar/error)
      factor=p*rh*alph*alph/(rhor*alphar)
      g=(factor*dihdel/(sin(del*xonst)*cos(angi0)))**0.5
```



```
c      compute receiver function
      p2=p*p/(error*error)
      betar2=betar*betar
      etaa=(1./(alphar*alphar)-p2)**.5
      etab=(1./betar2-p2)**.5
      denom=betar2*(etab*etab-p2)**2. + 4.*p2*betar2*etaa*etab
      rpz=2.*etaa*(etab*etab-p2)/denom
      rpz=alphar*rpz

      close(1)
      close(2)
      return
      goto 2345
2343   write(6,*)d2tdd2p//" does not exist. Exiting!"
      goto 9999
2344   write(6,*)d2tdd2pcp//" does not exist. Exiting!"
9999  stop

2345  continue
      end
c --------------------------------------------------
      SUBROUTINE bc10(disd,edepth,fai,delta,alamda,rho,vel,
     *   p,g,rpz,fp,fpp,fsp,PP,SP,jfbup,d2tdd2p,d2tdd2pcp)
c      first lines are read in.. second line are determined within
c       the subroutine
c      Boatwright & Choy (10) p.2097
c     'Equivilent' radiation pattern coefficient

      dimension dist(113),depth(15),t(113,15)
      character*72 jfbup
      character*72 d2tdd2p,d2tdd2pcp
      reth=6371.
      pi=4.*atan(1.)
      open(unit=4,file=jfbup, status='old', err=2344)
      read(4,1)ajunk,(depth(k),k=1,15)
1      format(16f5.1)
      do 2 j=1,113
      read(4,1) dist(j),(t(j,k),k=1,15)
2      continue
      call mysert(edepth,depth,15,adep,bdep,ndep,itest)
      call mysert(disd,dist,113,adis,bdis,ndis,itest)
      dtda=(t(ndis,ndep)-t(ndis+1,ndep))/(dist(ndis)-dist(ndis+1))
      dtdb=(t(ndis,ndep+1)-t(ndis+1,ndep+1))/(dist(ndis)-dist(ndis+1))
      dtddel=dtda*adep+dtdb*bdep
      p=dtddel
      alphar=vel/1000.
      rhor=rho/1000.
      betar=alphar/sqrt(3.)
      iray=1
      call georpz(disd,edepth,p,alphar,betar,rhor,ilayer,iray,g,rpz,
     * d2tdd2p,d2tdd2pcp)
c -- compute radiation coefficients
      aih=asin(p*alphar*180./(pi*reth))
      ajh=asin(sin(aih)/sqrt(3.))
C       write(7,*) 'Take-off angles : ',aih/pi*180,ajh/pi*180
      si=sin(aih)
      ci=cos(aih)
      sj=sin(ajh)
      cj=cos(ajh)
      s2i=2.*si*ci
      c2i=2.*ci*ci-1.
      sd=sin(delta*pi/180.)
      cd=cos(delta*pi/180.)
      sl=sin(alamda*pi/180.)
```

```
      cl=cos(alamda*pi/180.)
      sf=sin(fai*pi/180.)
      cf=cos(fai*pi/180.)
      s2f=2.*sf*cf
      c2f=2.*cf*cf-1.
      c2d=2.*cd*cd-1.
      sr=sd*cd*sl
      pr=cl*sd*s2f-sr*c2f
      qr=sl*c2d*sf+cl*cd*cf

C     write(7,10112) pr,qr,sr
C 10112 format('pR, qR, sR = ',3f8.3)

      pl=sr*s2f+cl*sd*c2f
      ql=-cl*cd*sf+sl*c2d*cf
      fp=sr*(3.*ci*ci-1.)-qr*s2i-pr*si*si
      fpp=sr*(3.*ci*ci-1.)+qr*s2i-pr*si*si
      s2j=sin(2.*pi-2.*ajh)
      c2j=cos(2.*pi-2.*ajh)
      fsp=1.5*sr*s2j+qr*c2j+0.5*pr*s2j
c -- compute reflection coefficients
c     pbeta is the product p*beta used in Aki and Richards p. 140
c --
      pbeta=p*betar*180./(pi*reth)
c      a=4.*pbeta*(betar/alphar)*ci*cj
       a=4.*pbeta*pbeta*(betar/alphar)*ci*cj
      b=(1.-2.*pbeta*pbeta)**2.
      c=4.*(betar/alphar)*pbeta*cj*(1.-2.*pbeta*pbeta)
      PP=(a-b)/(a+b)
      SP=c/(a+b)
      SP=SP*ci/cj


      close(4)
      return
      goto 2345
2344   write(6,*)jfbup//" does not exist. Exiting!"
      stop
2345  continue
      end
C*****************************************************************
      FUNCTION tst(x)
c      Choy and Cormier 86 Part 1
      if (x.lt.0.1)then
         y2=0.9 - .1*alog10(x)
      elseif(x.ge.0.1.and.x.lt.1.)then
         y2=.5 -.5*alog10(x)
      else
         y2=.5 -.10*alog10(x)
      endif
      tst=y2
      return
      end
c-----------------------------------------------------------------------
---
      SUBROUTINE mygrt(ALAT1,ALON1,ALAT2,ALON2,DISD,AZ12,AZ21,GC)
c Great circle program. Given epicenter and station, finds distance,
c take-off and back- azimuths, and length of great circle
      PI = 4.*atan(1.0)
      ATH=6378.388
      BTH=6356.912
      RAD = PI/180.
      H = 1. - BTH*BTH/(ATH*ATH)
      P = H/(1. - H)
```



```
      GR = ALON1*RAD
      TR = ALAT1*RAD
      SINTR = SIN(TR)
      COSTR = COS(TR)
      IF (SINTR .EQ. 0.) SINTR = .000001
      IF (COSTR .EQ. 0.) COSTR = .000001
      R1 = ATH/SQRT(1. - H*SINTR*SINTR)
      Z1 = R1*(1. - H)*SINTR
      G = ALON2*RAD
      T = ALAT2*RAD
      IF (T .EQ. 0.) T = .00001
      SINT = SIN(T)
      COST = COS(T)
      R2 = ATH/SQRT(1. - H*SINT*SINT)
      DG = G - GR
      COSDG = COS(DG)
      SINDG = SIN(DG)
      DGR = GR - G
      DT = T - TR
      Q = SINT*COSTR/((1. + P)*COST*SINTR) + H*R1*COSTR/(R2*COST)
      X = R2*COST*COSDG
      Y = R2*COST*SINDG
      Z = R2*(1. - H)*SINT
      AZ12 = ATAN2(SINDG,(Q - COSDG)*SINTR)
      Q = SINTR*COST/(COSTR*SINT*(1. + P)) + H*R2*COST/(R1*COSTR)
      AZ21 = ATAN2(SIN(DGR),SINT*(Q - COS(DGR)))
      COS12 = COS(AZ12)
      CTA2 = COSTR*COSTR*COS12*COS12
      P0 = P*(CTA2 + SINTR*SINTR)
      B0 = (R1/(1. + P0))*SQRT(1. + P*CTA2)
      E0 = P0/(1. + P0)
      GC = 2.*PI*B0*SQRT(1. + P0)*(1. - E0*(.25 + E0*(3./64.
     *                                       + 5.*E0/256.)))
      C0 = 1. + P0*(.25 - P0*(3./64 - 5.*P0/256.))
      C2 = P0*(-.125 + P0*(1./32. - 15.*P0/1024.))
      C4 = (-1./256. + 3.*P0/1024.)*P0*P0
      U0 = ATAN2(SINTR,COSTR*COS12*SQRT(1. + P0))
      U = ATAN2(R1*SINTR + (1. + P0)*(Z - Z1),(X*COS12 - Y*SINTR*
     *                                      SIN(AZ12))*SQRT(1. + P0))
      DISD = U - U0
      IF (U .LT. U0) DISD = PI + PI + DISD
      DIST = B0*(C0*( DISD ) + C2*(SIN(U + U) - SIN(U0 + U0))
     *                       + C4*(SIN(4.*U) - SIN(4.*U0)))
      DISD = DISD/RAD
      AZ12 = AZ12/RAD
      AZ21 = AZ21/RAD
      IF (AZ12 .LT. 0.) AZ12 = 360. + AZ12
      IF (AZ21 .LT. 0.) AZ21 = 360. + AZ21
      if(disd.gt.355.) disd=360.-disd
      RETURN
      END
c-----------------------------------------------------------------------
---
      SUBROUTINE myfnd(JA,JB,JC)
c Given number JA, Finds JC such that  2**JC is next smallest power of 2
c  (JC is order of FFT to process JA points). Also returns JB=2**JC.
      DIMENSION POWER(25)
      POWER(1)=1.
      DO 1 L=2,25
      POWER(L)=2.*POWER(L-1)
    1 CONTINUE
      X=JA
      CALL MYSERT(X,POWER,25,AX,BX,JC,IA)
      JB=POWER(JC+1)+0.5
```

```
      RETURN
      END
c-------------------------------------------------------------------------
---
      SUBROUTINE mydtr(A,N)
c  Detrend array by suppressing average value
      DIMENSION A(1)
      S=0.
      DO 1 J=1,N
      S=S+A(J)
   1  CONTINUE
      AN=N
      S=S/AN
      DO 2 J=1,N
   2  A(J)=A(J)-S
      RETURN
      END
      SUBROUTINE mytpr(A,N,B,E)
c  Cosine taper of array A of N points, by B at beginning and E at end
c   B and E are fractions of the entire length
      DIMENSION A(1)
      PI=3.14159265378
      AN=N
      M1=AN*B+0.5
      M2=M1+1
      IF(M1)10,10,11
  11  ANG=PI/FLOAT(M1)
      DO 12 I=1,M1
      XI=I
      CS=(1.-COS(XI*ANG))/2.
  12  A(I)=A(I)*CS
  10  M3=AN*E+0.5
      M5=N-M3
      M4=M5+1
      IF(M3)13,13,14
  14  ANG=PI/FLOAT(M3)
      DO 15 I=M4,N
      XI=I-N-1
      CS=(1.-COS(XI*ANG))/2.
  15  A(I)=A(I)*CS
  13  RETURN
      END
c-------------------------------------------------------------------------
---
      SUBROUTINE mytpr2(A,N,B,E)
c  Cosine taper of array A of N points, by B at beginning and E at end
c   B and E are number of points being tapered
      DIMENSION A(1)
      PI=3.14159265378
      AN=N

C front end
      M1=B
      M2=M1+1
      IF(M1)10,10,11
  11  ANG=PI/FLOAT(M1)

      DO 12 I=1,M1
      XI=I
      CS=(1.-COS(XI*ANG))/2.
  12  A(I)=A(I)*CS

  10  M3=E
      M5=N-M3
```



```
      M4=M5+1
      IF(M3)13,13,14
  14  ANG=PI/FLOAT(M3)

      DO 15 I=M4,N
      XI=I-N-1
      CS=(1.-COS(XI*ANG))/2.

  15  A(I)=A(I)*CS
  13  RETURN
      END
c-------------------------------------------------------------------------
---
      SUBROUTINE coolb(NN,DATAI,SIGNI)
c a simple FFT program
C version from emile okal, however very similar
C to version in 1989 draft of Seth Stein's introduction
C to seismology.

      DIMENSION DATAI(1)
      N=2**(NN+1)
      J=1
      DO 5 I=1,N,2
      IF(I-J)1,2,2
   1  TEMPR=DATAI(J)
      TEMPI=DATAI(J+1)
      DATAI(J)=DATAI(I)
      DATAI(J+1)=DATAI(I+1)
      DATAI(I)=TEMPR
      DATAI(I+1)=TEMPI
   2  M=N/2
   3  IF(J-M)5,5,4
   4  J=J-M
      M=M/2
      IF(M-2)5,3,3
   5  J=J+M
      MMAX=2
   6  IF(MMAX-N)7,10,10
   7  ISTEP=2*MMAX
      THETA=SIGNI*6.28318531/FLOAT(MMAX)
      SINTH=SIN(THETA/2.)
      WSTPR=-2.*SINTH*SINTH
      WSTPI=SIN(THETA)
      WR=1.
      WI=0.
      DO 9 M=1,MMAX,2
      DO 8 I=M,N,ISTEP
      J=I+MMAX
      TEMPR=WR*DATAI(J)-WI*DATAI(J+1)
      TEMPI=WR*DATAI(J+1)+WI*DATAI(J)
      DATAI(J)=DATAI(I)-TEMPR
      DATAI(J+1)=DATAI(I+1)-TEMPI
      DATAI(I)=DATAI(I)+TEMPR
   8  DATAI(I+1)=DATAI(I+1)+TEMPI
      TEMPR=WR
      WR=WR*WSTPR-WI*WSTPI+WR
   9  WI=WI*WSTPR+TEMPR*WSTPI+WI
      MMAX=ISTEP
      GO TO 6
  10   RETURN
      END
c-------------------------------------------------------------------------
---
      SUBROUTINE mysert(X,A,N,AX,BX,NX,ITEST)
```

```
c Inserts x into array A(N); returns index NX, and barycentral coeffs. AX,
 BX.
c ITEST =1 if screw-up.  A can be increasing or decreasing.
c Returns AX=x-a(j+1); BX=a(j)-x, so that  interp. goes X=A(nx)*AX+A(NX+1)
*BX
      DIMENSION A(1)
      if(a(N).lt.a(1)) go to 100
c  Case of an increasing array
      IF(X.LT.A(1)) GO TO 3
      IF(X.GT.A(N)) GO TO 4
      DO 1 J=1,N
      IF(X.GT.A(J).AND.X.LE.A(J+1)) GO TO 2
   1  CONTINUE
   2  NX=J
      ITEST=0
      BX=A(J)-X
      AX=X-A(J+1)
      CX=AX+BX
      AX=AX/CX
      BX=BX/CX
      RETURN
   3  NX=-1
      GO TO 5
   4  NX=N
        go to 5
c case of a decreasing array A
100     IF(X.GT.A(1)) GO TO 103
      IF(X.LT.A(N)) GO TO 104
      DO 101 J=1,N
      IF(X.LT.A(J).AND.X.GE.A(J+1)) GO TO 102
 101  CONTINUE
 102  NX=J
      ITEST=0
      BX=A(J)-X
      AX=X-A(J+1)
      CX=AX+BX
      AX=AX/CX
      BX=BX/CX
      RETURN
 103  NX=-1
      GO TO 5
 104  NX=N
   5  ITEST=1
      AX=0
      BX=0
      RETURN
      END
c-----------------------------------------------------------
      subroutine irispzersp(filein,iyr,idoy,np,nz,poles,zeros,amp,units
     *                    ,loc)
c     Subroutine to read response paramenters from downloaded response fro
m FetchBulkdata
c     This is to accomodate to the IRIS format of the pole-zero response f
ile
c     by Jaime Convers Nov 2012
      complex zeros,poles
      dimension zeros(50), poles(50)
      integer iyr,imm,idd,syr,smm,sdd,eyr,emm,edd,np,nz,nxz,nxp,idoy
      real amp,a0,sd,const,convfact
      real rz,iz,rp,ip
      integer units,locflag
      character*2 ch_units,loc
      character*72 filein
      character*8 head1
```



```
      character*7 head2
      character*31 head3
      character trash
      np=0
      nz=0
      nxp=0
      nxz=0
      rz=0
      iz=0
      rp=0
      ip=0
      a0=0
      sd=0
      jpz=0
      locflag=0
      const=0
C Open Response file downloaded from CWBquery
      open(unit=1,file=filein,status='old',err=2345)

      do j=1, 5000
        read (1,51,end=2350)head1,head2,head3
C Reads station location code
              if(head1.eq.'* LOC'.and.head2.eq.'ATION '
     *  .and.locflag.eq.0) then
                      backspace 1
                      read(1,57) loc
                      if(loc.eq.' '.or.loc.eq.'??') loc='__'
                      locflag=1
              endif

              ! UNITS in the IRIS pz file are now after SENSITIVITY
              if(head1.eq.'* INP'.and.head2.eq.'UT UNIT') then ! Reads conv
ersion factor UNITS are now after SENSITIVITY
                      backspace 1
                      read(1,57)ch_units
                      if(ch_units.eq.'NM') then
                              units=0 ! means don't add zeros
                              convfact=1E09
                      elseif(ch_units.eq.'UM') then
                              units=0 ! means don't add zeros
                              convfact=1E06
                      elseif(ch_units.eq.'M ') then
                              convfact=1
                              units=0 ! means don't add zeros
                      else convfact=1 ! this in case I can't read the conv
ersion factor
                              !units=1 ! I don't see this case happening (
always NM or UM or M)

                      endif
              endif
C Sensitivity
              if(head1.eq.'* SEN'.and.head2.eq.'SITIVIT'.and.sd.eq.0)
     * then
                      backspace 1
                      read(1,58) sd
              endif

C  Reads A0 normalization, this number is different from RESP files
              if(head1.eq.'* A0 '.and.a0.eq.0) then
                      backspace 1
                      read(1,58) a0
              endif
C read CONSTANT HERE, this replaces Sd x A0 that is found in RESP files
```

```
             if(head1.eq.'CONST'.and.const.eq.0) then
                     backspace 1
                     read(1,*)trash,const
                     !write(6,*) const
             endif
C Number of Zeros
             if(head1.eq.'ZEROS  '.and.nz.eq.0) then
                     backspace 1
                     read(1,*)trash,nz
                     !write(6,*) nz
                     do i=1,nz
                       read(1,*) rz,iz
                       !write(6,*)rz,iz
                       zeros(i)=cmplx(rz,iz)
                       !write(6,*)zeros(i)
                     enddo
             endif
C Reads number of poles and poles
             if(head1.eq.'POLES  '.and.np.eq.0) then
                     backspace 1
                     read(1,*)trash,np
                     do i=1,np
                       read(1,*) rp,ip
                       !write(6,*)rp,ip
                       poles(i)=cmplx(rp,ip)
                       !write(6,*) poles(i)
                     enddo
             endif

c      endif

      enddo
51    format(a5,a7,a31)
52    format(15x,i4,1x,i2,1x,i2) ! fomat for reading dates
c53    format(15x,a2) ! format for reading chanel units
c54    format(15x,E9.6)  ! format to read a0
55    format(8x,i2)   ! for reading npoles and nzeros
c56    format(22x,E10.6) ! for CONSTANT
C to READ in the IRIS formatting of the file.
57    format(22x,a2) ! format for reading chanel units (NM,UM,M) Also LOC
58    format(22x,E12.6) ! format for reading A0 and Sensitivity value

59    format(16x,E12.6)       ! for reading value of CONSTANT
      goto 2350
2345  write(6,*)"Response file '",filein,"' does not exist... Exiting"
      stop

2350  close(1)
      amp=const*convfact
      !write(6,*) "Loc ",loc," a0:",a0," sd:",sd," amp:",amp ! test jconve
rs
      !write(6,*) "const:",const,"convfact",convfact
      !write(6,*) "npoles",np," nzeros",nz
      !write(6,*) "poles= ",poles
      !write(6,*) "zeros= ",zeros
      RETURN
      END

c-----------------------------------------------------------
      subroutine cwbresp(filein,iyr,idoy,np,nz,poles,zeros,amp,units
     *                    ,loc)
c     Subroutine to read response paramenters from downloaded response
c     files from CWBquery
c     by Jaime Convers Dec 2008
```



```
      complex zeros,poles
      dimension zeros(50), poles(50)
      integer iyr,imm,idd,syr,smm,sdd,eyr,emm,edd,np,nz,nxz,nxp,idoy
      real amp,a0,sd,const,convfact
      real rz,iz,rp,ip
      integer units,locflag
      character*2 ch_units,loc
      character*72 filein
      character*8 head1
      character*7 head2
      character*31 head3
      np=0
      nz=0
      nxp=0
      nxz=0
      rz=0
      iz=0
      rp=0
      ip=0
      a0=0
      sd=0
      jpz=0
      locflag=0
      const=0
C Open Response file downloaded from CWBquery
      open(unit=1,file=filein,status='old',err=2345)

      do j=1, 5000
        read (1,51,end=2350)head1,head2,head3
c Checks if event is later than EFFECTIVE starting date date of response
c        if(head1.eq.'* EFFECT'.and.head2.eq.'IVE    ') then
c                backspace 1
c                read(1,52)syr,smm,sdd
c                if (iyr.gt.syr) then
c                        isgood=1
c                elseif(iyr.eq.syr.and.imm.gt.smm) then
c                        isgood=1
c                elseif(iyr.eq.syr.and.imm.eq.smm.and.idd.ge.sdd) then
c                        isgood=1
c                else
c                        isgood=0
c                endif
c        endif
c         if(head1.eq.'* ENDDAT'.and.head2.eq.'E      '.and.isgood.eq.1)
c     * then
c                 backspace 1
c                 read(1,52)eyr,emm,edd
c                 if(iyr.lt.eyr) then
c                         iegood=1
c                 elseif(iyr.eq.eyr.and.imm.lt.emm) then
c                         iegood=1
c                 elseif(iyr.eq.eyr.and.imm.eq.emm.and.idd.le.edd) then
c                         iegood=1
c                 else
c                         iegood=0
c                 endif
c         endif
C only for dates inside time span of rsponse file:
c      if(isgood.eq.1.and.iegood.eq.1) then
C Reads station location code
                if(head1.eq.'* LOCATI'.and.head2.eq.'ON   '
     *  .and.locflag.eq.0) then
                        backspace 1
                        read(1,53) loc
```

```
                      if(loc.eq.' '.or.loc.eq.'??') loc='__'
                      locflag=1
              endif


              if(head1.eq.'* INPUT '.and.head2.eq.'UNIT  ') then ! Reads uni
ts
                      backspace 1
                      read(1,53)ch_units
                      if(ch_units.eq.'NM') then
                              units=0 ! means don't add zeros
                              convfact=1E09
                      elseif(ch_units.eq.'UM') then
                              units=0 ! means don't add zeros
                              convfact=1E06
                      else units=1 ! I don't see this case happening (alwa
ys NM or UM)
                      endif
              endif
C  Reads A0 normalization, this number is different from RESP files
              if(head1.eq.'* A0-CAL'.and.head2.eq.'C   ') then
                      backspace 1
                      read(1,54) a0
              endif
C sensitivity Calculated
              if(head1.eq.'* SENS-C'.and.head2.eq.'ALC  '.and.sd.eq.0)
     * then
                      backspace 1
                      read(1,54) sd
              endif
C read CONSTANT HERE, this replaces Sd x A0 in the RESP files
              if(head1.eq.'CONSTANT'.and.const.eq.0) then
                      backspace 1
                      read(1,56) const
              endif
C Number of Zeros
              if(head1.eq.'ZEROS  '.and.nz.eq.0) then
                      backspace 1
                      read(1,55) nz
                      do i=1,nz
                        read(1,*) rz,iz
                        zeros(i)=cmplx(rz,iz)
                      enddo
              endif
C Reads number of poles and poles
              if(head1.eq.'POLES  '.and.np.eq.0) then
                      backspace 1
                      read(1,55) np
                      do i=1,np
                        read(1,*) rp,ip
                        poles(i)=cmplx(rp,ip)
c                        write(6,*) poles(i)
                      enddo
              endif
c      endif

      enddo
51    format(a8,a7,a31)
52    format(15x,i4,1x,i2,1x,i2) ! fomat for reading dates
53    format(15x,a2) ! format for reading chanel units
54    format(15x,E9.6)  ! format to read a0
55    format(8x,i2)   ! for reading npoles and nzeros
56    format(22x,E10.6) ! for CONSTANT
      goto 2350
```



```
2345  write(6,*)"Response file '",filein,"' does not exist... Exiting"
      stop

2350  close(1)
      amp=const*convfact
C      write(6,*) "Loc ",loc," a0:",a0," sd:",sd," amp:",amp ! test jconve
rs
C      write(6,*) "poles= ",poles
C      write(6,*) "zeros= ",zeros
      RETURN
      END
c-----------------------------------------------------------------
      subroutine rresp2(filein,iyr,idoy,np,nz,poles,zeros,amp,units)
c     Subroutine to read in EVALRESP format
c     written by AVN on Tue May  3 15:02:25 MDT 2005
c     written by AVN on Tue Sep  2 19:15:56 EDT 2008
      complex zeros,poles
      dimension zeros(99),poles(99)
      integer iyr,idoy,syr,sdoy,eyr,edoy,np,nz,nxz,nxp
      real    amp,a0,sd
      real    rz,iz,rp,ip
      integer units
      character*6 ch_units
      character*72 filein
      character*10 head
      character*31 head2,head3
      character*41 head4
      character*30 head5
      character*10 junk1

      np=0
      nz=0
      nxp=0
      nxz=0
      rz=0
      iz=0
      rp=0
      ip=0
      a0=0
      sd=0
      jpz=0
C  open RESP file
      open(unit=1,file=filein,status='old',err=2345)

      do 100 j=1,50000
      read(1,51,end=2350)head,head2,head3
       if(head.eq.'B052F22 ') then
              backspace 1
              read(1,52) syr,sdoy
c             get out if event is before this time
              if (iyr.gt.syr) then
                      isgood=1
              elseif (iyr.eq.syr.and.idoy.ge.sdoy) then
                      isgood=1
              else
                      isgood=0
              endif
       endif
       if(head.eq.'B052F23  '.and.isgood.eq.1) then
c             get out if event is after this time
              if(head3.eq.'No Ending Time') then
                  iegood=1
              else
                 backspace 1
```

```
                   read(1,52) eyr,edoy
c                  get out if event is after this time
                   if (iyr.lt.eyr) then
                          iegood=1
                   elseif(iyr.eq.eyr.and.idoy.le.edoy) then
                       iegood=1
                   else
                       iegood=0
                   endif
                endif
         endif
C       ONLY READ IF DATE IS WITHIN SPAN (as determined above)
        if (isgood.eq.1.and.iegood.eq.1) then
c               print *, "iyr,idoy=",iyr,idoy
c               print *, "  syr,sdoy=",syr,sdoy
c               print *, "  eyr,edoy=",eyr,edoy
c        determine units
         if(head.eq.'B053F05  ') then
            backspace 1
           read(1,15) ch_units
           if(ch_units.eq.'M/S  '.or.ch_units.eq.'M/S - ') then
                   units=1
           else if(ch_units.eq.'M/S**2'.or.ch_units.eq.'M/S/S')then
                   units=2
           else units=0
           endif
         endif
c        print *, "UNITS =",ch_units,units

c        A0 normalization (reads only first occurrence)
         if(head.eq.'B053F07 '.and.a0.eq.0) then
            backspace 1
            read(1,4) head1,head4,head5
            read(head5,*) a0
         endif
c        Sensitivity (reads only first occurrence)
         if(head.eq.'B058F04 '.and.head2.eq.' Sensitivity: '.and.
     *       sd.eq.0) then
            backspace 1
            read(1,4) head1,head4,head5
            read(head5,*) sd
         endif
c        Number of zeroes
         if(head.eq.'B053F09 '.and.nz.eq.0) then
          backspace 1
          read(1,22) nz
          endif
c        Number of POLES
         if(head.eq.'B053F14 '.and.np.eq.0) then
          backspace 1
          read(1,22) np
          endif
c        B053F10-13=zeros, B053F10-18=poles
         if(head.eq.'B053F10-13'.or.head.eq.'B053F15-18'
     *     .and.jpz.le.(nz+np)) then
           jpz=jpz+1
           if(head.eq.'B053F10-13') then
              backspace 1
              read(1,*) junk1,nxz,rz,iz
           endif
           if(head.eq.'B053F15-18') then
              backspace 1
              read(1,*) junk1,nxp,rp,ip
           endif
```



```
              zeros(nxz+1)=cmplx(rz,iz)
              poles(nxp+1)=cmplx(rp,ip)
            endif


          endif
c ----
100       continue
c --------------- End read loop

51         format(a10,a15,a15)
52         format(25x,i4,1x,i3)

4         format(a10,a41,a30)
15        format(51x,a6)
20        format(51x,f10.2)
21        format(51x,e13.6)
22        format(51x,i2)

          goto 2350
2345      write(6,*)"Response file '",filein,"' does not exist... Exiting"
          stop

2350      close(1)
          amp=a0*sd
          return
          end

c-----------------------------------------------------
          subroutine rresploc(filein,loc)
c         Subroutine to read loc EVALRESP format response file
c         written by AVN on Fri May 20 17:14:54 MDT 2005
          character*2 loc
          character*100 line
          character*72 filein
          character*10 head
          character*31 head2,head3

          open(unit=99,status='SCRATCH')
          open(unit=98,status='SCRATCH')
          open(unit=1,file=filein,status='old',err=2345)


          do 100 j=1,1000
            read(1,1,end=2350) line
            write(99,1) line
            rewind 99
            read(99,4)head,head2,head3
            write(98,*) head3

            rewind 99
            rewind 98
c         get loc
            if(head.eq.'B052F03 ') read(99,22) loc
100       rewind 99
c --------------- End read loop

1         format(a100)
4         format(a10,a31,a31)
22        format(25x,a2)

          goto 2350

2345      write(6,*)"Response file '",filein,"' does not exist... Exiting"
```

```
      stop

2350  close(1)
      if(loc.eq.'??') loc='__'

      return
      end
```

REFERENCES

Abercrombie, R. E., M. Antolik, K. Felzer, and G. Ekstrom (2001), The 1994 Java tsunami earthquake: Slip over a subducting seamount, *J. Geophys. Res.-Solid Earth*, *106*(B4), 6595-6607.

Aki, K. (1966), Generation and propagation of G waves from the Niigata earthquake of June 14, 1964. 2. Estimation of earthquake moment, released energy and stress-strain drop from G wave spectrum". , *Bulletin of the Earthquake Research Institute, Tokyo University*, *44*, 73-88.

Aki, K., and P. G. Richards (1980), *Quantitative Seismology: Theories and Methods*, W.H. Freeman and Company, San Francisco.

Allmann, B. P., and P. M. Shearer (2009), Global variations of stress drop for moderate to large earthquakes, *J. Geophys. Res.-Solid Earth*, *114*, 22.

Ammon, C. J., H. Kanamori, T. Lay, and A. A. Velasco (2006), The 17 July 2006 Java tsunami earthquake, *Geophys. Res. Lett.*, *33*(24).

Ammon, C. J., et al. (2005), Rupture Process of the 2004 Sumatra-Andaman Earthquake, *Science*, *308*(5725), 1133-1139.

Beresnev, I. A. (2009), The reality of the scaling law of earthquake-source spectra?, *J. Seismol.*, *13*(4), 433-436.

Bilek, S. L. (2007), Using earthquake source durations along the Sumatra-Andaman subduction system to examine fault-zone variations, *Bull. Seismol. Soc. Amer.*, *97*(1), S62-S70.

Bilek, S. L., and T. Lay (1999), Rigidity variations with depth along interplate megathrust faults in subduction zones, *Nature*, *400*(6743), 443-446.

Boatwright, J., and J. B. Fletcher (1984), The Partition of Radiated Energy Between P-wave and S-wave, *Bull. Seismol. Soc. Amer.*, *74*(2), 361-376.

Boatwright, J., and G. L. Choy (1986), Telsesismic estimates of the energy radiated by shallow earthquakes, *Journal of Geophysical Research-Solid Earth and Planets*, *91*(B2), 2095-2112.

Briggs, R. W., et al. (2006), Deformation and slip along the Sunda Megathrust in the great 2005 Nias-Simeulue earthquake, *Science*, *311*(5769), 1897-1901.

Caldeira, B., M. Bezzeghoud, and J. F. Borges (2010), DIRDOP: a directivity approach to determining the seismic rupture velocity vector, *J. Seismol.*, *14*(3), 565-600.

Chen, T., A. V. Newman, L. J. Feng, and H. M. Fritz (2009), Slip distribution from the 1 April 2007 Solomon Islands earthquake: A unique image of near-trench rupture, *Geophys. Res. Lett.*, *36*.

Choy, G. L., and J. L. Boatwright (1995), Global patterns of radiated seismic energy and apparent stress, *J. Geophys. Res.-Solid Earth*, *100*(B9), 18205-18228.

Choy, G. L., and A. McGarr (2002), Strike-slip earthquakes in the oceanic lithosphere: observations of exceptionally high apparent stress, *Geophysical Journal International*, *150*(2), 506-523.

Choy, G. L., and S. H. Kirby (2004), Apparent stress, fault maturity and seismic hazard for normal-fault earthquakes at subduction zones, *Geophysical Journal International*, *159*(3), 991-1012.

Choy, G. L., and J. Boatwright (2007), The energy radiated by the 26 December 2004 Sumatra-Andaman earthquake estimated from 10-minute P-wave windows, *Bull. Seismol. Soc. Amer.*, *97*(1), S18-S24.

Choy, G. L., and J. Boatwright (2009), Differential Energy Radiation from Two Earthquakes in Japan with Identical M-w: The Kyushu 1996 and Tottori 2000 Earthquakes, *Bull. Seismol. Soc. Amer.*, *99*(3), 1815-1826.

Choy, G. L., A. McGarr, S. H. Kirby, and J. Boatwright (2006), An overview of the global variability in radiated energy and apparent stress, in *Earthquakes: Radiated Energy and the Physics of Faulting*, edited by R. Abercrombie, A. McGarr, G. DiToro and H. Kanamori, pp. 43-57, Amer Geophysical Union, Washington.

Convers, J. A., and A. V. Newman (2011), Global Evaluation of Large Earthquake Energy from 1997 Through mid-2010, *J. Geophys. Res.*, *116*.

DeMets, C. (2001), A new estimate for present-day Cocos-Caribbean plate motion: Implications for slip along the Central American volcanic arc, *Geophys. Res. Lett.*, *28*(21), 4043-4046.

Der, Z. A., T. W. McElfresh, and A. Odonnell (1982), An investigation of the regional variations and frequency-dependence of anelastic attenuation in the mantle under the united-states in the 0.5-4Hz band, *Geophysical Journal of the Royal Astronomical Society*, *69*(1), 67-99.

Douglas, A., J. A. Hudson, and R. G. Pearce (1988), Direcivity and the Doppler-effect, *Bull. Seismol. Soc. Amer.*, *78*(3), 1367-1372.

Duputel, Z., L. Rivera, H. Kanamori, and G. Hayes (2012), W phase source inversion for moderate to large earthquakes (1990-2010), *Geophysical Journal International*, *189*(2), 1125-1147.

Dziewonski, A. M., and J. H. Woodhouse (1983), An Experiment in systematic study of global seismicity - Centroid-Moment Tensor Solutions for 201 moderate and large earthquakes of 1981, *Journal of Geophysical Research*, *88*(NB4), 3247-3271.

Dziewonski, A. M., T. A. Chou, and J. H. Woodhouse (1981), Determination of earthquake source parameters from waveform data for studies of global and regional seismicity, *Journal of Geophysical Research*, *86*(NB4), 2825-2852.

Ebeling, C. W., and E. A. Okal (2012), An extension of the E/M0 tsunami earthquake discriminant T to regional distances, *Geophysical Journal International*, *190*(3), 1640-1656.

Eissler, H., L. Astiz, and H. Kanamori (1986), Tectonic setting and source parameters of the september 19, 1985 michoacan, mexico earthquake, *Geophys. Res. Lett.*, *13*(6), 569-572.

Ekstrom, G., A. M. Dziewonski, N. N. Maternovskaya, and M. Nettles (2005), Global seismicity of 2003: centroid-moment-tensor solutions for 1087 earthquakes, *Physics of the Earth and Planetary Interiors*, *148*(2-4), 327-351.

Fritz, H. M., et al. (2007), Extreme runup from the 17 July 2006 Java tsunami, *Geophys. Res. Lett.*, *34*(12).

Geist, E. L., and T. Parsons (2005), Triggering of tsunamigenic aftershocks from large strike-slip earthquakes: Analysis of the November 2000 New Ireland earthquake sequence, *Geochem. Geophys. Geosyst.*, *6*.

Hanks, T. C., and H. Kanamori (1979), A moment magnitude scale, *Journal of Geophysical Research*, *84*(NB5), 2348-2350.

Hara, T. (2007), Measurement of the duration of high-frequency energy radiation and its application to determination of the magnitudes of large shallow earthquakes, *Earth Planets and Space*, *59*(4), 227-231.

Hayes, G. P. (2011), Rapid source characterization of the 2011 M-w 9.0 off the Pacific coast of Tohoku Earthquake, *Earth Planets and Space*, *63*(7), 529-534.

Hayes, G. P., P. S. Earle, H. M. Benz, D. J. Wald, R. W. Briggs, and U. N. E. R. Team (2011), 88 Hours: The US Geological Survey National Earthquake Information Center Response to the 11 March 2011 M-W 9.0 Tohoku Earthquake, *Seismol. Res. Lett.*, *82*(4), 481-493.

Henstock, T. J., L. C. McNeill, and D. R. Tappin (2006), Seafloor morphology of the Sumatran subduction zone: Surface rupture during megathrust earthquakes?, *Geology*, *34*(6), 485-488.

Hill, E. M., et al. (2012), The 2010 M_W 7.8 Mentawai earthquake: Very shallow source of a rare tsunami earthquake determined from tsunami field survey and near-field GPS data, *J. Geophys. Res.-Solid Earth*, *117*.

Houston, H. (2001), Influence of depth, focal mechanism, and tectonic setting on the shape and duration of earthquake source time functions, *J. Geophys. Res.-Solid Earth*, *106*(B6), 11137-11150.

Husseini, M. I., and M. J. Randall (1976), Rupture velocity and radiation efficiency, *Bull. Seismol. Soc. Amer.*, *66*(4), 1173-1187.

Ide, S., and G. C. Beroza (2001), Does apparent stress vary with earthquake size?, *Geophys. Res. Lett.*, *28*(17), 3349-3352.

Ide, S., F. Imamura, Y. Yoshida, and K. Abe (1993), Source characteristics of the Nicaraguan tsunami earthquake of september 2, 1982, *Geophys. Res. Lett.*, *20*(9), 863-866.

Iglesias, A., S. K. Singh, J. F. Pacheco, L. Alcantara, M. Ortiz, and M. Ordaz (2003), Near-trench Mexican earthquakes have anomalously low peak accelerations, *Bull. Seismol. Soc. Amer.*, *93*(2), 953-959.

Imamura, F., N. Shuto, S. Ide, Y. Yoshida, and K. Abe (1993), Estimate of the tsunami source of the 1992 nicaraguan earthquake from tsunami data, *Geophys. Res. Lett.*, *20*(14), 1515-1518.

ISC (2009), International Seismological Center - Earthquake Hypocentral Bulletin., edited, Available at http://www.isc.ac.uk, Thatcham, U.K.

Ji, C., D. J. Wald, and D. V. Helmberger (2002), Source description of the 1999 Hector Mine, California, earthquake, part I: Wavelet domain inversion theory and resolution analysis, *Bull. Seismol. Soc. Amer.*, *92*(4), 1192-1207.

Kanamori, H. (1972), Mechanism of Tsunami Earthquakes, *Physics of the Earth and Planetary Interiors*, *6*, 346-359.

Kanamori, H., and L. Rivera (2006), Energy partitioning during an earthquake, in *Earthquakes: Radiated Energy and the Physics of Faulting*, edited by R. Abercrombie, A. McGarr, G. DiToro and H. Kanamori, pp. 3-13, Amer Geophysical Union, Washington.

Kanamori, H., L. Rivera, and W. H. K. Lee (2010), Historical seismograms for unravelling a mysterious earthquake: The 1907 Sumatra Earthquake, *Geophysical Journal International*, *183*(1), 358-374.

Lay, T., C. J. Ammon, H. Kanamori, Y. Yamazaki, K. F. Cheung, and A. R. Hutko (2011), The 25 October 2010 Mentawai tsunami earthquake (M_w 7.8) and the tsunami hazard presented by shallow megathrust ruptures, *Geophys. Res. Lett.*, *38*.

Lay, T., H. Kanamori, C. J. Ammon, K. D. Koper, A. R. Hutko, L. L. Ye, H. Yue, and T. M. Rushing (2012), Depth-varying rupture properties of subduction zone megathrust faults, *J. Geophys. Res.-Solid Earth*, *117*.

Lomax, A. (2005), Rapid estimation of rupture extent for large earthquakes: Application to the 2004, M9 Sumatra-Andaman mega-thrust, *Geophys. Res. Lett.*, *32*(10).

Lomax, A., A. Michelini, and A. Piatanesi (2007), An energy-duration procedure for rapid determination of earthquake magnitude and tsunamigenic potential, *Geophysical Journal International*, *170*(3), 1195-1209.

Natawidjaja, D. H., K. Sieh, M. Chlieh, J. Galetzka, B. W. Suwargadi, H. Cheng, R. L. Edwards, J. P. Avouac, and S. N. Ward (2006), Source parameters of the great Sumatran megathrust earthquakes of 1797 and 1833 inferred from coral microatolls, *J. Geophys. Res.-Solid Earth*, *111*(B6).

Newcomb, K. R., and W. R. McCann (1987), SEISMIC HISTORY AND SEISMOTECTONICS OF THE SUNDA ARC, *Journal of Geophysical Research-Solid Earth and Planets*, *92*(B1), 421-439.

Newman, A. V., and E. A. Okal (1998), Teleseismic estimates of radiated seismic energy: The E/M_0 discriminant for tsunami earthquakes, *Journal of Geophysical Research*, *103*(B11), 26885-26898.

Newman, A. V., G. Hayes, Y. Wei, and J. A. Convers (2011a), The 25 October 2010 Mentawai Tsunami Earthquake, from real-time discriminants, finite-fault rupture, and tsunami excitation, *Geophys. Res. Lett.*, *38*.

Newman, A. V., L. J. Feng, H. M. Fritz, Z. M. Lifton, N. Kalligeris, and Y. Wei (2011b), The energetic 2010 M_W 7.1 Solomon Islands tsunami earthquake, *Geophysical Journal International*, *186*(2), 775-781.

Ni, S., H. Kanamori, and D. Helmberger (2005), Seismology - Energy radiation from the Sumatra earthquake, *Nature*, *434*(7033), 582-582.

Okal, E. A. (1992), Use of the mantle magnitude m(m) for the reassessment of the moment of historical earthquakes .1. shallow events, *Pure and Applied Geophysics*, *139*(1), 17-57.

Okal, E. A., and A. V. Newman (2001), Tsunami earthquakes: the quest for a regional signal, *Physics of the Earth and Planetary Interiors*, *124*(1-2), 45-70.

Perez-Campos, X., and G. C. Beroza (2001), An apparent mechanism dependence of radiated seismic energy, *J. Geophys. Res.-Solid Earth*, *106*(B6), 11127-11136.

Polet, J., and H. Kanamori (2000), Shallow subduction zone earthquakes and their tsunamigenic potential, *Geophysical Journal International*, *142*(3), 684-702.

Press, W. H., S. A. Teukolsky, W. T. Vetterling, and B. P. Flannery (1992), *Numerical Recipes in FORTRAN*, 935 pp., Cambridge University Press, New York, NY, USA.

Protti, M., F. Gundel, and K. McNally (1994), The geometry of the Wadati-Benioff zone under southern Central-America and its tectonic significance: Results from a high-resolution local seismographic network, *Physics of the Earth and Planetary Interiors*, *84*(1-4), 271-287.

Richter, C. F. (1935), An instrumental earthquake magnitude scale, *Bull. Seismol. Soc. Amer.*, *25*(1), 1-32.

Sahal, A., B. Pelletier, J. Chatelier, F. Lavigne, and F. Schindele (2010), A catalog of tsunamis in New Caledonia from 28 March 1875 to 30 September 2009, *C. R. Geosci.*, *342*(6), 434-447.

Satake, K., and Y. Tanioka (1999), Sources of tsunami and tsunamigenic earthquakes in subduction zones, *Pure and Applied Geophysics*, *154*(3-4), 467-483.

Schorlemmer, D., S. Wiemer, and M. Wyss (2005), Variations in earthquake-size distribution across different stress regimes, *Nature*, *437*(7058), 539-542.

Stein (1999), The role of stress transfer in earthquake occurrence, *Nature*, *402*(6762), 605-609.

Stein, S., and Wysession (2003), *An Introduction To Seismology, Earthquakes, And Earth Structure*, 498 pp., Blackwell Publishing.

Tsuboi, S., P. M. Whitmore, and T. J. Sokolowski (1999), Application of M-wp to deep and teleseismic earthquakes, *Bull. Seismol. Soc. Amer.*, *89*(5), 1345-1351.

Tsuboi, S., K. Abe, K. Takano, and Y. Yamanaka (1995), Rapid determination of Mw from broad-band p-wave-forms, *Bull. Seismol. Soc. Amer.*, *85*(2), 606-613.

Vassiliou, M. S., and H. Kanamori (1982), The energy release in earthquakes, *Bull. Seismol. Soc. Amer.*, *72*(2), 371-387.

Venkataraman, A., and H. Kanamori (2004), Effect of directivity on estimates of radiated seismic energy, *J. Geophys. Res.-Solid Earth*, *109*(B4).

Vidale, J. E., and H. Houston (1993), The depth dependence of earthquake duration and implications for rupture mechanisms, *Nature*, *365*(6441), 45-47.

Warren, L. M., and P. G. Silver (2006), Measurement of differential rupture durations as constraints on the source finiteness of deep-focus earthquakes, *J. Geophys. Res.-Solid Earth*, *111*(B6).

Weinstein, S. A., and E. A. Okal (2005), The mantle magnitude M_m and the slowness parameter Θ: Five years of real-time use in the context of Tsunami warning, *Bull. Seismol. Soc. Amer.*, *95*(3), 779-799.

Wyss, M., and J. N. Brune (1968), Seismic moment stress and source dimensions for earthquakes in California-Nevada region, *Journal of Geophysical Research*, *73*(14), 4681-4694.